eCAM Evidence-Based Complementary and Alternative Medicine

Role of Natural Products in Ameliorating Drugs and Chemicals Toxicity

Guest Editors: Mohamed M. Abdel-Daim, Salah M. Aly, Khaled Abo-el-Sooud, Mario Giorgi, and Sorin Ursoniu

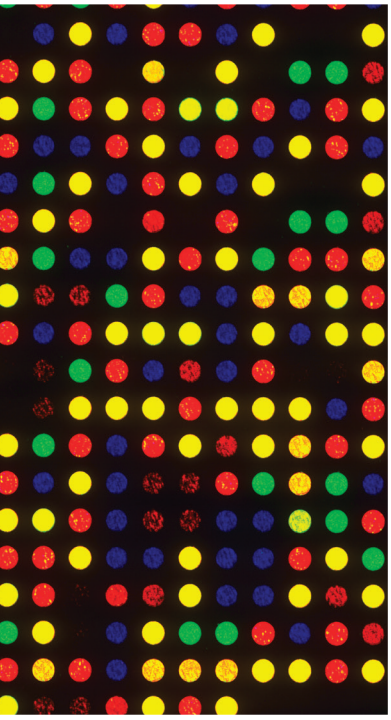

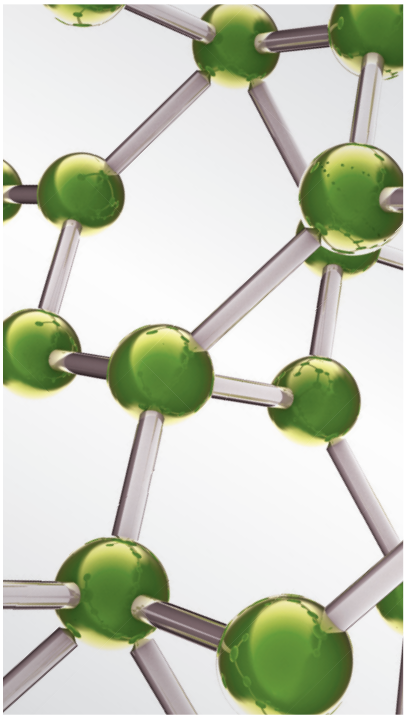


Role of Natural Products in Ameliorating Drugs and Chemicals Toxicity

Evidence-Based Complementary and Alternative Medicine

Role of Natural Products in Ameliorating Drugs and Chemicals Toxicity

Guest Editors: Mohamed M. Abdel-Daim, Salah M. Aly, Khaled Abo-el-Sooud, Mario Giorgi, and Sorin Ursoniu

Editorial Board

Contents

Hindawi Publishing Corporation
Evidence-Based Complementary and Alternative Medicine
Volume 2016, Article ID 7879406, 2 pages
http://dx.doi.org/10.1155/2016/7879406

Editorial

Role of Natural Products in Ameliorating Drugs and Chemicals Toxicity

Mohamed M. Abdel-Daim,[1] Salah M. Aly,[2] Khaled Abo-el-Sooud,[3] Mario Giorgi,[4] and Sorin Ursoniu[5]

[1] *Pharmacology Department, Faculty of Veterinary Medicine, Suez Canal University, Ismailia 41522, Egypt*
[2] *Pathology Department, Faculty of Veterinary Medicine, Suez Canal University, Ismailia 41522, Egypt*
[3] *Pharmacology Department, Faculty of Veterinary Medicine, Cairo University, Giza, Egypt*
[4] *Pharmacology and Toxicology Division, Department of Veterinary Sciences, University of Pisa, Pisa, Italy*
[5] *Department of Functional Sciences, Discipline of Public Health, "Victor Babes" University of Medicine and Pharmacy, Timisoara, Romania*

Correspondence should be addressed to Mohamed M. Abdel-Daim; abdeldaim.m@vet.suez.edu.eg

Received 26 July 2016; Accepted 26 July 2016

Herbal medicines have a long history over than 7000 years in traditional treatment, therapeutic experiences, and clinical trials including Egypt, China, and Korea. This practice is still the mainstay of about 75–80% of the world population, mainly in the developing countries, for primary health care and promotion because of better cultural acceptability, better compatibility with the human body, and lesser side effects. However, the last few years have seen a major increase in their use in the developed world. Nowadays, we can find a bipolarised market for the active ingredients: those chemically produced and mainly supported by the pharmaceutical companies and those natural constituents that are demanded by an increased number of patients. Although natural products have not been always active as supposed, some of them are scientifically recognised as therapeutically active. Indeed, it has to be noted that some drugs, still used in the current therapies, are extracted from plants. Some of these can have additive action if coadministered with synthesized drugs or ameliorate the drug toxicity.

Potentially there are hundred thousands of natural compounds on the heart. Countries where the flora and fauna are variegated have more potentiality. That is the reason why research on natural compound is especially developed in these areas. However, the increased global demand of these active ingredients has led to a worldwide research in this field. The reason why this special issue has been set up is because the natural compounds are taking place in our society, and their combination with synthesized drugs is an "on the edge" topic.

Nine manuscripts have been published.

L.-J. Cao et al. concluded that isoliquiritigenin and glycyrrhetinic acid could activate the nuclear factor erythroid 2-related factor 2 (Nrf2) antioxidant response in HepG2 cells, protecting against triptolide-induced oxidative damage.

X. Jing et al. suggest that electroacupuncture is an effective approach for inhibiting weight gain in type 2 diabetic rats treated by rosiglitazone through increased levels of leptin receptor and STAT3 and decreased PPARγ expression.

S. Paul et al. examined the possible protective effects of Satkara, *Citrus macroptera* fruit ethanol extract against acetaminophen-induced rats hepatorenal toxicity through its inhibition of lipid peroxidation.

A. Hanafy et al. evaluated the hepatoprotective and antioxidant activities of the methanol extract of *Adansonia digitata* fruit pulp on acetaminophen-induced hepatotoxicity in rats.

Y. Luo et al. conducted a randomized, parallel-group, multicenter clinical application study in order to confirm the

Kangfuxin solution superiority to compound borax gargle on chemoradiotherapy-mucositis.

D. L. Valle Jr. et al. isolated and identified the antimicrobial compounds of Philippine *Piper betle* L. leaf ethanol extracts by thin layer chromatography- (TLC-) bioautography and gas chromatography-mass spectrometry (GC-MS) and tested them against two Gram-positive multidrug-resistant (MDR) bacteria.

N. H. AbdelAllah et al. used an alternative natural adjuvant system (chitosan and sodium alginate) allowing for a reduction in dose and cost in the antihepatitis B vaccine.

I. J. Asiedu-Gyekye et al. investigated the elemental composition of unsweetened natural cocoa powder, its effect on nitric oxide, and its hepatoprotective potential during simultaneous administration with high-dose artemether/lumefantrine (recommended therapy for malaria). They found that unsweetened natural cocoa powder increases nitric oxide levels and has hepatoprotective potential during artemether/lumefantrine administration.

S. Sabiu et al. evaluated membrane stabilization and detoxification potential of ethyl acetate fraction of *Zea mays* L., *Stigma maydis* in acetaminophen-induced renal oxidative damage through its antioxidant effect.

Mohamed M. Abdel-Daim
Salah M. Aly
Khaled Abo-el-Sooud
Mario Giorgi
Sorin Ursoniu

Hindawi Publishing Corporation
Evidence-Based Complementary and Alternative Medicine
Volume 2016, Article ID 2046298, 14 pages
http://dx.doi.org/10.1155/2016/2046298

Research Article

Membrane Stabilization and Detoxification of Acetaminophen-Mediated Oxidative Onslaughts in the Kidneys of Wistar Rats by Standardized Fraction of *Zea mays* L. (Poaceae), *Stigma maydis*

S. Sabiu,[1,2] F. H. O'Neill,[2] and A. O. T. Ashafa[1]

[1] *Phytomedicine and Phytopharmacology Research Group, Department of Plant Sciences, University of the Free State, QwaQwa Campus, Phuthaditjhaba 9866, South Africa*
[2] *Department of Microbial, Biochemical, and Food Biotechnology, University of the Free State, Nelson Mandela Drive, P.O. Box 339, Bloemfontein 9301, South Africa*

Correspondence should be addressed to A. O. T. Ashafa; ashafaaot@ufs.ac.za

Received 18 March 2016; Accepted 22 May 2016

Academic Editor: Khaled Abo-el-Sooud

This study evaluated membrane stabilization and detoxification potential of ethyl acetate fraction of *Zea mays* L., *Stigma maydis* in acetaminophen-induced oxidative onslaughts in the kidneys of Wistar rats. Nephrotoxic rats were orally pre- and posttreated with the fraction and vitamin C for 14 days. Kidney function, antioxidative and histological analyses were thereafter evaluated. The acetaminophen-mediated significant elevations in the serum concentrations of creatinine, urea, uric acid, sodium, potassium, and tissue levels of oxidized glutathione, protein-oxidized products, lipid peroxidized products, and fragmented DNA were dose-dependently assuaged in the fraction-treated animals. The fraction also markedly improved creatinine clearance rate, glutathione, and calcium concentrations as well as activities of superoxide dismutase, catalase, glutathione reductase, and glutathione peroxidase in the nephrotoxic rats. These improvements may be attributed to the antioxidative and membrane stabilization activities of the fraction. The observed effects compared favorably with that of vitamin C and are informative of the fraction's ability to prevent progression of renal pathological conditions and preserve kidney functions as evidently supported by the histological analysis. Although the effects were prominently exhibited in the fraction-pretreated groups, the overall data from the present findings suggest that the fraction could prevent or extenuate acetaminophen-mediated oxidative renal damage via fortification of antioxidant defense mechanisms.

1. Introduction

The kidney is a highly specialized organ that maintains the body's homeostasis by selectively excreting or retaining various substances according to specific body needs. In its role as a detoxifier and primary eliminator of xenobiotics, it becomes vulnerable to developing injuries. Such injuries have been linked with reactive oxygen species (ROS) mediated oxidative stress on renal biomolecules [1]. The kidney's response to toxicants varies by multiple morphological patterns beginning with tubular or interstitial changes to nephropathy [2]. Kidney disorders account for 1 in 10 deaths, making Chronic Kidney Disease (CKD) one of the most sought after public health concerns in recent years [3]. The prevalence of the disease is more disconcerting in sub-Saharan Africa countries like Nigeria and South Africa with an estimation of 23 and 40%, respectively [3, 4]. Till date, orthodox management therapies for kidney disorders have been embraced and identified to include the use of renal replacement therapy (dialysis and transplantation) and applications of angiotensin-converting enzyme (ACE) inhibitors, angiotensin II receptor blockers (ARBs), and erythropoietin to slow the progression of loss of kidney function [5]. The affordability, sensitivity, and inherent adverse effects of the aforementioned therapies have undermined their applications in the past. The availability of kidneys for transplantation and cost are other important

challenges consistent with renal replacement therapy [6]. Interestingly, traditional systems of medicine have offered effective drugs against kidney pathological conditions and thus can be used to protect renal function and prevent/slow the progression of renal diseases to CKD or end stage renal disease [7]. A number of drugs from herbal sources have been shown to be nephroprotective and there is a keen global interest on the development of such. The focus is mostly to protect or prevent injurious insults to the kidney as well as enhance the regeneration of tubular cells [8].

Zea mays L. (Poaceae), *Stigma maydis* (corn silk) is one of several herbs commonly used in the management of kidney stones, bedwetting, and urinary infections [9]. GCMS analysis of its aqueous extract from our laboratory revealed the presence of maizenic acid, β-carotene, ascorbic acid, gluten, o-diethyl phthalate, 2-methyl-naphthalene, thymol, $3'$-o-methyl-maysin, cyanidin, cinnamic acid, hordenine, luteolinidin, pelargonidin, and betaine as major identifiable adaptogenic phytonutrients [10]. Corn silk (CS) has found therapeutic applications as an insecticide, disinfectant, antioxidant, antibiotic, and immune booster [11–13]. Its pharmacological significance in Asian folkloric medicine as oral hypoglycemic and anti-inflammatory agents has also been reported [14–16]. Lamentably in Africa, particularly, Nigeria and South Africa, where corn is a common staple food, CS is still underutilized and its pharmacological significance is chiefly untapped.

Besides very limited research on the therapeutic importance of CS in Africa, opinions on its nephroprotective potential are divergent. While Sukandar et al. [17] demonstrated the potency of its ethanolic extract against gentamicin/piroxicam-induced kidney failure, Sepehri et al. [18] submitted that treatment with its methanolic extract does not result in complete reversal of gentamicin-induced alterations in kidney function parameters. More comprehensive research is however imperative in this direction and has prompted the present study with a view to providing detailed biochemical information on the ability of CS to preserve renal functions and delay/prevent the progression of renal pathological conditions. Hence, we evaluated its standardized fraction against acetaminophen-perturbed oxidative onslaughts in the kidneys of Wistar rats. In addition, the membrane stabilization capacity of the CS fraction was also investigated.

2. Materials and Methods

2.1. Chemicals, Reagents, and Assay Kits. Assay kits for kidney function parameters, glutathione peroxidase, and glutathione reductase were purchased from Randox Laboratories Limited, United Kingdom. Acetaminophen (APAP) and vitamin C were products of Emzor Pharmaceuticals, Lagos, Nigeria. The water used was glass-distilled and all other chemicals and reagents were of analytical grade.

2.2. Plant Collection and Authentication. Fresh corn silks were harvested from a maize plantation in the Phuthaditjhaba area of Maluti-A-Phofung, QwaQwa, Free State province, South Africa, between November 2014 and March 2015. They were authenticated by Dr. A. O. T. Ashafa of the Plant Sciences Department, University of the Free State, QwaQwa Campus, South Africa. Voucher specimen (number SabMed/01/2015/QHB) was thereafter prepared and deposited at the Herbarium of the University.

2.3. Extract Processing, Standardization, and Selection. The CS was shade dried to constant weight and subsequently milled by an electric blender (model MS-223; Labcon PTY, Durban, South Africa) to fine powder. The powdered sample (2 kg) was extracted with 70% methanol (10 L) with regular agitation for 24 h. The solution obtained was filtered (Whatman no. 1 filter paper) and the resulting filtrate concentrated to a yield of 455 g crude extract. Part of the crude extract (400 g) was suspended in distilled water (0.6 L) and subsequently partitioned in succession with n-hexane, dichloromethane, ethyl acetate, and n-butanol. This yielded 18 g, 24 g, 33 g, and 42 g of the respective fractions. About 10 μL of each (1 mg/mL) was spotted on silica gel TLC plates. The resulting chromatograms were thereafter developed in dichloromethane/methanol (8.5 : 1.5 v/v) solvent system and sprayed with 0.2% 1,1-diphenyl-2-picrylhydrazyl (DPPH) in methanol for detection of antioxidant metabolites. From the chromatograms, the ethyl acetate fraction of CS (CSEAF) had the highest number of antioxidant spots and was selected for the subsequent biochemical assays. CSEAF was kept air-tight and refrigerated prior to commencement of the study.

2.4. Experimental Animals. This study was approved (UFS-AED2015/0005) by the Ethical Committee of University of the Free State, South Africa, in accordance with the Guidelines of the National Research Council Guide for the Care and Use of Laboratory Animals [19] and principles of Good Laboratory Procedure [20]. Healthy Wistar rats (both sexes) of weight range 200–222 g were collected from the experimental animal facility of University of the Free State, Bloemfontein, South Africa. They were housed in clean metabolic cages placed in a well-ventilated animal house with optimal conditions (temperature 23 ± 1°C, photoperiod; 12 h natural light and 12 h dark; humidity; 45–50%). They were acclimatized to the animal house condition for 10 days and had *ad libitum* access to pelleted rat chow (Pioneer Food (Pty) Ltd., Huguenot, South Africa) and water.

2.5. Nephroprotective Study

2.5.1. Induction of Renal Injury. This was achieved as previously described [21]. Briefly, the animals were fasted overnight for 14 h and a single oral dose of APAP (750 mg/kg body weight (b.w.)) was thereafter administered. These animals essentially represent nephrotoxic rats.

2.6. Experimental Protocol. Fifty rats randomized into 9 experimental groups were used for this study. While the nephrotoxic control group had 10 animals that were further divided into 2 sets (with one of the sets designated as satellite group) to monitor possible self-recovery effects, the remaining animals (40) were evenly distributed into 8 treatment groups of 5 rats each and treated as in Table 1.

Table 1

Groups	Designation	Treatments
1	Control	Given sterile placebo.
2	Nephrotoxic rats in two sets	Animals induced with nephrotoxicity and not treated.
3	CSEAF-treated only	Given 200 $mgkg^{-1}$ b.w. of CSEAF only for 14 days.
4, 5, and 6	Pretreatment	Pretreated with CSEAF (100 and 200 $mgkg^{-1}$ b.w.) and vitamin C (200 $mgkg^{-1}$ b.w.), respectively, for 14 days prior to nephrotoxicity induction.
7, 8, and 9	Posttreatment	Nephrotoxic rats posttreated, respectively, with the fraction (100 and 200 $mgkg^{-1}$ b.w.) and vitamin C (200 $mgkg^{-1}$ b.w.) for 14 days.

Treatments were done once daily via oral intubation between 9.00 and 10.00 a.m. to minimize possible diurnal effects. A transition period of 24 h was observed between the two subsequential treatment periods in both pre- and posttreatment groups.

2.7. Serum Preparation and Kidney Isolation. Forty-eight hours after the last treatment in each case, the rats were humanely euthanized under halothane anaesthetization and blood was collected via cardiac puncture into plain sample bottles. For serum preparation, the blood was allowed to clot for 10 min and subsequently centrifuged (Beckman and Hirsch, Burlington, IO, USA) at 3,000 ×g for 15 minutes. Serum was carefully aspirated and used for kidney function tests. The rats were also immediately dissected and the kidneys were diligently harvested, blotted with clean tissue paper, cleaned of fat, and weighed and the relative kidney-body weight ratios (RKW) were evaluated. The left kidney was thereafter sliced into two portions with one of the portions homogenized in Tris-HCl buffer (0.05 mol/L Tris-HCl and 1.15% KCl, pH 7.4) for antioxidant analyses, while the other was used for histological examination.

2.8. Biochemical Analyses

2.8.1. Kidney Function Parameters. Following the procedures outlined in the assay kits, kidney function parameters were determined. Serum concentrations of creatinine, blood urea nitrogen, uric acid, potassium, sodium, and calcium were evaluated. Creatinine clearance rate (CCR) was estimated as earlier reported [22].

2.9. Antioxidant and Oxidative Stress Assays

2.9.1. Reduced Glutathione (GSH) and Oxidized Glutathione (GSSG). The procedure described by Ellman [23] was employed to determine the level of GSH in the homogenate. Briefly, 1.0 mL of the homogenate was added to 25% trichloroacetic acid (1 mL) and the precipitate was removed by centrifugation at 5,000 ×g for 10 min. Supernatant (0.1 mL) was added to 2 mL of 0.6 mM 5,5′-dithiobis-2-nitrobenzoic acid (DTNB) prepared in 0.2 M sodium phosphate buffer (pH 8.0). The absorbance of the yellow-colored complex was thereafter read at 420 nm and the extrapolated values from the standard calibration curve were expressed as the homogenate concentrations of GSH.

For GSSG level estimation, the described method of Hissin and Hilf [24] was adopted. The homogenate (50 μL) was mixed with 20 μL of 0.04 M *N*-ethylmaleimide (NEM) to prevent oxidation of GSH to GSSG. The mixture was subsequently incubated at room temperature for 30 min prior to consecutive addition of 0.3 M Na_2HPO_4 solution (1.68 mL) and 250 μL of DTNB reagent. The absorbance of the resulting mixture was thereafter read at 420 nm as concentration of GSSG in the homogenate expressed in nmol/mg protein.

2.10. Lipid Peroxidation Products. The homogenate levels of lipid peroxidation products (conjugated dienes, lipid hydroperoxides, and malondialdehyde) were estimated as reported by Reilly and Aust [25].

2.11. Protein Carbonyl and Advanced Oxidation Protein Product (AOPP). The method of Levine et al. [26] based on the reaction of carbonyl compounds with 2,4-dinitrophenyl hydrazine for 1 h and subsequent precipitation with 20% trichloroacetic acid was employed to determine the concentration of protein carbonyl in the renal homogenate. The released carbonyl compounds were measured spectrophotometrically at 380 nm and expressed as nmol/mg protein of the homogenate.

For the AOPP assay, the kidney homogenate (2 mL) was centrifuged at 2500 ×g for 10 min at 40°C. The resulting supernatant was thereafter added to a reaction mixture containing 50% acetic acid and 1.16 mol/L potassium iodide in phosphate buffered saline solution. The absorbance was read at 340 nm and the concentration of AOPP determined from the extrapolated standard curve of serially diluted AOPP standard solution using 500 μmol/L chloramines stock [27].

2.12. Fragmented DNA. The quantity of fragmented DNA in the kidney homogenates was determined using standard protocols [28]. In brief, kidney homogenate was centrifuged at 15,000 ×g, for 15 min at 4°C. While the supernatant was aspirated and treated with 10% trichloroacetic acid (1.50 mL), the resulting pellet was treated with 5% trichloroacetic acid (0.65 mL). The reaction mixture in each case was kept refrigerated (4°C) to precipitate overnight before centrifuging at 2500 ×g for 10 min. Each reaction mixture was subsequently boiled at 100°C for 15 min, cooled to room temperature, and further centrifuged at 2500 ×g for 5 min. Exactly 0.5 mL of the supernatant content was treated with diphenylamine reagent

(1 mL) and incubated at 37°C for 4 h. Absorbance readings for both the treated supernatant and pellet were taken at 600 nm using a spectrophotometer and the % fragmented DNA was calculated using the expression:

$$\%\ \text{Fragmented DNA} = 100 \times \left(\frac{A_s}{A_s + A_p} \right), \quad (1)$$

where A_s and A_p represent absorbance of the supernatant and pellet, respectively.

2.13. Glutathione Peroxidase and Glutathione Reductase. Homogenate activities of glutathione peroxidase (GPx) and glutathione reductase (GRx) were also evaluated as per the manufacturer's instructions in the assay kits.

2.14. Superoxide Dismutase. The activity of superoxide dismutase (SOD) in the tissue homogenate was determined as outlined by Misra and Fridovich [29]. In brief, 0.2 mL of the homogenate was added to 2.5 mL of 0.05 M carbonate buffer (pH 10.2) to equilibrate before addition of freshly prepared 0.3 mM epinephrine (0.3 mL) to commence the reaction. The change in absorbance was measured at 480 nm at 30 s intervals for 150 s. One unit of enzyme activity is defined as 50% inhibition of the rate of autooxidation of pyrogallol as determined by changes in absorbance/min at 480 nm.

2.15. Catalase. The homogenate activity of catalase (CAT) activity was evaluated adopting the method of Aebi [30]. Exactly 50 μL of the kidney homogenate was added to a cuvette containing 2 mL of phosphate buffer (pH 7.0) and 30 mM H_2O_2 (1 mL). Catalase activity was measured at 240 nm for 1 min using a spectrophotometer. The molar extinction coefficient (43.6 M/cm) of H_2O_2 was used to estimate catalase activity.

2.16. Histopathological Examination. Following previously reported standard protocol [31], the histopathological examination of the excised kidney was performed. Briefly, sliced portions of the kidney were washed in normal saline and fixed immediately in 10% buffered formalin solution for at least 24 h. They were further dehydrated with graded alcohol (50–100%) and subsequently processed in paraffin embedding using LEICA PT 1020 Automatic Tissue Processor. About 5 μm thick section of each tissue was stained with hematoxylin and eosin and observed for possible histopathological infiltrations. Microscopic features of the kidneys of CSEAF- and vitamin C-treated rats were compared with both normal and nephrotoxic control groups. Based on the degree of derangements and severity of renal damage observed, the kidney sections were further evaluated and scored by an independent histopathologist on a 0 to 4 scale as follows:

0: normal and well-preserved renal architecture;

1: proximal convoluted tubules dilatation, focal granulovacuolar epithelial cell degeneration, and granular debris in not more than 1% of the tubular lumen;

2: epithelial necrosis and desquamation involving less than 50% of cortical tubules;

3: epithelial desquamation and necrosis involving more than 50% of proximal tubules;

4: complete or almost entire tubular necrosis.

2.17. Membrane Stabilizing Activity

2.17.1. Preparation of Bovine Red Blood Cell Suspension. This was achieved following the method of Oyedapo et al. [32] with slight modification. Briefly, fresh bovine blood samples were collected into ethylenediaminetetraacetic acid (EDTA) bottles and centrifuged (Bench Centrifuge, Beckman and Hirsch, Burlington, IO, USA) at 3,000 ×g for 10 min. The supernatants (plasma and leucocytes) were carefully aspirated with a Pasteur pipette, while the packed red blood cells were washed five times with isotonic buffered solution (154 mM NaCl in 10 mM sodium phosphate buffer (pH 7.4)) and centrifuged (3000 ×g, 10 min) each time until the supernatants were clear. The resulting pellet was employed to prepare 2% (v/v) stock suspension of erythrocytes (RBC) that was subsequently used.

2.18. Hypotonic Solution-Induced Hemolysis. Earlier reported methods [32, 33] were adapted for this assay. In brief, 0.5 mL of stock erythrocyte (RBC) suspension was mixed with 4.5 mL of hypotonic solution (50 mM NaCl in 10 mM sodium phosphate buffered saline (pH 7.4)) containing 1.0 mL of either the fraction (0.25–2.0 mg/mL) or ibuprofen (standard drug (0.1 mg/mL)). For the control sample, 0.5 mL of RBCs was mixed with the hypotonic buffered saline alone. The resulting mixture in each case was incubated (20°C, 10 min) and subsequently centrifuged (3000 ×g, 10 min) prior to absorbance reading at 540 nm using a spectrophotometer (Beckman, DU 7400, USA). The percentage inhibition of either hemolysis or membrane stabilization was calculated using the following equation:

$$\%\ \text{inhibition of hemolysis} = 100 \times \left(\frac{A_c - A_s}{A_c} \right), \quad (2)$$

where A_c is absorbance of control (hypotonic buffered saline solution alone) and A_s is absorbance of test sample in hypotonic solution.

2.19. Statistical Analysis. Degrees of protection conferred on the DNA, kidney function parameters, and inhibition of hemolysis by the fraction were expressed as percentages. Other results were subjected to one-way analysis of variance (ANOVA) using SPSS software package for windows (Version 16, SPSS Inc., Chicago, USA) and presented as mean ± standard error of mean (SEM) of five determinations. Significant difference between the treatment means was determined at 95% confidence level using Duncan's Multiple Range Test.

3. Results

3.1. Body and Relative Organ Weight. Data obtained with respect to body weight gain revealed significant ($p < 0.05$)

Table 2: Effect of *Zea mays*, *Stigma maydis* ethyl acetate fraction on the body weight changes and relative organ weights of acetaminophen-treated rats ($n = 5$, mean ± SEM).

Treatments	Weight changes			Kidney weight (g)	RKW (g/100 g b.w.)
	Initial (g)	Final (g)	% weight gain		
Sterile placebo (control)	210.22 ± 0.90	224.01 ± 0.89	6.16^{a}	1.61 ± 0.01^{a}	0.72^{a}
APAP treatment	220.12 ± 0.77	215.00 ± 0.99	(2.34^{b})	0.97 ± 0.01^{b}	0.45^{b}
200 mg/kg b.w. CSEAF	200.05 ± 0.54	220.01 ± 0.86	9.07^{c}	1.69 ± 0.01^{a}	0.77^{a}
100 mg/kg b.w. CSEAF, then APAP	212.21 ± 0.75	223.09 ± 0.76	4.88^{a}	1.58 ± 0.02^{a}	0.71^{a}
200 mg/kg b.w. CSEAF, then APAP	206.15 ± 0.45	227.31 ± 0.69	9.31^{c}	1.73 ± 0.01^{a}	0.76^{a}
200 mg/kg b.w. vitamin C, then APAP	215.05 ± 0.39	228.19 ± 0.50	5.76^{a}	1.64 ± 0.02^{a}	0.72^{a}
APAP, then 100 mg/kg b.w. CSEAF	200.15 ± 0.31	205.99 ± 0.56	2.84^{d}	1.49 ± 0.02^{a}	0.73^{a}
APAP, then 200 mg/kg b.w. CSEAF	219.02 ± 0.97	232.00 ± 0.67	5.60^{a}	1.72 ± 0.01^{a}	0.74^{a}
APAP, then 200 mg/kg b.w. vitamin C	221.09 ± 0.75	227.23 ± 0.45	2.70^{d}	1.63 ± 0.01^{a}	0.72^{a}

Values bearing different superscripts along the same column for each parameter are significantly different ($p < 0.05$).
Parenthesis signifies reduced value for the parameter. RKW: relative kidney-body weight.

Table 3: Effect of *Zea mays*, *Stigma maydis* ethyl acetate fraction on serum concentrations of some kidney function parameters of acetaminophen-treated rats ($n = 5$, mean ± SEM).

Treatments	Creatinine (mg/dL)	BUN (mg/dL)	Uric acid (mg/dL)	CCR (mL/min)
Sterile placebo (control)	0.63 ± 0.02^{a}	15.66 ± 0.17^{a}	4.09 ± 0.01^{a}	10.48 ± 0.01^{a}
APAP treatment	2.50 ± 0.04^{b}	49.00 ± 0.26^{b}	15.99 ± 0.02^{b}	2.64 ± 0.01^{b}
200 mg/kg b.w. CSEAF	0.62 ± 0.01^{a}	14.99 ± 0.43^{a}	4.10 ± 0.03^{a}	10.65 ± 0.02^{a}
100 mg/kg b.w. CSEAF, then APAP	0.99 ± 0.03^{c}	22.11 ± 0.23^{c}	8.11 ± 0.09^{c}	6.67 ± 0.01^{c}
200 mg/kg b.w. CSEAF, then APAP	0.57 ± 0.02^{a}	15.99 ± 0.13^{a}	4.51 ± 0.03^{a}	11.58 ± 0.02^{a}
200 mg/kg b.w. vitamin C, then APAP	0.56 ± 0.02^{a}	16.00 ± 0.12^{a}	4.51 ± 0.09^{a}	11.79 ± 0.01^{a}
APAP, then 100 mg/kg b.w. CSEAF	1.11 ± 0.03^{c}	25.12 ± 0.18^{c}	8.99 ± 0.06^{c}	5.95 ± 0.02^{c}
APAP, then 200 mg/kg b.w. CSEAF	0.63 ± 0.05^{a}	15.79 ± 0.12^{a}	9.01 ± 0.06^{c}	10.48 ± 0.01^{a}
APAP, then 200 mg/kg b.w. vitamin C	1.25 ± 0.01^{c}	16.09 ± 0.23^{a}	8.88 ± 0.04^{c}	5.28 ± 0.01^{c}

[abc]Values with different superscripts for each parameter are significantly different ($p < 0.05$). APAP: acetaminophen, CSEAF: corn silk ethyl acetate fraction, BUN: blood urea nitrogen, and CCR: estimated creatinine clearance rate.

reduction in the body weight of the nephrotoxic rats (APAP-treated) compared to control (Table 2). In contrast, when compared with the nephrotoxic group, the CSEAF pre- and posttreated groups had significantly ($p < 0.05$) higher weight gain with the effect elicited by the fraction administered at 200 mg/kg b.w. competing favorably with vitamin C. However, only marginal variation was observed in this parameter between the 200 mg/kg b.w. fraction-pretreated groups and those placed on 200 mg/kg b.w. of the fraction alone (Table 2). In addition, while there was marked reduction in the RKW of the APAP-treated animals, those of the fraction and vitamin C-administered groups were only marginally different from the normal control group (Table 2).

3.2. Kidney Function Indices. Significantly ($p < 0.05$) elevated serum levels of creatinine, urea, uric acid, sodium, and potassium were observed in the APAP-administered group when compared with the normal control (Tables 3 and 4). However, treatments with the fraction for 14 days dose-dependently and significantly ($p < 0.05$) prevented and extenuated the APAP-mediated increases in these parameters with most prominent effects elicited at the highest investigated dose in the pretreated groups. This is also consistent with the increased CCR and serum calcium levels observed in the fraction-supplemented rats as compared to the significantly ($p < 0.05$) reduced value for this parameter in the nephrotoxic rats (Tables 3 and 4). There were no evidences of nephrotoxic tendencies in the animals given 200 mg/kg b.w. of the CSEAF alone, as they compared favorably with the control for these parameters. However, the marked improvements observed in the fraction-treated animals were not evident in the satellite self-recovery group whose assayed parameters were essentially those of the nephrotoxic animals. The degree of protection conferred on the serum levels of creatinine and blood urea nitrogen by CSEAF treatments is presented in Figure 1. While treatments with 200 $mgkg^{-1}$ b.w. CSEAF compared favorably with vitamin C for overall modulation of blood urea nitrogen, it elicited a better and most prominent effect on creatinine metabolism (Figure 1).

3.3. Antioxidants and Oxidative Stress Markers

3.3.1. Nonenzymic Antioxidants and Oxidative Stress Markers. The effects of 14-day treatment with CSEAF on the nonenzymic antioxidant status and oxidative stress markers of the experimental rats are presented in Table 5 and Figure 2. The APAP-induced significant ($p < 0.05$) reduction in the level of GSH and the elevations in the levels of GSSG, protein

Table 4: Effect of *Zea mays*, *Stigma maydis* ethyl acetate fraction on serum concentrations of selected electrolytes of acetaminophen-treated rats ($n = 5$, mean ± SEM).

Treatments	Sodium (mEq/L)	Potassium (mEq/L)	Calcium (mg/dL)
Sterile placebo (control)	135.44 ± 1.35^{a}	3.50 ± 1.01^{a}	8.95 ± 1.01^{a}
APAP treatment	338.22 ± 1.65^{b}	10.11 ± 1.02^{b}	3.33 ± 1.00^{b}
200 mg/kg b.w. CSEAF	145.01 ± 1.21^{a}	3.59 ± 1.00^{a}	9.83 ± 1.02^{a}
100 mg/kg b.w. CSEAF, then APAP	198.22 ± 1.11^{c}	5.55 ± 1.02^{c}	5.99 ± 1.01^{c}
200 mg/kg b.w. CSEAF, then APAP	138.94 ± 1.26^{a}	3.75 ± 1.06^{a}	9.01 ± 1.00^{a}
200 mg/kg b.w. vitamin C, then APAP	143.12 ± 1.70^{a}	3.55 ± 1.01^{a}	9.17 ± 1.01^{a}
APAP, then 100 mg/kg b.w. CSEAF	226.21 ± 1.13^{d}	7.09 ± 1.01^{d}	6.99 ± 1.02^{d}
APAP, then 200 mg/kg b.w. CSEAF	200.12 ± 1.42^{c}	5.99 ± 1.00^{c}	8.99 ± 1.02^{a}
APAP, then 200 mg/kg b.w. vitamin C	139.01 ± 1.22^{a}	3.79 ± 1.02^{a}	9.15 ± 1.01^{a}

[abcd]Values with different superscripts for each parameter are significantly different ($p < 0.05$). APAP: acetaminophen and CSEAF: corn silk ethyl acetate fraction.

Table 5: Effect of *Zea mays*, *Stigma maydis* ethyl acetate fraction on the levels of nonenzymic antioxidant system, protein-oxidized products, and fragmented DNA of acetaminophen-treated rats ($n = 5$, mean ± SEM).

Treatment	GSH (X)	GSSG (X)	GSH/GSSG	PC (X)	AOPP (Y)	F/DNA (%)
Sterile placebo (control)	35.11 ± 1.35^{a}	0.20 ± 0.01^{a}	175.55 ± 0.20^{a}	3.72 ± 0.25^{a}	195.98 ± 1.99^{a}	10.12 ± 0.10^{a}
APAP treatment	7.56 ± 1.09^{b}	1.99 ± 0.02^{b}	3.80 ± 0.08^{b}	15.12 ± 0.22^{b}	501.23 ± 1.59^{b}	65.15 ± 0.19^{b}
200 mg/kg b.w. CSEAF	25.02 ± 1.08^{c}	0.12 ± 0.03^{c}	208.50 ± 0.32^{c}	3.66 ± 0.40^{a}	190.23 ± 1.45^{a}	11.75 ± 0.14^{a}
100 mg/kg b.w. CSEAF, then APAP	30.19 ± 1.11^{a}	0.21 ± 0.02^{a}	143.29 ± 0.19^{d}	8.00 ± 0.25^{c}	275.99 ± 1.40^{c}	30.16 ± 0.15^{c}
200 mg/kg b.w. CSEAF, then APAP	31.01 ± 1.06^{a}	0.16 ± 0.03^{a}	193.81 ± 0.15^{c}	4.67 ± 0.32^{a}	193.01 ± 1.34^{a}	12.01 ± 0.18^{a}
200 mg/kg b.w. vitamin C, then APAP	36.11 ± 1.32^{a}	0.19 ± 0.02^{a}	190.05 ± 0.17^{c}	3.89 ± 0.25^{a}	200.45 ± 1.29^{a}	11.21 ± 0.19^{a}
APAP, then 100 mg/kg b.w. CSEAF	15.99 ± 1.11^{d}	0.22 ± 0.01^{a}	72.68 ± 0.15^{e}	9.04 ± 0.22^{c}	287.32 ± 1.88^{c}	31.00 ± 0.10^{c}
APAP, then 200 mg/kg b.w. CSEAF	16.21 ± 1.00^{d}	0.19 ± 0.05^{a}	85.32 ± 0.09^{e}	9.14 ± 0.35^{c}	203.19 ± 1.25^{a}	12.09 ± 0.11^{a}
APAP, then 200 mg/kg b.w. vitamin C	15.15 ± 1.72^{d}	0.19 ± 0.05^{a}	79.74 ± 0.10^{e}	8.01 ± 0.29^{c}	212.34 ± 1.67^{a}	12.13 ± 0.15^{a}

[abcde]Values with different superscripts for each parameter are significantly different ($p < 0.05$). APAP: acetaminophen, CSEAF: corn silk ethyl acetate fraction, GSH: reduced glutathione, GSSG: peroxidized glutathione, PC: protein carbonyl, AOPP: advanced oxidation protein product, F/DNA: fragmented DNA, X: nmol mg protein^{-1}, and Y: μmol mg protein^{-1}.

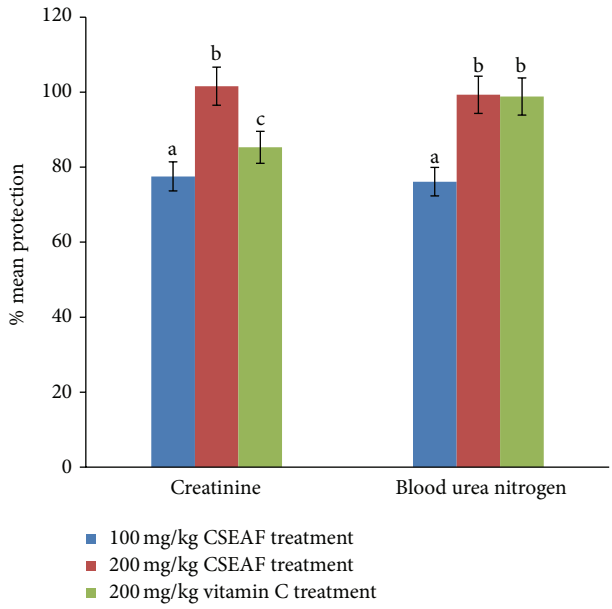

Figure 1: Mean percentage protection offered by *Zea mays*, *Stigma maydis* and vitamin C against acetaminophen-induced renal injury as assessed by serum creatinine and blood urea nitrogen. The percent protection was calculated as follows: 100 × (values of APAP treatment − values of test)/(values of APAP treatment − values of control). [abc]Bars with different superscripts for each parameter are significantly different ($p < 0.05$). CSEAF: corn silk ethyl acetate fraction.

Table 6: Effect of *Zea mays*, *Stigma maydis* ethyl acetate fraction on specific activities of enzymic antioxidant system of acetaminophen-treated rats ($n = 5$, mean ± SEM).

Treatments	Antioxidant enzymes (nmol min^{-1} mgprotein^{-1})			
	SOD	Catalase	Glutathione Rx	Glutathione Px
Sterile placebo (control)	43.12 ± 0.15^{a}	33.99 ± 0.11^{a}	56.11 ± 0.45^{a}	123.15 ± 1.10^{a}
APAP treatment	10.11 ± 0.10^{b}	13.29 ± 0.12^{b}	18.11 ± 0.23^{b}	43.66 ± 1.15^{b}
200 mg/kg b.w. CSEAF	59.21 ± 0.03^{c}	45.35 ± 0.11^{c}	55.19 ± 0.20^{a}	144.11 ± 1.10^{c}
100 mg/kg b.w. CSEAF, then APAP	32.12 ± 0.11^{d}	22.76 ± 0.15^{d}	30.21 ± 0.25^{c}	102.31 ± 1.10^{d}
200 mg/kg b.w. CSEAF, then APAP	41.24 ± 0.12^{a}	32.99 ± 0.19^{a}	53.99 ± 0.23^{a}	125.03 ± 1.11^{a}
200 mg/kg b.w. vitamin C, then APAP	42.07 ± 0.21^{a}	33.09 ± 0.11^{a}	56.04 ± 0.35^{a}	100.19 ± 1.09^{d}
APAP, then 100 mg/kg b.w. CSEAF	32.11 ± 0.12^{d}	22.18 ± 0.13^{d}	31.14 ± 0.31^{c}	98.22 ± 1.15^{d}
APAP, then 200 mg/kg b.w. CSEAF	31.99 ± 0.15^{d}	31.00 ± 0.13^{a}	55.09 ± 0.26^{a}	120.11 ± 1.10^{a}
APAP, then 200 mg/kg b.w. vitamin C	30.98 ± 0.20^{d}	30.01 ± 0.12^{a}	33.04 ± 0.35^{c}	96.12 ± 1.12^{d}

^{abcd}Values with different superscripts for each parameter are significantly different ($p < 0.05$). APAP: acetaminophen, CSEAF: corn silk ethyl acetate fraction, SOD: superoxide dismutase, Rx: reductase, and Px: peroxidase.

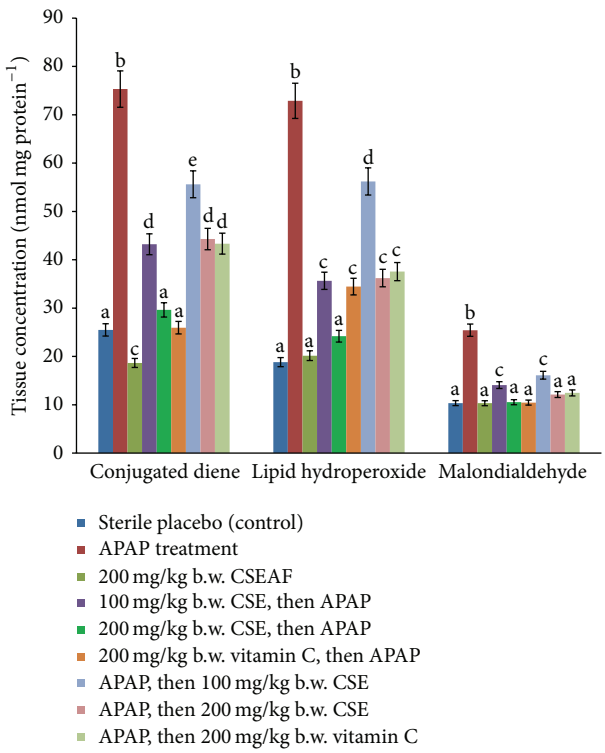

Figure 2: Effect of *Zea mays*, *Stigma maydis* ethyl acetate fraction on tissue concentrations of conjugated dienes, lipid hydroperoxides, and malondialdehyde of acetaminophen-treated rats. Values are mean ± standard error of mean (SEM) of five determinations. ^{abcde}Bars with different superscripts for each parameter are significantly different ($p < 0.05$). APAP: acetaminophen and CSEAF: corn silk ethyl acetate fraction.

carbonyls, AOPP, fragmented DNA, malondialdehyde, conjugated dienes, and lipid hydroperoxides were significantly ($p < 0.05$) and dose-dependently normalized in the CSEAF-treated animals. Although the fraction (at 200 mgkg^{-1} b.w.) compared well with reference drug (vitamin C) in both pre- and posttreatment modes, better results comparable to those of the control were observed in the fraction-pretreated group. However, while other nonenzymic antioxidant parameters were not significantly altered by treatment with 200 mgkg^{-1} b.w. of CSEAF alone, the homogenate level of GSH was significantly increased when compared with the control (Table 5).

3.3.2. Enzymic Antioxidants. Kidney homogenate activities of GRx, GPx, SOD, and CAT were significantly ($p < 0.05$) induced by CSEAF in a concentration-dependent manner in the two treatment models. These inductions markedly ($p < 0.05$) improved the observed APAP-mediated reduction in their activities and at the highest investigated dose the effect compared well with that of vitamin C (Table 6).

3.4. Histopathological Investigation. Macroscopic examination of kidneys from the control group revealed that they were essentially normal with characteristic fine texture and dark maroon appearance. While kidneys from the fraction-administered animals showed mild spots of brown color changes, those of the APAP-intoxicated animals revealed color changes from maroon to brown with characteristic uneven texture. Detailed histoarchitectural examination of the kidney sections of the control and 200 mgkg^{-1} b.w. CSEAF groups showed no histological derangements, as evidenced by the normal and well-preserved renal architecture with characteristic intact glomeruli and tubules (Figures 3(a) and 3(c)). In contrast, kidney sections from the APAP-administered group exhibited altered architecture with extensive destruction of glomeruli and tubular structures, as demonstrated by marked necrotic areas (Figure 3(b)). Hypercellularity in Bowman's capsule indicating leukocyte infiltration, glomerular atrophy, and dilated proximal tubules with loss of the cellular boundary and brush border were also evident (Figure 3(b)). Treatment with CSEAF at the investigated doses in the pre- and posttreatment modes showed dose-dependent protective and ameliorative capabilities in the kidneys that compared favorably with that of vitamin C (Figures 3(d)–3(i)). This was evident by the less severe tubular and glomerular damage, with the best and most prominent effect

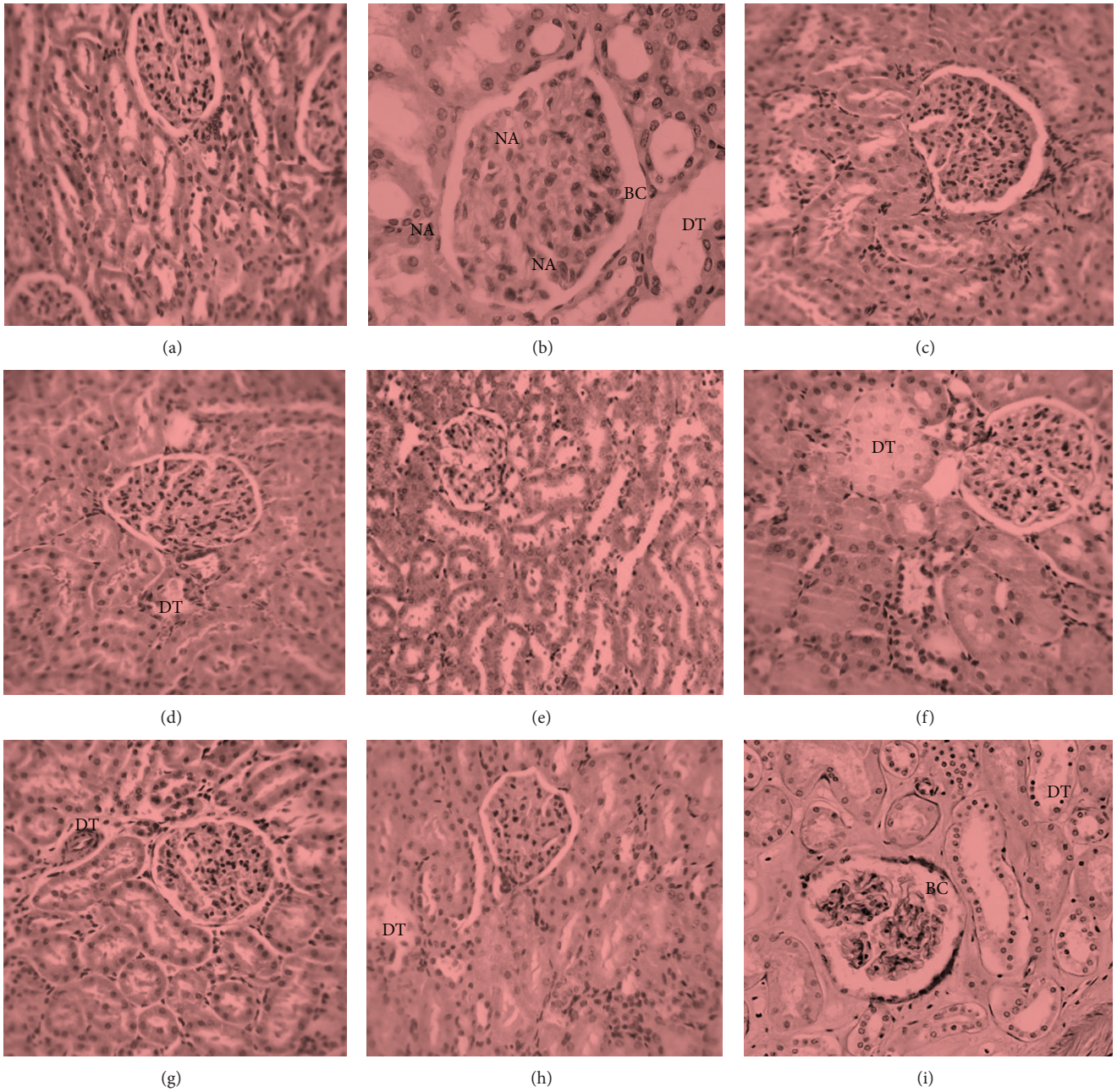

Figure 3: Kidney micrographs (×400, hematoxylin and eosin stained) of (a) control rat, (b) nephrotoxic rat, (c) CSEAF (200 mg/kg b.w.) treated rat, (d) nephrotoxic rat pretreated with CSEAF (100 mg/kg b.w.), (e) nephrotoxic rat pretreated with CSEAF (200 mg/kg b.w.), (f) nephrotoxic rat pretreated with vitamin C (200 mg/kg b.w.), (g) nephrotoxic rat posttreated with CSEAF (100 mg/kg b.w.), (h) nephrotoxic rat posttreated with CSEAF (200 mg/kg b.w.), and (i) nephrotoxic rat posttreated with vitamin C (200 mg/kg b.w.). CSEAF: corn silk ethyl acetate fraction, BC: Bowman's capsule showing leukocyte infiltration, DT: dilated proximal tubule, and NA: necrotic area.

observed in the 200 $mgkg^{-1}$ b.w. dose treated groups (Figures 3(e) and 3(h)). Furthermore, histopathological scoring of the kidney sections of CSEAF-treated groups showed that the obvious epithelial desquamation and tubular necrosis present in the kidney sections of the APAP-intoxicated animals were significantly and dose-dependently assuaged in a manner comparable to the vitamin C-treated animals (Table 7).

3.5. Membrane Stabilization. The result of membrane stabilizing activity of CSEAF is shown in Figure 4. Treatment with the fraction dose-dependently protected bovine RBC against hypotonic solution-induced infiltrations. The elicited effect at a 2 mg/mL dose of the fraction compared favorably with ibuprofen (0.1 mg/mL), standard drug used in this study.

Table 7: Histopathological grading of liver tissue sections of *Zea mays*, *Stigma maydis* ethyl acetate fraction-treated animals.

Treatments	Scores				
	0	1	2	3	4
Control	(5)	(0)	(0)	(0)	(0)
APAP treatment	(0)	(0)	(1)	(3)	(1)
200 mg/kg of CSEAF	(5)	(0)	(0)	(0)	(0)
100 mg/kg b.w. CSEAF, then APAP	(3)	(2)	(0)	(0)	(0)
200 mg/kg b.w. CSEAF, then APAP	(5)	(0)	(0)	(0)	(0)
200 mg/kg b.w. vitamin C, then APAP	(3)	(2)	(0)	(0)	(0)
APAP, then 100 mg/kg b.w. CSEAF	(2)	(2)	(1)	(0)	(0)
APAP, then 200 mg/kg b.w. CSEAF	(4)	(1)	(0)	(0)	(0)
APAP, then 200 mg/kg b.w. vitamin C	(3)	(2)	(0)	(0)	(0)

($n = 5$; figure in parenthesis represents number of rats affected in the group). APAP: acetaminophen and CSEAF: corn silk ethyl acetate fraction.

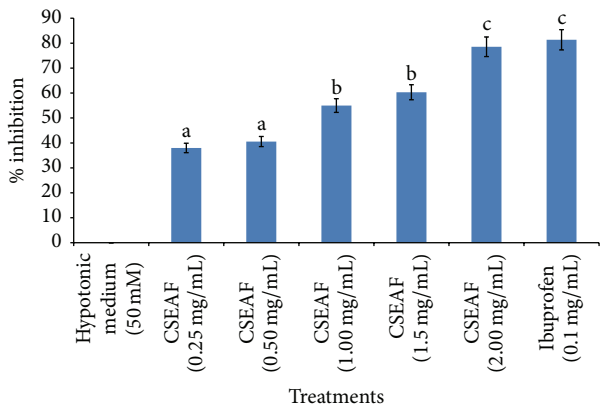

Figure 4: Effect of *Zea mays*, *Stigma maydis* ethyl acetate fraction on hypotonic solution-induced hemolysis of bovine erythrocyte membrane. Values are mean ± standard error of mean (SEM) of three determinations. [abc]Bars with different superscripts for the parameter are significantly different ($p < 0.05$). CSEAF: corn silk ethyl acetate fraction.

4. Discussion

Acetaminophen-mediated oxidative nephrotoxicity has been well documented and is characterized by morphologic and functional evidence of proximal tubular injury in humans and experimental animals [34, 35]. Acute and chronic renal failures in the course of therapeutic APAP administration have also been described in alcoholics and case-control studies [36]. Although molecular studies have linked APAP renal proximal tubular damage to translocation of GADD153 (growth arrest- and DNA damage-inducible gene 153) to the nucleus and subsequent proteolysis of caspase-12 [37], involvement of a reactive intermediate metabolite, N-acetyl-*p*-benzoquinone imine (NAPQI), cannot be excluded from renal damage [21]. NAPQI arylates selenium binding protein and glutamine synthetase in the S3 segment of the proximal tubule with consequential depletion of GSH [38]. This subsequently results in autooxidation of renal macromolecules (lipids, proteins, and DNA) with associated tubular cell necrosis. Tubular cell loss is an important feature of both acute renal failure and chronic renal disease [35] and is accompanied by concomitant increased serum concentrations of creatinine, urea, uric acid, and electrolyte imbalance. Creatinine, urea, and uric acid are major catabolic products of muscle, protein, and purine metabolism, respectively, and their serum concentrations give clues to the functional capacity of the nephrons at the glomerular and tubular levels [39]. These waste products (urea and creatinine) are passed into the blood stream for removal by the kidneys and their increased level in blood is a direct indication of renal dysfunction [40].

In this study, the increased serum concentrations of creatinine, blood urea nitrogen, and uric acid coupled with the attenuated CCR in the APAP-intoxicated animals may be indicative of renal injury and cell necrosis resulting from formation of NAPQI in excess of GSH detoxification ability. This is consistent with previous studies [21, 34], where APAP administration proved toxic to renal tubular cells. However, the significant and dose-dependent reversal in the levels of these parameters in the CSEAF-treated rats suggests that CSEAF was able to prevent or extenuate the deleterious influence of APAP. This observation also indicates that CSEAF at the investigated doses could preserve renal functions and delay progression of renal pathological conditions.

The most common cause of electrolyte imbalance or disturbance is associated with renal failure [40]. Calcium ions play a vital role in muscle contraction and serves as an intracellular second messenger for hormones. Hypocalcaemia is most commonly found in terminal stages of chronic generalized renal failure. Hence, the low level of calcium ion in the serum of APAP-administered rats may be associated with derangement of renal function resulting from interference with ions transport across the renal tubules [41]. The improvement observed in the calcium concentration in CSEAF-treated animals is a probable indication of its nephroprotective tendency. Sodium and potassium are the major extracellular and intracellular cations, respectively, in a living system. Sodium regulates the total amount of water in the body and its transmission across cells plays roles critical to body functions while adequate levels of potassium ions are essential for normal cell function. Many processes in the body, especially in the nervous system, muscles, and renal selective reabsorption, require electrical signals for communication. The movement of these ions is critical in generation of electrical signals [42]. In this study, the concentration-related significant normalization of APAP-mediated increases in serum levels of sodium and potassium ions in the fraction-administered rats is suggestive of its ability to maintain the levels of water and sodium at optimum equilibrium, thereby enhancing selective reabsorption capability of the nephron. Since membrane integrity is vital to signalling, the effect observed may also be due to the potential of the fraction to maintain membrane integrity of the kidney cells. This agrees with a previous report [43] where treatment with plant extracts reversed an acetaminophen-induced electrolyte imbalance in experimental animals.

Changes in the body weight of animals have been used to predict the nature and extent of drug-induced toxicity

and may give important information on their overall health status [44]. It could also dictate the impact of the drug on the overall growth and developmental metabolism of the animals. Therefore, the observed reduction in the body weight of the APAP-treated animals may imply possible impairment in growth-linked metabolic processes. That the CSEAF-administered animals had relatively normal and marginal body weight gain is an obvious indication of the tendency of the fraction to aid normal metabolism and sustain growth and developmental mechanisms in the animals. This could be attributed to enhanced appetite in the animals that may be ascribed to the phytoconstituents in CSEAF as previously reported for the crude aqueous extract of CS [45]. The effect of fraction on the body weight of the animals not only was further supported by the significant weight gain in the rats placed on 200 $mgkg^{-1}$ b.w. dose of CSEAF alone, but also lent credence to the nonnephrotoxic effect of the fraction. This observation is consistent with the finding of Abdul Hamid et al. [46], where administration of standardized leaf extract of *Zingiber zerumbet* was linked to both mean body weight gain and nephroprotective effects in experimental animals. The relative organ weight in pharmacological studies is imperative to understanding crucial treatment-induced organ weight variations in animals [47]. While an increase in the relative organ weight may depict either inflammation or increased secretory ability of the organ, a reduction could be informative of cellular shrinkage. In addition to defining toxicity as pathological changes observed in the organs of interest, the relative organ weight could also be suggestive of organ swelling, atrophy, or hypertrophy [48]. In this study, the sustained kidney weights in all the fraction-administered animals relative to the significantly reduced kidney weight in the APAP-intoxicated rats could imply that the constriction of renal tubular cells caused by the ravaging oxidative insults of APAP was well prevented or extenuated by the fraction. This suggests that CSEAF could protect renal tubular cells against oxidative routs at the tested doses and was closely supported by the histopathological findings where the kidney sections of fraction-treated animals revealed distinct and well-preserved histoarchitectural features.

Studies have implicated NAPQI formation and oxidative stress in APAP-induced nephrotoxicity [49, 50], and their overwhelming effects result in significantly impaired and insufficient levels of both enzymic and nonenzymic antioxidant defense mechanisms in the body [51]. Hence, the observed reduction in the renal level of GSH of APAP-intoxicated rats in this study might be due to depletion of GPx and GR, as well as formation of NAPQI that exceeds GSH detoxification capacity [49]. Also, the APAP-mediated elevation in GSSG levels may be ascribed to either GSH autooxidation or its mobilization towards GPx formation. The reduction in the ratio of GSH to GSSG caused by APAP administration reveals possible oxidative damage on the renal tubular cells. However, the significantly and dose-dependently increased GSH level coupled with the corresponding high GSH: GSSG ratio and low GSSG levels in the kidneys of the CSEAF-treated rats is suggestive of the inherent antioxidative effect of the fraction and further supports that it offered a considerable level of nephroprotection. Palani et al. [52] also reported similar improvement on the nonenzymic antioxidant status in APAP-intoxicated rats following treatment with *Pimpinella tirupatiensis* ethanolic extract.

An elevated level of malondialdehyde in tissues is an obvious indication of cellular damage due to lipid peroxidation resulting from malfunctioning of the antioxidant defense system [53]. Furthermore, APAP has been linked with lipid peroxidation and may facilitate elevated level of peroxidized products (conjugated dienes, lipid hydroperoxides, and malondialdehydes) in nephrotoxicity [46]. Therefore, the significant elevation in the levels of these products could be indicative of uncontrolled oxidative attacks of APAP's reactive metabolites and ROS on membrane-bound lipids. This might have disrupted membrane fluidity as well as modified and inflicted functional loss on the proteins and DNA of the renal tubular cells. The attenuation of APAP-enhanced increases in these peroxidative products by the CSEAF could mean that it was able to offer a considerable level of protection to the renal membrane lipids. This may be adduced to the ability of the CSEAF to aid with detoxification of reactive metabolites, which could have initiated and propagated peroxidation of membrane-bound polyunsaturated lipids of the tubular cells. It may also suggest that the fraction is rich in phytonutrients capable of stabilizing the cellular membranes of renal tubules against oxidative onslaughts of APAP. In the same vein, unguided influence of ROS can trigger protein autooxidation with consequential formation of protein carbonyls and AOPP [54]. These protein oxidative products have been employed as invaluable markers to ascertain the degree of oxidant-mediated protein damage in cells [55]. In this study, the significant increase in the tissue concentrations of these markers in the nephrotoxic animals relative to the fraction-treated rats could be attributable to the capacity of NAPQI to arylate selenium binding protein and glutamine synthetase in the S3 segment of the proximal tubule, thereby facilitating autooxidation of renal proteins [38]. This may also imply covalent binding of NAPQI to mitochondrial proteins which resultantly induced nitrate ion formation that incapacitates the Ca^{2+} pump of the renal membrane. Incapacitation of the Ca^{2+} pump further hinders mitochondrial function and ATP production which could have enhanced the observed elevated levels of AOPP and carbonyl product [54, 55]. The pre- and posttreatments with CSEAF reversed this trend which is a further attestation to its possible potential to incapacitate NAPQI, nitrate ions, and other reactive metabolites through enhancement and fortification of the antioxidant defense mechanisms of the renal tubular cells. Our findings are in agreement with previous assertions [46] that linked restoration to normal of APAP-mediated elevated levels of renal protein-oxidized products with seven-day treatment with ethyl acetate extract of *Zingiber zerumbet*.

Similar to protein-oxidized products, calcium ion accumulation and hydroxyl radical mediated oxidative damage are important events in the pathogenesis of DNA fragmentation. These events promote either tissue necrosis

or carcinogenesis, which subsequently results in cell death [56]. Thus, the significantly increased level of fragmented DNA in the kidneys of APAP-intoxicated rat is indicative of either genotoxicity or probable initiation of carcinogenesis. Jaeschke and Bajt [57] have earlier reported a similar increase in the level of damaged DNA due to APAP administration. The CSEAF-enhanced attenuation in the level of fragmented DNA in the kidneys of APAP-treated rats is a tenable fact that the fraction is endowed with antioxidative and antigenotoxic attributes. The CSEAF might have mimicked an antigenotoxic agent, thereby facilitating DNA repair or synthesis system [58].

During renal damage, superoxide radicals are formed at the site of injury and if their accumulation exceeds the body's antioxidant capacity it could overwhelm the defensive activities of SOD and CAT, thereby aggravating the severity of existing damage [52]. Therefore, exogenous optimization of preventive (CAT, GPx) and chain-breaking (SOD, GRx) enzymic antioxidants that subsequently increase cellular GSH content is not only imperative to annihilating catastrophic influence of free radicals/ROS but also crucial to stalling ravaging impacts of drug-induced oxidative stress. In this study, the decreased tissue activities of the assayed antioxidant enzymes (SOD, CAT, GRx, and GPx) could be due to their excessive mobilization towards detoxification of NAPQI and ROS during APAP-induced nephrotoxicity. This might have led to haphazard oxidative attack on cellular macromolecules that consequently results in necrosis [59]. This report is in agreement with the findings of Aslam et al. [60] and Kadir et al. [61], where the authors also studied drug-mediated renal damage in rats. They noted similar reductions in the activities of ROS detoxifying enzymes that were associated with the formation of reactive metabolites and ROS. Thus, the dose-dependent auspicious reversion of the APAP-induced reduction in the activities of these detoxifying enzymes by the CSEAF is indicative of its antioxidative activity. This could either be attributed to the tendency of the fraction to scavenge NAPQI and ROS or enhance tissue activity of ROS detoxifying enzymes.

In addition to complementing biochemical analyses, histopathological examination of kidney sections may provide invaluable information on how pharmacologically potent an agent is against renal damage. The significant alterations in glomerular structure, the thickening of the glomerular basement membrane, widening of the filtration slits, basal infolding patterns with the presence of cytoplasmic vacuolation, and the increase in collagen deposition around the tubules as observed in the kidney sections of APAP-intoxicated rats could be responsible for their impaired renal function. The consequently decreased glomerular filtration rate with associated elevated serum levels of urea and creatinine was evident in the present study and agreed with a previous report [62]. However, the apparently repudiated oxidative threats inflicted by APAP on the architectural features of renal tubular cells in the fraction pre- and posttreated rats suggest that the CSEAF offered a significant degree of protection and stabilization on the overall histoarchitectural integrity of the kidneys. In fact, the preservation of the tubular cells and architectural organization of some of the kidney sections was almost completely normalized with an increasing number of viable cells. The effects noticed compared favorably with that of vitamin C and are consistent with the results of the biochemical investigations performed in this study. Our observations agree with previous reports [21, 46, 63], where recovery from APAP-mediated derangements towards normalization of serum kidney function parameters and renal histological architecture was attributed to treatment with plant extracts.

During inflammatory events, lysosomal enzymes and hydrolytic constituents are released from phagocytes into the extracellular space. This release consequently inflicts injuries on the surrounding organelles and tissues as well as aggravating the severity of any existing infection [33]. The exposure of an erythrocyte to injurious substances like hypotonic medium and heat results in lysis of its membrane with associated hemolysis and autooxidation of hemoglobin. The autooxidation and hemolysis are direct consequences of the vulnerability of the cells to secondary insults of free radical chain reactions [64]. This hemolytic effect is closely linked to excessive accumulation of fluid within the cell which consequently results in membrane disorientation and disruption. This notion is consistent with the observation that the breakdown of biomembranes generates free radicals that invariably enhance cellular damage as normally observed in renal tubular oxidative damage [61]. Medicinal plants with good antioxidative and anti-inflammatory attributes have been reported to provide succor either by annihilating the ravaging activity of lysosomal enzymes or by enhanced stabilization of biomembranes via maintenance of membrane fluidity and ion gradients [32, 65]. This was evidently displayed in this study with the CSEAF at the highest investigated dose conferring a membrane stabilization potential of 78.55% against hypotonic solution infiltration on bovine erythrocytes. This may be ascribed to either the capability of the fraction to bind tenaciously to the erythrocyte membranes with concomitant prevention of deleterious assaults of the hypotonic solution or its potential in promoting dispersion by mutual repulsion of charges involved in the hemolysis of RBCs. While studies have shown flavonoids to exert stabilizing effects on lysosomes [33], tannin and saponins have been reported as being capable of binding cations, thereby stabilizing the erythrocyte membrane [66]. In addition to the various antioxidative phytoconstituents revealed by GC-MS analysis of CS, alkaloids, sterols, phenols, tannins, flavonoids, and saponins have also been qualitatively and quantitatively evaluated in its crude aqueous extract [67]. Therefore, the remarkable RBC membrane stabilization activity with good protection against hypotonic solution-induced lysis elicited by the CSEAF in this study may be attributed to the presence of these phytochemicals. This might have also enhanced restoration to normal of APAP-perturbed alterations in the assayed biochemical indices and preserved the membrane integrity of renal tubular cells as evidently revealed in both pre- and posttreatment groups in this study.

5. Conclusion

The reduction of oxidative onslaughts posed by APAP via treatments with the ethyl acetate fraction of corn silk is a

manifestation of its capabilities to preserve renal function and delay progression of renal pathological conditions to end stage disease/death. The engendered nephroprotective effect by the fraction could, in rats, be ascribed to its antioxidative and membrane stabilization potential. This is achieved by facilitating detoxification of APAP-mediated nephrotoxicity via induction of ROS detoxifying enzymes, thereby stalling autooxidation of cellular macromolecules and renal tubular damage. Though the effects were prominently exhibited in the fraction-pretreated groups, the overall effects elicited in both treatment groups were remarkable and indicative of an excellent candidate for the management of drug-induced renal oxidative disorders.

Competing Interests

The authors declare that there are no competing interests.

Acknowledgments

While appreciating the provision of Community Development Action Research Grant (no. KWA-SUCCD/2014AR/1/32) by Kwara State University, Malete, Nigeria, and the supportive grant of Nigerian Tertiary Education Trust Fund (TETFund) to S. Sabiu to South Africa, the expertise enjoyed at the laboratory of Phytomedicine and Phytopharmacology Research Group, University of the Free State, QwaQwa Campus, South Africa is also gratefully acknowledged.

References

[1] E. Ozbek, "Induction of oxidative stress in kidney," *International Journal of Nephrology*, vol. 2012, Article ID 465897, 9 pages, 2012.

[2] F. G. Silva, "Chemical-induced nephropathy: a review of the renal tubulointerstitial lesions in humans," *Toxicologic Pathology*, vol. 32, no. 2, pp. 71–84, 2004.

[3] World Health Organization (WHO), *Track Records of Global Chronic Kidney Disorders: An Update for the Sub-Saharan African Countries 2011–2014*, DR: SSAFR/TR121/Doc, World Health Organization, Harare, Zimbabwe, 2014.

[4] National Kidney Foundation of South Africa (NKFS), "Fact sheet on the prevalence of kidney disorders," 2015, http://www.nkf.org.za/kidney_disease.htm.

[5] Q. Z. Ahmad, N. Jahan, G. Ahmad, and G. Tajuddin, "An appraisal of nephroprotection and the scope of natural products in combating renal disorders," *Journal of Nephrology and Therapeutics*, vol. 4, article 170, 2014.

[6] World Health Organization, *Preventing Chronic Disease: A Vital Investment*, World Health Organization, Geneva, Switzerland, 2005.

[7] N. Ullah, M. A. Khan, T. Khan, and W. Ahmad, "Nephroprotective potentials of *Citrus Aurantium*: a prospective pharmacological study on experimental models," *Pakistan Journal of Pharmaceutical Sciences*, vol. 27, no. 3, pp. 505–510, 2014.

[8] N. Hamid and R. Mahmoud, "Tubular kidney protection by antioxidants," *Iranian Journal of Public Health*, vol. 42, pp. 1194–1196, 2013.

[9] F. Grases, J. G. March, M. Ramis, and A. Costa-Bauzá, "The influence of *Zea mays* on urinary risk factors for kidney stones in rats," *Phytotherapy Research*, vol. 7, no. 2, pp. 146–149, 1993.

[10] S. Sabiu, F. H. O'Neill, and A. O. T. Ashafa, "*Zea mays, Stigma maydis* prevents and extenuates acetaminophen-perturbed oxidative onslaughts in rat hepatocytes," *Pharmaceutical Biology*, 2016.

[11] P. Guevara, M. C. Pérez-Amador, B. Zúñiga, and M. Snook, "Flavones in corn silks and resistance to insect attacks," *Phyton-International Journal of Experimental Botany*, vol. 69, no. 1, pp. 151–156, 2000.

[12] Z. A. Maksimović and N. Kovačević, "Preliminary assay on the antioxidative activity of *Maydis stigma* extracts," *Fitoterapia*, vol. 74, no. 1-2, pp. 144–147, 2003.

[13] K. A. Kim, S.-K. Choi, and H.-S. Choi, "Corn silk induces nitric oxide synthase in murine macrophages," *Experimental and Molecular Medicine*, vol. 36, no. 6, pp. 545–550, 2004.

[14] G.-Q. Wang, T. Xu, X.-M. Bu, and B.-Y. Liu, "Anti-inflammation effects of corn silk in a rat model of carrageenin-induced pleurisy," *Inflammation*, vol. 35, no. 3, pp. 822–827, 2012.

[15] W. Zhao, Y. Yin, Z. Yu, J. Liu, and F. Chen, "Comparison of anti-diabetic effects of polysaccharides from corn silk on normal and hyperglycemia rats," *International Journal of Biological Macromolecules*, vol. 50, no. 4, pp. 1133–1137, 2012.

[16] M. Ghada, M. S. Eltohami, H. N. Adurahman, M. E. Mahmoud, and I. Mudawi, "*In Vitro* study of the effect of corn silk on glucose uptake by isolated rat hemi-diaphragm," *World Journal of Pharmaceutical Research*, vol. 3, no. 4, pp. 2190–2195, 2014.

[17] E. Y. Sukandar, J. I. Sigit, and L. F. Adiwibowo, "Study of kidney repair mechanisms of corn silk (*Zea mays* L. Hair)-binahong (*Anredera cordifolia* (Ten.) Steenis) leaves combination in rat model of kidney failure," *International Journal of Pharmacology*, vol. 9, no. 1, pp. 12–23, 2013.

[18] G. Sepehri, A. Derakhshanfar, and F. Y. Zadeh, "Protective effects of corn silk extract administration on gentamicin-induced nephrotoxicity in rat," *Comparative Clinical Pathology*, vol. 20, no. 1, pp. 89–94, 2011.

[19] National Research Council (NRC), *Guide for the Care and Use of Laboratory Animals*, National Research Council, 8th edition, 2011.

[20] World Health Organization, *Basic OECD Principles of GLP. Geneva*, World Health Organization, Geneva, Switzerland, 1998.

[21] B. Parameshappa, M. S. Ali Basha, S. Sen et al., "Acetaminophen-induced nephrotoxicity in rats: protective role of *Cardiospermum halicacabum*," *Pharmaceutical Biology*, vol. 50, no. 2, pp. 247–253, 2012.

[22] G. J. Schwartz, A. Muñoz, M. F. Schneider et al., "New equations to estimate GFR in children with CKD," *Journal of the American Society of Nephrology*, vol. 20, no. 3, pp. 629–637, 2009.

[23] G. L. Ellman, "Tissue sulfhydryl groups," *Archives of Biochemistry and Biophysics*, vol. 82, no. 1, pp. 70–77, 1959.

[24] P. J. Hissin and R. Hilf, "A fluorometric method for determination of oxidized and reduced glutathione in tissues," *Analytical Biochemistry*, vol. 74, no. 1, pp. 214–226, 1976.

[25] C. A. Reilly and S. D. Aust, "Measurement of lipid peroxidation," *Current Protocols in Toxicology*, vol. 2, pp. 2–4, 2001.

[26] R. L Levine, D. Garland, C. N. Oliver, A. Amici, I. Climent, A. G. Lenz et al., *Oxygen Radicals in Biological Systems Part B: Oxygen Radicals and Antioxidants*, Methods in Enzymology, Elsevier, Amsterdam, Netherlands, 1990.

[27] V. Witko-Sarsat, M. Friedlander, C. Capeillère-Blandin et al., "Advanced oxidation protein products as a novel marker of oxidative stress in uremia," *Kidney International*, vol. 49, no. 5, pp. 1304–1313, 1996.

[28] K. Burton, "A study of the conditions and mechanism of the diphenylamine reaction for the colorimetric estimation of deoxyribonucleic acid," *The Biochemical journal*, vol. 62, no. 2, pp. 315–323, 1956.

[29] H. P. Misra and I. Fridovich, "The role of superoxide anion in the autoxidation of epinephrine and a simple assay for superoxide dismutase," *The Journal of Biological Chemistry*, vol. 247, no. 10, pp. 3170–3175, 1972.

[30] H. Aebi, "Catalase *in vitro*," *Methods in Enzymology*, vol. 105, pp. 121–126, 1984.

[31] R. A. B. Drury and E. A. Wallington, *Carleton's Histological Techniques*, Oxford University Press, New York, NY, USA, 5th edition, 1980.

[32] O. O. Oyedapo, B. A. Akinpelu, K. F. Akinwunmi, M. O. Adeyinka, and F. O. Sipeolu, "Red blood cell membrane stabilizing potentials of extracts of *Lantana camara* and its fractions," *International Journal of Plant Physiology and Biochemistry*, vol. 2, no. 4, pp. 46–51, 2010.

[33] M. Hossain, S. Ahamed, S. M. Dewan et al., "*In vivo* antipyretic, antiemetic, *in vitro* membrane stabilization, antimicrobial, and cytotoxic activities of different extracts from *Spilanthes paniculata* leaves," *Biological Research*, vol. 47, article 45, 2014.

[34] M. Cekmen, Y. O. Ilbey, E. Ozbek, A. Simsek, A. Somay, and C. Ersoz, "Curcumin prevents oxidative renal damage induced by acetaminophen in rats," *Food and Chemical Toxicology*, vol. 47, no. 7, pp. 1480–1484, 2009.

[35] S. Palani, S. Raja, R. P. Kumar, P. Parameswaran, and B. S. Kumar, "Therapeutic efficacy of *Acorus calamus* on acetaminophen induced nephrotoxicity and oxidative stress in male albino rats," *Acta Pharmaceutica Sciencia*, vol. 52, no. 1, pp. 89–100, 2010.

[36] A. L. Jones and L. F. Prescott, "Unusual complications of paracetamol poisoning," *Quarterly Journal of Medicine*, vol. 90, no. 3, pp. 161–168, 1997.

[37] C. Lorz, P. Justo, A. Sanz, D. Subirá, J. Egido, and A. Ortiz, "Paracetamol-induced renal tubular injury: a role for ER stress," *Journal of the American Society of Nephrology*, vol. 15, no. 2, pp. 380–389, 2004.

[38] A. A. Adeneye and A. S. Benebo, "Protective effect of the aqueous leaf and seed extract of *Phyllanthus amarus* on gentamicin and acetaminophen-induced nephrotoxic rats," *Journal of Ethnopharmacology*, vol. 118, no. 2, pp. 318–323, 2008.

[39] M. T. Yakubu, L. S. Bilbis, M. Lawal, and M. A. Akanji, "Evaluation of selected parameters of rat liver and kidney function following repeated administration of yohimbine," *Biochemistry*, vol. 15, pp. 50–56, 2003.

[40] O. B. Oloyede and T. O. Sunmonu, "Potassium bromate content of selected bread samples in Ilorin, Central Nigeria and its effect on some enzymes of rat liver and kidney," *Food and Chemical Toxicology*, vol. 47, no. 8, pp. 2067–2070, 2009.

[41] D. G. Shirley and R. J. Unwin, "The structure and function of tubules," in *The Oxford Textbook of Clinical Nephrology*, A. M. Davison, S. J. Cameron, J. P. Grunfeld et al., Eds., Oxford University Press, Oxford, UK, 3rd edition, 2005.

[42] A. Devine, R. A. Criddle, I. M. Dick, D. A. Kerr, and R. L. Prince, "A longitudinal study of the effect of potassium, sodium and calcium intake on regional bone density in post-menopausal women," *American Journal of Clinical Nutrition*, vol. 18, pp. 3735–3785, 1999.

[43] S. I. Alqasoumi, "Evaluation of the hepatroprotective and nephroprotective activities of *Scrophularia hypericifolia* growing in Saudi Arabia," *Saudi Pharmaceutical Journal*, vol. 22, no. 3, pp. 258–263, 2014.

[44] S. Sireeratawong, N. Lertprasertsuke, U. Srisawat et al., "Acute and subchronic toxicity study of the water extract from *Tiliacora triandra* (Colebr.) Diels in rats," *Songklanakarin Journal of Science and Technology*, vol. 30, no. 5, pp. 611–619, 2008.

[45] S. Saheed, A. E. Oladipipo, A. A. Abdulazeez et al., "Toxicological evaluations of *Stigma maydis* (corn silk) aqueous extract on hematological and lipid parameters in Wistar rats," *Toxicology Reports*, vol. 2, pp. 638–644, 2015.

[46] Z. Abdul Hamid, B. B. Siti, N. W. Jie, H. Asmah, H. Khairana, and M. Jamaludin, "Nephroprotective effects of *Zingiber zerumbet* Smith ethyl acetate extract against paracetamol-induced nephrotoxicity and oxidative stress in rats," *Journal of Zhejiang University of Science (Biotechnology and Biomedicine)*, vol. 13, no. 3, pp. 176–185, 2012.

[47] A. Wooley, *A Guide to Practical Toxicology Evaluation, Prediction and Risk Determination in General and Reproductive Toxicology*, Taylor & Francis, New York, NY, USA, 2003.

[48] G. R. Amresh, P. N. Singh, and C. V. Rao, "Toxicological screening of traditional medicine Laghupatha (*Cissampelos pareira*) in experimental animals," *Journal of Ethnopharmacology*, vol. 116, no. 3, pp. 454–460, 2008.

[49] J. Das, J. Ghosh, P. Manna, and P. C. Sil, "Taurine protects acetaminophen-induced oxidative damage in mice kidney through APAP urinary excretion and CYP2E1 inactivation," *Toxicology*, vol. 269, no. 1, pp. 24–34, 2010.

[50] M. I. Yousef, S. A. M. Omar, M. I. El-Guendi, and L. A. Abdelmegid, "Potential protective effects of quercetin and curcumin on paracetamol-induced histological changes, oxidative stress, impaired liver and kidney functions and haematotoxicity in rat," *Food and Chemical Toxicology*, vol. 48, no. 11, pp. 3246–3261, 2010.

[51] K. R. Basma and F. S. Mona, "The renoprotective effect of honey on paracetamol-induced nephrotoxicity in adult male albino rats," *Life Science Journal*, vol. 8, no. 3, pp. 8–12, 2011.

[52] S. Palani, S. Raja, K. R. Praveen, J. Soumya, and K. B. Senthil, "Therapeutic efficacy of *Pimpinella tirupatiensis* (Apiaceae) on acetaminophen induced nephrotoxicity and oxidative stress in male albino rats," *International Journal of Pharmacy and Technology Research*, vol. 1, no. 3, pp. 925–934, 2009.

[53] N. Kaplowitz, "Mechanisms of liver cell injury," *Journal of Hepatology*, vol. 32, supplement 1, pp. 39–47, 2000.

[54] P. I. Margetis, M. H. Antonelou, I. K. Petropoulos, L. H. Margaritis, and I. S. Papassideri, "Increased protein carbonylation of red blood cell membrane in diabetic retinopathy," *Experimental and Molecular Pathology*, vol. 87, no. 1, pp. 76–82, 2009.

[55] C. J. J. Alderman, S. Shah, J. C. Foreman, B. M. Chain, and D. R. Katz, "The role of advanced oxidation protein products in regulation of dendritic cell function," *Free Radical Biology and Medicine*, vol. 32, no. 5, pp. 377–385, 2002.

[56] M. S. Cooke, M. D. Evans, M. Dizdaroglu, and J. Lunec, "Oxidative DNA damage: mechanisms, mutation, and disease," *The FASEB Journal*, vol. 17, no. 10, pp. 1195–1214, 2003.

[57] H. Jaeschke and M. L. Bajt, "Intracellular signaling mechanisms of acetaminophen-induced liver cell death," *Toxicological Sciences*, vol. 89, no. 1, pp. 31–41, 2006.

[58] D. Brahmi, C. Bouaziz, Y. Ayed, H. Ben-Mansour, L. Zourgui, and H. Bacha, "Chemopreventive effect of cactus *Opuntia ficus*

indica on oxidative stress and genotoxicity of aflatoxin B1," *Nutrition & Metabolism*, vol. 8, article 73, 2011.

[59] H. Parlakpinar, S. Tasdemir, A. Polat et al., "Protective role of caffeic acid phenethyl ester (cape) on gentamicin-induced acute renal toxicity in rats," *Toxicology*, vol. 207, no. 2, pp. 169–177, 2005.

[60] M. Aslam, S. T. Ahmad, R. Dayal et al., "Nephroprotective action of *Peucedanum grande* against cadmium chloride induced renal toxicity in Wistar rats," *EXCLI Journal*, vol. 11, pp. 444–452, 2012.

[61] F. A. Kadir, N. M. Kassim, M. A. Abdulla, and W. A. Yehye, "Effect of oral administration of ethanolic extract of *Vitex negundo* on thioacetamide-induced nephrotoxicity in rats," *BMC Complementary and Alternative Medicine*, vol. 13, article 294, 2013.

[62] E. Marieb, "Urinary system," in *Essentials of Human Anatomy and Physiology*, pp. 501–526, Pearson Benjamin Cummings, San Fransisco, Calif, USA, 8th edition, 2006.

[63] M. Naggayi, N. Mukiibi, and E. Iliya, "The protective effects of aqueous extract of *Carica papaya* seeds in paracetamol induced nephrotoxicity in male wistar rats," *African Health Sciences*, vol. 15, no. 2, pp. 598–605, 2015.

[64] S. Umukoro and R. B. Ashorobi, "Evaluation of anti-inflammatory and membrane stabilizing property of aqueous leaf extract of *Momordica charantia* in rats," *African Journal of Biomedical Research*, vol. 9, no. 2, pp. 119–124, 2009.

[65] O. O. Amujoyegbe, J. M. Agbedahunsi, B. A. Akinpelu, and O. O. Oyedapo, "*In vitro* evaluation of membrane stabilizing activities of leaf and root extracts of *Calliandra portoricensis* (JACQ) benth on sickle and normal human erythrocytes," *International Research Journal of Pharmacy and Pharmacology*, vol. 2, no. 8, pp. 198–203, 2012.

[66] I. Khan, M. Nisar, F. Ebad et al., "Anti-inflammatory activities of Sieboldogenin from *Smilax china* Linn.: experimental and computational studies," *Journal of Ethnopharmacology*, vol. 121, no. 1, pp. 175–177, 2009.

[67] S. Sabiu, F. H. O'Neill, and A. O. T. Ashafa, "Kinetics of α-amylase and α-glucosidase inhibitory potential of *Zea mays* Linnaeus (Poaceae), *Stigma maydis* aqueous extract: an in vitro assessment," *Journal of Ethnopharmacology*, vol. 183, pp. 1–8, 2016.

Hindawi Publishing Corporation
Evidence-Based Complementary and Alternative Medicine
Volume 2016, Article ID 7387286, 11 pages
http://dx.doi.org/10.1155/2016/7387286

Research Article

Unsweetened Natural Cocoa Powder Has the Potential to Attenuate High Dose Artemether-Lumefantrine-Induced Hepatotoxicity in Non-Malarious Guinea Pigs

Isaac Julius Asiedu-Gyekye,[1] Kennedy Kwami Edem Kukuia,[1] Abdulai Mahmood Seidu,[2] Charles Antwi-Boasiako,[3] Benoit Banga N'guessan,[1] Samuel Frimpong-Manso,[4] Samuel Adjei,[5] Jonathan Zobi,[1] Abraham Terkpertey Tettey,[1] and Alexander Kwadwo Nyarko[1]

[1] *Department of Pharmacology and Toxicology, University of Ghana School of Pharmacy, College of Health Sciences, Legon, Ghana*
[2] *Department of Chemical Pathology, School of Biomedical and Allied Health Sciences, College of Health Sciences, Korle-Bu, Ghana*
[3] *Department of Physiology, School of Biomedical and Allied Health Sciences, College of Health Sciences, Korle-Bu, Ghana*
[4] *Department of Pharmaceutical Chemistry, University of Ghana School of Pharmacy, College of Health Sciences, Legon, Ghana*
[5] *Department of Animal Experimentation, Noguchi Memorial Institute for Medical Research, College of Health Sciences, Accra, Ghana*

Correspondence should be addressed to Isaac Julius Asiedu-Gyekye; ijasiedu-gyekye@ug.edu.gh

Received 29 March 2016; Revised 30 May 2016; Accepted 8 June 2016

Academic Editor: Mohamed M. Abdel-Daim

Objective. This study investigated the elemental composition of unsweetened natural cocoa powder (UNCP), its effect on nitric oxide, and its hepatoprotective potential during simultaneous administration with high-dose artemether/lumefantrine (A/L). *Method*. Macro- and microelements in UNCP were analyzed with EDXRF spectroscopy. Thirty (30) male guinea-pigs were then divided into five groups. For groups 3 (low-dose), 4 (medium-dose), and 5 (high-dose), the animals received oral UNCP prophylactically for 14 days. Group 1 received distilled water (14 days) and group 2 A/L for the last 3 days (days 12 to 14). After euthanisation, biochemical and histopathological examinations were carried out in all groups. *Results*. Phytochemical analysis of UNCP showed the presence of saponins, flavonoids, tannins, and cardiac glycosides. Thirty-eight (38) macro- and microelements were found. UNCP produced significant decreases in ALT, ALP, GGT, and AST levels. A significant increase in total protein levels was observed during A/L+UNCP administration in comparison to 75 mg/kg A/L group. Histopathological examinations buttressed the protective effects of cocoa administration. UNCP administration increased nitric oxide levels 149.71% ($P < 0.05$) compared to controls. *Conclusion*. UNCP increases nitric oxide levels and has hepatoprotective potential during A/L administration. A high level of copper was observed which may be detrimental during high daily consumptions of UNCP.

1. Introduction

Malaria is an infection transmitted by the female anopheles mosquito. It is a major public health issue in the tropics and one of the world's leading infectious killer diseases. The high death rate resulting from malaria cannot be overemphasised especially in some parts of Africa. In Ghana 3.5 million people contract malaria every year [1, 2]. Resistance is a major setback in the management of malaria and has therefore necessitated countries to review and implement new antimalarial drug policies to ensure effective case management to reduce both morbidity and mortality [3]. Due to increased therapeutic efficacy, decreased cytotoxicity, and delay or prevention of the development of drug resistance, combination drug regimens is recommended over monotherapy [4]. Artemisinin-based combination therapy

(ACT) has been recommended for use by the WHO [5, 6]. Artemether/lumefantrine (A/L) is one of the combination therapies currently used.

Artemisinin derivatives have impressive parasiticidal properties *in vivo* and *in vitro* but currently there have been issues of treatment failures, resistance, and increasing cases of hepatotoxic effects [7–9]. Some countries have considered increasing the dose of the A/L in treatment in order to arrest the issue of resistance [10] but increase in dose implies that there will be increased side effects, adverse reactions, and hepatotoxic effects [9]. In fact, there are concerns about frequent usage of A/L on some organ systems [9]. Considering the fact that so far A/L is one of the most effective combination therapies, the issue of drug-induced hepatotoxicity needs to be addressed. Another effect of A/L is its effect on nitric oxide levels, where it has been found to reduce nitric oxide levels. However, other studies show that A-L increase nitric oxide levels as a compensatory mechanism in cases of reduced nitric oxide levels [9].

Unsweetened natural Cocoa powder (UNCP) is used as a beverage and nutraceutical amongst Ghanaians. The antioxidant properties of cocoa powder have been well studied [11–13] and even found to be unchanged after various manufacturing processes [14]. It contains antioxidant polyphenols called flavonols reported to have hepatoprotective [15, 16] and antimalarial effects [17, 18]. The chemical composition of cocoa has been well investigated using various methods. UNCP contains about 1.9% theobromine and 0.21% caffeine [19–21]. Polyphenols in various compounds have also been proven in several studies to exert hepatoprotective activity [22–25]. For example, polyphenol-rich fractions prepared from walnut kernel pellicles have been assessed for its hepatoprotective effect in mice [23]. Studies conducted on cocoa powder has shown its quantitative components such as 14 N-phenylpropenoyl-L-amino acids, N-[4′-hydroxy-(E)-cinnamoyl]-L-tryptophan, and N-[4′-hydroxy-3′-methoxy-(E)-cinnamoyl]-L-tyrosine [26]. Other studies have also proven the roles of polyphenols such as cynarin, isochlorogenic acid, chlorogenic acid, luteolin-7-glucoside, and two organic acids, caffeic and quinic, from Cynara scolymus in the hepatoprotective activity [27]. Besides, cocoa or flavonols increase nitric oxide levels which have also been found to have hepatoprotective effects in acute liver injury by virtue of their antioxidant properties [18, 28, 29]. Further, the tannin, glycoside, flavonoid, and saponins have also been implicated in their hepatoprotective effect in several studies. The total flavonoid content of UNCP has also been determined [30–34]. This is a strong background to investigate the beneficial effect UNCP might have in ameliorating the hepatotoxic effect of this important drug A/L.

It is important in spite of all these component-based effects of UNCP to note that both micro- and macroelements present in UNCP are also capable of interfering with the availability of secondary metabolites in UNCP which may easily modulate their pharmacological effects [35]. The presence of toxic heavy metals in medicinal plants can on the other hand pose a threat to the health of consumers [35, 36]. Though UNCP contains some elemental particles, correlation between the pharmacological activity of UNCP and these macro- and microelements has not been established. It has been established, for example, that zinc has beneficial hepatoprotective action [37, 38]. Simultaneous ingestion of UNCP and A/L is a common practice amongst Ghanaians suffering from uncomplicated malaria undergoing treatment with A/L. It is important to establish the beneficial effect and visible adverse effect of the simultaneous consumption of UNCP and A/L which is a way of life for Ghanaians especially with the affordable price of UNCP and highly subsidised A/L.

This study seeks to determine the elemental composition of UNCP and its effect on nitric oxide levels and to assess its hepatoprotective potential against A/L-induced liver toxicity during their simultaneous ingestion in male guinea pigs.

2. Materials and Methods

2.1. Energy Dispersive X-Ray (EDXRF) Measurements. Sample of UNCP (Batch number BT620IT; FDA/DK06-070) was acquired from a supermarket. The sample was sieved using sieve of 180 microns and three samples prepared and sieved with a mesh size (aperture) of 180 μm into fine powder. This was kept in dry well-labelled containers. Before pelletation, the sample was kept in an oven at 60°C overnight. Triplicate weighed samples, 4000 mg/sample, were added separately to 900 mg Fluxana H Elektronik BM-0002-1 (Licowax C micropowder PM-Hoechstwax) as binder (due to their morphology and the loose nature); the mixture was homogenized using the RETSCH Mixer Mill (MM301) for 3 min and pressed manually with SPECAC hydraulic press for 2 min with a maximum pressure limit of 15 tons (15000 kg) into pellets of 32 mm in diameter and 3 mm thickness for subsequent XRF measurements. Time between pelletation and measurement was kept short to avoid deformation of the flat surfaces of the pellets [39]. A factory calibrated Spectro X-Lab 2000 spectrometer (from the Geological Survey Department, Accra, Ghana) enhanced with three-axial geometry was used for the simultaneous analysis and measurement of the elemental content of the samples.

2.2. Preparation of UNCP Solution. Calculated amount (9.6 g) of UNCP was dissolved in warm distilled water (40 mL) with stirring (till everything went into solution) making a concentration of 240 mg/mL (of the UNCP). This was administered to the guinea pigs in groups 3, 4, and 5 at their respective doses via oral gavage.

2.3. Preparation of A/L Solution. A concentration of 20 mg/mL of dispersible A/L (with reference to artemether) was prepared and administered to the guinea pigs in the UNCP treated groups at a dose of 75 mg/kg body weight daily for 3 days via oral gavage. Dosage was calculated with reference to the dose of artemether in the drug combination. To achieve this, seventy (70) tablets of Novartis Coartem® dispersible tablets (20/120 mg), which are equivalent to 1400 mg of artemether, were dissolved in 70 mL of distilled water and stirred until completely homogenous.

In all cases, fresh solutions of UNCP and A/L were prepared before each dosing.

2.4. Phytochemical Analysis. Phytochemical analysis was conducted to determine the various constituents in the unsweetened natural cocoa [40].

2.4.1. Saponin Test. About 0.5 g of UNCP was added to water in a test tube. The test tube was shaken to observe foam formation.

2.4.2. Tannins Test. About 0.5 g of UNCP was dissolved in 80% of aqueous methanol (10 cm^3). Freshly prepared iron (III) chloride solution was added and observations were made on colour changes.

2.4.3. Flavonoids Test. About 0.1 g of UNCP was added to 80% ethanol (15 cm^3). Magnesium turnings were added to the filtrate followed by concentrated HCl (0.5 cm^3) and observed for colour changes within 10 minutes.

2.4.4. Cardiac Glycoside Test. About 0.5 g of UNCP was dissolved in chloroform (2 cm^3) in a test tube after which concentrated sulphuric acid was carefully added down the side of the test tube to form a lower layer.

2.5. Animal Husbandry. Thirty (30) male guinea pigs (450 g and 600 g) were purchased from the Noguchi Memorial Institute for Medical Research, University of Ghana, for this experiment. The animals were acclimatized to the laboratory environment for one week before being used in the study and were provided with Sankofa pellet feeds and tap water *ad libitum*. The room temperature was maintained at 20–23°C with 12 : 12 hour light/dark cycle. Spontaneous behaviours of all guinea pigs were observed in cages before experimental procedures were carried out. No animals showed signs of illness before the experimental phase. The study protocol was approved by the departmental ethical and protocol review committee and the Noguchi Memorial Institute for Medical Research Institutional Animal Care and Use Committee with protocol approval number 2013-01-3E.

2.6. Drug Administration. The guinea pigs were grouped into five, with groups 3 to 5 receiving the UNCP at 300, 900, and 1500 mg/kg, respectively, for 14 days. Doses of A/L were administered for the last 3 days of cocoa administration. Group 2 animals were given only A/L for the last 3 days whereas group 1 received vehicle (water) only. The weights of the animals were taken weekly and the doses administered adjusted accordingly. All experiments carried out on animals conformed to the guidelines on ethical standards for inducing toxicity in animals (NLC, 1996).

Group 1. Control (distilled water only)

Group 2. 75 mg/kg A/L (last 3 days)

Group 3. Cocoa 300 mg/kg (14 days) + 75 mg/kg A/L (last 3 days)

Group 4. Cocoa 900 mg/kg (14 days) + 75 mg/kg A/L (last 3 days)

Group 5. Cocoa 1500 mg/kg (14 days) + 75 mg/kg A/L (last 3 days).

2.7. Biochemical Assays. Blood samples were collected from the descending aorta and aliquoted into EDTA-2K tubes and plain tubes, respectively, at the end of the dosing period. This was done after euthanisation of the animals under ether anaesthesia. The EDTA blood was immediately analyzed for haematological parameters using the SYSMEX Haematology Autoanalyser (Kobe, Japan) while sera prepared from blood in plain tubes were used for biochemical examinations including clinical chemistry measurements such as alanine aminotransferase (ALT) or glutamic pyruvic transaminase (SGPT) levels, alkaline phosphatase (ALP), Serum Glutamic Oxaloacetic Transaminase (SGOT) or aspartate transaminase, and Gamma Glutamyl Transpeptidase (GGT). These were measured as liver function tests (LFT) to give an indication of the state of the liver.

Nitric oxide levels were also measured using the Griess Reagent System. The total nitric oxide kit by R&D Systems was used in this study. In this system, nitrate is converted to nitrite using nitrate reductase after which the total nitrite is measured.

The principle of this assay determines nitric oxide concentration based on the enzymatic conversion of nitrate to nitrite by nitrate reductase. The reaction is followed by colorimetric detection of nitrite as an azo dye product of the Griess Reaction. The Griess Reaction is then based on the two-step diazotization reaction in which acidified NO_2^- produces a nitrosating agent, which reacts with sulfanilic acid to produce the diazonium ion. This ion is then coupled to *N*-(1-naphthyl) ethylenediamine to form the chromophoric azo-derivative which absorbs light at 540–570 nm.

2.8. Histopathological Studies. Guinea pigs were euthanized and their livers were swiftly excised and washed with 0.9% saline. The livers were stored in 10% neutral buffered formaldehyde. The liver tissues were then cut and sectioned. A microtone was used to cut 2 μm thick liver slices and stained with haematoxylin-eosin for examination. The stained tissues were observed with an Olympus microscope (BX-51) and photographed by INFINITY 4 USB Scientific Camera (Lumenera Corporation, Otawa, Canada).

The study protocol was approved by the departmental ethical and protocol review committee and the Noguchi Memorial Institute for Medical Research Institutional Animal Care and Use Committee with protocol approval number 2013-01-3E.

2.9. Statistics. The results are reported as mean ± SEM. Statistical analysis was performed using one-way analysis of variance (ANOVA) followed by student *Newman-Keuls post hoc* test. Statistical significance was set at $P < 0.05$; Dunnet Multiple Comparison Test was used in the analysis of the nitric oxide levels. All statistical analyses were performed using Graph Pad prism 5 software.

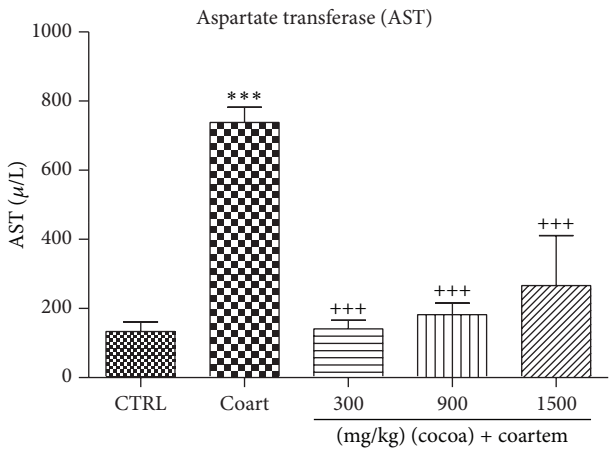

Figure 1: Changes in AST levels during a 14-day administration of UNCP in male guinea pigs followed by a 3-day A/L administration. Values are expressed as mean ± SEM, $n = 6$. The differences among the mean were analyzed using one-way ANOVA followed by *Newman-Keuls post hoc* analysis. *** means $P < 0.0001$ when compared to the control (distilled water) and $^{+++}$ means $P < 0.0001$ when compared to the A/L group.

3. Results

3.1. Energy Dispersive X-Ray (EDXRF) Measurements. A total of thirty-eight (38) elements comprising 12 macroelements, (sodium (Na), magnesium (Mg), aluminium (Al), silicon (Si), phosphorus (P), sulphur (S), chlorine (Cl), potassium (K), calcium (Ca), titanium (Ti), manganese (Mn), and iron (Fe), and 26 microelements, vanadium (V), chromium (Cr), cobalt (Co), nickel (Ni), copper (Cu), zinc (Zn), gallium (Ga), arsenic (As), rubidium (Rb), strontium (Sr), yttrium (Y), zirconium (Zr), niobium (Nb), molybdenum (Mo), antimony (Sb), iodine (I), cesium (Cs), barium (Ba), lanthanum (La), cerium (Ce), hafnium (Hf), tantalum (Ta), lead (Pb), bismuth (Bi), thorium (Th), and uranium (U)) (Table 1), were identified and evaluated.

3.2. Phytochemical Analysis. Phytochemical analysis of unsweetened natural cocoa powder showed the presence of saponins, flavonoids, tannins, and cardiac glycosides.

3.3. Biochemical Assays

3.3.1. Liver Function Tests. AST levels increased in animals that received A/L 75 mg/kg by 81.97% when compared to the group that received distilled water (control group) while those in the UNCP administered group decreased with percentage change of 80.91%, 75.33%, and 63.86%, respectively, when compared with the A/L administered group ($P < 0.05$) (Figure 1).

ALP levels decreased in group 2 by 10.82% when compared to group 1. ALP levels in groups 3, 4, and 5 increased with percentage change of 14.95%, 9.13%, and 36.94%, respectively, when compared with group 2 ($P < 0.05$) (Figure 2).

Table 1: Mean and standard deviation (SD) of measured elements (mg/4000 mg).

Element	Mean/SD mg/4000 mg
Macroelements	
Na	2.4666 ± 0.00
Mg	33.0133 ± 0.02
Al	14.0093 ± 0.01
Si	15.3880 ± 0.02
P	64.3866 ± 0.00
S	30.9120 ± 0.00
Cl	2.3616 ± 0.00
K	149.0667 ± 0.03
Ca	11.0146 ± 0.00
Ti	0.0232 ± 0.00
Mn	0.4093 ± 0.00
Fe	1.0309 ± 0.00
Microelements	
V	0.2320 ± 1.73
Cr	0.4200 ± 17.44
Co	0.0108 ± 0.10
Ni	0.0638 ± 1.16
Cu	0.2984 ± 1.71
Zn	0.4086 ± 0.74
Ga	0.0024 ± 0.00
As	0.0020 ± 0.00
Rb	0.1698 ± 0.49
Sr	0.1064 ± 0.20
Y	0.0016 ± 0.00
Zr	0.0125 ± 0.42
Nb	0.0070 ± 0.29
Mo	0.0044 ± 0.00
Sb	0.0043 ± 0.06
I	0.0133 ± 0.15
Cs	0.0232 ± 0.10
Ba	0.0620 ± 5.81
La	0.0480 ± 0.00
Ce	0.0849 ± 4.97
Hf	0.0148 ± 0.17
Ta	0.0213 ± 0.06
Pb	0.0036 ± 0.00
Bi	0.0024 ± 0.00
Th	0.0020 ± 0.00
U	0.0112 ± 0.10

Levels of GGT increased in animals that received 75 mg/kg A/L by 37.61% and a decrease by 39.5% in the cocoa treated group when compared to the control group ($P > 0.05$) (Figure 3).

ALT levels increased in the group dosed at 75 mg/kg A/L by 35.76% when compared to the control group. ALT

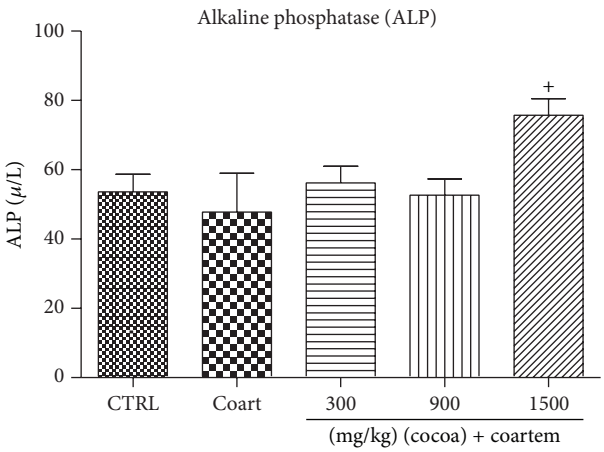

Figure 2: Changes in ALP levels during a 14-day administration of UNCP in male guinea pigs followed by a 3-day A/L administration. Values are expressed as mean ± SEM, $n = 6$. The differences among the mean were analyzed using one-way ANOVA followed by *Newman-Keuls post hoc* analysis. $^{+}$ means $P < 0.05$ when compared with A/L group.

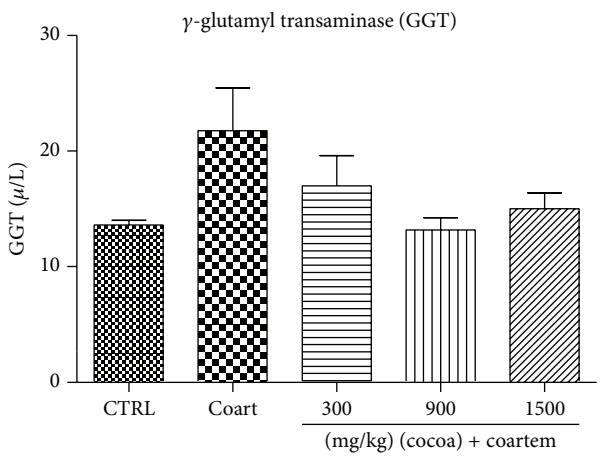

Figure 3: Changes in GGT levels during a 14-day administration of UNCP in male guinea pigs followed by a 3-day A/L administration. Values are expressed as mean ± SEM, $n = 6$. The differences among the mean were analyzed using one-way ANOVA followed by *Newman-Keuls post hoc* analysis.

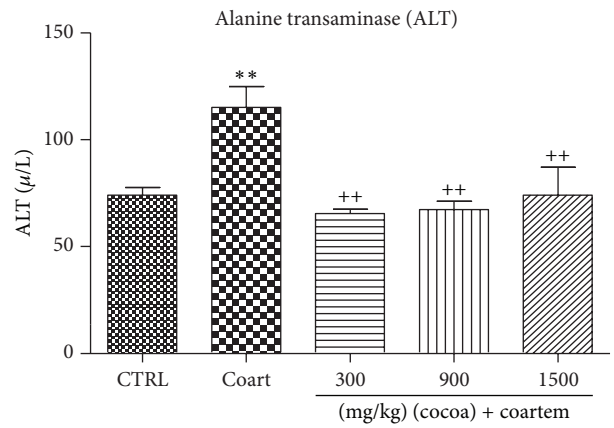

Figure 4: Changes in ALT levels during a 14-day administration of UNCP in male guinea pigs followed by a 3-day A/L administration. Values are expressed as mean ± SEM, $n = 6$. The differences among the mean were analyzed using one-way ANOVA followed by *Newman-Keuls post hoc* analysis. ** means $P < 0.001$ when compared to the control (distilled water) and $^{++}$ means $P < 0.001$ when compared to the A/L group.

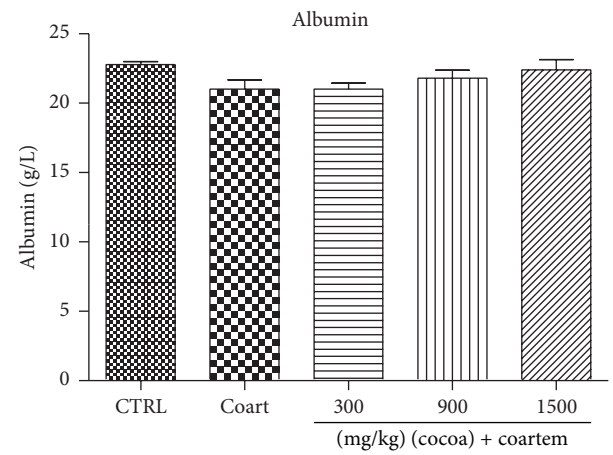

Figure 5: Changes in ALP levels during a 14-day administration of UNCP in male guinea pigs followed by a 3-day A/L administration. Values are expressed as mean ± SEM, $n = 6$. The differences among the mean were analyzed using one-way ANOVA followed by *Newman-Keuls post hoc* analysis.

levels at doses of 300 mg/kg, 900 mg/kg, and 1500 mg/kg decreased with percentage change of 43.05%, 41.49%, and 35.76%, respectively, when compared to the A/L administered group ($P < 0.05$) (Figure 4).

Serum albumin levels reduced slightly in the A/L administered group while the levels slightly increased in the animals treated with UNCP compared to the controls ($P > 0.05$). Total protein levels decreased in the A/L group by 7.89% (Figure 5) while bilirubin levels increased by 80.4% when compared to the control groups (Figure 7). In the UNCP administered group, total protein levels increased up to 12.77% in the 1500 mg/kg group while the bilirubin levels reduced up to 39.35% in the 900 mg/kg group, ($P > 0.05$) (Figure 6).

3.3.2. Nitric Oxide Levels. Group 3 produced the greatest increase (147.33 ± 117.78, $P < 0.05$, i.e., 149.71%) in nitric oxide followed by group 4 (79.21 ± 36.24, $P < 0.05$, i.e., 34.25%) and then group 5 (61.88 ± 3.83, $P < 0.05$, i.e., 4.88%) when compared to group 1 (Figure 9). At a dosage of 900 mg/kg (cocoa only), considered to be the optimal in most studies, there was just a slight increase in nitric oxide (36.92 ± 3.65, $P = 00.0024$).

3.3.3. Histopathological Analysis. The histological examination of liver samples was based on changes associated with exposure of liver tissues to toxins. This is mainly inflammatory associated changes ranging from acute to chronic changes such as dilation of central and microcirculatory

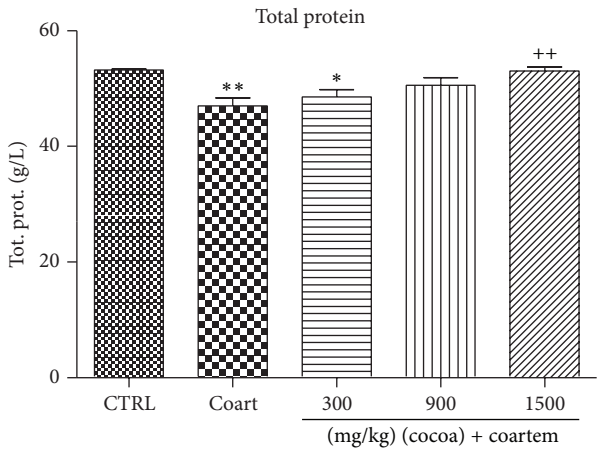

Figure 6: Changes in total protein levels during a 14-day administration of UNCP in male guinea pigs followed by a 3-day A/L administration. Values are expressed as mean ± SEM, $n = 6$. The differences among the mean were analyzed using one-way ANOVA followed by *Newman-Keuls post hoc* analysis. * means $P < 0.05$, ** means $P < 0.001$ when compared with control (distilled water), and $^{++}$ means $P < 0.001$ when compared with the A/L group.

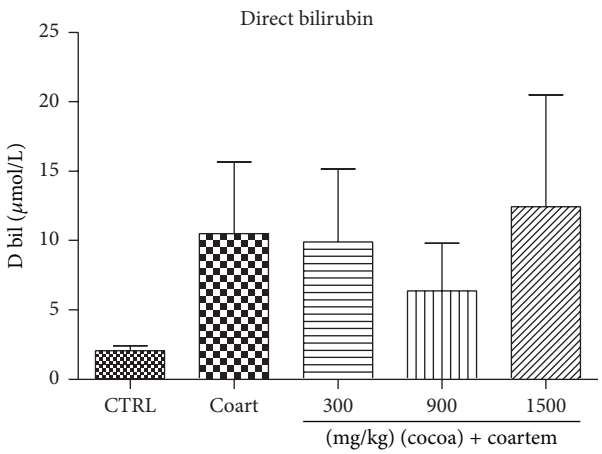

Figure 7: Changes in direct bilirubin levels during a 14-day administration of UNCP in male guinea pigs followed by a 3-day A/L administration. Values are expressed as mean ± SEM, $n = 6$. The differences among the mean were analyzed using one-way ANOVA followed by *Newman-Keuls post hoc* analysis.

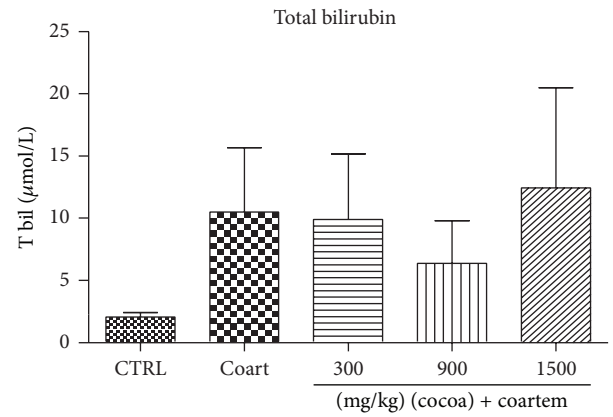

Figure 8: Changes in total bilirubin levels during a 14-day administration of UNCP in male guinea pigs followed by a 3-day A/L administration. Values are expressed as mean ± SEM, $n = 6$. The differences among the mean were analyzed using one-way ANOVA followed by *Newman-Keuls post hoc* analysis.

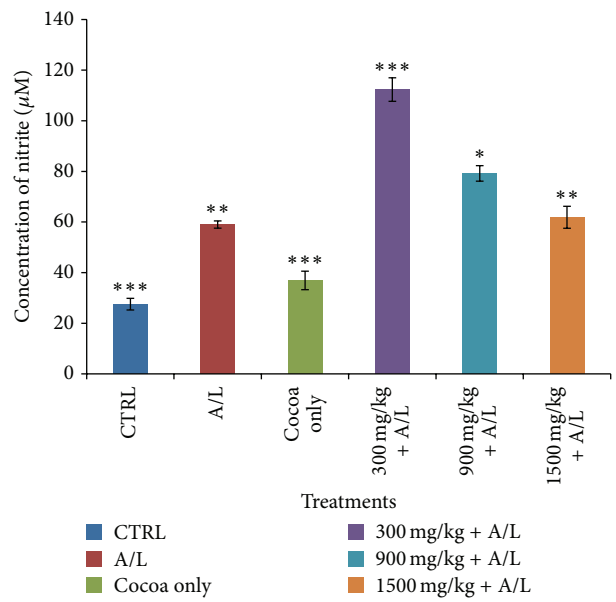

Figure 9: Effect of UNCP (LD = 300, MD = 900, and HD = 1500 mg/kg) on nitrite concentrations in plasma of guinea pigs during A/L administration. Values are mean ± SD ($n = 5$) and $^{*}P < 0.05$, $^{**}P < 0.01$, and $^{***}P < 0.001$ compare to the control (one-way ANOVA followed by a *Dunnett's* multiple comparison test). The low dose UNCP (300 mg/kg) + A/L produced the greatest increase (147.33 ± 117.78, $P < 0.05$, i.e., 149.71%) in nitric oxide followed by medium dose UNCP + A/L (79.21 ± 36.24, $P < 0.05$, i.e., 34.25%) and then high dose UNCP + A/L (61.88 ± 3.83, $P < 0.05$, i.e., 4.88%) when compared to the A/L only group.

vessels, congestion of the central vein, leucocyte infiltration, and disturbances in the liver parenchyma (necrosis). Sections of liver from guinea pigs that received only a 3-day HD A/L administration (75 mg/kg) revealed disturbed liver parenchyma (necrotised liver cells) with highly congested and dilated central vein as well as lymphocyte infiltration (Figure 10(a)). This finding is indicative of a severe liver damage (LDS of 4-5) [41].

In contrast, examination of liver sections from 14-day unsweetened natural cocoa administration (300, 900, and 1500 mg/kg) followed by a 3-day A/L administration (75 mg/kg) showed undisturbed liver parenchyma, uncongested but dilated central vein, and slightly dilated sinusoids (Figures 10(c), 10(d), and 10(e)). This is indicative of a mild change (LDS of 1-2) with a high degree of reversibility. Liver sections from the control group that received only distilled water showed undisturbed liver parenchyma with uncongested central veins (Figure 10(b)).

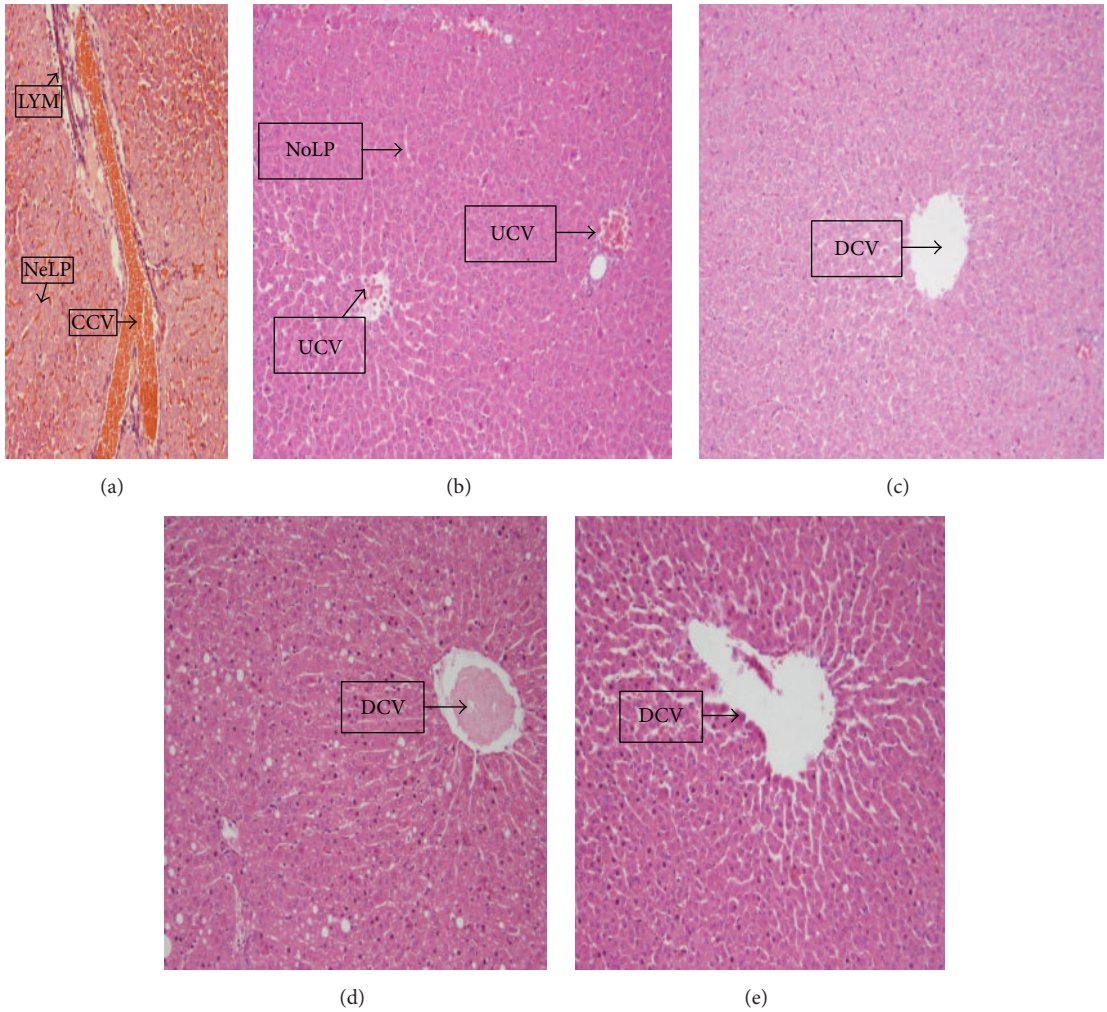

Figure 10: A representation of sections of liver from guinea pigs that received (a) only a 3-day HD A/L administration (75 mg/kg/bwt) showing disturbed (necrotic) liver parenchyma (NeLP), a highly congested and dilated central vein (CCV), and lymphocytic infiltration (LYM). (b) Distilled water (control) showing undisturbed liver parenchyma (NoLP) with uncongested central veins (UCV). Note the regularity of liver cell plates, microcirculatory zones, and sinusoids. (c) A 14-day UNCP administration (300 mg/kg/bwt) followed by a 3-day A/L administration (75 mg/kg/bwt) showing undisturbed liver parenchyma with an uncongested but dilated central vein (DCV). (d) A 14-day UNCP administration (900 mg/kg/bwt) followed by a 3-day A/L administration (75 mg/kg/bwt) showing undisturbed liver parenchyma with an uncongested but dilated central vein (DCV). (e) A 14-day UNCP administration (1500 mg/kg/bwt) followed by a 3-day A/L administration (75 mg/kg/bwt) showing undisturbed liver parenchyma with an uncongested but dilated central vein (DCV) (H & E stain ×40).

4. Discussion

The above study has shown that UNCP contains 38 elemental particles comprising 12 macro- and 26 microelements believed to play roles in executing pharmacological effect of natural products. The phytochemical constituents of the powder were also identified as flavonoids, tannins, saponins, terpenoids, and glycosides.

Hepatocyte membrane distortion is associated with membrane leakage of the hepatocyte cytosolic contents which manifests by significant elevation of serum or plasma enzymes. ALT, AST, and ALP have been shown to be reliable markers of acute hepatocellular damage. Among the marker enzymes, ALT is the most reliable because AST is known to be abundant in the cardiac muscles, skeletal muscles, kidneys, and testes. Thus, any disease state affecting hepatic tissues significantly elevates the serum level of these enzymes [42, 43].

In our study, A/L increased the levels of ALT, AST, GGT, and bilirubin, while the levels of albumin and total protein were reduced indicating the presence of hepatotoxicity (Figures 1–4). The increases in AST and ALT were dose dependent. Normally, hepatotoxicity is accompanied by a significant rise in ALT levels more than three times the upper limit of normal. ALP levels also increase more than twice the upper limit level or total bilirubin more than twice when associated with increased ALP or ALT. Further, liver damage could be either hepatocellular (predominately initial alanine transferase elevation) or cholestatic (initial alkaline phosphatase rise) types. However, they are no mutually exclusive

and mixed types of injuries that are often encountered [44]. In order to differentiate liver diseases from elevated ALP related conditions, serum GGT measurement was conducted. Elevations in GGT may indicate that the integrity of the hepatocyte membranes has been compromised [44, 45].

A/L administration was accompanied by a high elevation of GGT levels. Similar studies have also found A/L and other artemisinin derivatives to have hepatotoxic effects [9, 45–47]. Besides, other antimalarial drugs such as chloroquine, amodiaquine, quinine, and halofantrine have also been reported to elevate serum ALT and ALP and may induce hepatic damage [9, 46, 48–50]. It has also been shown in other studies that A/L increases the level of oxidants such as superoxides (O^{2-}) and peroxides (H_2O_2) which leads to oxidative stress [48]. Though this was not measured in this study, it is known that reactive oxygen species (ROS) generated during the process of drug biotransformation can bind and react with cellular components in the liver to cause hepatic injury, thus impairing liver function [49]. Taking these mechanisms into consideration, it is plausible that drugs that have antioxidant activity or have the ability to reduce oxidative stress can be useful in preventing the deleterious effects of A/L on the liver. It is noteworthy that the elevations in serum liver enzymes were absent in guinea pigs pretreated with UNCP for 14 days before A/L administration. UNCP and its derived products have been shown to contain important antioxidant polyphenols that inhibit different tumoral processes and exhibit antioxidant and anti-inflammatory properties [50–53]. The hepatoprotective effect exhibited by cocoa may likely be due to the antioxidative effects of their polyphenols [54–56].

Furthermore, UNCP increased total proteins and albumin levels in the animals unlike the A/L administered group (Figures 5 and 6). Total protein and albumins are used to assess the synthetic functions of the liver. The diminution of total protein and albumin levels further support the hepatotoxic effects of A/L. In contrast, UNCP induced significant elevation in total proteins, which may be a reflection of its hepatoprotective effect. UNCP did not cause significant increase in albumin. Also, studies indicate that cocoa does not significantly increase albumin levels [57]. This buttresses the finding from this experiment. Bilirubin levels were not significantly affected by both A/L and UNCP (Figure 8).

Hepatoprotective effect of UNCP was further corroborated by the fact that there were no histological abnormalities following the administration of UNCP before A/L administration. Our histopathological studies showed damaged liver tissues in animals that received A/L alone evidenced by disturbed (necrotic) liver parenchyma (NeLP), a highly congested and dilated central vein (CCV) and lymphocytic infiltration (LYM) in all animals (Figure 10(b)), a situation that could be described as severe with a LDS between 4 and 5 according to Krastev [41]. UNCP administration reduced the extent of liver damage evidenced by the undisturbed liver parenchyma with an uncongested but dilated central vein (mild liver damage). The total protein levels tend to be restored (Figure 6).

Animals that received various doses (300 mg/kg, 900 mg/kg, and 1500 mg/kg) of UNCP showed a normal uncongested and dilated central vein. However, in one of the animals that received 1500 mg/kg UNCP, there was observed, dilated, and congested central vein. High levels of copper in the blood have been shown to be responsible for liver and gastrointestinal disorders [58]. Thus, this observation of the compromised liver integrity might probably be due to the high levels of copper (Table 1) at this high dose of UNCP. This level of copper has also been observed in our study where energy dispersive X-ray (EDXRF) analyses of UNCP showed the presence of both macro- and microelements including copper 0.2984 mg ± 1.71 per 4 g of UNCP (Table 1). The copper content of 1500 mg/kg UNCP exceeds the normal recommended daily allowance (RDA) of 900 μg (i.e., more than 103.6% of RDA). Thus, caution should be taken against frequent high consumption of UNCP as a beverage.

This study reports for the first time the hepatoprotective effect of UNCP against A/L-induced hepatic damage in guinea pigs. Similar effect of UNCP has been demonstrated in other studies where it was shown that UNCP reduced liver damage in mice infected with *Plasmodium berghei* [59], prevented alcohol-induced hepatic damage in rats [60], and protected against liver and renal damage by carbon tetrachloride [61].

The effect of UNCP on nitric oxide was also investigated. Nitric oxide has been found to have hepatoprotective effects in acute liver injury. The 900 mg/kg UNCP administered group showed an increase in nitric oxide levels. This dose level has been identified by other researchers as the optimum dose for beneficial effects of cocoa. The observed moderate nitric oxide increases that are beneficial [30] could be attributed to the flavonoid content of the unsweetened natural cocoa [29]. Cocoa increases nitric oxide levels in humans as observed for studies involving consumption for flavonoid rich chocolate and cocoa drinks [62, 63]. Superoxides and peroxides have been found to scavenge nitric oxide [61]. The rise in nitric oxide caused by A/L observed in the present study may be consistent with others who have suggested that to be as a result of a compensatory mechanism trying to restore the nitric oxide level [62]. Nitric oxide increased in the UNCP and A/L combinations with the greatest increments in animals receiving 300 mg/kg and 900 mg/kg UNCP. This may indicate that the hepatoprotective effect is likely to be more pronounced in the animals in these groups as confirmed by both the biochemical (Figures 1, 4, and 9) and histopathological results (Figure 10(c)).

This study suggests that the normal practice of UNCP consumption during malaria infection and treatment with A/L may have additional beneficial effects [17, 18, 59] in view of the fact that cocoa is also reported to have antimalarial properties. It is recommended that more studies be conducted to evaluate the possible synergistic antimalarial effect during concomitant administration of UNCP and A/L in addition to further investigating the mechanism of the hepatoprotective effect of UNCP. The findings from this study are consistent with previous studies that have shown that UNCP had reduced liver damage in mice infected with *Plasmodium berghei* [59], prevented alcohol-induced hepatic damage in rats [60], and shown hepatoprotective activity against carbon tetrachloride toxicity [61]. Further, it is highly

possible that the hepatoprotective potential of UNCP could be due to both pharmacological properties of the macro- and microelements and its phytochemical composition. Regular consumption of UNCP has immense health benefits and its simultaneous administration with A/L during malaria treatment could be beneficial and should be encouraged. The daily administration 300 mg/kg, 900 mg/kg, and 1500 mg/kg bwt UNCP in these animals is equivalent to a daily amount of 4.54 g, 13.42 g, and 22.70 g of UNCP, respectively, in a 70 kg man according to Reagan-Shaw et al. [64].

5. Conclusion

Unsweetened natural cocoa powder has 38 macro- and microelements, increases nitric oxide levels, and has hepatoprotective potential during high dose A/L administration. The simultaneous consumption of UNCP and A/L is not likely to result in liver injury or dysfunction. Care must however be taken during high daily consumptions due to the high copper content.

Abbreviations

FDA: Food and Drugs Authority
EDXRF: Energy dispersive X-ray
RDA: Recommended daily allowance
UNCP: Unsweetened natural cocoa powder
A/L: Artemether/lumefantrine
ALT: Alanine aminotransferase
AST: Aspartate aminotransferase
ALB: Albumin
ALP: Alkaline phosphatase
ANOVA: Analysis of variance
GAFCO: Ghana Agriculture Food Company
LD: Low dose
MD: Medium dose
HD: High dose
S-D: Sprague-Dawley
SDR: Sprague-Dawley rats
NeLP: Necrotic liver parenchyma
CCV: A highly congested and dilated central vein
LYM: Lymphocytic infiltration
DCV: Dilated central vein
UCV: Uncongested central veins.

Additional Points

Availability of data and materials: Coartem sample and unsweetened natural cocoa powder are legally registered products in Ghana and samples deposited at the University of Ghana School of Pharmacy. Data of the above studies and the photomicrographs are available in the Department of Pharmacology and Toxicology, University of Ghana. The limitations of this study was the fact that animals infected with specific malaria parasites could have been used as a source of comparison and the fact that other species of animals could also be used to conduct this research. It is recommended that a separate study be conducted to investigate the effect of UNCP on parasitemia during A/L administration in malaria infected animals and specific mechanisms under which this protective effect occurs.

Ethical Approval

The study protocol was approved by the departmental ethical and protocol review committee and the Noguchi Memorial Institute for Medical Research Institutional Animal Care and Use Committee with protocol approval number 2013-01-3E.

Competing Interests

The authors hereby declare there is no conflict of interests in the above research conducted and publication of the paper.

References

[1] World Health Organisation, *World Malaria Report*, World Health Organisation, Geneva, Switzerland, 2012.
[2] World Health Organization, *World Malaria Report*, World Health Organization, Geneva, Switzerland, 2007.
[3] P. B. Bloland, M. Ettling, and S. Meek, "Combination therapy for malaria in Africa: hype or hope?" *Bulletin of the World Health Organization*, vol. 78, no. 12, pp. 1378–1388, 2000.
[4] World Health Organization, *Guidelines for the Treatment of Malaria*, World Health Organisation (WHO), Geneva, Switzerland, 3rd edition, 2015.
[5] B. K. Brice, Y. William, O. Lacina et al., "In vitro susceptibility of *Plasmodium falciparum* isolates from Abidjan, Côte d'Ivoire, to artemisinin, chloroquine, dihydroartemisinin and pyronaridine," *Tanzania Journal of Health Research*, vol. 12, no. 1, pp. 73–79, 2010.
[6] World Health Organization, *Antimalarial Drug Combination Therapy: Report of a Technical Consultation*, World Health Organisation (WHO), Geneva, Switzerland, 2007.
[7] A. M. Dondorp, F. Nosten, P. Yi et al., "Artemisinin resistance in *Plasmodium falciparum* malaria," *The New England Journal of Medicine*, vol. 361, no. 5, pp. 455–467, 2009.
[8] A. P. Phyo, S. Nkhoma, K. Stepniewska et al., "Emergence of artemisinin-resistant malaria on the western border of Thailand: a longitudinal study," *The Lancet*, vol. 379, no. 9830, pp. 1960–1966, 2012.
[9] S. E. Owumi, M. A. Gbadegesin, O. A. Odunola, A. M. Adegoke, and A. O. Uwaifo, "Toxicity associated with repeated administration of artemether-lumefantrine in rats," *Environmental Toxicology*, vol. 30, no. 3, pp. 301–307, 2015.
[10] Worldwide Antimalarial Resistance Network (WWARN) AL Dose Impact Study Group, "The effect of dose on the antimalarial efficacy of artemether-lumefantrine: a systematic review and pooled analysis of individual patient data," *The Lancet Infectious Diseases*, vol. 15, no. 6, pp. 692–702, 2015.
[11] M. J. A. Maleyki and A. Ismail, "Antioxidant properties of cocoa powder," *Journal of Food Biochemistry*, vol. 34, no. 1, pp. 111–128, 2010.
[12] A. H. Azizah, N. M. Nik Ruslawati, and T. Swee Tee, "Extraction and characterization of antioxidant from cocoa by-products," *Food Chemistry*, vol. 64, no. 2, pp. 199–202, 1999.
[13] M. Karim, K. McCormick, and C. Tissa Kappagoda, "Effects of cocoa extracts on endothelium-dependent relaxation," *The Journal of Nutrition*, vol. 130, no. 8, pp. 2105S–2108S, 2000.

[14] L. Stahl, K. B. Miller, J. Apgar et al., "Preservation of cocoa antioxidant activity, total polyphenols, flavan-3-ols, and procyanidin content in foods prepared with cocoa powder," *Journal of Food Science*, vol. 74, no. 6, pp. C456–C461, 2009.

[15] I. Amin, B. Koh, and R. Asmah, "Effect of cacao liquor on tumor marker enzymes 492 during chemical hepatocarcinogenesis in rats," *Journal of Medicinal Food*, vol. 7, no. 1, pp. 7–12, 2004.

[16] I. Cordero-Herrera, M. A. Martín, L. Goya, and S. Ramos, "Cocoa flavonoids protect hepatic cells against high-glucose-induced oxidative stress: relevance of MAPKs," *Molecular Nutrition and Food Research*, vol. 59, no. 4, pp. 597–609, 2015.

[17] S. K. Amponsah, K. A. Bugyei, D. Osei-Safo et al., "*In vitro* activity of extract and fractions of natural cocoa powder on *Plasmodium falciparum*," *Journal of Medicinal Food*, vol. 15, no. 5, pp. 476–482, 2012.

[18] F. K. Addai, "Natural cocoa as diet-mediated antimalarial prophylaxis," *Medical Hypotheses*, vol. 74, no. 5, pp. 825–830, 2010.

[19] C. Andres-Lacueva, M. Monagas, N. Khan et al., "Flavanol and flavonol contents of cocoa powder products: influence of the manufacturing process," *Journal of Agricultural and Food Chemistry*, vol. 56, no. 9, pp. 3111–3117, 2008.

[20] A. Caligiani, D. Acquotti, M. Cirlini, and G. Palla, "1H NMR study of fermented cocoa (*Theobroma cacao* L.) beans," *Journal of Agricultural and Food Chemistry*, vol. 58, no. 23, pp. 12105–12111, 2010.

[21] M. Del Rosario Brunetto, L. Gutiérrez, Y. Delgado et al., "Determination of theobromine, theophylline and caffeine in cocoa samples by a high-performance liquid chromatographic method with on-line sample cleanup in a switching-column system," *Food Chemistry*, vol. 100, no. 2, pp. 459–467, 2007.

[22] L. Tian, X. Shi, L. Yu, J. Zhu, R. Ma, and X. Yang, "Chemical composition and hepatoprotective effects of polyphenol-rich extract from houttuynia cordata tea," *Journal of Agricultural and Food Chemistry*, vol. 60, no. 18, pp. 4641–4648, 2012.

[23] H. Shimoda, J. Tanaka, M. Kikuchi et al., "Walnut polyphenols prevent liver damage induced by carbon tetrachloride and D-galactosamine: hepatoprotective hydrolyzable tannins in the kernel pellicles of walnut," *Journal of Agricultural and Food Chemistry*, vol. 56, no. 12, pp. 4444–4449, 2008.

[24] J. Yang, Y. Li, F. Wang, and C. Wu, "Hepatoprotective effects of apple polyphenols on CCl4-induced acute liver damage in mice," *Journal of Agricultural and Food Chemistry*, vol. 58, no. 10, pp. 6525–6531, 2010.

[25] S. M. Sabir, S. D. Ahmad, A. Hamid et al., "Antioxidant and hepatoprotective activity of ethanolic extract of leaves of *Solidago microglossa* containing polyphenolic compounds," *Food Chemistry*, vol. 131, no. 3, pp. 741–747, 2012.

[26] T. I. Stark, H. Justus, and T. Hofmann, "Quantitative analysis of *N*-phenylpropenoyl-L-amino acids in roasted coffee and cocoa powder by means of a stable isotope dilution assay," *Journal of Agricultural and Food Chemistry*, vol. 54, no. 8, pp. 2859–2867, 2006.

[27] T. Adzet, J. Camarasa, and J. C. Laguna, "Hepatoprotective activity of polyphenolic compounds from *Cynara scolymus* against CCl4 toxicity in isolated rat hepatocytes," *Journal of Natural Products*, vol. 50, no. 4, pp. 612–617, 1987.

[28] T. Rassaf and M. Kelm, "Cocoa flavanols and the nitric oxide-pathway: targeting endothelial dysfunction by dietary intervention," *Drug Discovery Today: Disease Mechanisms*, vol. 5, no. 3-4, pp. e273–e278, 2008.

[29] W. M. Hon, K. H. Lee, and H. E. Khoo, "Nitric oxide in liver diseases: friend, foe, or just passerby?" *Annals of the New York Academy of Sciences*, vol. 962, pp. 275–295, 2002.

[30] Y. Li, D.-M. Zhang, J.-B. Li, S.-S. Yu, Y. Li, and Y.-M. Luo, "Hepatoprotective sesquiterpene glycosides from sarcandra glabra," *Journal of Natural Products*, vol. 69, no. 4, pp. 616–620, 2006.

[31] M. Yoshikawa, T. Morikawa, Y. Kashima, K. Ninomiya, and H. Matsuda, "Structures of new dammarane-type triterpene saponins from the flower buds of *Panax n otoginseng* and hepatoprotective effects of principal ginseng saponins 1," *Journal of Natural Products*, vol. 66, no. 7, pp. 922–927, 2003.

[32] E. A. Adewusi and A. J. Afolayan, "A review of natural products with hepatoprotective activity," *Journal of Medicinal Plants Research*, vol. 4, no. 13, pp. 1318–1334, 2010.

[33] Y. Wu, F. Wang, Q. Zheng et al., "Hepatoprotective effect of total flavonoids from *Laggera alata* against carbon tetrachloride-induced injury in primary cultured neonatal rat hepatocytes and in rats with hepatic damage," *Journal of Biomedical Science*, vol. 13, no. 4, pp. 569–578, 2006.

[34] A. J. Mungole, R. Awati, A. Chaturvedi, and P. Zanwar, "Preliminary phytochemical screening of *Ipomoea obscura* (L)—a hepatoprotective medicinal plant," *International Journal of PharmTech Research*, vol. 2, no. 4, pp. 2307–2312, 2010.

[35] E. Ronen, "Micro-elements in agriculture," *Practical Hydroponics and Greenhouses*, pp. 39–48, 2007.

[36] World Health Organization, *Quality Control Methods for Medicinal Plant Materials*, WHO Offset, Geneva, Switzerland, 1998.

[37] E. H. Jihen, M. Imed, H. Fatima, and K. Abdelhamid, "Protective effects of selenium (Se) and zinc (Zn) on cadmium (Cd) toxicity in the liver and kidney of the rat: histology and Cd accumulation," *Food and Chemical Toxicology*, vol. 46, no. 11, pp. 3522–3527, 2008.

[38] I. Messaoudi, J. El Heni, F. Hammouda, K. Saïd, and A. Kerkeni, "Protective effects of selenium, zinc, or their combination on cadmium-induced oxidative stress in rat kidney," *Biological Trace Element Research*, vol. 130, no. 2, pp. 152–161, 2009.

[39] M. J. Anjos, R. T. Lopes, E. F. O. Jesus, S. M. Simabuco, and R. Cesareo, "Quantitative determination of metals in radish using X-ray fluorescence spectrometry," *X-Ray Spectrometry*, vol. 31, no. 2, pp. 120–123, 2002.

[40] J. B. Harborne, *Phytochemical Methods: A Guide to Modern Techniques of Plant Analysis*, Chapman & Hall, London, UK, 1998.

[41] Z. Krastev, "Liver Damage Score—a new index for evaluation of the severity of chronic liver diseases," *Hepato-Gastroenterology*, vol. 45, no. 19, pp. 160–169, 1998.

[42] P. Alavinejad, F. Farsi, A. Rezazadeh et al., "The effects of dark chocolate consumption on lipid profile, fasting blood sugar, liver enzymes, inflammation, and antioxidant status in patients with non-alcoholic fatty liver disease: a randomized, placebo-controlled, pilot study," *Journal of Gastroenterology and Hepatology Research*, vol. 4, no. 12, pp. 1858–1864, 2015.

[43] E. T. Olayinka and A. Ore, "Alterations in antioxidant status and biochemical indices following administration of dihydroartemisinin-piperaquine phosphate (p-ALAXIN®)," *IOSR Journal of Pharmacy and Biological Sciences*, vol. 5, no. 4, pp. 43–53, 2013.

[44] N. Mumoli, M. Cei, and A. Cosimi, "Drug-related hepatotoxicity," *The New England Journal of Medicine*, vol. 354, no. 20, pp. 2192–2193, 2006.

[45] C. U. Ugokwe, H. C. Asomba, and I. O. Onwuzulike, "Hepatotoxicity potential of coartemether on wistar albino rat using liver enzyme assay," *Journal of Pharmacy and Biological Sciences*, vol. 10, pp. 66–70, 2015.

[46] A. A. Ngokere, T. C. Ngokere, and A. P. Ikwudinma, "Acute study of histomorphological and biochemedical changes caused by artesunate in visceral organs of the rabbit," *Journal of Experimental and Clinical Anatomy*, vol. 3, no. 4, pp. 11–16, 2004.

[47] A. Udobre, E. J. Edoho, O. Esevin, and E. I. Etim, "Effect of artemisinin with folic acid on the activities of aspartate amino transferase, alanine amino transferase and alkaline phosphatase in rat," *Asian Journal of Biochemistry*, vol. 4, no. 2, pp. 55–59, 2009.

[48] O. A. Adaramoye, D. O. Osaimoje, A. M. Akinsanya, C. M. Nneji, M. A. Fafunso, and O. G. Ademowo, "Changes in antioxidant status and biochemical indices after acute administration of artemether, artemether-lumefantrine and halofantrine in rats," *Basic and Clinical Pharmacology and Toxicology*, vol. 102, no. 4, pp. 412–418, 2008.

[49] A. S. Adekunle, C. O. Falade, E. O. Agbedana, and A. Egbe, "Assessment of side-effects of administration of artemether in humans," *Biology and Medicine*, vol. 1, no. 3, pp. 15–19, 2009.

[50] H. U. Nwanjo and G. Oze, "Acute hepatotoxicity following administration of artesunate in Guinea pigs," *The Internet Journal of Toxicology*, vol. 4, no. 1, pp. 1–2, 2007.

[51] A. Ismail, Z. M. Marjan, and C. W. Foong, "Total antioxidant activity and phenolic content in selected vegetables," *Food Chemistry*, vol. 87, no. 4, pp. 581–586, 2004.

[52] R. M. Lamuela-Raventós, A. I. Romero-Pérez, C. Andrés-Lacueva, and A. Tornero, "Review: health effects of cocoa flavonoids," *Food Science and Technology International*, vol. 11, no. 3, pp. 159–176, 2005.

[53] A. B. Granado-Serrano, M. A. Martín, L. Bravo, L. Goya, and S. Ramos, "A diet rich in cocoa attenuates N-nitrosodiethylamine-induced liver injury in rats," *Food and Chemical Toxicology*, vol. 47, no. 10, pp. 2499–2506, 2009.

[54] M. A. Martín, S. Ramos, R. Mateos et al., "Protection of human HepG2 cells against oxidative stress by cocoa phenolic extract," *Journal of Agricultural and Food Chemistry*, vol. 56, no. 17, pp. 7765–7772, 2008.

[55] M. Natsume, N. Osakabe, M. Yamagishi et al., "Analyses of polyphenols in cacao liquor, cocoa, and chocolate by normal-phase and reversed-phase HPLC," *Bioscience, Biotechnology and Biochemistry*, vol. 64, no. 12, pp. 2581–2587, 2000.

[56] M. Yamagishi, M. Natsume, A. Nagaki et al., "Antimutagenic activity of cacao: inhibitory effect of cacao liquor polyphenols on the mutagenic action of heterocyclic amines," *Journal of Agricultural and Food Chemistry*, vol. 48, no. 10, pp. 5074–5078, 2000.

[57] M. Yamagishi, M. Natsume, N. Osakabe et al., "Effects of cacao liquor proanthocyanidins on PhIP-induced mutagenesis in vitro, and in vivo mammary and pancreatic tumorigenesis in female Sprague-Dawley rats," *Cancer Letters*, vol. 185, no. 2, pp. 123–130, 2002.

[58] *Health Effects of Excess Copper; Copper in Drinking Water*, The National Academies Press, Washington, DC, USA, 2000.

[59] E. Aidoo, F. K. Addai, J. Ahenkorah et al., "Natural cocoa ingestion reduced liver damage in mice infected with *Plasmodium berghei* (NK65)," *Research and Reports in Tropical Medicine*, vol. 3, pp. 107–116, 2012.

[60] G. Sokpor, F. K. Addai, R. K. Gyasi et al., "Voluntary ingestion of natural cocoa extenuated hepatic damage in rats with experimentally induced chronic alcoholic toxicity," *Functional Foods in Health and Disease*, vol. 2, no. 5, pp. 166–187, 2012.

[61] K. Suzuki, K. Nakagawa, T. Yamamoto et al., "Carbon tetrachloride-induced hepatic and renal damages in rat: Inhibitory effects of cacao polyphenol," *Bioscience, Biotechnology and Biochemistry*, vol. 79, no. 10, pp. 1669–1675, 2015.

[62] D. Taubert, R. Roesen, C. Lehmann, N. Jung, and E. Schömig, "Effects of low habitual cocoa intake on blood pressure and bioactive nitric oxide: a randomized controlled trial," *The Journal of the American Medical Association*, vol. 298, no. 1, pp. 49–60, 2007.

[63] G. J. Dusting and P. S. Macdonald, "Endogenous nitric oxide in cardiovascular disease and transplantation," *Annals of Medicine*, vol. 27, no. 3, pp. 395–406, 1995.

[64] S. Reagan-Shaw, M. Nihal, and N. Ahmad, "Dose translation from animal to human studies revisited," *The FASEB Journal*, vol. 22, no. 3, pp. 659–661, 2008.

Hindawi Publishing Corporation
Evidence-Based Complementary and Alternative Medicine
Volume 2016, Article ID 7659684, 8 pages
http://dx.doi.org/10.1155/2016/7659684

Research Article

Chitosan and Sodium Alginate Combinations Are Alternative, Efficient, and Safe Natural Adjuvant Systems for Hepatitis B Vaccine in Mouse Model

Nourhan H. AbdelAllah,[1] Nourtan F. Abdeltawab,[2] Abeer A. Boseila,[3] and Magdy A. Amin[2]

[1] *Viral Control Unit, National Organisation for Research and Control of Biologicals (NORCB), Cairo 12654, Egypt*
[2] *Department of Microbiology and Immunology, Faculty of Pharmacy, Cairo University, Cairo 11562, Egypt*
[3] *National Organization for Drug Control and Research (NODCAR), Cairo 11562, Egypt*

Correspondence should be addressed to Nourtan F. Abdeltawab; nourtan.abdeltawab@pharma.cu.edu.eg

Received 1 April 2016; Accepted 9 June 2016

Academic Editor: Mario Giorgi

Hepatitis B viral (HBV) infections represent major public health problem and are an occupational hazard for healthcare workers. Current alum-adjuvanted HBV vaccine is the most effective measure to prevent HBV infection. However, the vaccine has some limitations including poor response in some vaccinee and being a frost-sensitive suspension. The goal of our study was to use an alternative natural adjuvant system strongly immunogenic allowing for a reduction in dose and cost. We tested HBV surface antigen (HBsAg) adjuvanted with chitosan (Ch) and sodium alginate (S), both natural adjuvants, either alone or combined with alum in mouse model. Mice groups were immunized subcutaneously with HBsAg adjuvanted with Ch or S, or triple adjuvant formula with alum (Al), Ch, and S, or double formulations with AlCh or AlS. These were compared to control groups immunized with current vaccine formula or unadjuvanted HBsAg. We evaluated the rate of seroconversion, serum HBsAg antibody, IL-4, and IFN-γ levels. The results showed that the solution formula with Ch or S exhibited comparable immunogenic responses to Al-adjuvanted suspension. The AlChS gave significantly higher immunogenic response compared to controls. Collectively, our results indicated that Ch and S are effective HBV adjuvants offering natural alternatives, potentially reducing dose.

1. Introduction

Hepatitis B virus (HBV) is one of the most common viral infectious diseases of the liver and is considered as a major public health problem. HBV is an important occupational hazard for health workers according to the World Health Organization (WHO) [1]. About 240 million people are chronically infected with HBV which is defined as being hepatitis B surface antigen (HBsAg) positive for at least 6 months [2]. HBV infection accounts for 30% of cirrhosis and 53% of primary liver cancer throughout most of the world [2]. Almost 80% of all cases of hepatocellular carcinoma worldwide may be related to HBV which is second to tobacco among known human carcinogens [3].

There is no specific treatment for HBV; however, since 1982 a vaccine against HBV was proven to be safe and effective [1]. The vaccine had been recommended by WHO to be included in the national immunization system. By May 2002, 154 countries had routine infant immunization with hepatitis B vaccine [4]. Although the vaccine is effective in preventing infection, there are limitations which include an estimated five to 15 percent of vaccine nonresponder [5]. In addition, low rates of completion of vaccinations are another problem of current vaccine [6–8]. Many reasons are proposed for poor responsiveness or nonresponsiveness, including concurrent infections or immunocompromised patients or genetic factors as HLA haplotypes or cytokine and chemokine SNPs. In addition to technical errors as intragluteal injection or inappropriate storage conditions (reviewed in [5]), studies have shown potential need for boosters, use of carriers, including preS-epitope, or using more-potent immunogenic adjuvants [5].

Although alum is currently the most commonly used adjuvant with human and veterinary vaccines, it provides

Table 1: Composition of adjuvant systems formulations used in the study.

	1 (Negative control)	2 (Unadjuvanted)	3 (Al)	4 (Ch)	5 (S)	6 (AlCh)	7 (AlS)	8 (AlChS)
PBS	x							
HBsAg (1 μg/mL)		x						
HBsAg (0.1 μg/mL)			x	x	x	x	x	x
Alum (0.5 mg/mL)			x			x	x	x
Chitosan (0.5 mg/mL)				x		x		x
Sodium alginate (5 mg/mL)					x		x	x

some obstacles that need to be resolved. Alum, like any mineral adjuvants, is difficult to manufacture in a physicochemically reproducible way. This failure affects its formulation immunogenicity. In addition, alum cannot be frozen or easily lyophilized as both of these processes cause the collapse of the gel resulting in gross aggregation and precipitation [9]. Alum adjuvant also induces inflammation and local reactions at the site of injection [10], augmenting the production of IgE antibody responses as part of the overall Th2 profile which is not likely to protect against diseases in which Th1 immunity and MHC class I restricted CTL are essential for protection, for example, viral infections, intracellular parasites, or tuberculosis [11].

There is a general tendency on using natural products as potential source of immune modulating compounds [12, 13]. Different compounds derived from natural origin such as plants, microorganism, algae, or insects have been used in the development of new adjuvants for vaccines and drugs for the treatment of other diseases such as allergy and cancer where immune modulating therapies are needed [12–14]. Two natural adjuvant candidates are chitosan and alginate salts. Studies showed significant evidence supporting their use as adjuvants [9, 10, 15]. Chitosan is a natural polysaccharide, which is converted by deacetylation from chitin that is considered the main component of the cell walls of fungi, the exoskeletons of arthropods, the radula of mollusks, and the beaks of cephalopods, including squids and octopuses. Chitosan has been used in several preclinical and clinical studies with good tolerability, excellent immune stimulation, and positive clinical results across a number of infections [11, 12, 14]. Sodium alginate, a naturally occurring polysaccharide, is the sodium salt of alginic acid. It is a gum, extracted from the cell walls of brown algae. Sodium alginate is generally regarded as nontoxic and nonirritant material. It poses many ideal characteristics as it is biodegradable and mucoadhesive polymer that does not produce toxicity in administration which makes it suitable polymer to use in vaccine developments [15]. In the current study, we compared the improvement of the immunogenic response of hepatitis B vaccine using adjuvants system of chitosan and sodium alginate compared to the currently used adjuvant system.

2. Materials and Methods

2.1. Animals. Male and female Balb/c mice (6–8 weeks of age, 20–30 g) were included in this study and were obtained from VACSERA vivarium, Helwan, Egypt. Animals were housed in accordance with standard laboratory conditions, under controlled environment with temperature 22 ± 3°C, 55 ± 5% humidity, and 12-hour light/dark cycle. Animals were provided with a standard laboratory diet and water ad libitum. The mice were adapted for one week before starting the experiment to their environment. Animals handling was according to guidelines [13, 16]. Permission to conduct the study was obtained from Ethics Committee in Faculty of Pharmacy, Cairo University.

2.2. Preparation of Chitosan and Sodium Alginate Solution. Chitosan powder (Sigma-Aldrich, USA) was dissolved in 0.8% (v/v) acetic acid and 0.9% (w/v) saline and then heated at 37°C with constant stirring. Sodium alginate (Sigma-Aldrich, USA) was dissolved in distilled water and heated at 37°C with constant stirring until complete dissolving; then both solutions were sterilized by autoclaving.

2.3. Adjuvant Systems and Vaccine Formulations Preparation. The hepatitis B surface (HBsAg) antigen, produced by GSK Biologicals (Rixensart, Belgium), was diluted in phosphate buffer solution (PBS) to a final concentration of 1 μg/mL (Table 1, formulation 2). The different formulations of adjuvanted vaccine combinations are explained in Table 1. In brief, we diluted the HBsAg in PBS with either aluminum hydroxide gel (alum) (Sanofi-Pasteur, France) or chitosan solution or sodium alginate to obtain a final concentration of HBsAg of 0.1 μg/mL. We used alum at concentration of 0.5 mg/mL (Al) or chitosan at concentration of 0.5 mg/mL (Ch) or sodium alginate at concentration of 5 mg/mL (S). Each adjuvant-antigen mixture was shaken for two hours at 25°C to ensure complete absorbtion of the antigen onto the adjuvant system (Table 1, formulations 3–5). The formulations consisting of alum with either chitosan (AlCh) or sodium alginate (AlS) were prepared by addition of alum to the diluted antigen and shaken for one hour; then either chitosan or sodium alginate was added and shaken again for one

hour. Finally the combined adjuvanted vaccine formulation of the three adjuvants (AlChS) was prepared by diluting HBsAg then adding alum, chitosan, and sodium alginate consequently with shaking for half an hour after first and second adjuvant addition; then the final mixture was shaken for an additional hour.

2.4. Evaluation of the Loading Efficacy of HBsAg in Suspension Vaccine Formulations. The loading efficacy of each vaccine formulation suspension, namely, Al, AlCh, AlS, and AlChS, was calculated indirectly by quantifying the free antigen remaining in the supernatant after the mixture was centrifuged at 10,000 rpm for ten minutes as described previously [17, 18]. The loading efficacy (LE) values were calculated according to the following equations:

LE(%) = (total amount of HBsAg − free HBsAg)/(total amount of HBsAg) ∗ 100.

2.5. Experimental Design of Immunization Studies. Balb/c mice were randomly assigned to eight groups ($n = 6$ mice) as shown in Table 1. The groups were control groups (1–3) where group (1) negative control (PBS alone); (2) HBsAg 1 μg/mL in PBS solution (1 μg); and (3) HBsAg 0.1 μg/mL loaded on alum (Al). Groups 4–8 were immunized with the following formulations: group (4) HBsAg 0.1 μg/mL in chitosan solution (Ch); (5) HBsAg 0.1 μg/mL in sodium alginate (S); (6) HBsAg 0.1 μg/mL loaded on alum and chitosan (AlCh); (7) HBsAg 0.1 μg/mL loaded on alum and sodium alginate (AlS); and (8) HBsAg 0.1 μg/mL loaded on alum, chitosan, and sodium alginate (AlChS). Mice groups were inoculated subcutaneously with 1 mL of respective formulations following guidelines for *in vivo* assay [19–22]. Blood samples were collected at four weeks after immunization. Sera were separated by centrifugation at 4000 rpm for ten minutes and stored at −20°C until tested.

2.6. In Vivo Safety Assay. Each mouse in each group was monitored for 14 days and the toxicity was assessed by survival rate. In addition, local inflammation symptoms as redness, local swelling, and loss of hair at the site of injection were monitored for each mouse.

2.7. Measurement of Rate of Seroconversion. The rate of positive seroconversion was measured by using commercial enzyme-linked immunosorbent assay (ELISA) (Diasorin, Italy). The rate of seroconversion was calculated by the following formula:

Rate of seroconversion (%) = (number of mice with specific IgG to HBsAg in their sera that is equal or above 10 mIU/mL)/(total number of mice injected immunized in each group) ∗ 100.

2.8. Measurement of Total HBsAg-Specific Antibodies and Antibodies Subclasses. Sera in each mice group were pooled and used for measurement of HBsAg-specific antibodies (IgG) and IgG subclasses. Total IgG was measured using commercial ELISA quantification kit (Diasorin, Italy) as described by the manufacturer and the results were represented as mIU/mL. For measuring HBsAg-specific IgG1, IgG2a, and IgG2b, purified HBsAg (1 μg/mL) was dissolved in 0.05 M carbonate-bicarbonate buffer, pH 9.6, and dispensed into 96-well microtiter plate. Coated plates were incubated at 4°C overnight, washed with PBST (PBS with 0.05% Tween 20) three times, and blocked with 5% bovine serum albumin (BSA) in PBST for two hours at 37°C. After washing the plates with PBST, the sera of each group were added to the wells. Plates were incubated at 37°C for two hours. After washing the plates with PBST, horseradish peroxidase-labelled anti-mouse isotypes (anti-IgG1, anti-IgG2a, and anti-IgG2b) (Komabiotech, Korea) were added and incubated for one hour at 37°C. The plates were washed again with PBST and the bound antibodies were revealed by adding 3,3′,5,5′-Tetramethylbenzidine (TMB) (Sigma, USA). The reaction was stopped with 0.2 M of H_2SO_4 and the absorbance was read at 450/630 nm in an automatic ELISA reader (Dynex, USA). ELISA titers were expressed in mIU/mL, where 1 mIU is the mean of absorbance readings for the control group serum plus two times the standard deviation (SD).

2.9. Cytokines Measurements. The pooled sera of each group were used for quantification of anti-mouse interferon gamma (IFN-γ) and interleukin- (IL-) 4 using commercial ELISA kit (Bosterbio, USA), as recommended by the manufacturer. Cytokines levels were expressed in pg/mL.

2.10. Statistical Analysis. Data were analyzed using GraphPad Prism 6.01 (Graph-Pad Software Inc., California, USA). We used one-way analysis of variance (ANOVA) followed by multiple comparisons using Fisher's LSD test for comparison of cytokine and antibody levels means. P values less than 0.05 were considered significant.

3. Results

3.1. Addition of Chitosan and Sodium Alginate Significantly Improved HBsAg Adsorption in Vaccine Formulations. The loading efficacy (LE) of HBsAg antigen on alum suspension formulations (AlCh, AlS, and AlChS) was measured to confirm that addition of either chitosan or sodium alginate or both to alum did not decrease the adsorption of antigen to the alum. In contrast the LE% of HBsAg in formulation which contained either chitosan or sodium alginate or both increased significantly from alum alone ($P < 0.05$) (Figure 1). The LE% of Al, AlCh, AlS, and AlChS was 67.72 ± 7.92%, 83.93 ± 0.6%, 77.93 ± 7.04%, and 89.73 ± 3.67% (mean ± SD), respectively (Figure 1). Therefore, new formulations of adjuvant composed of alum with either chitosan or sodium alginate or both showed significantly positive impact compared to alum alone AlCh versus Al ($P < 0.01$), AlS versus Al ($P < 0.05$), and AlChS versus Al ($P < 0.01$) on the adsorption of the antigen (Figure 1).

3.2. Natural Adjuvanted Formulations Had No Mortality and Showed No Skin Irritation When Tested in In Vivo Model. Mice groups were subcutaneously immunized with different formulations (Table 1) and observed for 14 days. There was no mortality nor weight changes in the immunized animal groups. In addition, we observed that mice immunized

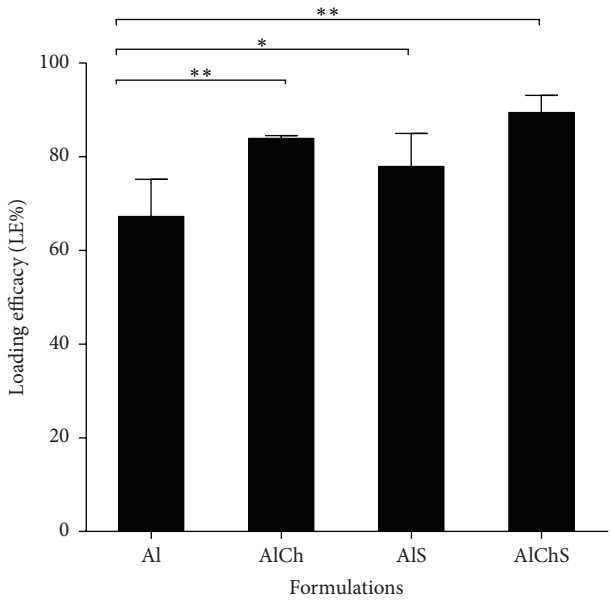

Figure 1: The loading efficacy (LE%) of HBsAg in alum suspension vaccine formulations (Al, AlCh, AlS, and AlChS). Each bar represents mean LE% ± standard deviation. Natural adjuvant formulations showed significantly higher LE% compared to alum-adjuvanted HBsAg. $^{*}P < 0.05$ and $^{**}P < 0.01$ compared against alum adjuvant formulation.

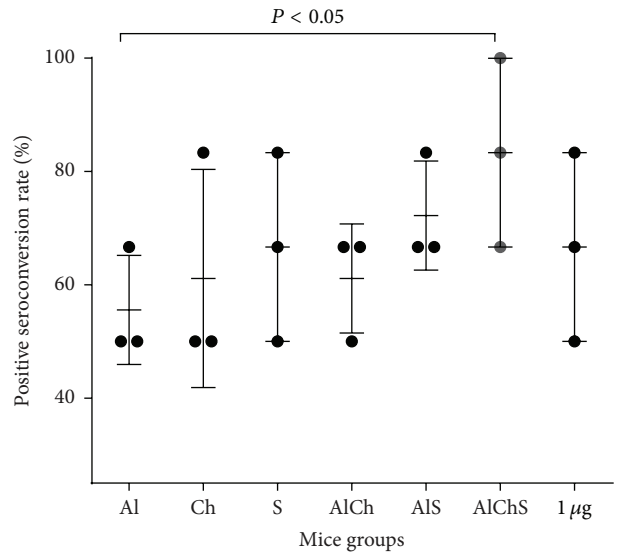

Figure 2: The rate of positive seroconversion expressed in percentage among immunized mice groups. Mice sera were assayed for anti-HBsAg and a cut-off at ≥10 mIU/mL was set as positive. The seroconversion rate was calculated by dividing the number of mice (anti-HBsAg ≥ 10 mIU/mL) on the total number of mice in each group. Data points represent mean ± SD from three independent experiments.

with formulations containing natural adjuvants showed no signs for local swelling nor hair loss at the site of injection compared to alum-adjuvanted formulation (data not shown).

3.3. Chitosan and Sodium Alginate Showed Comparable Seroconversion to Alum-Adjuvanted Formulation in Mice. Specific antibodies against HBsAg (anti-HBsAg) of at least 10 milli-international units per milliliter (mIU/mL) are considered a reliable marker of the protective level of immunity [1, 6]. The percentage of mice with sera having anti-HBsAg ≥ 10 mIU/mL divided by the total number of mice vaccinated in each group was evaluated as percent of positive seroconversion rate. All groups showed a percentage of positive seroconversion over 50% (Figure 2). Mice immunized with formulations containing Ch or S or Al as single adjuvants showed no significant difference compared to unadjuvanted control.

3.4. Addition of Chitosan and Sodium Alginate to Alum Formula Significantly Increased Seroconversion in Mice Immunized with AlChS Triple Formulation. Mice groups immunized with double adjuvant formulations had no significant difference compared to single adjuvanted formulation or unadjuvanted control (Figure 2). The highest percentage of seroconversion was observed in the triple adjuvant formulation AlChS with seroconversion rate being up to 90% ($P < 0.05$) (Figure 2).

3.5. Chitosan and Sodium Alginate Elicited HBsAg-Specific IgG in Immunized Animals. A pool of the mice sera from each group after 28 days from vaccination were used for determination of total HBsAg-specific IgG levels. In general, the naturally adjuvanted formulations whether single adjuvanted or combined with alum elicited HBsAg-specific IgG comparable to alum-adjuvanted formulation (Figure 3). Moreover, the triple adjuvanted formulation AlChS induced significantly higher HBsAg-specific IgG levels than alum-adjuvanted group ($P < 0.05$) (Figure 3) suggesting some sort of synergism between the three adjuvants.

3.6. Formulations Containing Chitosan and Sodium Alginate Elicited Broad Range of Anti-HBsAg IgG Subclasses in Mice. Formulations adjuvanted with Al and Ch elicited IgG1, IgG2a, and IgG2b in mice sera (Figure 4). However, sodium alginate adjuvanted group showed higher serum IgG2b levels compared to the other two groups (Al, Ch) with $P \leq 0.05$. Similarly, AlS, AlCh, and AlChS adjuvanted formulations elicited a broad range of anti-HBsAg IgG subclasses (Figure 4). All IgG subclasses were elicited in AlChS group, with an increase in IgG1 subclass (Figure 5). In addition, triple formulation showed significant enhancement of IgG2b levels observed in AlChS group especially compared with Al and Ch group ($P < 0.01$) and AlS group ($P < 0.05$) (Figure 4).

3.7. Use of Combination of Chitosan and Sodium Alginate with Alum Triple Formulation Elicited Highest IL-4 Response In Vivo While Combination of Chitosan or Sodium Alginate with Alum as Double Formulation Elicited Highest IFN-γ Response In Vivo. We evaluated IL-4 and IFN-γ to further study immune responses and cytokine production induced by each adjuvant system formulation. Mice groups immunized with single adjuvants of Al and Ch showed comparable levels of

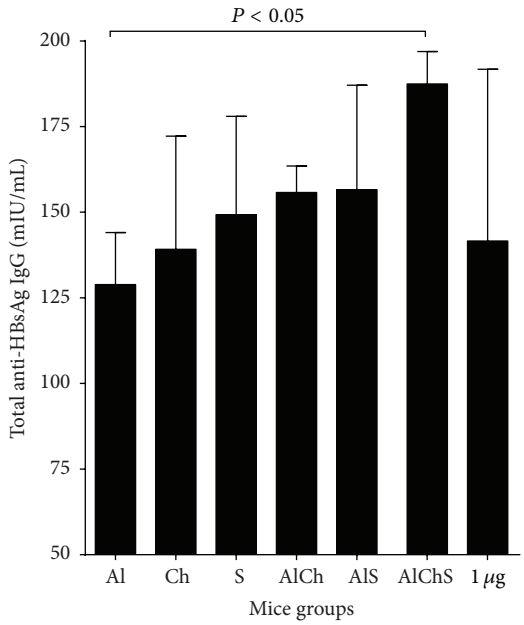

Figure 3: HBsAg-specific IgG titers of mice immunized with different formulations of hepatitis B adjuvanted vaccine. Group of 6 mice was immunized with various HBsAg formulations. Pool of sera for each group collected after 28 days and serum anti-HBs antibody was determined. Each bar corresponds to the group means ± SD from 3 independent experiments.

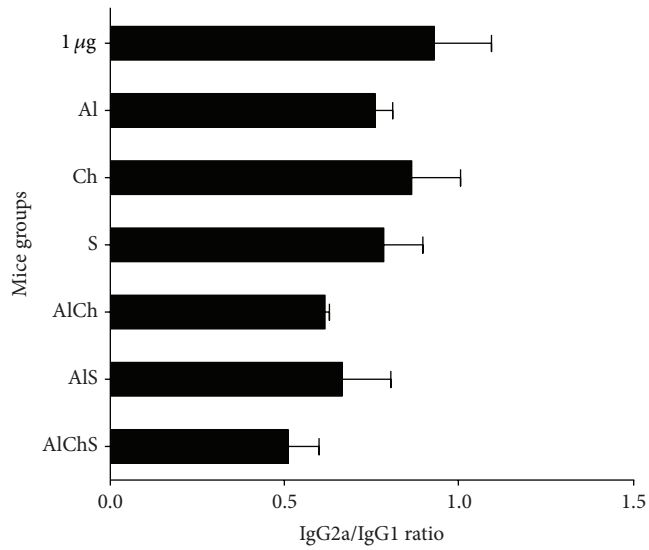

Figure 5: Ratios of IgG2a/IgG1 in mice sera groups immunized with different vaccine adjuvant systems. Ratios depict the percentage of IgG2a divided by the percentage of IgG1. Any ratio >1 is associated with a Th1 response and any ratio <1 is associated with a Th2 response. Each bar represents mean ratio ± standard deviation.

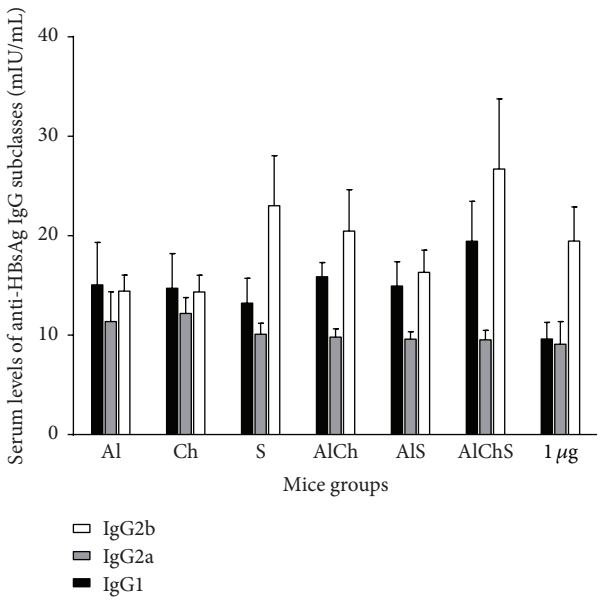

Figure 4: Levels of serum anti-HBsAg IgG subclass elicited in mice immunized with different formulations of the hepatitis B vaccine. Values are expressed as mean of antibody level from 3 independent experiments ± standard variation. $P < 0.05$ (AlChS versus unadjuvanted group) in levels of IgG1; $P \leq 0.05$ (S versus AlCh group), $P < 0.01$ (AlChS versus AlCh group), and $P < 0.05$ (AlChS versus AlS group) levels of IgG2b.

IL-4 and significantly higher levels than control (Figure 6(a)). Formulation containing S showed the lowest IL-4 levels that is comparable to control (Figure 6(a)). Meanwhile, double and triple formulations produced significantly higher IL-4 levels than the control and unadjuvanted groups (Figure 6(a)). Mice immunized with triple adjuvant system AlChS elicited the highest levels of IL-4 compared to all groups ($P < 0.001$) (Figure 6(a)).

On the other hand, all adjuvanted groups elicited IFN-γ levels higher than unadjuvanted and control groups (Figure 6(b)). The combined adjuvanted groups AlCh, AlS, and AlChS showed higher levels of IFN-γ than single adjuvanted groups ($P < 0.01$) (Figure 6(b)). Sodium alginate adjuvanted formulation induced higher IFN-γ production compared to alum or chitosan single adjuvanted formulation ($P < 0.01$) (Figure 6(b)). AlS induced the highest IFN-γ levels among all adjuvanted formulations (Figure 6(b)).

4. Discussion

Hepatitis B vaccine is composed of purified recombinant proteins, which, despite of its better tolerability, is unfortunately less immunogenic when administrated alone. Therefore, there is a constant need to develop new adjuvants to increase the immunogenicity of HBV vaccine so lower doses of HBsAg can be used. In the present study, we compared the safety and immunogenic response of different natural adjuvant systems chitosan, sodium alginate, or both compared to the currently used adjuvant alum. Despite the fact that alum adjuvant has been used in practical vaccination for over 80 years, its drawbacks cannot be ignored. One major drawback is that traditional alum-adsorbed vaccines are frost-sensitive

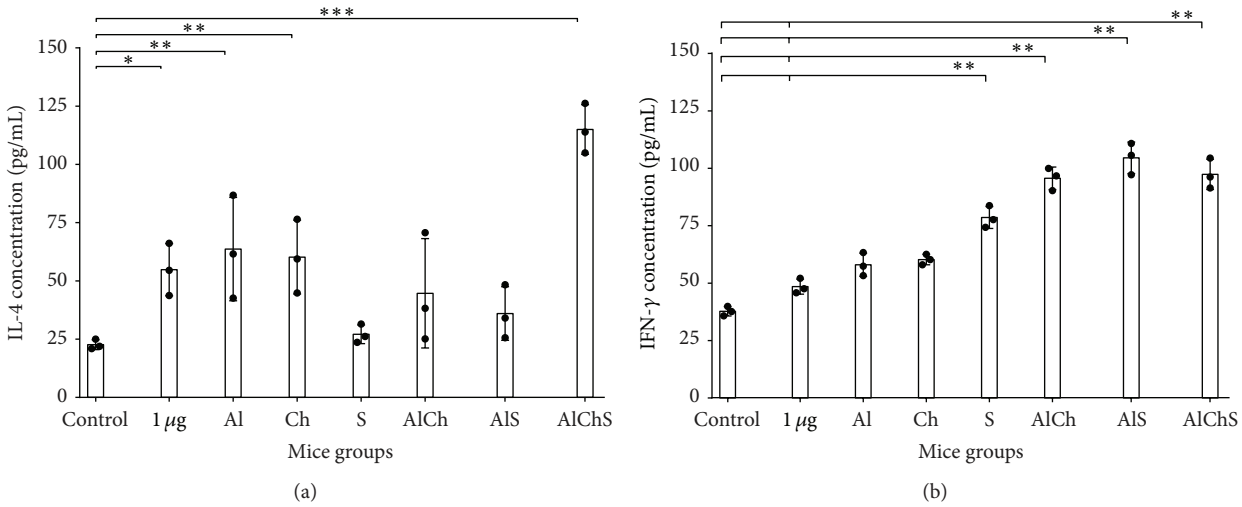

Figure 6: IL-4 and IFN-γ levels in mice sera immunized with different formulation of HBsAg. Cytokine values are expressed as means ± SD of three pools. Levels of (a) IL-4 and (b) IFN-γ in mice sera immunized with different formulation of HBsAg. $^{*}P < 0.05$, $^{**}P < 0.01$, and $^{***}P < 0.001$ compared to control group.

suspensions and thus cannot be lyophilized, hence making transportation and long-term storage a problem. Also alum elicits Th2-driven antibody responses with little Th1-type responses, which restricts the protection against many intracellular pathogens especially virus. In addition, there are safety issues concerning inflammation at the site of injection [23, 24].

Natural products can be a vast source of compounds that modulate immune function [12, 13, 16]. In this study, the potential of some naturally derived compounds was examined to be considered as a natural source of vaccine adjuvants with biological activity equivalent to the current commercially available adjuvants. Both chitosan and sodium alginate are naturally abundant polysaccharides. Chitosan was proven to be safe, nontoxic, nonirritable, nonantigenic, biocompatible, and biodegradable [25, 26]. Similarly, sodium alginate is recognized as a safe food and pharmaceutical ingredient by US Food and Drug Administration (FDA). Sodium alginate is also biodegradable and cheap to produce a stable long shelf life [9, 27]. In our study, chitosan and sodium alginate adjuvanted HBV vaccine showed to be safe whether used alone as single adjuvant or in combination with alum. However, our *in vivo* safety assessment would need to be conducted for formulations containing alum over longer periods of time to observe any possible long-term neurological or systemic adverse effects known to be associated with alum.

We first examined the replacement of alum with either chitosan or sodium alginate in the single solution adjuvanted formulation. Both chitosan and sodium alginate adjuvanted vaccine gave comparable immunogenic response to alum and to each other. This was evident by the rate of the positive seroconversion in immunized mice that provided above 50% of anti-HBsAg that is at least 10 mIU/mL (Figure 2). In addition, Ch and S elicited similar levels of total anti-HBsAg IgG (Figure 3); moreover Ch elicited mixed Th1-Th2 IgG subclasses similar to Al (Figure 4). Meanwhile, S elicited more IgG2b, a more Th-1-like response (Figure 4); also S elicited the least IL-4 levels and one of the highest IFNγ in mice sera (Figure 6).

It has been shown that Th1 and Th2 responses could be characterized by their cytokine production [28]. The Th1 immune response is indicated by the production of IFN-γ and production of IgG2a and IgG2b in mice while the Th2 immune response is indicated by the production of IL-4 and enhanced production of IgG1 (Figures 4 and 6) [19, 29]. The ratio of IgG2a/IgG1 of all formulations indicated a more IgG1, Th2 response (Figure 5). However, sodium alginate group induced high level of IgG2b versus alum and chitosan group which indicate a tendency toward Th1-like response. Overall, this indicates that there is a variety of IgG subclasses elicited by natural alternative adjuvant systems, which offers more protection against hepatitis B. Another marker of Th1/Th2 response is IgG2a/IgG1 ratio. It provides an indication of the Th1/Th2 bias of the ongoing immune response [28]. Mice immunized with chitosan adjuvanted formulation exhibited the highest ratio among all groups which gave a good indication of a balanced Th1/Th2 immune response as indicated by the increase in IgG1, IgG2a, and IgG2b antibody isotypes (Figures 4 and 5). Overall these findings are not far from what was reported in using chitosan with different types of antigen and different route of administration [11, 20, 21]. For example, adjuvanted chitosan solution with OVA antigen when injected parentally in mice produced similar levels of IgG1, IgG2a, and IgG2b [20]. Meanwhile, chitosan solution with *Helicobacter pylori* antigen administrated orally gave IgG2a/IgG1 of 1.06 ± 0.4 which is similar to our result 0.9 (Figure 5) [21].

Our single adjuvant systems results are also in agreement with previous studies where sodium alginate elicited response shifted toward Th1-like response in sodium alginate adjuvanted vaccine of Bacillus Calmett-Guerin (BCG) administrated subcutaneously in mice [15]. We also found a

significant increase in the production of IFN-γ but a decrease in the production of IL-4 in sodium alginate adjuvanted vaccine compared to alum and chitosan groups which had approximate levels in both IL-4 and IFN-γ (Figure 6). These results were consistent with those found in other studies using alginate encapsulated influenza virus preserving its immunogenicity and stimulating potent CD8+ T cell responses by secretion of antiviral cytokines, such as IFN-γ [22]. These findings supported the use of either chitosan or sodium alginate alone as a replacement natural safe adjuvant instead of alum for hepatitis B vaccine.

Next, we used chitosan and sodium alginate in combination with alum as either double or triple formulation to enhance the potency of the vaccine by protecting the antigen from degradation *in vivo*, trying to decrease the amount of HBsAg and alum used, thus a more cost-effective vaccine [30, 31]. We found that double and triple formulation offered best immunogenic responses. This was evident as triple formulation had the highest rate of seroconversion (Figure 2) and elicited highest total IgG levels with a mixed IgG1, 2a, and 2b giving a more comprehensive protection (Figures 3 and 4). Finally, triple formulation showed significantly highest level of Th2 cytokine IL-4 and was second to AlS in IFNγ levels (Figure 6). Our data supports the use of combined adjuvants to decrease the amount of alum and HBsAg used. This is in line with many of the successful examples as AS04 containing aluminum and the bacterial lipid, monophosphoryl lipid A [32]. This adjuvant system is already licensed in Europe and used in many vaccines like HBV vaccine (Fendrix®) and Human Papilloma Virus (HPV) vaccine (Cervarix®).

Another important parameter was to evaluate the adsorption efficacy of the alum-adjuvanted vaccine (Figure 1). Adsorption of antigen to aluminum-containing adjuvants prior to administration is essential for the enhancement of immunogenicity and essential in avoiding fast degradation of the antigen after administration [33, 34]. In addition, the degree of adsorption became one of the parameters for evaluation of the efficacy of the final vaccine product [33, 34]. Addition of either chitosan or sodium alginate to alum provided efficient loading of the antigen on the adjuvant system (Figure 1). These results are in line with that reported when different formulation of hepatitis B antigen was efficiently associated with alginate coated chitosan nanoparticles with loading efficacy equal to 77.1 ± 3.0% [28]. However in our studies the presence of alum increased the loading efficiently when combined with either chitosan or sodium alginate adjuvant and reached its maximum when the three adjuvants combined together in the AlChS formulation (Figure 1). As expected between all adjuvant formulations in this study, the three-adjuvant combined group (AlChS) stands out as the most immunogenic formulation (Figures 3, 4, and 6).

While addition of chitosan or sodium alginate to alum in a combined adjuvant system gave comparable results to each other on the level of HBsAg-specific IgG antibodies, IgG isotypes, and cytokine production, their immunogenic effect did not increase significantly compared to the single adjuvanted vaccine group. Similar observation was found when both antigen and another adjuvant (CpG ODN 1826) were adsorbed to chitosan nanoparticles as the formulation did not give additional important benefit compared to other formulations containing unadjuvanted antigen and single adjuvant (CpG ODN 1826) formulation [17].

Additionally, in the current study, a group of mice has been immunization subcutaneously with 1 μg HBsAg unadjuvanted, which on its own induced low but detectable anti-HBs. When we reduced unadjuvanted HBsAg doses ten times (0.1 μg) or to 0.5 μg/mL, we found that there were no responses (data not shown). All adjuvanted vaccine formulation induced equivalent peak titers of anti-HBsAg as unadjuvanted vaccine (1 μg), about 10-fold higher with ten times less antigen (0.1 μg), except for AlChS group which induced even more anti-HBs titer than 1 μg HBsAg (Figure 3). Interestingly, regarding IFN-γ levels, all adjuvanted vaccine formulations were significantly higher than 1 μg unadjuvanted vaccine which seemed particularly strong in the presence of sodium alginate whether alone or in combination (Figure 3), while the IL-4 levels of 1 μg unadjuvanted group were comparable with the less antigen adjuvanted group with the exception of the group adjuvanted with sodium alginate which produce lower IL-4 (Figure 6). On the contrary AlChS group produce significant higher IL-4 level about 2-fold than produced by the 1 μg unadjuvanted vaccine (Figure 6). Similar observation was obtained with the same mice strain using the same antigen (HBsAg) with alum alone or combined with different adjuvant (CPG ODN) [35]. This result indicates that both chitosan and sodium alginate could induce 10-fold immunogenic response compared to the same dose of unadjuvanted vaccine whether used alone or in combination with alum.

5. Conclusions

Our study revealed that natural products can be used as an alternative safe, highly immunogenic adjuvant to HBV vaccine. It is advantageous to use natural alternatives with good biocompatibility and immunological activity on the specific cellular and humoral immune responses to HBsAg in mice. Collectively our results suggested that the use of natural adjuvants, chitosan or sodium alginate, as single adjuvant or in combination with alum can help in production of lower dose of HBV vaccine that can potentially be less expensive. The combined formulation of triple adjuvant where the antigen is enclosed in the adjuvant system with strong adsorption showed strong impact on the immune response. These responses were expressed with the highest level in the cytokine levels, rate of seroconversion, anti-HBsAg, and their isotypes with balanced Th2 and Th1. Our study provides a great opportunity for the improvement of the currently licensed HBV vaccines. However, more studies are needed to assess the long-term safety and application of our findings in clinical settings.

Competing Interests

The authors declare that they have no competing interests.

References

[1] World Health Organization, *Hepatitis B. Fact Sheet No. 204, 2000*, World Health Organization, Geneva, Switzerland, 2007.

[2] J. F. Perz, G. L. Armstrong, L. A. Farrington, Y. J. F. Hutin, and B. P. Bell, "The contributions of hepatitis B virus and hepatitis C virus infections to cirrhosis and primary liver cancer worldwide," *Journal of Hepatology*, vol. 45, no. 4, pp. 529–538, 2006.

[3] B. N. Fields, D. M. Knipe, P. M. Howley, and D. E. Griffin, *Fields Virology*, Lippincott Williams & Wilkins, Philadelphia, Pa, USA, 2001.

[4] D. Lavanchy, "Hepatitis B virus epidemiology, disease burden, treatment, arid current and emerging prevention and control measures," *Journal of Viral Hepatitis*, vol. 11, no. 2, pp. 97–107, 2004.

[5] A. Shlomai and Y. Shaul, "Inhibition of hepatitis B virus expression and replication by RNA interference," *Hepatology*, vol. 37, no. 4, pp. 764–770, 2003.

[6] Centers for Disease Control and Prevention (CDC), *Epidemiology and Prevention of Vaccine-Preventable Diseases*, Public Health Foundation, Washington, DC, USA, 2011.

[7] R. Clemens, R. Sänger, J. Kruppenbacher et al., "Booster immunization of low- and non-responders after a standard three dose hepatitis B vaccine schedule—results of a post-marketing surveillance," *Vaccine*, vol. 15, no. 4, pp. 349–352, 1997.

[8] K. Cardell, B. Åkerlind, M. Sällberg, and A. Frydén, "Excellent response rate to a double dose of the combined hepatitis A and B vaccine in previous nonresponders to hepatitis B vaccine," *Journal of Infectious Diseases*, vol. 198, no. 3, pp. 299–304, 2008.

[9] A. E. Itodo, J. U. Umoh, J. O. Adekeye, M. O. Odugbo, G. Haruna, and M. Y. Sugun, "Field trial of sodium alginate-adsorbed *Clostridium perfringens* types C and D toxoid against clostridial enterotoxemia in sheep," *Israel Journal of Veterinary Medicine*, vol. 64, no. 1, pp. 2–5, 2009.

[10] Y. Kato, H. Onishi, and Y. Machida, "Application of chitin and chitosan derivatives in the pharmaceutical field," *Current Pharmaceutical Biotechnology*, vol. 4, no. 5, pp. 303–309, 2003.

[11] M. J. Heffernan, D. A. Zaharoff, J. K. Fallon, J. Schlom, and J. W. Greiner, "In vivo efficacy of a chitosan/IL-12 adjuvant system for protein-based vaccines," *Biomaterials*, vol. 32, no. 3, pp. 926–932, 2011.

[12] Y. M. Vasiliev, "Chitosan-based vaccine adjuvants: incomplete characterization complicates preclinical and clinical evaluation," *Expert Review of Vaccines*, vol. 14, no. 1, pp. 37–53, 2015.

[13] S. Leary, W. Underwood, R. Anthony et al., *AVMA Guidelines for the Euthanasia of Animals*, 2013.

[14] R. Scherließ, S. Buske, K. Young, B. Weber, T. Rades, and S. Hook, "In vivo evaluation of chitosan as an adjuvant in subcutaneous vaccine formulations," *Vaccine*, vol. 31, no. 42, pp. 4812–4819, 2013.

[15] F. Dobakhti, T. Naghibi, M. Taghikhani et al., "Adjuvanticity effect of sodium alginate on subcutaneously injected BCG in BALB/c mice," *Microbes and Infection*, vol. 11, no. 2, pp. 296–301, 2009.

[16] L. C. Chosewood and D. E. Wilson, *Biosafety in Microbiological and Biomedical Laboratories*, Diane Publishing, 2007.

[17] O. Borges, M. Silva, A. de Sousa, G. Borchard, H. E. Junginger, and A. Cordeiro-da-Silva, "Alginate coated chitosan nanoparticles are an effective subcutaneous adjuvant for hepatitis B surface antigen," *International Immunopharmacology*, vol. 8, no. 13-14, pp. 1773–1780, 2008.

[18] X. Y. Li, X. Y. Kong, S. Shi et al., "Preparation of alginate coated chitosan microparticles for vaccine delivery," *BMC Biotechnology*, vol. 8, article 89, 2008.

[19] T. L. Stevens, A. Bossie, V. M. Sanders et al., "Regulation of antibody isotype secretion by subsets of antigen-specific helper T cells," *Nature*, vol. 334, no. 6179, pp. 255–258, 1988.

[20] Z.-S. Wen, Y.-L. Xu, X.-T. Zou, and Z.-R. Xu, "Chitosan nanoparticles act as an adjuvant to promote both Th1 and Th2 immune responses induced by ovalbumin in mice," *Marine Drugs*, vol. 9, no. 6, pp. 1038–1055, 2011.

[21] Y. Xie, N.-J. Zhou, Y.-F. Gong et al., "Th immune response induced by *H pylori* vaccine with chitosan as adjuvant and its relation to immune protection," *World Journal of Gastroenterology*, vol. 13, no. 10, pp. 1547–1553, 2007.

[22] A. C. Boesteanu, N. S. Babu, M. Wheatley, E. S. Papazoglou, and P. D. Katsikis, "Biopolymer encapsulated live influenza virus as a universal CD8+ T cell vaccine against influenza virus," *Vaccine*, vol. 29, no. 2, pp. 314–322, 2010.

[23] R. K. Gherardi, M. Coquet, P. Cherin et al., "Macrophagic myofasciitis lesions assess long-term persistence of vaccine-derived aluminium hydroxide in muscle," *Brain*, vol. 124, no. 9, pp. 1821–1831, 2001.

[24] E. B. Lindblad, "Aluminium compounds for use in vaccines," *Immunology and Cell Biology*, vol. 82, no. 5, pp. 497–505, 2004.

[25] K. Arai, T. Kinumaki, and T. Fujita, "Toxicity of chitosan," *Bulletin of Tokai Regional Fisheries Research Laboratory*, no. 56, pp. 89–94, 1968.

[26] T. Kean and M. Thanou, "Biodegradation, biodistribution and toxicity of chitosan," *Advanced Drug Delivery Reviews*, vol. 62, no. 1, pp. 3–11, 2010.

[27] W. Wang and M. Singh, "Selection of adjuvants for enhanced vaccine potency," *World Journal of Vaccines*, vol. 1, no. 2, pp. 33–78, 2011.

[28] S. Romagnani, "T-cell subsets (Th1 versus Th2)," *Annals of Allergy, Asthma & Immunology*, vol. 85, no. 1, pp. 9–21, 2000.

[29] J. A. Gracie and J. A. Bradley, "Interleukin-12 induces interferon-γ-dependent switching of IgG alloantibody subclass," *European Journal of Immunology*, vol. 26, no. 6, pp. 1217–1221, 1996.

[30] B. Levast, S. Awate, L. Babiuk et al., "Vaccine potentiation by combination adjuvants," *Vaccines*, vol. 2, no. 2, pp. 297–322, 2014.

[31] Y. Perrie, A. R. Mohammed, D. J. Kirby, S. E. McNeil, and V. W. Bramwell, "Vaccine adjuvant systems: enhancing the efficacy of sub-unit protein antigens," *International Journal of Pharmaceutics*, vol. 364, no. 2, pp. 272–280, 2008.

[32] M. E. Pichichero, "Improving vaccine delivery using novel adjuvant systems," *Human Vaccines*, vol. 4, no. 4, pp. 262–270, 2008.

[33] T. Clapp, P. Siebert, D. Chen, and L. Jones Braun, "Vaccines with aluminum-containing adjuvants: optimizing vaccine efficacy and thermal stability," *Journal of Pharmaceutical Sciences*, vol. 100, no. 2, pp. 388–401, 2011.

[34] B. Hansen, A. Sokolovska, H. HogenEsch, and S. L. Hem, "Relationship between the strength of antigen adsorption to an aluminum-containing adjuvant and the immune response," *Vaccine*, vol. 25, no. 36, pp. 6618–6624, 2007.

[35] R. Weeratna, L. Comanita, and H. L. Davis, "CPG ODN allows lower dose of antigen against hepatitis B surface antigen in BALB/c mice," *Immunology and Cell Biology*, vol. 81, no. 1, pp. 59–62, 2003.

Hindawi Publishing Corporation
Evidence-Based Complementary and Alternative Medicine
Volume 2016, Article ID 4976791, 7 pages
http://dx.doi.org/10.1155/2016/4976791

Research Article

Thin Layer Chromatography-Bioautography and Gas Chromatography-Mass Spectrometry of Antimicrobial Leaf Extracts from Philippine *Piper betle* L. against Multidrug-Resistant Bacteria

Demetrio L. Valle Jr.,[1] Juliana Janet M. Puzon,[1,2] Esperanza C. Cabrera,[3] and Windell L. Rivera[1,2]

[1] *Institute of Biology, College of Science, University of the Philippines, Diliman, 1101 Quezon City, Philippines*
[2] *Natural Sciences Research Institute, University of the Philippines, Diliman, 1101 Quezon City, Philippines*
[3] *Biology Department, De La Salle University, Taft Avenue, 1004 Manila, Philippines*

Correspondence should be addressed to Windell L. Rivera; wlrivera@science.upd.edu.ph

Received 1 April 2016; Revised 20 May 2016; Accepted 6 June 2016

Academic Editor: Mohamed M. Abdel-Daim

This study isolated and identified the antimicrobial compounds of Philippine *Piper betle* L. leaf ethanol extracts by thin layer chromatography- (TLC-) bioautography and gas chromatography-mass spectrometry (GC-MS). Initially, TLC separation of the leaf ethanol extracts provided a maximum of eight compounds with R_f values of 0.92, 0.86, 0.76, 0.53, 0.40, 0.25, 0.13, and 0.013, best visualized when inspected under UV 366 nm. Agar-overlay bioautography of the isolated compounds demonstrated two spots with R_f values of 0.86 and 0.13 showing inhibitory activities against two Gram-positive multidrug-resistant (MDR) bacteria, namely, methicillin-resistant *Staphylococcus aureus* and vancomycin-resistant *Enterococcus*. The compound with an R_f value of 0.86 also possessed inhibitory activity against Gram-negative MDR bacteria, namely, carbapenem-resistant Enterobacteriaceae-*Klebsiella pneumoniae* and metallo-β-lactamase-producing *Acinetobacter baumannii*. GC-MS was performed to identify the semivolatile and volatile compounds present in the leaf ethanol extracts. Six compounds were identified, four of which are new compounds that have not been mentioned in the medical literature. The chemical compounds isolated include ethyl diazoacetate, tris(trifluoromethyl)phosphine, heptafluorobutyrate, 3-fluoro-2-propynenitrite, 4-(2-propenyl)phenol, and eugenol. The results of this study could lead to the development of novel therapeutic agents capable of dealing with specific diseases that either have weakened reaction or are currently not responsive to existing drugs.

1. Introduction

Piper betle L. belonging to the family Piperaceae is a climbing vine used in alternative medicine due to its numerous therapeutic properties, which include its antibacterial, antifungal, antioxidant, cytotoxic, antihelminthic, antiprotozoal, antidiabetic, hepatoprotective, and immunomodulatory properties [1]. The plant is known to be widely distributed in India, Sri Lanka, Malaysia, Indonesia, Thailand, China, Philippines, and other subtropical countries [2]. It has been reported to have broad spectrum antimicrobial activities against various bacterial strains [1] and fungi [3, 4].

Results of our previous studies have proven the great potential of *P. betle* as a cure for multidrug-resistant (MDR) bacteria [5, 6]. Out of 12 Philippine medicinal plants subjected to antimicrobial assays, the *P. betle* exceptionally presented significant inhibitory effects against selected MDR isolates [5]. Moreover, the antimicrobial activities of the ethanol, methanol, and supercritical CO_2 extracts from *P. betle* were determined on clinical isolates of MDR bacteria which have been identified by the Infectious Disease Society of America as being among the currently more challenging strains in clinical management. The assay methods used in the study included the standard disc diffusion method and the broth

microdilution method for the determination of the minimum inhibitory concentration (MIC) and the minimum bactericidal concentrations (MBC) of the extracts for the test microorganisms. The study revealed the bactericidal activities of all the *P. betle* leaf crude extracts with MBC ranging from 19 μg/mL to 1250 μg/mL. The extracts proved to be more potent against the Gram-positive methicillin-resistant *Staphylococcus aureus* (MRSA) and vancomycin-resistant *Enterococcus* (VRE) than for the Gram-negative test bacteria. VRE isolates were more susceptible to all the extracts than the MRSA isolates. Generally, the ethanol extracts proved to be more potent than the methanol extracts and supercritical CO_2 extracts as shown by their lower MICs for both the Gram-positive and Gram-negative MDRs. It is in this light that an investigation on the efficacy of *P. betle* as a source of antimicrobial agents was conducted by performing bioassay-guided isolation and identification of its antimicrobial compounds.

Although there are several studies focusing on the phytochemistry of *P. betle*, there are varying outcomes concerning the constituents or bioactive compounds of the plant, implying that the habitat plays a significant role in the phytochemistry of medicinal plants. One such documentation is a local study made on the Philippine variety of *P. betle*, where it was observed that unlike the Indian variety the major constituents of the essential oil and ether soluble fraction of the Philippine *P. betle* are chavibetol and chavibetol acetate, whereas allylpyrocatechol is the major constituent of the leaves [7]. Information on the particular pharmacologically active constituents of medicinal plants and the subsequent isolation of important compounds are vital in the search for new therapeutic drugs. In the development of new treatment for MDR bacteria, we should be able to identify which bioactive compounds are responsible for significant antagonistic effects against such pathogens, taking into consideration the mechanisms of action and possible toxicity.

Several spectroscopic and chromatographic analytical methods have been developed for standardization of products from medicinal plants, which include mass spectrometry (MS), gas chromatography-mass spectrometry (GC-MS), liquid chromatography (LC), thin layer chromatography (TLC), high performance liquid chromatography (HPLC), and high performance thin layer chromatography (HPTLC) to guarantee their quality, efficacy, and safety [8].

To determine the biologically active natural products in plant extracts, the choice of the bioassay method is critical. The bioassay tests should be sensitive, reliable, simple, and prompt [9]. The type of extraction method, duration of extraction, temperature, and the polarity of solvent used influence the quality and the concentration of bioactive components isolated from the raw material [2, 10]. Activity-guided fractionation is essential, as all fractions should be thoroughly examined and monitored, to detect or identify highly active compounds for further isolation and purification until active monosubstances are obtained [9].

This study aimed to identify and isolate the antibacterial compounds of *P. betle* extracts using TLC, agar-overlay, and contact (indirect) bioautographic assays and to identify the semivolatile and volatile compounds using GC-MS.

2. Materials and Methods

2.1. Collection and Preparation of Plant Materials. The leaves of the *P. betle* were collected at the foot of Sierra Madre Mountain Range in the Municipality of General Nakar, Quezon, Philippines. The plant was identified and authenticated at the Jose Vera Santos Memorial Herbarium of the Institute of Biology, University of the Philippines, Diliman, Quezon City, Philippines. The leaves were washed thoroughly and then air-dried at room temperature for seven days, finely powdered, and stored in sterile airtight containers until further use.

2.2. Preparation of Ethanol Leaf Extracts. Powdered dried leaves of *P. betle* were extracted in accordance with the method of Basri and Fan [11] with minor modifications. Briefly, 150 g of powdered plant material was soaked in 500 mL of ethanol for seven days with occasional stirring and then filtered using Whatman filter paper number 1 (Whatman Ltd., England). The filtrate was concentrated under reduced pressure using a rotary evaporator at 50°C. The crude ethanol extract was collected and allowed to dry at room temperature. The stock solution was prepared by dissolving the dried extract in DMSO at 1×10^5 μg/mL concentration.

2.3. Multidrug-Resistant (MDR) Bacterial Strains. The MDR bacterial strains used in this study were the following: Gram-positive MDR bacteria, namely, methicillin-resistant *Staphylococcus aureus* (MRSA) and vancomycin-resistant *Enterococcus* (VRE); Gram-negative MDR bacteria, namely, carbapenem-resistant Enterobacteriaceae- (CRE-) *Klebsiella pneumoniae* and metallo-β-lactamase- (MβL-) producing *Acinetobacter baumannii*. These MDR bacterial strains were isolated from anonymized patients admitted to Makati Medical Center and Ospital ng Makati. Both are Level III training hospitals located in Makati City, Philippines. All isolates were identified by automated biochemical tests using Vitek®MS (bioMérieux, Marcy l'Etoile, France) GP colorimetric identification card. The susceptibility patterns were obtained by Vitek MS AST (bioMérieux, Marcy l'Etoile, France) following MIC interpretive standard from Clinical Laboratory Standard Institute M100-S24 [12].

2.4. Thin Layer Chromatography (TLC). A TLC system (CAMAG) equipped with a sample applicator was used for application of samples. Five microliters of leaf ethanol extracts was separately applied on 5 cm × 10 cm chromatographic precoated silica gel plates (Merck, TLC grade) as the stationary phase. The TLC plates were developed in a twin trough glass chamber containing mixture of ethyl acetate and *n*-hexane (7 : 3 v/v) as the mobile phase. The plates were removed when the solvent front has moved to 15 cm from the original extract position and subsequently allowed to dry. After drying, the spots on the developed plates were visualized under visible (white), short UV (254 nm), and long UV (366 nm) light. As postderivatization, the plates were sprayed with vanillin-sulfuric acid for color reaction and allowed to dry. A visualizer and a scanner were used for photodocumentation at UV 254 nm and UV 366 nm and under the

visible light before and after application of the vanillin-sulfuric acid spray. The movement of each separating spot of the extract was expressed by its retention factor (R_f). Values were calculated for each spot using the following formula:

$$R_f = \frac{\text{distance traveled by the solute from the point of application to the center of spot}}{\text{distance traveled by the solvent front}}. \quad (1)$$

2.5. TLC-Contact (Indirect) Bioautography Technique. The inocula of representative MDR bacterial strains with 1.5×10^8 CFU/mL concentration, namely, MRSA, VRE, MβL-*A. baumannii*, and CRE-*K. pneumoniae*, were swabbed onto Mueller-Hinton agar plates for use in contact bioautography technique adopted from the method of Wedge and Nagle [13] with slight modifications. The dried TLC plates with corresponding spots were placed aseptically onto the seeded Mueller-Hinton agar plate overlaid with sterile lens paper. The TLC plate was placed face downward with the silica-coated side in contact evenly with the lens paper and was incubated for 12 to 18 hours at $4 \pm 2^\circ$C. Then, the TLC plate was removed, and the inoculated agar plate was further incubated at $35 \pm 2^\circ$C for 24 hours in an ambient air incubator. The zone of inhibition was observed and compared with TLC plate R_f value results.

2.6. TLC-Agar-Overlay Bioautography Technique. One milliliter of representative MDR bacterial strains with 1.5×10^8 CFU/mL concentration was used for every 10 mL of Mueller-Hinton agar. Developed TLC plates were placed in a sterile Petri dish (150 mm). The culture was added to the melted Mueller-Hinton agar and a thin layer was poured over the TLC plate. After the solidification of the medium, TLC plate was incubated for 24 hours at $35 \pm 2^\circ$C. The TLC-bioautography plates were sprayed with an aqueous solution (2.5 mg/mL) of methylthiazol tetrazolium (Sigma, USA). Clear zone of inhibition was observed against a purple background [14]. Identification of specific compounds was limited by the unavailability of prepared reference standards.

2.7. Gas Chromatography-Mass Spectrometry (GC-MS). The GC-MS analysis of leaf ethanol extracts was performed using a Perkin Elmer GC-MS (Perkin Elmer Clarus 680 GC-Clarus SQ 8T MS) equipped with Elite-5 MS 30 m $\times$ 0.25 mm $\times$ 25 μm capillary column (5% diphenyl, 95% dimethylpolysiloxane). For GC-MS detection, an electron ionization system with ionization energy of 70 eV was used. Ultrapure helium gas was used as a carrier gas at a constant flow rate of 1 mL/min. Ion source, mass transfer line, and injector temperature were set at 230°C, 250°C, and 290°C, respectively. The oven temperature was programmed from 50 to 150°C at a rate of 3°C/min and then held in isothermal condition for 10 min and finally raised to 250°C at 10°C/min. Diluted samples (1/100, v/v in ethanol) of 1 μL were manually injected in the split mode of 120. Mass spectral scan range was at 45–450 *m/z*, with a solvent delay of 2 min. The components of the extracts were identified based on the comparison of their GC relative retention time and mass spectra with those of NIST MS Search Library Software version 2.0.

3. Results and Discussion

3.1. Thin Layer Chromatography (TLC). To isolate and identify the bioactive compounds of the *P. betle* leaf extract, TLC was initially performed as a qualitative method to document the extract constituents. This method has been widely used to separate secondary metabolites like polyphenols, flavonoids, saponins, alkaloids, and steroids, including amino acids, proteins, peptides, hormones, and pesticides [15]. Although TLC does not provide specific measurements, it is very effective when used in combination with other techniques. In our study, TLC of the *P. betle* leaf ethanol extracts revealed a maximum of 9 compounds in the order of decreasing R_f values, as shown in Table 1. Five bands were evident in the TLC plate visualized under visible light (Figure 1(a)), six bands when viewed under short UV radiation (254 nm wavelength) as shown in Figure 1(b), eight bands when viewed under long UV radiation (366 nm wavelength) as shown in Figure 1(c), and seven bands from the TLC plate sprayed with vanillin-sulfuric acid reagent (Figure 1(d)). The best resolutions were obtained when examined under UV light and after derivatization with the vanillin-sulfuric acid spray. Compounds with R_f values of 0.92, 0.86, and 0.13 were visualized in all TLC chromatograms. It is interesting to note that the compound with R_f 0.70 was evident in all visualization methods, except when viewed under long UV radiation.

3.2. TLC-Bioautography. In the agar-overlay and contact (indirect) bioautography assays, the antibacterial activity of the compounds separated on TLC was determined.

Representative MDR bacteria from each group with correspondingly similar MIC and MBC values as indicated in parentheses, namely, MRSA (78 μg/mL), VRE (19 μg/mL), MβL-*A. baumannii,* (312 μg/mL), and CRE-*K. pneumonia* (312 μg/mL), were used for bioautography. Significant antibacterial activity against MRSA was demonstrated by compounds with R_f values of 0.86 and 0.13 on agar-overlay bioautography, as evident by the significant clear zone of inhibition on a purple background (Figure 2). In the contact (indirect) method, only the compound with R_f 0.86 was visible, shown as a large clear zone of inhibition on a purple background sprayed with methylthiazol tetrazolium (Figure 3). The same compounds were also demonstrated to be active against VRE, as seen on the agar-overlay bioautography result in Figure 2. For the Gram-negative antimicrobial activity, only the compound with R_f value of 0.86 exhibited significant activity against MβL-*A. baumannii* and CRE-*K. pneumoniae* (Figures 2 and 3). From the results, a compound with R_f value of 0.86 was found to have inhibitory activity against both

Table 1: Thin layer chromatography (TLC) profile of *P. betle* L. leaf ethanol extract.

R_f value	Visual	UV-254 nm	UV-366 nm	Vanillin-sulfuric acid spray
0.92	Light yellow	Faint dark	Faint red	Violet spot
0.86	Dark gray	Dark gray	Pinkish red	Light brown
0.76	—	Faint dark	Red	Brown
0.70	Green	Dark gray	—	Green
0.53	Yellow	Light dark	Green	Light green
0.40	—	—	Light blue	—
0.25	—	—	Blue	—
0.13	Dark green	Dark gray	Pink	Green
0.013	—	—	Red	Light green

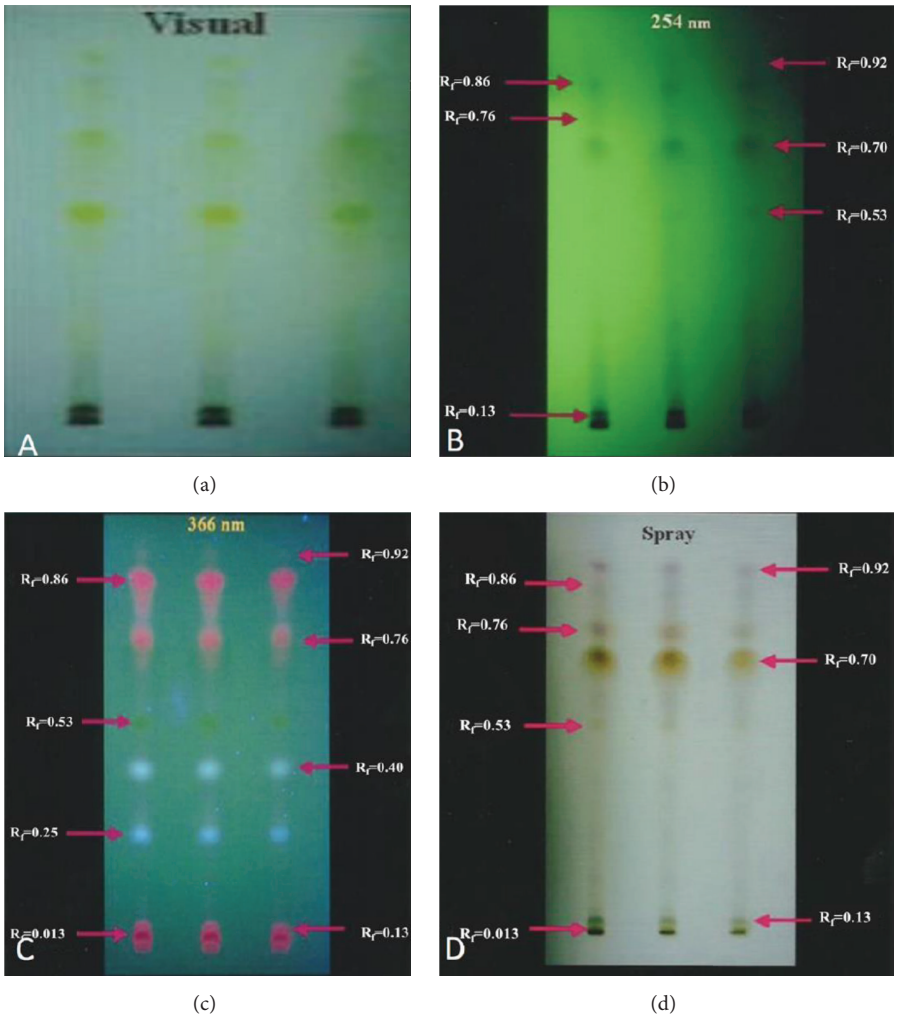

Figure 1: TLC plates of *P. betle* L. leaf ethanol extracts visualized under visible light, UV at 254 nm, and UV at 366 nm and after derivatization with vanillin-sulfuric acid. Mobile phase: ethyl acetate : *n*-hexane (7 : 3 v/v).

Gram-positive and Gram-negative MDR bacteria. Based on earlier studies about TLC of plant compounds, R_f values of 0.86 were exhibited by flavonoids and terpenoids, whereas R_f values of 0.13 were exhibited by alkaloids, saponins, and some flavonoids [16, 17].

The agar-overlay bioautography assay proved to be an excellent method of identifying and localizing compounds with specific antibacterial activity in *P. betle* leaf extract, justifying its value in the search for new antimicrobial agents. It is appropriate for evaluating compounds that can be

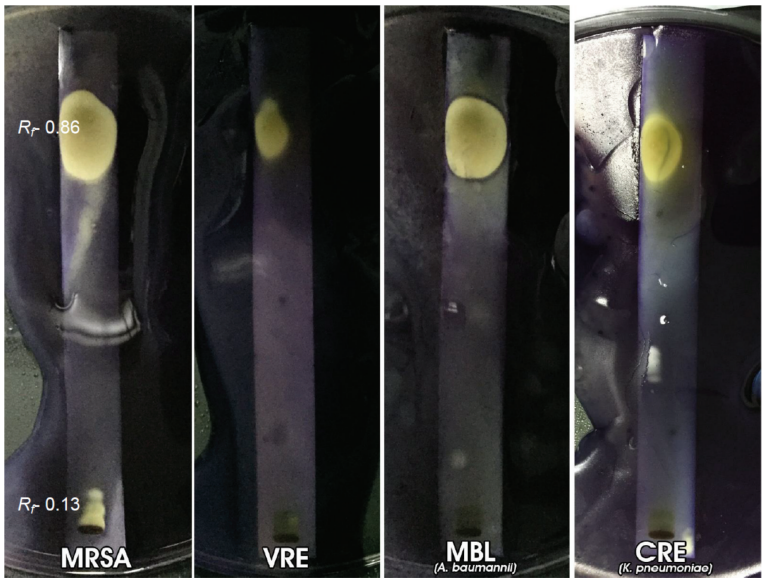

Figure 2: TLC-agar-overlay bioautography of *P. betle* L. leaf ethanol extracts against MRSA, VRE, MβL-*A. baumannii*, and CRE-*K. pneumoniae*.

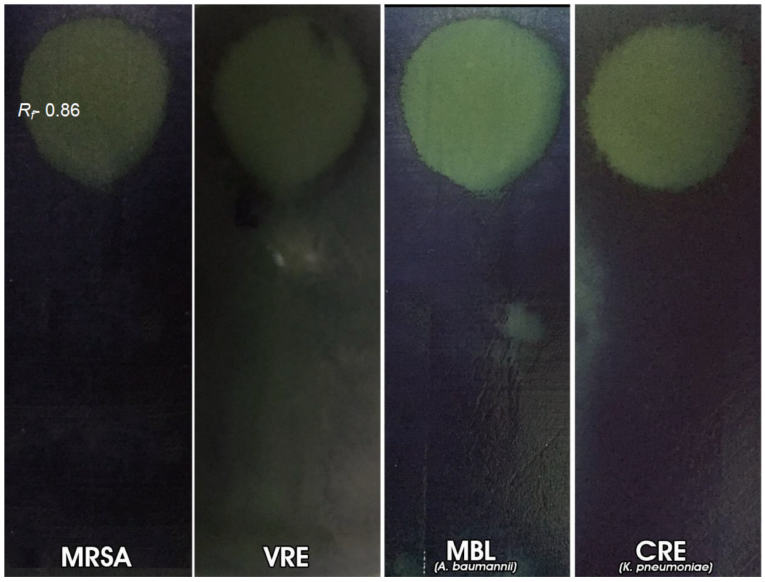

Figure 3: TLC-contact (indirect) bioautography of *P. betle* L. leaf ethanol extracts against MRSA, VRE, MβL-*A. baumannii*, and CRE-*K. pneumoniae*.

separated by TLC, against bacteria that grow directly on the TLC plate. This particular assay has the advantages of being cost-effective, rapid, uncomplicated, requiring a simple set-up, a small amount of test sample, and simple interpretation of results, and associated with a high sample output.

3.3. GC-MS Analysis. Six volatile and semivolatile compounds in the *P. betle* leaf ethanol extracts were identified based on the comparison of their GC relative retention time and mass spectra with those of NIST MS Search Library Software version 2.0. The antimicrobial compounds identified include ethyl diazoacetate, 4-(2-propenyl)phenol, eugenol, tris(trifluoromethyl)phosphine, heptafluorobutyrate, and 3-fluoro-2-propynenitrite (Table 2). In a previous study on *P. betle* collected from various provinces in the Philippines, namely, La Union, Abra, Iloilo, Palawan, and Bukidnon, twenty compounds were identified as constituents of the plant leaf essential oil [4]. Eugenol is one of the compounds with the highest retention time, as similarly revealed in the result of the GC-MS analysis in our study. Another study of six Indian cultivars of *P. betle* revealed that out of several compounds identified in the leaf extracts eugenol likewise was found to be a common and major compound [18]. Eugenol has documented antibacterial activities against various plant

Table 2: GC-MS data of *P. betle* L. leaf ethanol extracts.

RT (min)	Compound name	Chemical formula
2.04	Heptafluorobutyrate	$C_4F_7NaO_2$
2.72	Ethyl diazoacetate	$C_4H_6N_2O_2$
5.69	4-(2-Propenyl)phenol	$C_9H_{10}O$
12.97	3-Fluoro-2-propynenitrite	C_3FN
8.15	Eugenol	$C_{10}H_{12}O_2$
35.21	Tris(trifluoromethyl)phosphine	C_3F_9P

and human pathogens, including an MRSA [19]. Its mechanism of action is reported to be the deformation of macromolecules in the cytoplasmic membrane as verified by FT-IR spectroscopy [20]. Therefore, the presence of high concentration of eugenol and eugenol isomers in the leaf extracts is a possible phytochemical characteristic feature among *P. betle* cultivars, pointing to the potential of the plant species and its cultivars as promising sources of these antimicrobial metabolites against human pathogens. The variation in the chemical composition of the *P. betle* extracts provides evidence that ecological conditions for growth greatly affect the bioactive properties and functions of the medicinal plant.

4. Conclusion

The results of this study confirmed the presence of various bioactive compounds in the Philippine variant of *P. betle*, responsible for its different physiological or therapeutic activities. We have identified two compounds via TLC-bioautography with R_f values 0.86 and 0.13 that showed significant activities against selected MDR bacteria. This result points to the potential development of novel therapeutic antimicrobial agents from *P. betle* capable of dealing with specific diseases or medical conditions that either have weakened reaction or are currently not responsive to existing drugs. Analysis through GC-MS has identified the volatile and semivolatile compounds present in the leaf ethanol extract. In-depth phytochemical analysis of the secondary metabolites in *P. betle*, that is, flavonoids, phenolic acids, alkaloids, terpenoids, and saponin, is underway. Future studies are directed towards the development of purified bioactive compounds and quantitative determination of safe concentrations that can be used to improve existing drugs or to create new agents against MDR bacteria.

Competing Interests

The authors declare that there are no competing interests regarding the publication of this paper.

Acknowledgments

The authors acknowledge Makati Medical Center and Ospital ng Makati, Makati City, Philippines, for the clinical bacterial isolates used in this study. This work was financially supported by the LVV Educational Research Foundation, Inc., to Demetrio L. Valle, Jr.

References

[1] D. Pradhan, K. Suri, and P. Biswasroy, "Golden heart of the nature: *Piper betle* L.," *Journal of Pharmacognosy and Phytochemistry*, vol. 1, no. 6, pp. 147–167, 2013.

[2] H. Annegowda, P. Tan, M. Mordi et al., "TLC-bioautography-guided isolation, HPTLC and GC-MS-assisted analysis of bioactives of piper betle leaf extract obtained from various extraction techniques: in vitro evaluation of phenolic content, antioxidant and antimicrobial activities," *Food Analytical Methods*, vol. 6, no. 3, pp. 715–726, 2013.

[3] K. Nagori, M. Singh, A. Alexander et al., "*Piper betle* L.: a review on its ethnobotany, phytochemistry, pharmacological profile and profiling by new hyphenated technique DART-MS (Direct Analysis in Real Time Mass Spectrometry)," *Journal of Pharmacy Research*, vol. 4, no. 9, pp. 2991–2997, 2011.

[4] A. Caburian and M. Osi, "Characterization and evaluation of antimicrobial activity of the essential oil from the leaves of *Piper betle* L," *E-International Scientific Research Journal*, vol. 2, no. 1, 2010.

[5] D. L. Valle Jr., J. I. Andrade, J. J. M. Puzon, E. C. Cabrera, and W. L. Rivera, "Antibacterial activities of ethanol extracts of Philippine medicinal plants against multidrug-resistant bacteria," *Asian Pacific Journal of Tropical Biomedicine*, vol. 5, no. 7, pp. 532–540, 2015.

[6] D. L. Valle Jr., E. C. Cabrera, J. J. M. Puzon, and W. L. Rivera, "Antimicrobial activities of methanol, ethanol and supercritical CO_2 extracts of Philippine *Piper betle* L. on clinical isolates of Gram positive and Gram negative bacteria with transferable multiple drug resistance," *PLoS ONE*, vol. 11, no. 1, Article ID e0146349, 2016.

[7] A. M. Rimando, B. H. Han, J. H. Park, and M. C. Cantoria, "Studies on the constituents of Philippine *Piper betle* leaves," *Archives of Pharmacal Research*, vol. 9, no. 2, pp. 93–97, 1986.

[8] M. Rajani, M. N. Ravishankara, N. Shrivastava, and H. Padh, "HPTLC-aided phytochemical fingerprinting analysis as a tool for evaluation of herbal drugs. A case study of ushaq (Ammoniacum gum)," *Journal of Planar Chromatography*, vol. 14, no. 1, pp. 34–41, 2001.

[9] A. Marston and K. Hostettmann, "Biological and chemical evaluation of plant extracts and subsequent isolation strategy," in *Bioassay Methods in Natural Product Research and Drug Development*, L. Bohlin and J. G. Bruhn, Eds., Kluwer Academic Publishers, New York, NY, USA, 1999.

[10] W. Nantitanon, S. Yotsawimonwat, and S. Okonogi, "Factors influencing antioxidant activities and total phenolic content of guava leaf extract," *LWT—Food Science and Technology*, vol. 43, no. 7, pp. 1095–1103, 2010.

[11] D. Basri and S. Fan, "The potential of aqueous and acetone extracts of galls of *Quercus infectoria* as antibacterial agents," *Indian Journal of Pharmacology*, vol. 37, no. 1, pp. 26–29, 2005.

[12] Clinical and Laboratory Standards Institute, "Performance standards for antimicrobial susceptibility testing," in *Proceedings of the 24th Informational Supplement*, M100-S24, Wayne, Pa, USA, 2014.

[13] D. E. Wedge and D. G. Nagle, "A new 2D-TLC bioautography method for the discovery of novel antifungal agents to control plant pathogens," *Journal of Natural Products*, vol. 63, no. 8, pp. 1050–1054, 2000.

[14] I. Ahmad and F. Aqil, "In vitro efficacy of bioactive extracts of 15 medicinal plants against ESβL-producing multidrug-resistant

enteric bacteria," *Microbiological Research*, vol. 162, no. 3, pp. 264–275, 2007.

[15] S. A. Bhawani, M. N. Mohamad Ibrahim, O. Sulaiman, R. Hashim, A. Mohammad, and S. Hena, "Thin-layer chromatography of amino acids: a review," *Journal of Liquid Chromatography and Related Technologies*, vol. 35, no. 11, pp. 1497–1516, 2012.

[16] S. R. Biradar and B. D. Rachetti, "Extraction of some secondary metabolites &thin layer chromatography from different parts of *Centella asiatica* L. (URB)," *American Journal of Life Sciences*, vol. 1, no. 6, pp. 243–247, 2013.

[17] K. Karthika, S. Jamuna, and S. Paulsamy, "TLC and HPTLC fingerprint profiles of different bioactive components from the tuber of *Solena amplexicaulis*," *Journal of Pharmacognosy and Phytochemistry*, vol. 3, no. 1, pp. 198–206, 2014.

[18] A. K. S. Rawat, R. D. Tripathi, A. J. Khan, and V. R. Balasubrahmanyam, "Essential oil components as markers for identification of *Piper betle* L. cultivars," *Biochemical Systematics and Ecology*, vol. 17, no. 1, pp. 35–38, 1989.

[19] G. Horváth, N. Jámbor, A. Végh et al., "Antimicrobial activity of essential oils: the possibilities of TLC-bioautography," *Flavour and Fragrance Journal*, vol. 25, no. 3, pp. 178–182, 2010.

[20] K. P. Devi, S. A. Nisha, R. Sakthivel, and S. K. Pandian, "Eugenol (an essential oil of clove) acts as an antibacterial agent against *Salmonella typhi* by disrupting the cellular membrane," *Journal of Ethnopharmacology*, vol. 130, no. 1, pp. 107–115, 2010.

Hindawi Publishing Corporation
Evidence-Based Complementary and Alternative Medicine
Volume 2016, Article ID 8692343, 7 pages
http://dx.doi.org/10.1155/2016/8692343

Research Article

Effect of *Kangfuxin* Solution on Chemo/Radiotherapy-Induced Mucositis in Nasopharyngeal Carcinoma Patients: A Multicenter, Prospective Randomized Phase III Clinical Study

Yangkun Luo,[1] Mei Feng,[1] Zixuan Fan,[1] Xiaodong Zhu,[2] Feng Jin,[3] Rongqing Li,[4] Jingbo Wu,[5] Xia Yang,[6] Qinghua Jiang,[1] Hongfang Bai,[1] Yecai Huang,[1] and Jinyi Lang[1]

[1]*Department of Radiation Oncology, Sichuan Cancer Hospital, Chengdu 610041, China*
[2]*Department of Radiation Oncology, Affiliated Cancer Hospital of Guangxi Medical University, Nanning 530021, China*
[3]*Department of Oncology, Guizhou Cancer Hospital, Affiliated Hospital of Guiyang Medical College, Guiyang 550003, China*
[4]*Department of Radiation Oncology, First Affiliated Hospital of Kunming Medical University, Kunming 650032, China*
[5]*Department of Oncology, Affiliated Hospital of Sichuan Medical University, Luzhou 646000, China*
[6]*Kelun Pharmaceutical Research Institute, Sichuan Kelun Pharmaceutical Co., Ltd., Chengdu 610071, China*

Correspondence should be addressed to Jinyi Lang; ljy610610@163.com

Received 27 October 2015; Accepted 29 December 2015

Academic Editor: Mohamed M. Abdel-Daim

Objective. To evaluate the efficacy and safety of *Kangfuxin* Solution, a pure Chinese herbal medicine, on mucositis induced by chemoradiotherapy in nasopharyngeal carcinoma patients. *Methods*. A randomized, parallel-group, multicenter clinical study was performed. A total of 240 patients were randomized to receive either *Kangfuxin* Solution (test group) or compound borax gargle (control group) during chemoradiotherapy. Oral mucositis, upper gastrointestinal mucositis, and oral pain were evaluated by Common Terminology Criteria for Adverse Events (CTCAE) v3.0 and the Verbal Rating Scale (VRS). *Results*. Of 240 patients enrolled, 215 were eligible for efficacy analysis. Compared with the control group, the incidence and severity of oral mucositis in the test group were significantly reduced ($P = 0.01$). The time to different grade of oral mucositis occurrence (grade 1, 2, or 3) was longer in test group ($P < 0.01$), and the accumulated radiation dose was also higher in test group comparing to the control group ($P < 0.05$). The test group showed lower incidence of oral pain and gastrointestinal mucositis than the control group ($P < 0.01$). No significant adverse events were observed. *Conclusion*. *Kangfuxin* Solution demonstrated its superiority to compound borax gargle on mucositis induced by chemoradiotherapy. Its safety is acceptable for clinical application.

1. Introduction

Mucositis refers to secondary mucosal damage in the oral cavity, pharynx, larynx, esophagus, or other parts of the gastrointestinal tract. It normally occurs during cancer treatment. Almost all head and neck cancer patients who receive radiotherapy experience mucositis [1]. Oral mucositis usually starts with mucosal inflammation, characterized by erythema, and fused ulcers [2]. The main clinical symptom includes pain that affects normal eating, with secondary effects such as dehydration, dysgeusia, and malnutrition. Patients with bone marrow suppression may manifest secondary infection that leads to mucositis [3]. Gastrointestinal mucositis is characterized by pain, nausea, vomiting, and diarrhea [4]. On the one hand, severe mucositis leads to chemotherapy dose reduction or radiotherapy interruption, which affects the prognosis [5, 6]. On the other hand, it also leads to a lower quality of life, weight loss, and prolonged hospitalization as well as additional analgesic treatment, parenteral nutrition, liquid replacement therapy, and drugs for the treatment and prevention of serious infections, which increase the economic burden of patients [7–10].

Nasopharyngeal carcinoma (NPC) is one of the most common head and neck cancers in South China [11]. Chemoradiotherapy is the standard treatment. The incidence of mucositis is 100% in patients receiving radiotherapy [12]. The main symptom is pain, and the pain grade gradually

rises with increasing radiation dose [13]. Since oral mucositis caused by chemoradiotherapy is "easy to diagnose, difficult to handle," several drugs aimed at preventing and treating mucositis have been reported in recent years. However, drugs with clear efficacy for clinical recommendation have yet to be developed or discovered [14]. *Kangfuxin* Solution is a pure Chinese herbal medicine that is extracted from the American cockroach. It has been shown that *Kangfuxin* Solution may reduce the pain and discomfort of patients after chemoradiotherapy by inhibiting radiation damage-induced opening of the calcium-dependent potassium channel, thus maintaining normal cell function [15]. It is also believed to improve neutrophil muscle actin function and increase the number of neutrophils after radiation injury [16]. In addition, it promotes the synthesis and secretion of extracellular matrix in the wound site [17], thus improving the healing of mucositis caused by radiation. However, previous studies were limited by poor study design or small sample sizes and were not prospective. Therefore, the current study used a multicenter, randomized, parallel-group trial design to evaluate the efficacy and safety of *Kangfuxin* Solution in chemoradiotherapy-induced mucositis in nasopharyngeal carcinoma patients.

2. Materials and Methods

2.1. Study Patients. In this study, a multicenter, randomized, parallel-group clinical trial was performed from August 2012 to June 2014, including 240 patients with nasopharyngeal carcinoma who received treatment for the first time at one of the five hospitals including Sichuan Cancer Hospital; First Affiliated Hospital of Kunming Medical University; Guizhou Cancer Hospital, The Affiliated Cancer Hospital of Guizhou Medical University; Affiliated Cancer Hospital of Guangxi Medical University; and Affiliated Hospital of Sichuan Medical University. The study was approved by the respective hospital Ethics Committees. All the included patients provided signed informed consent. This clinical study was registered at the Chinese Clinical Trial Registry (http://www.chictr.org.cn/) with the registration number ChiCTR-IPR-15006687.

The inclusion criteria for this study were as follows: (1) histopathologically diagnosed patients without metastases; (2) patients at clinical stages I–IVB of nasopharyngeal carcinoma, according to the American Joint Committee on Cancer, 7th edition (2010); (3) patients aged 18 to 70 years, either male or female; (4) patients who underwent radical chemoradiotherapy; (5) patients with a Karnofsky score ≥70 points; and (6) patients with an expected survival of at least 6 months.

The exclusion criteria were as follows: (1) pregnant women, nursing mothers, and other female patients who were contraindicated for contraceptives during the test; (2) patients who already had active oral diseases, including oropharyngeal candidiasis and facial herpes, or other oral diseases; (3) patients with stomatitis; (4) patients with residual or recurrent nasopharyngeal carcinoma; (5) patients with severe heart, liver, kidney, blood, or nervous system or psychiatric disorders; (6) patients treated with neoadjuvant or concurrent chemotherapy with 5-fluorouracil; (7) patients treated with molecular targeted therapy; (8) diabetic patients with uncontrolled blood glucose levels; (9) patients with drug allergies, either known or suspected by a drug allergy test; (10) patients with a history of alcohol and/or drug abuse; and (11) patients who had participated in clinical trials of other drugs within the past 3 months.

2.2. Drugs. *Kangfuxin* Solution was manufactured by Hunan Kelun Pharmaceutical Co., Ltd. (Yueyanglou District, China) (Zhunzhi: Z43020995, 100 mL/bottle, lot number: M1204191; shelf-life: 36 months). Compound borax gargle was manufactured by Yunjia Huangpu Pharmaceutical Co., Ltd., Shanghai, China (Zhunzi H31022772, 250 mL/bottle, batch number: 120,308; shelf-life: 24 months).

2.3. Study Design. A multicenter, randomized, and controlled clinical trial was designed. A total of 240 subjects were randomly assigned to the test group (120 patients) or the control group (120 patients). In the test group, patients first rinsed their mouth with water before treatment to clean the oral cavity, followed by slow swallowing of 10 mL of *Kangfuxin* Solution, after gargling for 3 to 5 min with bulging cheeks alternating with sucking. In the control group, the patients first rinsed their mouth with water before treatment to clean the oral cavity, gargling with 10 mL of compound borax gargle for 3–5 min with bulging cheeks alternating with sucking, and spitting it out. Both *Kangfuxin* Solution and the compound borax gargle were administered to the patients on the first day of chemoradiotherapy, three times a day, after breakfast, lunch, and supper, respectively, until the patients were diagnosed with grade 3 oral mucositis or the patients finished the entire course of radiotherapy.

If the patients were diagnosed with grades 0–2 oral mucositis, drugs (such as *Koutai*, chlorhexidine, povidone iodine gargle, topical recombinant human epidermal growth factor, topical recombinant human basic fibroblast growth factor, topical recombinant bovine basic fibroblast growth factor, or watermelon cream) other than *Kangfuxin* Solution or compound borax gargle were used to treat oral mucositis. Hormones, antibiotics, or other treatments were not used. Any patient who received any of the above-mentioned pain control medications was excluded from the study. If the patients acquired oral fungal infections, $NaHCO_3$ and antifungal agents were used for mouthwash, with proper documentation. If the patients had grade 2 pain, lidocaine was administered in the form of a mouthwash, with proper documentation.

2.4. Evaluation Criteria. Patients were monitored from the first day of chemotherapy or radiotherapy until the emergence of grade 3 oral mucositis. During the course of treatment, the subjects were examined for oral mucosal inflammation, including posterior pharyngeal mucosa, upper gastrointestinal mucositis, and oral pain rating using on Common Terminology Criteria for Adverse Events (CTCAE) v3.0 standards [18] and the VRS standard [19], every day from 8:00 to 10:00. The grades of oral mucositis, upper gastrointestinal mucositis, and oral pain were recorded. The radiation dose was recorded with the start and end times of radiotherapy, break time, the cumulative radiation dose, drug-related

adverse reactions, and withdrawal time. The primary end-point criteria for efficacy evaluation included the incidence of oral mucositis and change of grades during radiation; the secondary end-point criteria for efficacy evaluation included the incidence of gastrointestinal mucositis and a change in the grade of oral pain during radiotherapy.

2.5. Chemotherapy and Radiotherapy. All patients were treated with radical radiotherapy, using intensity modulated radiation therapy, with a dose of 66–74 Gy (2.1–2.3 Gy each time) for gross tumor volume (GTV), 60–70 Gy (2.0–2.2 Gy each time) for gross tumor volume in lymph node (GTVln), 60–66 Gy (1.8–2.0 Gy each time) for clinical target volume-1 (CTV-1), 54–60 Gy (1.8–2.0 Gy each time) for clinical target volume-2 (CTV-2), and 50 Gy (1.8–2.0 Gy each time) for neck prevention. All patients received five treatments per week. The accelerator dose rate and the accuracy of the beam in all participating hospitals were based uniformly on quality assurance, which was measured and monitored to ensure the reliability of patient radiation dose during treatment.

2.6. Randomization and Statistical Analysis. Random codes were generated by stratified block randomization, stratified by center, using SAS software. The random numbers generated by the computer were assigned to drugs by pharmacists. The drugs were sequentially distributed to subjects according to the time of enrollment. In all participating hospitals, a smaller random number was assigned to a patient enrolled earlier. The SAS statistical package was used for statistical analysis. The rank-sum test and the t-test were used to evaluate the treatment for the primary end-point criteria, while the H chi-squared test and rank-sum test were used to evaluate the treatment for the secondary end-point criteria. $P < 0.05$ was considered statistically significant.

3. Results

3.1. Demographic Characteristics. A total of 240 patients were enrolled in this trial, including 120 in the test group and 120 in the compound borax gargle group. Twenty-five patients withdrew during the trial, and therefore data from 215 cases were eventually evaluated. The demographic data are listed in Table 1. The test and control groups were similar in terms of gender, age, height, weight, Karnofsky score, past medical history, allergies, staging, chemotherapy programs, and treatment time. The differences between the two groups were not statistically significant ($P > 0.05$).

3.2. Efficacy

3.2.1. Incidence, Timing, and Grade of Oral Mucositis. Compared with the control group, the incidence and grade of oral mucositis were significantly lower in the test group ($P = 0.0084$; Table 2). The incidence of grade 3 oral mucositis in the test and control groups was 40.19% and 53.70%, respectively. Comparing the grades of oral mucositis in the two groups, during the trial as well as at the end of the trial, the test drug was found to reduce the severity of oral mucositis ($P = 0.0098$; Table 3).

The test group delayed the occurrence of oral mucositis. The time between start of chemoradiotherapy and occurrence of grade 1, 2, or 3 oral mucositis was significantly different between the two groups ($P < 0.0001$, $P = 0.0014$, and $P = 0.0001$, resp.; Table 4).

When the same grade of mucositis occurred, the cumulative radiation dose in the test group was significantly greater than in the control group ($P < 0.0001$, $P = 0.0377$, and $P < 0.0001$, resp.; Table 5).

3.2.2. Incidence of Upper Gastrointestinal Mucositis and Oral Pain. Compared with the control group, the test group showed a reduced incidence and grade of gastrointestinal mucositis ($P < 0.0001$). Comparison of patients complaining of the highest level of oral pain between the two groups showed that the test drug reduced the incidence of high-grade oral pain. The difference between the two groups was statistically significant ($P = 0.0003$) (Table 6).

3.3. Safety Evaluation. A total of 108 cases (90.0%) of adverse events occurred in the test group, compared with 103 cases (85.3%) in the control group. However, using the chi-squared test for the incidence of adverse events in both groups, the difference was not statistically significant ($P = 0.3221$). Neither group experienced serious adverse events. The severity and outcome of adverse events in the two groups were not significantly different ($P = 0.1383$; $P = 0.5732$).

4. Discussion

Radiotherapy is the main treatment for NPC. For most patients with locoregionally advanced NPC, treatment includes chemotherapy, leading to further aggravation of oral mucositis. Almost 100% of such patients suffer from varying grades of mucositis [20]. Mucositis is considered the most painful side effect of radiotherapy, and approximately 15% of patients require hospitalization [21]. In addition, it also compromises the tolerance of normal tissue to radiation, thus limiting the radiation dose [22, 23]. Further, mucositis affects the efficacy of chemoradiotherapy and even leads to patient withdrawal. Recent studies have shown that abandonment or interruption of radiotherapy increases the number of residual tumor cells, the risk of recurrence, and metastasis, thus reducing the patient survival rate [24].

Radiation-induced mucositis involves a five-step mechanism [25]: (1) radiation first induces necrosis or apoptosis of epithelial cells and destruction of their compensation through proliferation, resulting in epithelial damage [26]; (2) severe damage is caused by the following mechanism [27]: oxidative stress, leading to cell, tissue, and vascular injury; (3) reactive oxygen may activate second messengers (such as nuclear transcription factor NF-κB), proinflammatory cytokines (such as tumor necrosis factor-α and interleukin 6), and metabolic byproducts in the microenvironment; (4) radiation or anticancer drugs cause saliva loss, which reduces the protective effect of the mucosal surface; and (5) chemoradiotherapy reduces the number of neutrophil cells, thus decreasing immunity [28].

Table 1: Demographics and baseline characteristics of the efficacy population N (%).

Characteristics	Test group	Control group	P
Gender			
F	70 (65.4)	83 (76.9)	0.064*
M	37 (34.6)	25 (23.2)	
Age	46.3 ± 11.0	48.0 ± 10.0	0.241***
Height (cm)	162.4 ± 7.7	163.4 ± 6.9	0.283***
Weight (kg)	59.3 ± 10.9	61.7 ± 10.5	0.100***
Allergic history			
No	102 (95.3)	105 (97.2)	0.499**
Yes	5 (4.7)	3 (2.8)	
Clinical stage			
I/II	12 (11.2)	18 (16.7)	0.649**
III/IV	95 (88.8)	90 (83.3)	
KPS			
100	3 (2.8)	3 (2.8)	
90	96 (89.7)	92 (85.2)	0.629**
80	8 (7.5)	12 (11.1)	
70	0 (0.00)	1 (0.92)	
TX			
XRT	3 (2.8)	8 (7.4)	0.126*
CRT	104 (97.2)	100 (92.6)	
TX time (day)	48.3 ± 37.3	43.6 ± 41.5	0.388***
Medical history			
No	87 (81.3)	85 (78.7)	0.633*
Yes	20 (18.7)	23 (21.3)	
Existing history of disease			
No	93 (86.9)	95 (88.0)	0.817*
Yes	14 (13.1)	13 (12.0)	

*Chi-squared test.
**Fisher exact probability method.
***t-test.
M, male; F, female; TX, treatment; XRT, radiotherapy; CRT, chemoradiotherapy.

Table 2: Comparison of incidence of oral mucositis at the end of trial N (%).

Group	G0	G1	G2	G3	P*
Test group (107)	5 (4.7)	26 (24.3)	33 (30.8)	43 (40.2)	0.0084
Control group (108)	0 (0.0)	15 (13.9)	35 (32.4)	58 (53.7)	

*Rank-sum test.
G, grade.

Table 3: Change in oral mucosa grade during the trial N (%)*.

Group	No change	Reducing 1 grade	P**
Test group (107)	96 (89.7)	11 (10.3)	0.0098
Control group (108)	106 (98.2)	2 (1.9)	

*Change refers to the highest grade of oral mucosa during the treatment subtracted from the oral mucosal grade at the end of treatment.
**Rank-sum test.

Kangfuxin Solution promotes the growth of granulation tissue and angiogenesis, accelerates shedding of necrotic tissue, and repairs all kinds of ulcers and wound surfaces. It acts as an anti-inflammatory agent by eliminating inflammatory edema. In addition, it improves the phagocytic capacity of macrophages and lymphocytes, increases serum lysozyme activity, enhances immunity, and regulates physiological equilibration and homeostasis. Studies on rats have shown that *Kangfuxin* Solution increases the number and function of neutrophils after simple trauma or radiation-induced

Table 4: Time to occurrence of oral mucositis (days).

Grade	Group	Number	Mean	SD	P^*
G1	Test group	106	18.6	8.1	<0.0001
	Control group	108	14.5	6.5	
G2	Test group	83	28.0	8.3	0.0014
	Control group	95	23.7	9.2	
G3	Test group	43	36.9	7.7	0.0002
	Control group	58	30.5	8.8	

*t-test.
SD, standard deviation.

Table 5: Cumulative radiation dose of occurrence of oral mucositis (Gy).

Grade	Group	Number	Mean	SD	P^*
G1	Test group	106	27.9	11.0	<0.0001
	Control group	108	22.1	8.9	
G2	Test group	82	42.0	11.0	0.0377
	Control group	95	37.3	18.7	
G3	Test group	43	56.2	10.2	<0.0001
	Control group	58	46.0	12.1	

*t-test.
SD, standard deviation.

wound. It also promotes synthesis of extracellular matrix and secretion in skin wounds caused by simple trauma or radiation damage [17]. Further, Chen et al. [16] reported that radiation-induced neutrophil actin dysfunction results in reduced neutrophil phagocytic activity as well as decreased wound neutrophil numbers and function. These effects delay healing after whole-body irradiation. *Kangfuxin* Solution restores actin function in neutrophils, thus increasing the neutrophil population in the wound. Ye et al. [29] have shown that the differences in membranous ion channel activity in peritoneal macrophages between *Kangfuxin* Solution-treated and control groups were not significant. However, *Kangfuxin* Solution activated opening of the anion channel partially in the irradiated group, reversing the inhibition after exposure to ionizing radiation [30]. *Kangfuxin* Solution inhibits the opening of calcium-dependent potassium channels after radiation damage, helping to maintain normal cell function. These effects may promote wound healing [15].

According to 2013 Multinational Association for Cancer Support Treatment (MASCC)/International Association of Oral Cancer (ISOO) guidelines for secondary mucositis after cancer treatment [31], treatments for mucositis include laser therapy, cryotherapy, and drug therapy, which involve cell growth factors, anti-inflammatory drugs, antibiotics, coating agent narcotic analgesics, and natural medicine. KGF-1 is so far the only Federal Drug Administration-approved drug for the prevention of oral mucositis, but it is suitable for blood cancer [32]. *Xiaoyanling* gargle can be used for prophylaxis of moderate head and neck cancer- (<50 Gy) induced oral mucositis, but it is only indicated for radiotherapy [31]. Laser therapy and cryotherapy are difficult to administer in clinical practice. Amifostine is recommended for treating gastrointestinal mucositis intravenously. Compound borax gargle contains borax, sodium bicarbonate, liquefied phenol, and glycerol. Glycerol has a protective effect on the oral mucosa. In addition, it also reacts with borax and sodium bicarbonate to produce glycerin sodium borate, which enhances the drug efficacy. Since compound borax gargle is the most commonly used gargle for treating oral mucositis, it was selected as the control drug in this study.

The study showed that the incidence of oral mucositis was significantly lower in test group ($P = 0.0084$). The incidence of grade 3 mucositis in the test and control groups was 40.19% and 53.70%, respectively. According to the definition of continuous ulcers or the pseudomembranes based on CTCAE v3.0, bleeding caused by small abrasions results in grade 3 mucositis. Patients often cannot eat orally, requiring hormone and antibiotic treatment, leading to radiotherapy interruption. Therefore, *Kangfuxin* Solution reduces the incidence of all levels of mucositis, especially high-grade mucositis, to improve patient's tolerance to radiation, ensuring the continuity of radiotherapy. These findings were consistent with previous studies. However, in contrast to previous studies, our trial used compound borax gargle as the control drug. The preventative effect of the control drug against mucositis was reported to be stronger than the methods used in the literature, such as the compound rinse oral fluid (0.9% NaCl + gentamicin + dexamethasone + Vitamin B_{12}) [30], 0.2% chlorhexidine tinidazole peptide [33], or mouthwash gargle (0.9% NaCl + gentamicin + dexamethasone + lidocaine + Vitamin B) [34]. Thus, *Kangfuxin* Solution significantly reduced the incidence of mucositis, compared with the current methods commonly used clinically. In this study, grade 3 mucositis was selected as the end-point because we primarily focused on prevention. Comparing the grades of oral mucositis in the two groups, during the trial as well as at the end of the trial, the test drug also was shown to reduce the severity of oral mucositis ($P = 0.0098$). This result suggested that *Kangfuxin* Solution was effective in reducing the incidence of high-grade mucositis. Severe mucositis is normally treated with hormones and antibiotics. Therefore, the therapeutic role of *Kangfuxin* Solution in severe mucositis needs further investigation.

Data from the trial showed that *Kangfuxin* Solution significantly delayed the time of occurrence of oral mucositis at all levels. The times of occurrence of grades 1, 2, and 3 mucositis were 18.59 ± 8.13 d, 27.98 ± 8.30 d, and 36.88 ± 7.68 d in the test group and 14.48 ± 6.51 d, 23.68 ± 9.22 d, and 30.48 ± 8.84 d in the control group, respectively ($P < 0.0001$, $P = 0.0014$, and $P = 0.0001$, resp.). In addition, the use of *Kangfuxin* Solution allowed the increase of cumulative radiation dose with the emergence of mucositis at grades 1, 2, and 3 ($P < 0.0001$, $P = 0.0377$, and $P < 0.0001$, resp.). Previous studies reported similar results. Peng [35] administered *Kangfuxin* Solution through inhalation to prevent radiotherapy-induced oropharyngeal mucosal reaction in 108 cases in the test group compared with 90 cases in the control group, treated with an anti-inflammatory mouthwash. The results showed that the occurrence of oral mucositis was delayed. Wang et al. [36] used *Kangfuxin* Solution to treat 37 NPC patients with radiation-induced oral mucosa damage. The Vitamin B_{12} and *Kangfuxin* Solution-treated group tolerated a significantly

Table 6: Incidence of upper gastrointestinal mucositis and oral pain.

Group	G0	G1	G2	G3	P^*
Upper gastrointestinal mucositis					
Test group (107)	33 (30.8)	36 (33.6)	35 (32.7)	3 (2.8)	<0.0001
Control group (108)	9 (8.3)	36 (33.3)	58 (53.7)	5 (4.6)	
Oral pain					
Test group (107)	12 (11.2)	43 (40.2)	49 (45.8)	3 (2.8)	0.0003
Control group (108)	1 (0.9)	30 (27.8)	73 (67.6)	4 (3.7)	

*Rank-sum test.

higher radiation dose for the same level of oral mucosal damage. Therefore, *Kangfuxin* Solution increased patients' tolerance to increased radiation dose for similar grade of oral mucositis to enable patient adherence to the complete course of radiotherapy. Therefore, treatment with *Kangfuxin* Solution may affect the prognosis. However, a follow-up study needs to be performed to confirm this hypothesis.

In this trial, VRS was used to evaluate oral pain. *Kangfuxin* Solution reduced the incidence of high-grade oral pain compared with the control group. Oral pain prevents feeding and affects the patients' general physiological condition. It requires additional analgesic treatments, parenteral nutrition, and liquid alternative therapy [7–10]. More importantly, patients often suffer from a psychological burden resulting in higher chances of treatment nonadherence due to subjective factors. *Kangfuxin* Solution reduces oral pain and increases patient compliance. *Kangfuxin* Solution can be either used as a mouth rinse or swallowed. As a secondary efficacy endpoint in this study, we also examined whether *Kangfuxin* Solution reduced the incidence of gastrointestinal mucositis. The results showed that *Kangfuxin* Solution reduced the incidence of upper gastrointestinal mucositis in the test group, compared with the control group ($P < 0.0001$), suggesting a potential role in the prevention and treatment of gastrointestinal inflammation. However, this efficacy of Kangfuxin Solution still needs to be confirmed by rigorous clinical trials.

No serious adverse events were observed during the trial. The rate of adverse events, adverse event severity, and outcome were not significantly different between the test and control groups. These data suggest that the safety of *Kangfuxin* Solution is not a concern in clinical practice. Due to the user-friendly approach via mouth rinsing, the patient may generally show a better compliance than other treatments.

The drawbacks of this trial include the following: (1) lack of consensus on the evaluation of efficacy for the treatment of mucositis, due to which the current trial was designed to test for general differences rather than superiority; (2) relatively small sample size and short observation period used in this trial failure to evaluate the long-term toxicity of *Kangfuxin* Solution and the prognosis of NPC patients following treatment; and (3) exclusion of 5-fluorouracil- (5-FU-) treated cases, even though 5-FU is one of the most commonly used chemotherapy drugs for nasopharyngeal carcinoma. The results do not indicate whether *Kangfuxin* Solution can be used in combination with 5-FU to treat patients with nasopharyngeal carcinoma. Additional studies are needed to address the foregoing limitations.

In summary, *Kangfuxin* Solution effectively prevents chemoradiotherapy-induced oral mucositis, reduces the incidence of upper gastrointestinal inflammation, and decreases the severity of oral pain, compared with compound borax gargle. It improves the quality of life in patients. It is effective, user-friendly, safe, and appropriate for clinical application.

Conflict of Interests

The authors declare that there is no conflict of interests regarding the publication of this paper.

Acknowledgment

This study was funded by West China Society of Therapeutic and Radiation Oncology-RTOG, CSWOG-RTOG001.

References

[1] M. Vera-Llonch, G. Oster, M. Hagiwara, and S. Sonis, "Oral mucositis in patients undergoing radiation treatment for head and neck carcinoma," *Cancer*, vol. 106, no. 2, pp. 329–336, 2006.

[2] C. Scully, J. Epstein, and S. Sonis, "Oral mucositis: a challenging complication of radiotherapy, chemotherapy, and radiochemotherapy. Part 2: diagnosis and management of mucositis," *Head and Neck*, vol. 26, no. 1, pp. 77–84, 2004.

[3] N. Yarom, A. Ariyawardana, A. Hovan et al., "Systematic review of natural agents for the management of oral mucositis in cancer patients," *Supportive Care in Cancer*, vol. 21, no. 11, pp. 3209–3221, 2013.

[4] D. M. Keefe, "Intestinal mucositis: mechanisms and management," *Current Opinion in Oncology*, vol. 19, no. 4, pp. 323–327, 2007.

[5] L. S. Elting, C. Cooksley, M. Chambers, S. B. Cantor, E. Manzullo, and E. B. Rubenstein, "The burdens of cancer therapy: clinical and economic outcomes of chemotherapy-induced mucositis," *Cancer*, vol. 98, no. 7, pp. 1531–1539, 2003.

[6] A. Trotti, L. A. Bellm, J. B. Epstein et al., "Mucositis incidence, severity and associated outcomes in patients with head and neck cancer receiving radiotherapy with or without chemotherapy: a systematic literature review," *Radiotherapy and Oncology*, vol. 66, no. 3, pp. 253–262, 2003.

[7] L. S. Elting, D. M. Keefe, S. T. Sonis et al., "Patient-reported measurements of oral mucositis in head and neck cancer patients treated with radiotherapy with or without chemotherapy: demonstration of increased frequency, severity, resistance to palliation, and impact on quality of life," *Cancer*, vol. 113, no. 10, pp. 2704–2713, 2008.

[8] B. A. Murphy, J. L. Beaumont, J. Isitt et al., "Mucositis-related morbidity and resource utilization in head and neck cancer patients receiving radiation therapy with or without chemotherapy," *Journal of Pain and Symptom Management*, vol. 38, no. 4, pp. 522–532, 2009.

[9] L. S. Elting, C. D. Cooksley, M. S. Chambers, and A. S. Garden, "Risk, outcomes, and costs of radiation-induced oral mucositis among patients with head-and-neck malignancies," *International Journal of Radiation Oncology Biology Physics*, vol. 68, no. 4, pp. 1110–1120, 2007.

[10] N. J. Nonzee, N. A. Dandade, T. Markossian et al., "Evaluating the supportive care costs of severe radiochemotherapy-induced mucositis and pharyngitis," *Cancer*, vol. 113, no. 6, pp. 1446–1452, 2008.

[11] Q. Liu, J.-O. Chen, Q.-H. Huang, and Y.-H. Li, "Trends in the survival of patients with nasopharyngeal carcinoma between 1976 and 2005 in Sihui, China: a population-based study," *Chinese Journal of Cancer*, vol. 32, no. 6, pp. 325–333, 2013.

[12] Y. Wang, G. Chen, W. Liu et al., "Clinical analysis of 479 cases of oral mucosa caused by radiotherapy for nasopharyngeal carcinoma," *People's Military Surgeon*, vol. 55, no. 8, pp. 758–759, 2012.

[13] J. Wang, F. Wang, and L. Kong, "Efficacy of rhGM-CSF in treatment of radiation induced oral mucosa," *Shandong Medical Journal*, vol. 49, no. 6, pp. 99–100, 2009.

[14] W. Parulekar, R. Mackenzie, G. Bjarnason, and R. C. K. Jordan, "Scoring oral mucositis," *Oral Oncology*, vol. 34, no. 1, pp. 63–71, 1998.

[15] Y. W. Wang, "Research and analysis of gastric cancer and study on inhibition of apoptosis of cell growth of gastric cancer by Kangfuxin Liquid and Rayport tablets," *China Journal of Clinical Medicine Hygiene*, vol. 4, no. 8, article 33, 2006.

[16] X. Chen, T. Chen, G. Ai et al., "Effects of system irradiation and W_{11}-a_{12} on neutrophils in wounds," *Journal of Third Military Medical University*, vol. 23, no. 3, pp. 287–289, 2001.

[17] C. Shu and T. Chen, "Study of the heal-promoting ef fect of kangfuxin on full thickness dermal wound and dermal wound complicated with systemic gamma ray radiation in rats," *Journal of Third Military Medical University*, vol. 21, pp. 64–168, 1999.

[18] National Cancer Institute.Common terminology criteria for adverse events v3.0 (CTCAE), 2006, http://ctep.cancer.gov/protocolDevelopment/electronic_applications/docs/ctcaev3.pdf.

[19] A. Williamson and B. Hoggart, "Pain: a review of three commonly used pain rating scales," *Journal of Clinical Nursing*, vol. 14, no. 7, pp. 798–804, 2005.

[20] A. Rodríguez-Caballero, D. Torres-Lagares, M. Robles-García, J. Pachón-Ibáñez, D. González-Padilla, and J. L. Gutiérrez-Pérez, "Cancer treatment-induced oral mucositis: a critical review," *International Journal of Oral and Maxillofacial Surgery*, vol. 41, no. 2, pp. 225–238, 2012.

[21] M. A. Stokman, F. K. L. Spijkervet, H. M. Boezen, J. P. Schouten, J. L. N. Roodenburg, and E. G. E. De Vries, "Preventive intervention possibilities in radiotherapy- and chemotherapy-induced oral mucositis: results of meta-analyses," *Journal of Dental Research*, vol. 85, no. 8, pp. 690–700, 2006.

[22] S. T. Sonis, G. Oster, H. Fuchs et al., "Oral mucositis and the clinical and economic outcomes of hematopoietic stem-cell transplantation," *Journal of Clinical Oncology*, vol. 19, no. 8, pp. 2201–2205, 2001.

[23] G. Russo, R. Haddad, M. Posner, and M. Machtay, "Radiation treatment breaks and ulcerative mucositis in head and neck cancer," *Oncologist*, vol. 13, no. 8, pp. 886–898, 2008.

[24] N. S. Bese, J. Hendry, and B. Jeremic, "Effects o f prolongation of overall treatment time due to unplanned interruptions during radiotheray of different tumor sites and practical methods for compensation," *International Journal of Radiation Oncology Biology Physics*, vol. 68, no. 3, pp. 654–661, 2007.

[25] S. T. Sonis, "The pathobiology of mucositis," *Nature Reviews Cancer*, vol. 4, no. 4, pp. 277–284, 2004.

[26] P. B. Lockhart and S. T. Sonis, "Relationship of oral complications to peripheral blood leukocyte and platelet counts in patients receiving cancer chemotherapy," *Oral Surgery, Oral Medicine, Oral Pathology*, vol. 48, no. 1, pp. 21–28, 1979.

[27] N. Al-Dasooqi, S. T. Sonis, J. M. Bowen et al., "Emerging evidence on the pathobiology of mucositis," *Supportive Care in Cancer*, vol. 21, no. 7, pp. 2075–2083, 2013.

[28] A. Shih, C. Miaskowski, M. J. Dodd, N. A. Stotts, and L. MacPhail, "Mechanisms for radiation-induced oral mucositis and the consequences," *Cancer Nursing*, vol. 26, no. 3, pp. 222–229, 2003.

[29] B. Ye, C. Shu, T. Chen et al., "Effect of ionizing radiation and Kangfuxin on 3T3 cell membrane calcium dependent potassium channe," *Chinese Journal of Applied Physiology*, vol. 3, article 290, 2002.

[30] S. Wu, J. Wen, S. Wu et al., "Kangfuxin combined with thymus protein in prevention of acute radiation oral mucositis," *Chinese Journal of Medicine*, vol. 47, no. 8, pp. 60–61, 2012.

[31] R. V. Lalla, J. Bowen, A. Barasch et al., "MASCC/ISOO clinical practice guidelines for the management of mucositis secondary to cancer therapy," *Cancer*, vol. 120, no. 10, pp. 1453–1461, 2014.

[32] R. Spielberger, P. Stiff, W. Bensinger et al., "Palifermin for oral mucositis after intensive therapy for hematologic cancers," *The New England Journal of Medicine*, vol. 351, no. 25, pp. 2590–2598, 2004.

[33] H. Deng, "Clinical observation of kangfuxin in prevention and treatment of radiotherapy-induced oral mucositis," *Guide of China Medicine*, vol. 9, no. 34, article 196, 2011.

[34] X. Lao, "Effect of Kangfuxin Solution's prevention and treatment on radiotherapy-induced oral mucositi," *Youjiang Medical Journal*, vol. 38, no. 6, pp. 745–746, 2010.

[35] X. Peng, "Clinical observation of Kangfuxin treatment of oropharyngeal mucosa reaction caused by radiotherapy for nasopharyngeal carcinoma," *Journal of Guangzhou Medical College*, vol. 23, no. 3, p. 290, 2009.

[36] Z. Wang, Y. Gao, and Y. Zhang, "Study of Kangfuxin on the prevention and treatment of acute radiation injury," *Chinese Journal of Coal Industry Medicine*, vol. 11, no. 7, pp. 1010–1011, 2008.

Hindawi Publishing Corporation
Evidence-Based Complementary and Alternative Medicine
Volume 2016, Article ID 4579149, 7 pages
http://dx.doi.org/10.1155/2016/4579149

Research Article

Evaluation of Hepatoprotective Activity of *Adansonia digitata* Extract on Acetaminophen-Induced Hepatotoxicity in Rats

Abeer Hanafy,[1] Hibah M. Aldawsari,[2] Jihan M. Badr,[3] Amany K. Ibrahim,[4] and Seham El-Sayed Abdel-Hady[2]

[1] *Department of Pharmacology and Toxicology, Faculty of Pharmacy, King Abdulaziz University, Jeddah 21589, Saudi Arabia*
[2] *Department of Pharmaceutics, Faculty of Pharmacy, King Abdulaziz University, Jeddah 21589, Saudi Arabia*
[3] *Department of Natural Products and Alternative Medicine, Faculty of Pharmacy, King Abdulaziz University, Jeddah 21589, Saudi Arabia*
[4] *Department of Pharmacognosy, Faculty of Pharmacy, Suez Canal University, Ismailia 41522, Egypt*

Correspondence should be addressed to Jihan M. Badr; jihanbadr2010@hotmail.com

Received 20 November 2015; Accepted 16 February 2016

Academic Editor: Mario Giorgi

The methanol extract of the fruit pulp of *Adansonia digitata* L. (Malvaceae) was examined for its hepatoprotective activity against liver damage induced by acetaminophen in rats. The principle depends on the fact that administration of acetaminophen will be associated with development of oxidative stress. In addition, hepatospecific serum markers will be disturbed. Treatment of the rats with the methanol extract of the fruit pulp of *Adansonia digitata* L. prior to administration of acetaminophen significantly reduced the disturbance in liver function. Liver functions were measured by assessment of total protein, total bilirubin, ALP, ALT, and AST. Oxidative stress parameter and antioxidant markers were also evaluated. Moreover, histopathological evaluation was performed in order to assess liver case regarding inflammatory infiltration or necrosis. Animals were observed for any symptoms of toxicity after administration of extract of the fruit pulp of *Adansonia digitata* L. to ensure safety of the fruit extract.

1. Introduction

Modern food styles, excessive medications, and exposure to pollutants besides many other factors have led to many serious diseases including liver damage [1]. Production of reactive oxygen species is considered as a crucial factor leading to oxidative damage of tissues. They react with cell membrane; accordingly, many clinical disorders could be attributed to these free radicals [2]. Recently, herbal products have gained attention as a major part of alternative medicine [3, 4]. It is reported that a significant percentage of population depend on natural derived medicines for maintaining health and treatment of diseases [5]. Nowadays, discovery of new drug leads seems to focus on those of plant origin. Herbal drugs play a significant role in the regeneration of liver cells and acceleration of healing process and hence management of many liver disorders [2]. One of the comprehensive examples is silymarin isolated from *Silybum marianum*. Silymarin is a mixture of phenolic compounds (flavonolignans) well known for their radical scavenging activities and thus plays a role in prevention and treatment of oxidative damage caused by reactive oxygen species. Nowadays, silymarin is considered as a major component of many important pharmaceutical preparations in the market introduced for treatment of liver diseases [2, 6, 7]. Based on the fact that a tremendous number of plants could be considered as a gold mine for discovery of hepatoprotective agents, we launched our study in a trial to investigate the fruit pulp of *Adansonia digitata* L.

Our aim here is to discover naturally derived therapeutic agents with hepatoprotective effect. Our work will focus on *Adansonia digitata* L. (commonly known as baobab) which is a tree native to Central Africa and belongs to family Malvaceae. The pulp of baobab fruit is a very important food. It is used by dissolving in milk or in water.

This solution is used as a drink, in baking, or as a sauce for food. The pulp is considered as a popular ingredient in ice products [8]. Previous chemical investigation reported that *A. digitata* accumulates flavonoids, terpenoids, steroids, amino acids, vitamins, lipids, and carbohydrates [9]. The dry fruit pulp possesses high percentage of carbohydrates, thiamine, nicotinic acid, and vitamin C; additionally, it reveals potent free radical scavenging activity [8, 10, 11]. Previous reports also indicated that the fruit pulp extract exhibited numerous activities such as anti-inflammatory, analgesic, and antipyretic activities [12]. Since free radical scavenging and anti-inflammatory activities are crucial factors in management of liver damage, so this plant is suggested to be an efficient hepatoprotective agent. In our study, the fruit extract was tested for hepatoprotective activity against liver damage induced by acetaminophen in rats. Assessment of liver function was performed by determination of its specific serum markers as well as oxidative stress. The study is also supported by histopathological studies to check any necrosis and inflammatory infiltration.

2. Materials and Methods

2.1. Animals. Seventy male adult Wistar rats of 200–250 g body weight were used in the present study. The rats had free access to food and water. They were maintained at a 12 h light and 12-h dark cycle during the experiment and were allowed to acclimatize for 1 week before starting the experiment. The animal experiments had been approved by the National Committee of Biomedical Ethics, King Abdulaziz University, Jeddah, Saudi Arabia (reference number: 163-15).

2.2. Drugs. Acetaminophen and silymarin were purchased from Sigma, Egypt. Silymarin was given orally once a day for one week by gavage at a dose of 100 mg/kg [13]. *Adansonia digitata* extract (200 mg/kg) was given orally once daily for one week. Drugs and extract were suspended in distilled water.

2.3. Plant Material and Extract. The fruits were collected from Sudan and identified at Faculty of Science, King Abdulaziz University, and a voucher sample was deposited at Natural Products and Alternative Medicine Department, Faculty of Pharmacy, King Abdulaziz University, Jeddah, Saudi Arabia, under registration number AD-2014. The pulp was extracted with methanol (3 × 2000 mL) by maceration at room temperature. The combined methanol extracts were concentrated under reduced pressure and kept in refrigerator till use.

2.4. Acute Toxicity in Rats. To test the acute toxicity of *Adansonia digitata* extract, four groups of rats were used, six animals each. *A. digitata* extract was suspended in distilled water and administered orally once daily for one week at four different doses (200, 500, 1000, and 2000 mg/kg). Six rats served as control. During the first hour, rats were observed continuously and then every hour for 12 hours and then every day for one week, to detect any toxicity signs or mortality.

2.5. Acetaminophen-Induced Acute Hepatotoxicity. Acute hepatotoxicity was induced by acetaminophen (2 g/kg) orally on the fifth day, 30 min posttreatment [13, 14].

2.6. Experimental Design. Forty rats were divided into four groups of ten animals each ($n = 10$) and treated orally as follows:

Group-I (normal): it was used as normal control rats and they were given distilled water orally for seven days.

Group-II (acetaminophen): rats received distilled water orally daily for seven days; on the fifth day rats received oral dose of acetaminophen.

Group-III (acetaminophen + silymarin): rats received silymarin (100 mg/kg) orally daily for seven days; on the fifth day rats received oral dose of acetaminophen.

Group-IV (acetaminophen + extract): rats received extract (200 mg/kg) orally daily for seven days; on the fifth day rats received oral dose of acetaminophen.

On the seventh day, two hours after treatments [14], blood samples were obtained via retroorbital sinus plexus and then rats were sacrificed. Blood was left to clot at room temperature and the serum was obtained by centrifugation at 4000 rpm for 15 min and kept at −20°C for further biochemical analysis. Two portions of liver tissues were obtained. The first portion was immediately stored at −80°C till it was used for the different biochemical measurements, while the second portion was embedded in 10% formalin and processed for histopathological assay. Tissue sections of liver were stained with hematoxylin and eosin (H&E).

2.7. Measurement of Liver Function. To evaluate liver function, Alanine Amino Transaminase (ALT), Aspartate Amino Transaminase (AST), alkaline phosphatase (ALP), and total bilirubin were measured spectrophotometrically using commercial kit from BioMed Diagnostics (White City, OR, USA). Total protein was measured by a colorimetric method using a kit from Diamond Diagnostics (Cairo, Egypt) following the manufacturer's protocol.

2.8. Measurement of Lipid Peroxide (Measured as MDA). MDA was determined in liver homogenates spectrophotometrically as thiobarbituric acid reactive substances (TBARS) [15].

2.9. Measurement of Glutathione (GSH). GSH level was determined in the homogenates of liver following the method of Ellman [16].

2.10. Measurement of Superoxide Dismutase (SOD). SOD activity was measured according to the method of Marklund [17].

2.11. Measurement of Catalase Activity (CATA). The activity of catalase was measured in the homogenate of liver by spectrophotometer using CATA assay kits (Bio-Diagnostic, Egypt) as described by Aebi, 1984 [18].

Table 1: Effect of *Adansonia digitata* extract on serum liver enzymes (ALT, AST, and ALP), total bilirubin, and total protein in acetaminophen-induced liver damage in rats.

Group	Regimen	ALT (IU/L)	AST (IU/L)	ALP (IU/L)	Total Bilirubin (mg/dL)	Total Protein (mg/dL)
I	Normal	57.4 ± 0.32	80.3 ± 0.60	130.5 ± 0.25	1.27 ± 0.20	9.8 ± 0.33
II	Acetaminophen	190.3 ± 0.24*	123.5 ± 0.74*	220.8 ± 0.55*	3.29 ±0.90*	4.6 ± 0.67*
III	Acetaminophen + silymarin	60.6 ± 0.22#	89.4 ± 0.29#	145.9 ± 0.73#	1.77 ± 0.48#	7.8 ± 0.79#
IV	Acetaminophen + extract	65.4 ± 0.11#	95.6 ± 0.82#	150.7 ± 0.67#	2.00 ± 0.60#	6.9 ± 0.61#

Results were expressed as mean ± SD and analyzed using one-way ANOVA followed by Bonferroni's post hoc test.
* $P < 0.05$ compared to normal control group.
# $P < 0.05$ compared to acetaminophen group, $n = 10$.

2.12. Statistical Analysis. The obtained data were represented as mean ± standard deviation (SD). Comparisons between groups were performed using one-way analysis of variance (ANOVA) followed by Bonferroni's multiple comparison test [19]. All P values reported are two-tailed. $P < 0.05$ was considered statistically significant. The data were analyzed using the Statistical Package of Social Sciences (SPSS) program version 16.

3. Results

3.1. Acute Toxicity Study. After oral administration of *Adansonia digitata* extract for seven days, no mortalities were reported up to 2000 mg/kg, and hence 1/10th of the maximum dose administered (i.e., 200 mg/kg, p.o.) was selected for the present study.

3.2. Effect of Adansonia digitata Extract and Silymarin on Liver Functions Measured as ALT, AST, ALP, Bilirubin, and Total Protein. The results of the liver function tests are shown in Table 1. Administration of acetaminophen resulted in a significant ($P < 0.05$) elevation of hepatospecific serum markers ALT, AST, ALP, and total bilirubin. On the other hand, there was a significant reduction in the total protein in comparison with the normal control rats. These deleterious effects of acetaminophen were significantly ($P < 0.05$) alleviated by pretreatment with either silymarin or *Adansonia digitata* extract compared to the acetaminophen group. We did not find any significant difference between silymarin treated rats and *Adansonia digitata* extract treated rats (Table 1).

3.3. Effect of Adansonia digitata Extract and Silymarin on Acetaminophen-Induced Changes in Liver MDA, GSH, SOD, and CAT Activities. Acetaminophen-induced oxidative stress in liver was in the form of significant elevation ($P < 0.05$) of MDA levels associated with significant ($P < 0.05$) reduction in SOD, GSH activities, and CATA levels compared with the normal animals (Figures 1–4). These deleterious findings induced by acetaminophen administration were improved significantly ($P < 0.05$) upon treating the animals with either silymarin or *Adansonia digitata* extract compared to acetaminophen group. There was no significant difference between silymarin and *Adansonia digitata* extract treated groups, suggesting that *Adansonia digitata* extract has the same ameliorating effect as the standard reference drug silymarin (Figures 1–4).

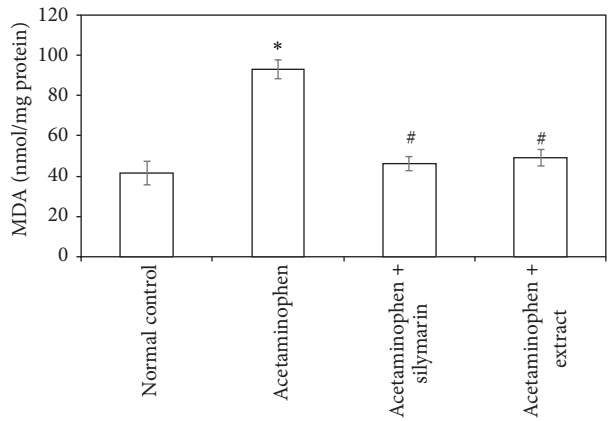

Figure 1: Effect of *Adansonia digitata extract* (200 mg/kg) and silymarin (100 mg/kg) on liver lipid peroxides (measured as MDA) concentration in acetaminophen-induced hepatotoxicity in rats. Each point represents the mean ± SD of ten rats. *Significant difference compared with the control group ($P < 0.05$). #Significant difference compared with the acetaminophen group ($P < 0.05$).

3.4. Histopathological Microscopic Study. The histopathologic study of liver tissues revealed that neither necrosis nor inflammation was noticed in the normal control animals which showed normal histologic structure with integrity of hepatic cells (Figure 5(a)). On the other hand, acetaminophen treated group showed necrosis of hepatic cells, inflammation, and lymphocytic infiltrations (Figure 5(b)). Pretreatment with silymarin showed nearly normal liver structure (Figure 5(c)). Pretreatment with *Adansonia digitata* extract showed parenchyma preservation of hepatocytes with mild necrosis and inflammation (Figure 5(d)).

4. Discussion

Liver is a large organ responsible for metabolism, detoxification, and protein synthesis [20, 21]. Drug-induced hepatotoxicity is one of the major causes of human mortality all over

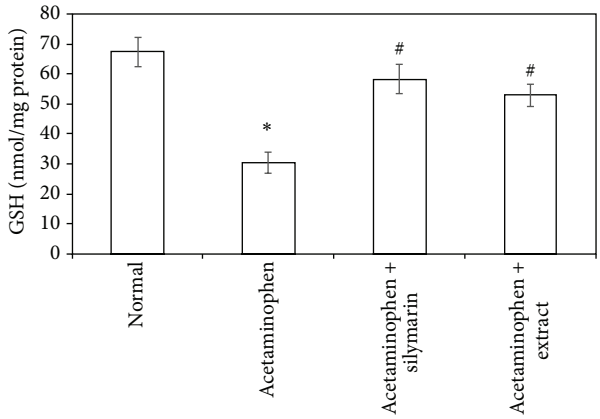

Figure 2: Effect of *Adansonia digitata extract* (200 mg/kg) and silymarin (100 mg/kg) on glutathione (GSH) level in acetaminophen-induced hepatotoxicity in rats. Each point represents the mean ± SD of ten rats. *Significant difference compared with the control group ($P < 0.05$). #Significant difference compared with the acetaminophen group ($P < 0.05$).

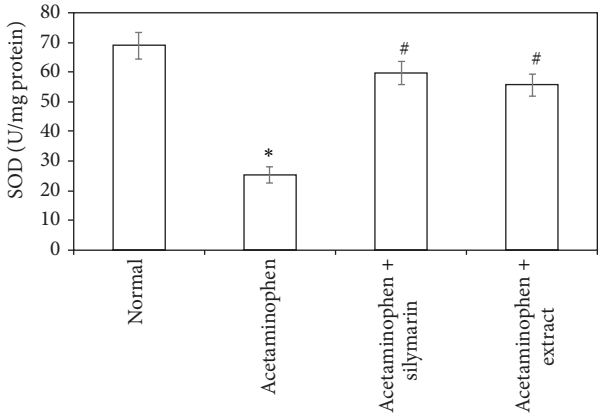

Figure 3: Effect of *Adansonia digitata extract* (200 mg/kg) and silymarin (100 mg/kg) on superoxide dismutase (SOD) activity in acetaminophen-induced hepatotoxicity in rats. Each point represents the mean ± SD of ten rats. *Significant difference compared with the control group ($P < 0.05$). #Significant difference compared with the acetaminophen group ($P < 0.05$).

the world [22]. Protection against acetaminophen-induced toxicity has been used as a test for a potential hepatoprotective agent by several investigators [23–26].

Acetaminophen is a common analgesic-antipyretic drug. It is safe in therapeutic doses. Many studies demonstrated the induction of necrosis of hepatic cells by high doses of acetaminophen in animals [2]. After high dosage of acetaminophen, it is extensively metabolized into N-acetyl-p-benzoquinoneimine (NAPQI) which depletes GSH and leads to hepatotoxicity [13, 14]. Acetaminophen is also shown to directly inhibit cellular proliferation, induce oxidative stress, resulting in lipid peroxidation, deplete ATP levels, and alter Ca++ homeostasis; all of these changes are considered potentially fatal to the cell [27, 28].

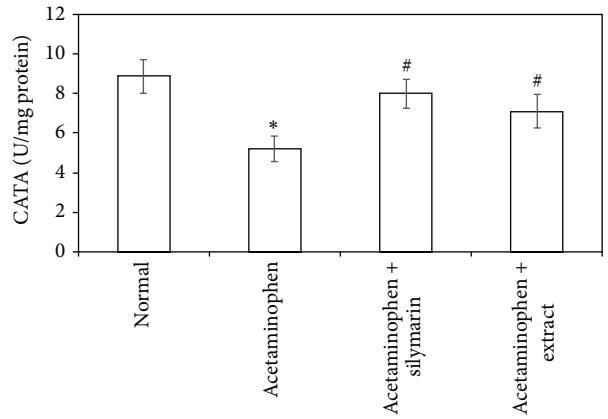

Figure 4: Effect of *Adansonia digitata extract* (200 mg/kg) and silymarin (100 mg/kg) on liver catalase activity (CATA) measured in acetaminophen-induced hepatotoxicity in rats. Each point represents the mean ± SD of ten rats. *Significant difference compared with the control group ($P < 0.05$). #Significant difference compared with the acetaminophen group ($P < 0.05$).

To evaluate liver injury, biochemical markers (ALT, AST, and ALP activity and serum bilirubin) levels are measured [29, 30]. In our study the hepatotoxicity due to acetaminophen was confirmed by elevated levels of biochemical parameters like ALT, AST, ALP, and total serum bilirubin with significant reduction in the total protein. This can be explained by the fact that hepatic cells contain a host of enzymes and possess a variety of metabolic activities. ALT was found in higher concentration in cytoplasm and AST particularly in mitochondria. The rise in the ALT is usually accompanied by an elevation in the levels of AST, which play a vital role in the conversion of amino acids to keto acids [31]. In hepatotoxicity the transport function of liver cells is disturbed, causing leakage of plasma membrane [32], therefore resulting in leakage of these enzymes leading to an increase in their serum level. The increased level of ALT and AST in acetaminophen-induced liver injury is an indicator of cellular leakage and loss of membrane integrity of liver cells [33]. Treatment with either silymarin or extract reversed the increased levels of ALT and AST as a result of the stabilization of plasma membrane and the repair of hepatic cell damage induced by acetaminophen [13, 27, 28].

The elevated serum level of alkaline phosphatase is due to its increased synthesis by bile canaliculi cells lining in response to the increased biliary pressure and cholestasis [27, 28]. Hyperbilirubinemia was due to excessive heme destruction and block of bile duct within the liver. Accordingly, there is a mass inhibition of the conjugation reaction and release of unconjugated bilirubin from damaged hepatocytes. Pretreatment with either silymarin or extract effectively controlled alkaline phosphatase activity and bilirubin level that point towards an enhancement in the hepatic cell secretary mechanism [2, 13, 30].

Total protein decreased level is a an indicator of liver damage due to significant fall in protein synthesis. Hypoproteinemia was observed after acetaminophen administration

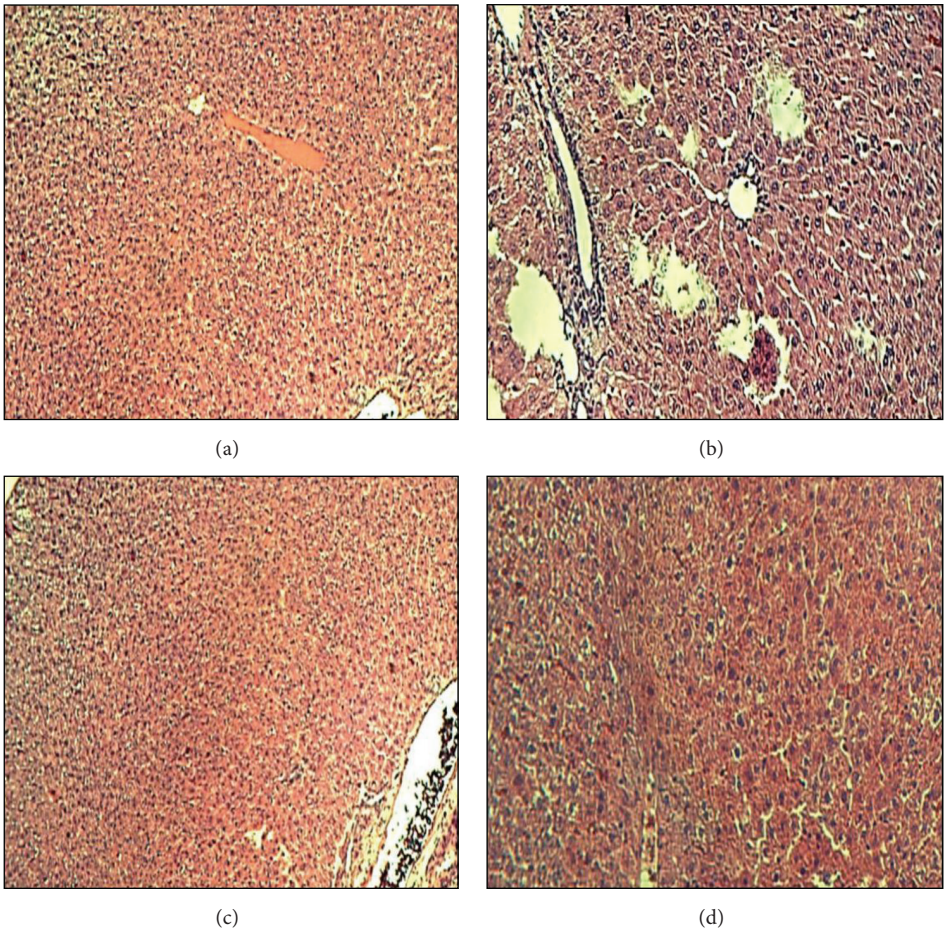

Figure 5: Histopathological study of liver tissue in control, acetaminophen, silymarin, and *Adansonia digitata* extract groups of rats. (a) Control group showed normal liver architecture (H&E ×40). (b) Acetaminophen group showed marked hepatic cell necrosis and moderate inflammation and lymphocytic infiltrations (H&E ×40). (c) Acetaminophen + Silymarin (100 mg/kg) showed nearly normal liver structure (H&E ×100). (d) Acetaminophen + *Adansonia digitata extract* (200 mg/kg) showed mild necrosis and inflammation (H&E ×100).

but the level turns towards normal upon pretreatment with either silymarin or extract.

Oxidation of lipids has been suggested for acetaminophen-induced liver injury. In agreement with previous studies [2, 13], we have found an elevation in MDA levels and depletion in antioxidant activity of SOD, CATA, and GSH. The elevated MDA in liver indicates failure of antioxidant defense mechanisms [34]. Pretreatment with silymarin or extract significantly restored these effects. The body defense mechanism prevents cell damage induced by free radicals [28]. This is established by the endogenous antioxidant enzymes, such as GSH, SOD, and CATA [35]. If there is no balance between the production of ROS and antioxidant defenses, oxidative stress results and leads to cell damage. Any compound that has antioxidant properties can prevent or alleviate this damage [28]. In our study, decreased levels of GSH, SOD, and CATA, observed in acetaminophen treated rats, are an indication of tissue damage produced by free radicals. The increase in the concentration of these antioxidant enzymes in liver tissues of silymarin- or extract-treated animals indicates antioxidant effect of silymarin and extract.

The histopathological findings confirmed the biochemical results. Rats that were treated with acetaminophen showed necrosis of hepatocytes which was manifested by disappearance of nuclei and aggregation of inflammatory cells. This may be a result of the formation of free radicals and oxidative stress induced by acetaminophen. These histopathologic findings were ameliorated significantly in the group of rats that were treated with either silymarin or *Adansonia digitata* extract.

Silymarin and *Adansonia digitata* extract showed similar hepatoprotective effect in the present study. The possible mechanism of hepatoprotection offered by silymarin is due to its high phenolic content which has been known to contribute to the antioxidant activity [2, 6, 7]. Our results on the extract are compatible with previous reports of chemical investigation of *Adansonia digitata* which reported that it accumulates flavonoids, terpenoids, steroids, amino acids, vitamins, lipids, and carbohydrates [9], while the dry fruit pulp possesses high percentage of carbohydrates, thiamine, nicotinic acid, and vitamin C. Accordingly, it is possible that the mechanism of hepatoprotective effect of extract might be

due to its antioxidant effect which is attributed to its content of vitamin C and the flavonoids that are well known for potent free radical scavenging activity and enhancement of the antioxidant defense system. Moreover, the steroid content with their anti-inflammatory activity can play a significant role in the hepatoprotective effect of the extract.

5. Conclusions

Our study suggested a significant protective effect of *Adansonia digitata* extract against acetaminophen-induced hepatotoxicity. *Adansonia digitata* extract exerts this protection through amelioration of lipid peroxidation by its scavenging activity of free radicals and enhancement of the antioxidant defense system.

Conflict of Interests

The authors declare that there is no conflict of interests regarding the publication of this paper.

Acknowledgments

This project was funded by the Deanship of Scientific Research (DSR), King Abdulaziz University, Jeddah, under Grant no. 166/896/D1435. The authors, therefore, acknowledge with thanks DSR technical and financial support.

References

[1] A. A. Elberry, F. M. Harraz, S. A. Ghareib et al., "Antihepatotoxic effect of *Marrubium vulgare* and *Withania somnifera* extracts on carbon tetrachloride—induced hepatotoxicity in rats," *Journal of Basic and Clinical Pharmacy*, vol. 1, no. 4, pp. 247–254, 2010.

[2] D. K. Dash, V. C. Yeligar, S. S. Nayak et al., "Evaluation of hepatoprotective and antioxidant activity of *Ichnocarpus frutescens* (Linn.) R.Br. on paracetamol-induced hepatotoxicity in rats," *Tropical Journal of Pharmaceutical Research*, vol. 6, no. 3, pp. 755–765, 2007.

[3] R. Ahmad, S. P. Srivastava, R. Maurya, S. M. Rajendran, K. R. Arya, and A. K. Srivastava, "Mild antihyperglycaemic activity in *Eclipta alba*, *Berberis aristata*, *Betula utilis*, *Cedrus deodara*, *Myristica fragrans* and *Terminalia chebula*," *Indian Journal of Science and Technology*, vol. 1, no. 5, pp. 1–6, 2008.

[4] S. Bent, "Herbal medicine in the United States: review of efficacy, safety, and regulation: grand rounds at University of California, San Francisco Medical Center," *Journal of General Internal Medicine*, vol. 23, no. 6, pp. 854–859, 2008.

[5] A. Kintzios and E. Spiridon, "Terrestrial plant derived anticancer agents and plant species used in anticancer research," *Critical Reviews in Plant Sciences*, vol. 25, pp. 79–135, 2006.

[6] F. Fraschini, G. Demartini, and D. Esposti, "Pharmacology of silymarin," *Clinical Drug Investigation*, vol. 22, no. 1, pp. 51–65, 2002.

[7] J. Kucharská, O. Uličná, A. Gvozdjáková et al., "Regeneration of coenzyme Q9 redox state and inhibition of oxidative stress by Rooibos tea (*Aspalathus linearis*) administration in carbon tetrachloride liver damage," *Physiological Research*, vol. 53, no. 5, pp. 515–521, 2004.

[8] E. De Caluwé, K. Halamová, and P. Van Damme, "*Adansonia digitata* L.—a review of traditional uses, phytochemistry and pharmacology," *Afrika Focus*, vol. 23, pp. 11–51, 2010.

[9] M. A. Osman, "Chemical and nutrient analysis of baobab (*Adansonia digitata*) fruit and seed protein solubility," *Plant Foods for Human Nutrition*, vol. 59, no. 1, pp. 29–33, 2004.

[10] S. Vertuani, E. Braccioli, V. Buzzoni, and S. Manfredini, "Antioxidant capacity of *Adansonia digitata* fruit pulp and leaves," *Acta Phytotherapeutica*, vol. 5, no. 2, pp. 1–7, 2002.

[11] A. A. Fagbohun, P. P. Ikokoh, M. O. Afolayan, O. O. Olajide, O. A. Fatokun, and F. T. Akanji, "Chemical composition and anti-oxidant capacity of the fruit pulp of *Adansonia digitata* L.," *International Journal of Applied Chemistry*, vol. 8, no. 3, pp. 165–172, 2012.

[12] A. Ramadan, F. M. Harraz, and S. A. El-Mougy, "Anti-inflammatory, analgesic and antipyretic effects of the fruit pulp of *Adansonia digitata*," *Fitoterapia*, vol. 65, no. 5, pp. 418–422, 1994.

[13] K. Biswas, A. Kumar, B. Babaria, K. Prabhu, and R. Setty, "Hepatoprotective effect of leaves of Peltophorum pterocarpum against paracetamol induced acute liver damage in rats ," *Journal of Basic and Clinical Pharmacy*, vol. 1, no. 1, pp. 10–15, 2010.

[14] S. Ramachandra Setty, A. A. Quereshi, A. H. M. Viswanath Swamy et al., "Hepatoprotective activity of *Calotropis procera* flowers against paracetamol-induced hepatic injury in rats," *Fitoterapia*, vol. 78, no. 7-8, pp. 451–454, 2007.

[15] H. G. Preuss, S. T. Jarrell, R. Scheckenbach, S. Lieberman, and R. A. Anderson, "Comparative effects of chromium, vanadium and gymnema sylvestre on sugar-induced blood pressure elevations in SHR," *Journal of the American College of Nutrition*, vol. 17, no. 2, pp. 116–123, 1998.

[16] G. L. Ellman, "SH groups determination in biological fluids," *Analytical Biochemistry*, vol. 46, pp. 237–240, 1970.

[17] S. L. Marklund, "Regulation by cytokines of extracellular superoxide dismutase and other superoxide dismutase isoenzymes in fibroblasts," *The Journal of Biological Chemistry*, vol. 267, no. 10, pp. 6696–6701, 1992.

[18] H. Aebi, "Catalase *in vitro*," *Methods in Enzymology*, vol. 105, pp. 121–126, 1984.

[19] M. Katz, *Study Design and Statistical Analysis: A Practical Guide for Clinicians*, Cambridge University Press, London, UK, 2006.

[20] R. Ahsan, K. M. Islam, A. Musaddik, and E. Haque, "Hepatoprotective activity of methanol extract of some medicinal plants against carbon tetrachloride induced hepatotoxicity in albino rats," *Global Journal of Pharmacology*, vol. 3, pp. 116–122, 2009.

[21] M. Angelico, B. Gridelli, and M. Strazzabosco, "Practice of adult liver transplantation in Italy: recommendations of the Italian Association for the Study of the Liver (A.I.S.F.)," *Digestive and Liver Disease*, vol. 37, no. 7, pp. 461–467, 2005.

[22] S. Bhawna and S. U. Kumar, "Hepatoprotective activity of some indigenous plants," *International Journal of PharmTech Research*, vol. 1, no. 4, pp. 1330–1334, 2009.

[23] Y. Dwivedi, R. Rastogi, N. K. Garg, and B. N. Dhawan, "Prevention of paracetamol-induced hepatic damage in rats by Picroliv, the standardized active fraction from *Picrorhiza kurroa*," *Phytotherapy Research*, vol. 5, no. 3, pp. 115–119, 1991.

[24] P. K. S. Visen, B. Shukia, G. K. Patnaik, and B. N. Dhawan, "Andrographolide protects rat hepatocytes against paracetamol-induced damage," *Journal of Ethnopharmacology*, vol. 40, no. 2, pp. 131–136, 1993.

[25] A. Singh and S. S. Handa, "Hepatoprotective activity of *Apium graveolens* and *Hygrophila auriculata* against paracetamol and thioacetamide intoxication in rats," *Journal of Ethnopharmacology*, vol. 49, no. 3, pp. 119–126, 1995.

[26] H. Kalantari, L. S. Khorsandi, and M. Taherimobarekeh, "The protective effect of the *Curcuma longa* extract on acetaminophen induced hepatotoxicity in mice," *Jundishapur Journal of Natural Pharmaceutical Products*, vol. 2, no. 1, pp. 7–12, 2007.

[27] H. Rabiul, M. Subhasish, S. Sinha, M. G. Roy, D. Sinha, and S. Gupta, "Hepatoprotective activity of *Clerodendron inerme* against paracetamol induced hepatic injury in rats for pharmaceutical product," *International Journal of Drug Development and Research*, vol. 3, no. 1, pp. 118–126, 2011.

[28] K. C. Gini and K. G. Muraleedhara, "Hepatoprotective effect of *Spirulina lonar* on paracetamol induced liver damage in rats," *Asian Journal of Experimental Biological Sciences*, vol. 1, pp. 614–623, 2010.

[29] E. Kozer, S. Evans, J. Barr et al., "Glutathione, glutathione-dependent enzymes and antioxidant status in erythrocytes from children treated with high-dose paracetamol," *British Journal of Clinical Pharmacology*, vol. 55, no. 3, pp. 234–240, 2003.

[30] C. Girish, B. C. Koner, S. Jayanthi, K. R. Rao, B. Rajesh, and S. C. Pradhan, "Hepatoprotective activity of six polyherbal formulations in paracetamol induced liver toxicity in mice," *Indian Journal of Medical Research*, vol. 129, no. 5, pp. 569–578, 2009.

[31] R. Sallie, J. M. Tredger, and R. Williams, "Drugs and the liver," *Biopharmaceutics & Drug Disposition*, vol. 12, no. 4, pp. 251–259, 1991.

[32] M. G. Rajesh and M. S. Latha, "Preliminary evaluation of the antihepatotoxic activity of Kamilari, a polyherbal formulation," *Journal of Ethnopharmacology*, vol. 91, no. 1, pp. 99–104, 2004.

[33] P. Abraham, "Oxidative stress in paracetamol-induced pathogenesis: (I). Renal damage," *Indian Journal of Biochemistry & Biophysics*, vol. 42, no. 1, pp. 59–62, 2005.

[34] H.-B. Shao, L.-Y. Chu, Z.-H. Lu, and C.-M. Kang, "Primary antioxidant free radical scavenging and redox signaling pathways in higher plant cells," *International Journal of Biological Sciences*, vol. 4, no. 1, pp. 8–14, 2008.

[35] J. Prakash, S. K. Gupta, V. Kochupillai, N. Singh, Y. K. Gupta, and S. Joshi, "Chemopreventive activity of Withania somnifera in experimentally induced fibrosarcoma tumours in swiss albino mice," *Phytotherapy Research*, vol. 15, no. 3, pp. 240–244, 2001.

Hindawi Publishing Corporation
Evidence-Based Complementary and Alternative Medicine
Volume 2016, Article ID 9470954, 11 pages
http://dx.doi.org/10.1155/2016/9470954

Research Article

Satkara (*Citrus macroptera*) Fruit Protects against Acetaminophen-Induced Hepatorenal Toxicity in Rats

Sudip Paul,[1] Md. Aminul Islam,[1] E. M. Tanvir,[1,2] Romana Ahmed,[1] Sagarika Das,[1] Nur-E-Noushin Rumpa,[1] Md. Sakib Hossen,[1] Mashud Parvez,[3] Siew Hua Gan,[4] and Md. Ibrahim Khalil[1,4]

[1] *Laboratory of Preventive and Integrative Biomedicine, Department of Biochemistry and Molecular Biology, Jahangirnagar University, Dhaka 1342, Bangladesh*
[2] *Department of Biochemistry and Molecular Biology, Gono University, Mirzanagar, Savar, Dhaka 1344, Bangladesh*
[3] *Dhaka Children Hospital and Bangladesh Institute of Children Health (BCIH), Sher-E-Bangla Nagar, Dhaka 1207, Bangladesh*
[4] *Human Genome Centre, School of Medical Sciences, Universiti Sains Malaysia, 16150 Kubang Kerian, Kelantan, Malaysia*

Correspondence should be addressed to Md. Ibrahim Khalil; drmikhalil@yahoo.com

Received 19 December 2015; Revised 18 January 2016; Accepted 24 January 2016

Academic Editor: Mohamed M. Abdel-Daim

Although *Citrus macroptera* (Rutaceae), an indigenous fruit in Bangladesh, has long been used in folk medicine, however, there is a lack of information concerning its protective effects against oxidative damage. The protective effects of an ethanol extract of *Citrus macroptera* (EECM) against acetaminophen-induced hepatotoxicity and nephrotoxicity were investigated in rats. Rats (treatment groups) were pretreated with EECM at doses of 250, 500, and 1000 mg/kg, respectively, orally for 30 days followed by acetaminophen administration. Silymarin (100 mg/kg) was administered as a standard drug over a similar treatment period. Our findings indicated that oral administration of acetaminophen induced severe hepatic and renal injuries associated with oxidative stress, as observed by 2-fold higher lipid peroxidation (TBARS) compared to control. Pretreatment with EECM prior to acetaminophen administration significantly improved all investigated biochemical parameters, that is, transaminase activities, alkaline phosphatase, lactate dehydrogenase, γ-glutamyl transferase activities and total bilirubin, total cholesterol, triglyceride and creatinine, urea, uric acid, sodium, potassium and chloride ions, and TBARS levels. These findings were confirmed by histopathological examinations. The improvement was prominent in the group that received 1000 mg/kg EECM. These findings suggested that *C. macroptera* fruit could protect against acetaminophen-induced hepatonephrotoxicity, which might be via the inhibition of lipid peroxidation.

1. Introduction

Complex redox reactions occur in the human body. Consequently, free radical formation is counteracted by specific endogenous enzymes, such as superoxide dismutase, catalase, and glutathione peroxidase, and by exogenous antioxidants from plant sources [1, 2]. *Citrus* fruits contain many pharmaceutically important bioactive compounds that are the main contributors to their inherent antioxidant properties [3].

Citrus macroptera var. annamensis (family, Rutaceae) is locally known as "Satkara" in Bengali and "Wild orange" in English [4]. The semiwild species is native to regions of Malesia and Melanesia [5]. The *C. macroptera* plant is grown in the yard of most homesteads and hill tracts of the Sylhet division of Bangladesh. The fruit is typically used during cooking and for pickle preparation and is popular for its medicinal purposes in Assam, India [6]. It is also used by locals in Northeast India as medicine for stomach pain and alimentary disorders [7].

The *C. macroptera* fruit has significant cytotoxic, antimicrobial [8], antihypertensive, antipyretic, and appetite stimulant potentials [9, 10]. Additionally, significant hypoglycemic and neuropharmacological effects were confirmed in a rat model [11, 12]. The antioxidant constituents in the *C. macroptera* fruit include phenolics, flavonoids, tannins, ascorbic acid, and proteins, and significant radical scavenging

activity was confirmed by an *in vitro* study [13]. Therefore, this fruit is postulated to play a therapeutic role in reducing the risk of some forms of fatal oxidative stress disorders, such as liver and kidney dysfunction, cardiovascular disease, and stroke [8, 14, 15].

The liver is a vital organ involved in the detoxification and elimination of toxic substances. The liver is often distressed by a large number of environmental pollutants and drugs, all of which burden, damage, or weaken it, ultimately leading to diseases such as hepatitis and cirrhosis [16]. Drug-induced toxicity of vital organs, including the liver and kidney, is frequently observed worldwide [17, 18]. Paracetamol (acetaminophen or *N*-acetyl-p-aminophenol; APAP) is a widely used over-the-counter analgesic and antipyretic drug [19]; APAP overdose can cause severe hepatocyte injury. APAP-induced hepatotoxicity is attributed to its reactive metabolite *N*-acetyl-p-benzoquinone imine (NAPQI), which is generated through cytochrome p450 and causes oxidative stress due to its ability to covalently react with proteins and nucleic acids and to deplete glutathione (GSH) [20–22]. There is also subtle evidence that APAP can cause harmful effects to the kidneys, which are important for drug elimination [23].

Interestingly, there is a plausible metabolic and pathophysiological link between the kidneys and the liver [24]. Both hepatotoxicity and nephrotoxicity are potential complications of APAP overdose, making the assessment of APAP-related toxicity indispensable [25]. There is particular interest in APAP-induced toxicity due to its overuse in Bangladesh, where no strong monitoring system is in place to regulate the utilization of over-the-counter drugs, such as APAP. Therefore, APAP-induced toxicity is a concern that affects many people.

Searching for novel medicinal plants with greater safety and efficacy has become the primary goal of medicinal chemists. We postulate that the high antioxidant potential of *C. macroptera* may confer protective effects when administered. Therefore, this study was designed to investigate the pharmaceutical effects of *C. macroptera* against APAP-induced hepatorenal toxicity in a rat model of liver and kidney diseases.

2. Materials and Methods

2.1. Chemicals. Acetaminophen was provided as a gift from Eskayef Bangladesh Limited (Dhaka, Bangladesh). 1,1,3,3-Tetraethoxypropane was purchased from NacalaiTesque, Inc. (Kyoto, Japan). Silymarin was obtained from Square Pharmaceuticals Ltd. (Bangladesh). All chemicals and reagents were of analytical grade.

2.2. Sample Collection. Fresh, mature *C. macroptera* fruit samples were collected from Sylhet district of Bangladesh in June 2014. The identification of the fruit was authenticated by Professor Nuhu Alam from the Botany Department, Jahangirnagar University. A voucher specimen (Acc. number 38619) was deposited in the Bangladesh National Herbarium for future reference.

2.3. Extract Preparation. The fresh, mature *C. macroptera* fruit samples were rinsed thoroughly under cold running water. The fruit pulp was separated from the peel and cut into small pieces using a sterile smooth steel knife and completely dried under sunlight for 28 h. Then, the dried samples were combined using a blender (Jaipan Commando, Mumbai-63, India). The blended samples were soaked in pure ethanol (100%) for 24 h and shaken (3 g) at 30°C for 72 h. Then, the extract was filtered through a cotton plug and then through Whatman No. 1 filters. The crude extract was evaporated under reduced pressure (100 psi) at a controlled temperature (40°C) and stored at −20°C prior to analysis.

2.4. Animals. Male Wistar Albino rats aged 12–14 weeks (140–150 g) were used in this study. The animals were bred and housed in an animal facility at the Department of Biochemistry and Molecular Biology, Jahangirnagar University, at a constant temperature of 25 ± 2°C with humidity ranging between 40% and 70%. The rats were housed in sterile plastic cages with soft wood-chip bedding and a natural 12 h day-night cycle. The animals had *ad libitum* access to standard food and water. The experiments were conducted according to the ethical guidelines approved by the Bangladesh Association for Laboratory Animal Science and the Biosafety, Biosecurity, and Ethical Committee of Jahangirnagar University [Approval number BBEC, JU/M2015 (2)].

2.5. Experimental Design. The animal experiments were designed based on the findings of the effective dose of acetaminophen as an agent for liver damage at subacute exposure while the outcomes of the study are the effects of *C. macroptera* investigated at multiple doses with some modifications (Figure 1) [13, 26]. Briefly, the animals were randomly divided into seven groups with six rats in each group. Group 1 was administered with normal saline, a solution of 0.90% of sodium chloride (5 mL/kg) perorally (p.o.) once daily for 30 days, and served as the "saline control" group. Group 2, the "EECM control" group, was treated with 1000 mg/kg EECM p.o. once daily for 30 days. Group 3, the "APAP control" group, received normal saline (5 mL/kg, p.o.) once daily for 30 days as well as 500 mg/kg APAP suspended in normal saline p.o. daily for the last 7 days. Groups 4, 5, and 6 received EECM at doses of 250, 500, and 1000 mg/kg p.o., respectively, for 30 days once a day and followed by administration of 500 mg/kg APAP p.o. daily for the last 7 days of the experiment; these groups were named the "T 250," "T 500," and "T 1000" groups, respectively. Group 7 was treated with a standard drug suspended in normal saline (silymarin, 100 mg/kg, p.o.) once daily for 30 days along with APAP (500 mg/kg, p.o.) for the last 7 days; this group was named the "silymarin" group.

At the end of the experimental period, the rats in each group were deeply anaesthetized with a ketamine hydrochloride injection (100 mg/kg) and sacrificed prior to dissection. Blood samples (5 mL) were collected from the inferior vena cava, and liver and kidney tissue samples were collected from each rat and stored in specimen containers (Thermo Scientific, USA) at −20°C prior to analysis.

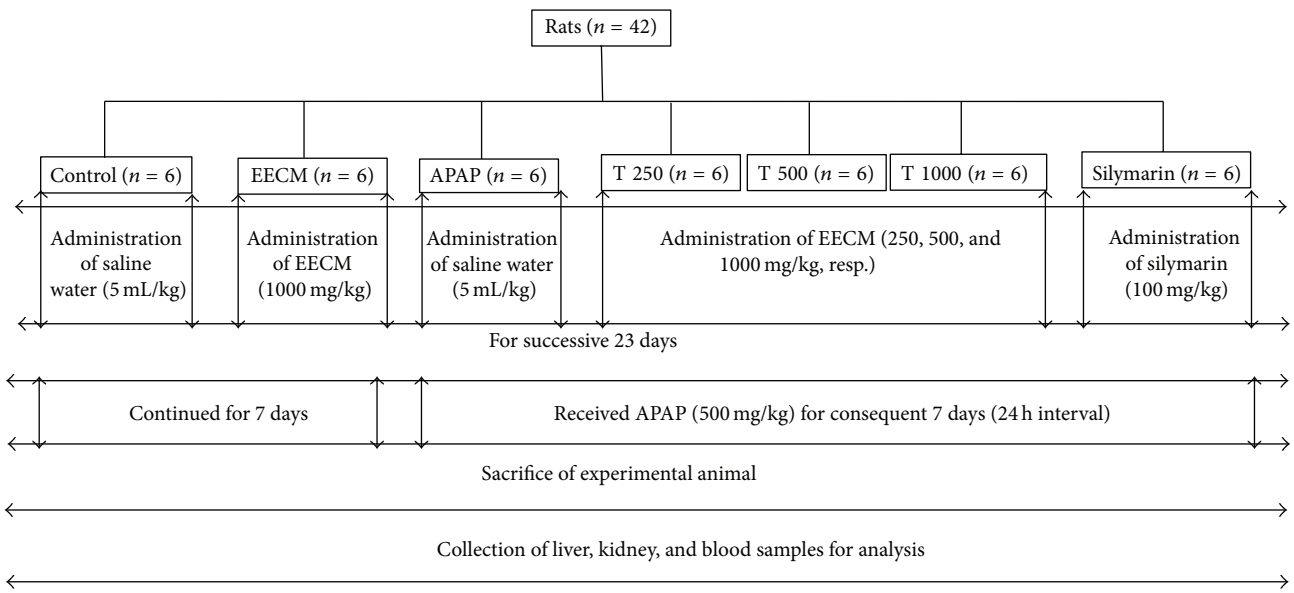

Figure 1: Schematic diagram of the experimental design of the study.

The changes in body weight (BW) and in absolute and relative liver and kidney weights were recorded. BW gain was calculated using the following formula:

$$\%\ \text{BW gain} = \left[\frac{(\text{final BW} - \text{initial BW})}{\text{final BW}}\right] \times 100. \quad (1)$$

2.6. Serum Preparation. Blood samples (3 mL) were collected in clot activator plastic tubes and allowed to coagulate at ambient temperature for 30 min prior to centrifugation at 358 g for 10 min to separate the serum. The serum was stored at −20°C for biochemical analysis.

2.7. Tissue Homogenate Preparation. The liver and kidney samples were homogenized in phosphate-buffered saline (25 mM, pH 7.4) to produce an approximately 10% (w/v) homogenate. The homogenate was centrifuged at 259 g for 10 min. The supernatant was collected and stored at −20°C prior to biochemical analysis. A portion of each liver and kidney sample was stored in 10% formalin for histopathological examination.

2.8. Biochemical Analysis. Biochemical parameters in serum, such as alanine aminotransferase (ALT), aspartate aminotransferase (AST), alkaline phosphatase (ALP), lactate dehydrogenase (LDH), γ-glutamyl transferase (GGT), total protein (TP), albumin (ALB), total bilirubin (TB), total cholesterol (TC), triglyceride (TG), creatinine (CRE), urea, uric acid (UA), sodium (Na^+), potassium (K^+), and chloride (Cl^-), were estimated following standard protocols using an automated chemistry analyzer (Dimension EXL with LM Integrated Chemistry System, Siemens Medical Solutions Inc., USA). Tissue TP levels were determined according to the method established by Lowry et al. [27]. Malondialdehyde (MDA) levels were investigated for products of lipid peroxidation (LPO) in the liver and kidney tissues. MDA, which is referred to as thiobarbituric acid reactive substance (TBARS), was measured at 532 nm according to the method described by Ohkawa et al. [28]. TBARS levels were expressed as nmol of TBARS per mg of protein.

2.9. Histopathological Examination. The liver and kidney tissues were dissected, fixed in 10% formalin, dehydrated in a graded ethanol series (50–100%), cleared in xylene, and embedded in paraffin wax. The tissues were sectioned at 5 μm thicknesses using a rotary microtome and then stained with hematoxylin and eosin for observation under a light microscope (MZ3000 Micros, St. Veit/Glan, Austria). The pathologist performing the histopathological evaluation was blinded to the treatment assignment of the different study groups.

2.10. Statistical Analysis. Data are presented as the mean ± standard deviation (SD). The data were analyzed using one-way analysis of variance (ANOVA), and the differences between groups were determined using Tukey's HSD *post hoc* test within Statistical Package for Social Sciences (SPSS) software version 13.0 (IBM Corporation, NY, USA) and Microsoft Excel 2007 (Redmond, WA, USA). A p value < 0.05 was considered statistically significant.

3. Results

The effects of oral EECM administration on liver function were investigated by measuring serum ALT, GGT, AST, ALP, and LDH activities as well as TP and ALB levels. Serum ALT and GGT activities were significantly higher in the APAP-treated group (Group 3) compared to the saline control group ($p < 0.05$). EECM pretreatment at 250, 500, and 1000 mg/kg significantly lowered ALT and GGT levels compared to

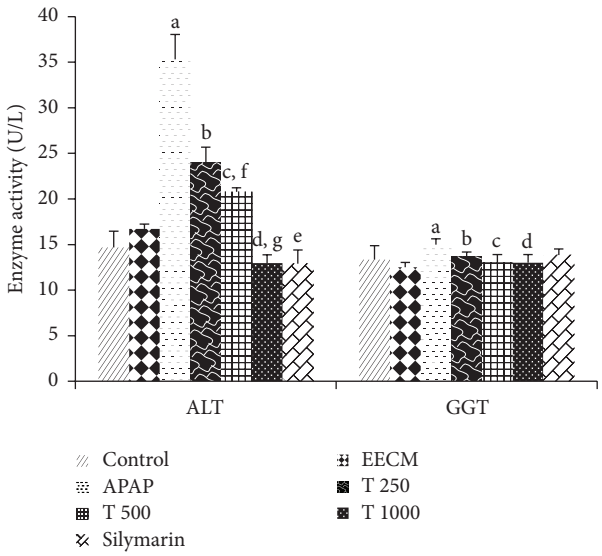

Figure 2: The effects of EECM and APAP on serum ALT and GGT activities. The results are presented as the mean ± SD ($n = 6$). In each dataset, each letter indicates a significant difference between two groups. a: a significant difference between saline control and APAP control groups, b: a significant difference between APAP control and T 250 groups, c: a significant difference between APAP control and T 500 groups, d: a significant difference between APAP control and T 1000 groups, e: a significant difference between APAP control and silymarin groups, f: a significant difference between T 250 and T 500 groups, and g: a significant difference between T 500 and T 1000 groups, respectively, at $p < 0.05$.

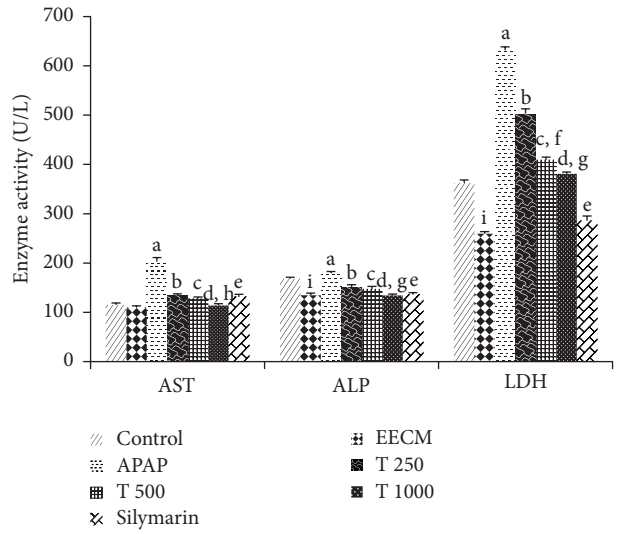

Figure 3: The effects of EECM and APAP on serum AST, ALP, and LDH activities. The results are presented as the mean ± SD ($n = 6$). In each dataset, each letter indicates a significant difference between two groups. a: a significant difference between saline control and APAP control groups, b: a significant difference between APAP control and T 250 groups, c: a significant difference between APAP control and T 500 groups, d: a significant difference between APAP control and T 1000 groups, e: a significant difference between APAP control and silymarin groups, f: a significant difference between T 250 and T 500 groups, g: a significant difference between T 500 and T 1000 groups, h: a significant difference between T 250 and T 1000 groups, and i: a significant difference between saline control and EECM control groups, respectively, at $p < 0.05$.

the APAP control group ($p < 0.05$). A significant reduction in serum ALT levels was also observed in Groups 4, 5, and 6. Silymarin treatment significantly reduced ALT levels but not GGT levels. The rats in the EECM control group showed no significant differences in ALT and GGT activities compared to the saline control group (Figure 2).

Figure 3 shows the significant increases in serum AST, ALP, and LDH activities in the APAP control group compared to the saline control group. Pretreatment with EECM at 250, 500, and 1000 mg/kg and silymarin significantly decreased the levels of the diagnostic markers compared to treatment with APAP alone (Group 3). Marked differences in serum AST and ALP levels were also found between Groups 4 and 6 and Groups 5 and 6, respectively, while LDH levels were significantly different among these three groups. Significant ($p < 0.05$) improvements in serum ALP and LDH activities were observed in the EECM control group compared to the saline control group.

Treatment with APAP increased serum TB levels compared to the saline control, while pretreatment with 1000 mg/kg EECM (T 1000 group) significantly ($p < 0.05$) decreased this parameter compared to the APAP control group. Silymarin and EECM pretreatment at doses of 500 and 1000 mg/kg significantly ($p < 0.05$) reduced serum ALB levels compared to treatment with APAP alone (Group 3); serum ALB levels in the APAP control group remained unchanged compared to the saline control group. A comparison of the different treatment groups showed that serum TP levels remained almost unchanged following APAP and EECM treatment (Table 1).

The effects of EECM and APAP on serum TC and TG levels are shown in Figure 4. Animals in the APAP control group showed a significant increase in TC and TG levels compared to the saline control group. However, the animals in the EECM pretreatment at 500 and 1000 mg/kg and silymarin groups exhibited significantly decreased TG and TC levels. Rats treated with EECM at 1000 mg/kg alone (Group 2) showed significantly higher TC levels and lower TG levels compared to saline control rats.

The effects of EECM and APAP on renal function were investigated by measuring serum CRE, urea, UA, Na^+, K^+, and Cl^- levels (Table 2). There were significant increases in CRE, urea, UA, Na^+, and K^+ levels and decreases in serum Cl^- levels among the APAP-treated animals (Group 3) compared to the saline control animals. However, the serum levels of CRE, urea, UA, Na^+, K^+, and Cl^- were improved in animals that received EECM at both 500 and 1000 mg/kg doses (Groups 5 and 6, resp.).

Based on the investigation of oxidative stress biomarkers, there was a significant increase in LPO levels in the animals treated with APAP alone (Group 3), as evidenced by the increase in liver MDA levels compared to the saline control

Table 1: The effects of EECM and APAP on serum TP, ALB, and TB levels.

Group	Parameters		
	TP (g/L)	ALB (g/L)	TB (mg/dL)
Saline control	60.00 ± 1.67	11.00 ± 0.63	0.12 ± 0.04
EECM control	61.83 ± 1.83	11.00 ± 0.89	0.12 ± 0.04
APAP control	60.83 ± 0.75	11.50 ± 0.54	0.18 ± 0.04[a]
T 250	59.54 ± 1.50	12.33 ± 0.52	0.15 ± 0.05
T 500	59.83 ± 1.72	10.83 ± 0.75[c,f]	0.13 ± 0.05
T 1000	62.12 ± 1.76	9.43 ± 0.89[d,g]	0.10 ± 0.00[d]
Silymarin	61.22 ± 1.47	10.00 ± 0.89[e]	0.12 ± 0.04

The data are presented as the mean ± SD ($n = 6$).
In each column, each letter indicates a significant difference between two groups.
a indicates a significant difference between saline control and APAP control group.
c indicates a significant difference between APAP control and T 500 groups.
d indicates a significant difference between APAP control and T 1000 groups.
e indicates a significant difference between APAP control and silymarin groups.
f indicates a significant difference between T 250 and T 500 groups and
g indicates a significant difference between T 500 and T 1000 groups, respectively, at $p < 0.05$.

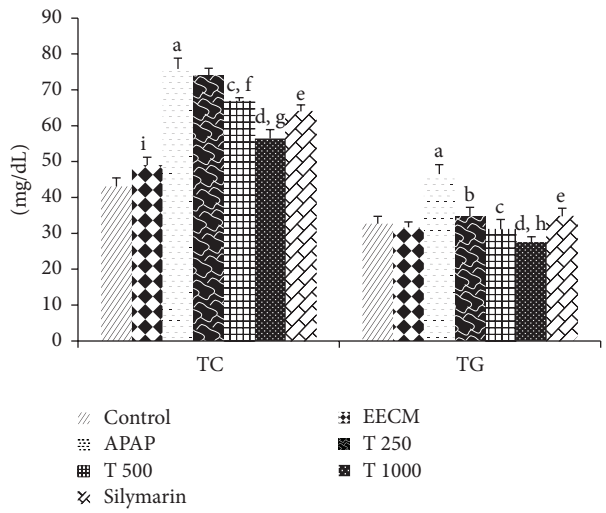

Figure 4: The effects of EECM and APAP on serum TC and TG levels. The results are presented as the mean ± SD ($n = 6$). In each dataset, each letter indicates a significant difference between two groups. a: a significant difference between saline control and APAP control groups, b: a significant difference between APAP control and T 250 groups, c: a significant difference between APAP control and T 500 groups, d: a significant difference between APAP control and T 1000 groups, e: a significant difference between APAP control and silymarin groups, f: a significant difference between T 250 and T 500 groups, g: a significant difference between T 500 and T 1000 groups, h: a significant difference between T 250 and T 1000 groups, and i: a significant difference between saline control and EECM control groups, respectively, at $p < 0.05$.

group (Group 1). However, EECM tended to confer a protective effect because the animals that were pretreated with EECM at 250, 500, and 1000 mg/kg had significantly lower MDA levels compared to the APAP control. Significantly reduced LPO levels were observed in both liver and kidney tissues from the rats treated with 1000 mg/kg EECM (Group 6) compared to those in Group 4. Treatment with silymarin also decreased LPO levels compared to APAP control treatment. No significant difference was observed between the saline control and EECM control groups (Figure 5).

Microscopic examination of the liver and kidney tissues revealed that the livers of the animals in Groups 1 and 2 had a normal hepatocyte arrangement, radiating from the central vein to the periphery of the lobule. The hepatocyte nuclei also exhibited normal vesicular structure with a normal and uniform cytoplasm (Figures 6(a) and 6(b)). In contrast, the livers of the animals in Groups 3 to 7 exhibited histopathological changes. The livers of the animals in Group 3 showed some degenerative changes, including inflammatory cell infiltration, vascular congestion, hepatocyte necrosis, and edema at different locations in the lobule (Figures 6(c) and 6(d)). The livers of the animals in Groups 4 to 7 showed improvements in all of the histopathological features (Figures 6(e)–6(h)), with a moderate to mild degree of hepatocyte degeneration, inflammatory cell infiltration, vascular congestion, and edema at all investigated doses (Table 3).

The saline control rats (Group 1) and those treated with EECM at 1000 mg/kg alone (Group 2) showed normal renal tubules and glomeruli (Figures 7(a) and 7(b)). However, rats treated with APAP (Group 3) showed severe tubular desquamation of the renal epithelium, cell necrosis, and vacuolization with the presence of intraluminal casts (Figures 7(c) and 7(d)). In contrast, rats treated with APAP and EECM at each of the three doses (Groups 4, 5, and 6) showed significant preservation of glomeruli architecture compared to rats treated with APAP alone (Group 3), although mild tubular degeneration and epithelial vacuolization were still present (Figures 7(e)–7(h)). Only mild to moderate degeneration of the tubular epithelium, vacuolization, and glomerular necrosis were observed (Table 3).

4. Discussion

Our study is the first to report the protective effects of *C. macroptera* against hepatonephrotoxicity induced by APAP in rats. The improvements in the biochemical parameters of the liver (i.e., ALT, AST, ALP, GGT, LDH, TB, TP, ALB, TC, and TG) and kidney (i.e., CRE, urea, UA, Na^+, K^+, and Cl^-) at the three different doses were supported by the inhibition of LPO and were confirmed histopathologically.

Investigation of the livers and kidneys of the experimental animals revealed a nonsignificant increase in both absolute and relative weight following APAP administration, although BW remained relatively unchanged.

Treatment with APAP for 7 consecutive days resulted in a profound increase in serum ALT, ALP, AST, GGT, and LDH activities that could potentially be attributed to hepatic injury and disturbances in the biosynthesis of these enzymes. The disruption of hepatocyte membrane permeability by APAP intoxication allows these enzymes to leak out from the liver

Table 2: The effects of EECM and APAP on serum CRE, urea, UA, Na^+, K^+, and Cl^- levels.

Group	Parameters					
	CRE (mmol/L)	Urea (mmol/L)	UA (mmol/L)	Na^+ (mmol/L)	K^+ (mmol/L)	Cl^- (mmol/L)
Saline control	48.58 ± 2.38	4.79 ± 0.07	40.33 ± 1.37	138.67 ± 2.73	3.60 ± 0.18	101.83 ± 1.33
EECM control	45.39 ± 2.85	5.27 ± 0.44	38.00 ± 2.00	142.83 ± 4.40	4.05 ± 0.05[i]	103.00 ± 1.79
APAP control	61.00 ± 2.28[a]	6.94 ± 0.41[a]	58.50 ± 2.26[a]	150.33 ± 2.66[a]	4.60 ± 0.28[a]	96.00 ± 3.35[a]
T 250	50.33 ± 2.88[b]	6.42 ± 0.12	51.33 ± 1.21[b]	143.17 ± 1.17[b]	3.42 ± 0.33[b]	99.33 ± 1.51
T 500	44.83 ± 1.72[c,f]	5.75 ± 0.36[c]	39.92 ± 2.46[c,f]	140.70 ± 4.38[c]	3.38 ± 0.12[c]	100.33 ± 3.20[c]
T 1000	31.88 ± 1.10[d,g]	4.99 ± 0.30[d,g]	37.95 ± 2.21[d]	141.80 ± 3.27[d]	3.52 ± 0.08[d]	103.17 ± 3.13[d]
Silymarin	41.33 ± 2.25[e]	5.77 ± 0.49	27.50 ± 1.64[e]	140.67 ± 1.03[e]	3.80 ± 0.09[e]	101.67 ± 1.37[e]

The data are presented as the mean ± SD ($n = 6$).
In each column, each letter indicates a significant difference between two groups.
a indicates a significant difference between saline control and APAP control groups.
b indicates a significant difference between APAP control and T 250 groups.
c indicates a significant difference between APAP control and T 500 groups.
d indicates a significant difference between APAP control and T 1000 groups.
e indicates a significant difference between APAP control and silymarin groups.
f indicates a significant difference between T 250 and T 500 groups.
g indicates a significant difference between T 500 and T 1000 groups.
i indicates a significant difference between saline control and EECM control groups, respectively, at $p < 0.05$.

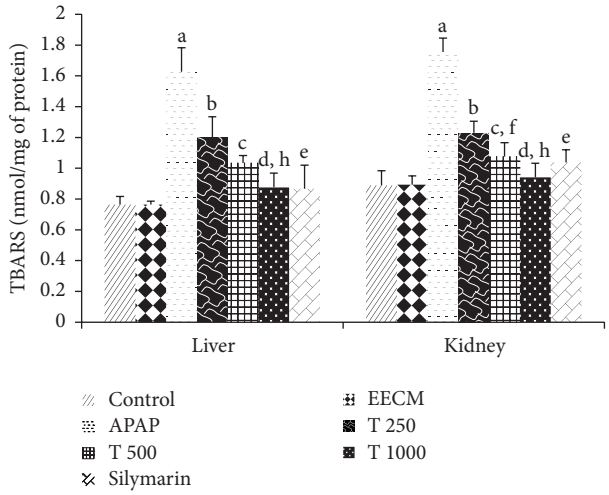

Figure 5: The effects of EECM and APAP on tissue MDA levels in rats. The results are presented as the mean ± SD ($n = 6$). In each dataset, each letter indicates a significant difference between two groups. a: a significant difference between saline control and APAP control groups, b: a significant difference between APAP control and T 250 groups, c: a significant difference between APAP control and T 500 groups, d: a significant difference between APAP control and T 1000 groups, e: a significant difference between APAP control and silymarin groups, f: a significant difference between T 250 and T 500 groups, g: a significant difference between T 500 and T 1000 groups, and h: a significant difference between T 250 and T 1000 groups, respectively, at $p < 0.05$.

cytosol into the blood circulation, thus inducing necrosis and inflammatory responses [25, 29]. Our findings are consistent with those of some previous studies [25, 26]. Pretreatment with EECM tended to alleviate the activities of the serum transaminases, ALP and LDH, thereby demonstrating that EECM maintained membrane integrity and restricted the leakage of hepatic enzymes via a mechanism that is not yet completely understood. Additionally, the rise in the TB level is an important clinical indicator of the severity of necrosis; TB accumulation is indicative of the binding, conjugation, and excretory capacity of hepatic cells [25, 30]. Treatment with 1000 mg/kg EECM restored all of the above diagnostic markers, thereby demonstrating its protective role in the liver.

Serum levels of TC and TG were also increased in the APAP-treated rats, suggesting that APAP affects liver cell membrane permeability. Additionally, blockage of liver bile ducts and the subsequent decreased secretion of cholesterol into the intestine may result in the elevation of serum cholesterol, which is another sign of liver damage [31, 32]. Elevated TG provides further evidence of increased hepatic glyceride synthesis that is directly proportional to the concentration of fatty acids and glycerophosphate [33] and may contribute to the increased VLDL-C involved in the transport of hepatic triglycerides to extrahepatic tissues [34]. Pretreatment with EECM ameliorated TC and TG levels, indicating its hepatoprotective effects.

The possible protective roles of EECM regarding oxidative damage generated by APAP-induced nephrotoxicity were confirmed by examining kidney histopathology. The considerable production of reactive NAPQI due to APAP overdose can result in covalent binding to macromolecules on cellular proteins, leading to the disruption of homeostasis, apoptosis, tissue necrosis, and, ultimately, organ dysfunction [35, 36]. In our study, treatment with APAP alone resulted in a marked elevation of serum CRE, urea, and UA levels that were indicative of decreased glomerular filtration and disrupted synthetic function in the kidney [37, 38]. Moreover, alterations in serum Na^+, K^+, and Cl^- levels in APAP-treated rats compared to saline control rats demonstrated the deterioration of renal function. These findings were consistent with those of previous studies that involved treating rats with APAP [25, 36]. However, EECM treatment ameliorated

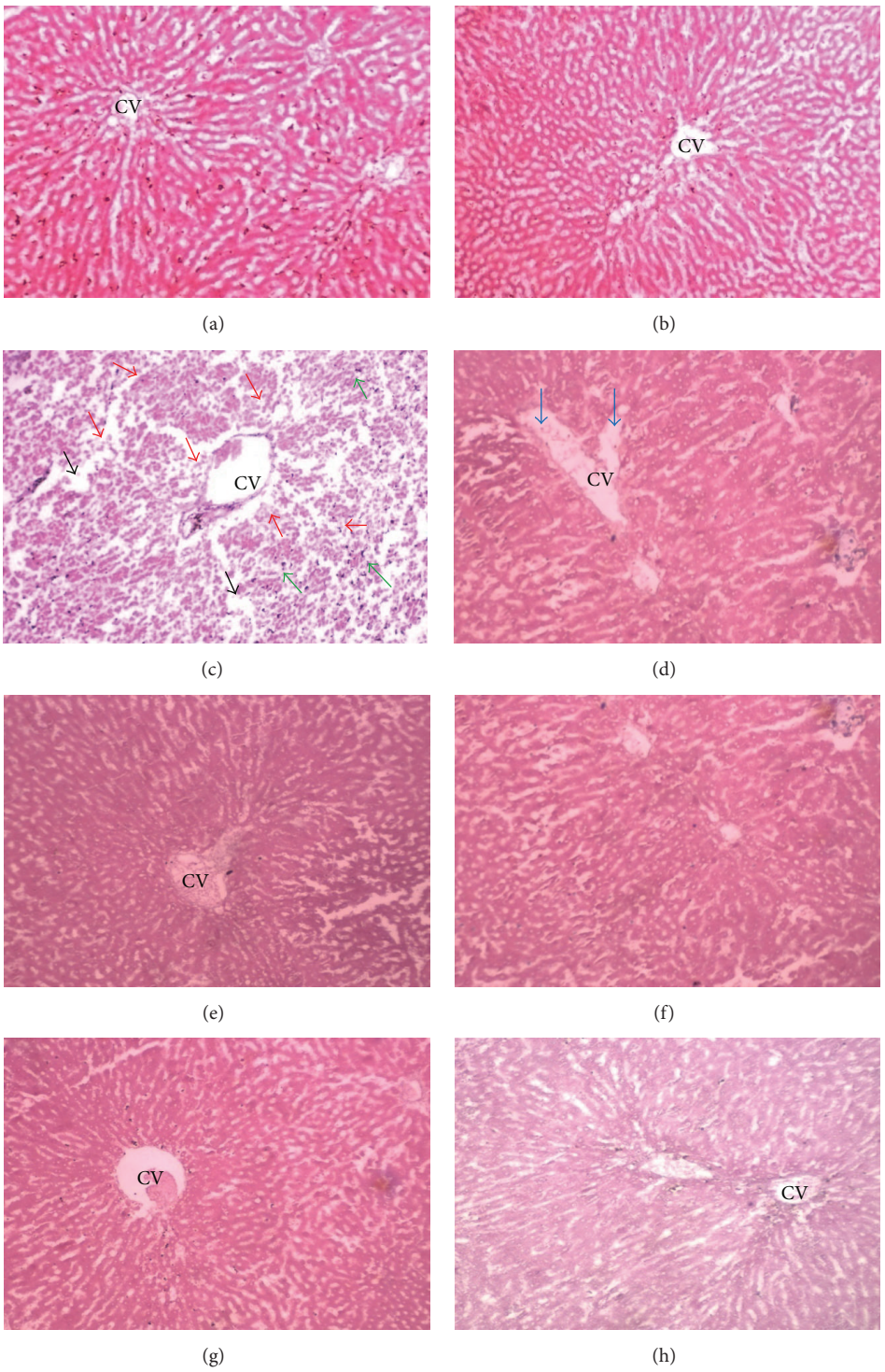

Figure 6: Liver sections from the experimental animals in (a) Group 1 (saline control) showing a normal liver with a hepatic lobule and a uniform pattern of polyhedral hepatocytes radiating from the central vein (CV) towards the periphery, (b) Group 2 (EECM control) showing a normal appearance of hepatocytes surrounding the CV, and (c) Group 3 (APAP control) demonstrating a disrupted arrangement of hepatocytes around the CV. There was also marked hepatocyte necrosis at the periphery of the CV (red arrow), inflammatory cell infiltration (green arrow), edema at different locations (black arrow), and severe congestion of the CV (d). (e–h) Groups 4, 5, 6 (T 250, T 500, and T 1000 groups, resp.), and 7 (silymarin control) showing a remarkable degree of preservation of the cellular arrangement with only mild inflammation [magnification: 40x; scale bar: 20 μm].

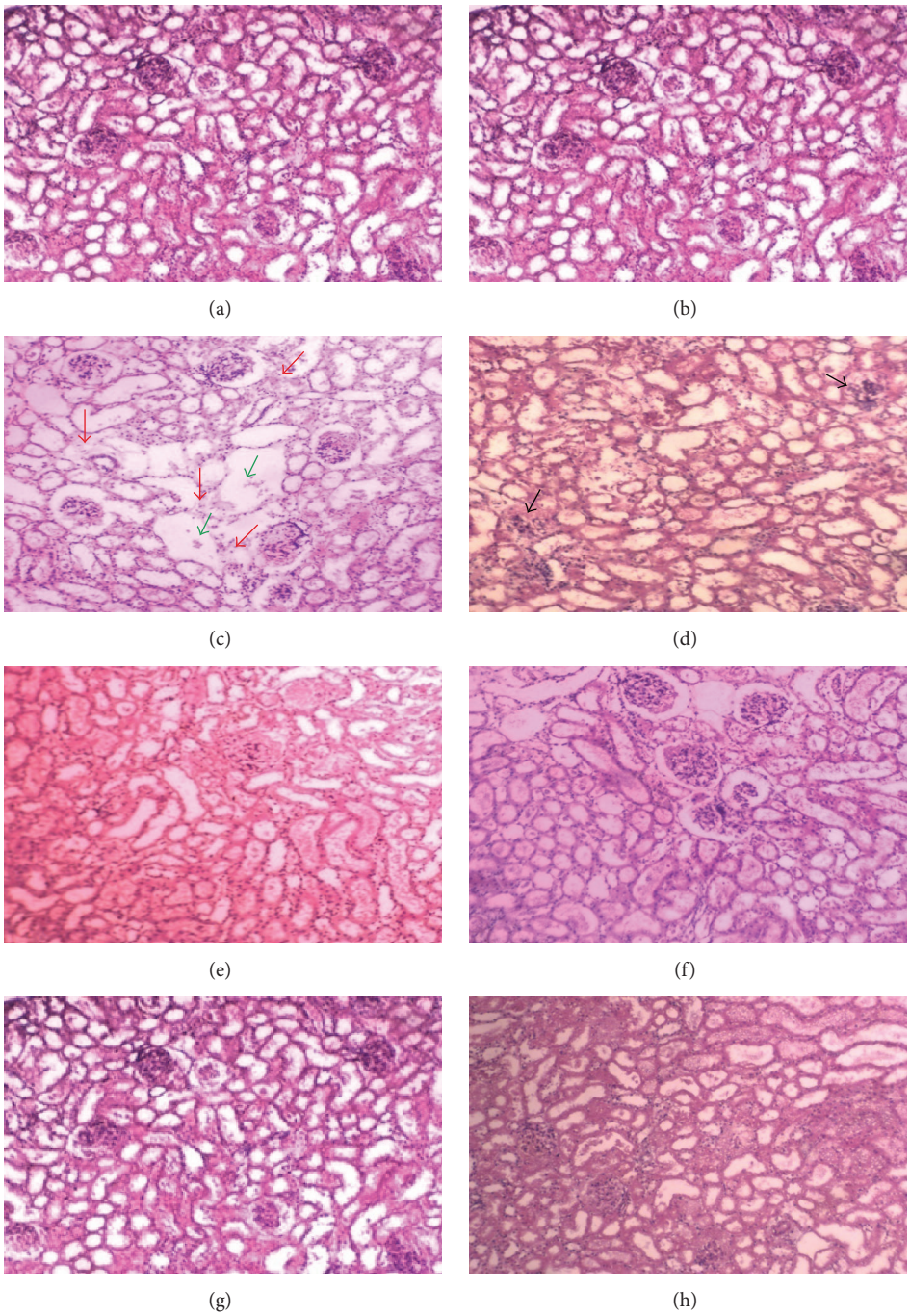

Figure 7: Kidney sections from the experimental animals in (a) Group 1 (saline control) showing a normal morphology of renal parenchyma with well-defined glomeruli and tubules; (b) Group 2 (EECM control) showing a normal appearance of the renal parenchyma; (c and d) Group 3 (APAP control) demonstrating marked degeneration of the tubular epithelium (red arrow), vacuolization (green arrow), and severe glomerular necrosis (black arrow); and (e–h) Groups 4, 5, 6 (T 250, T 500, and T 1000 groups, resp.), and 7 (silymarin control) showing a remarkable degree of morphological preservation with only moderate to mild inflammation [magnification: 40x; scale bar: 20 μm].

the kidney biomarkers, restored serum electrolytes, and restabilized the homeostatic function of the kidneys.

Oxidative injury in the liver and kidney was further evidenced by the elevation of LPO, which was suggestive of APAP-related tissue damage. LPO represents one of the most frequently measured parameters resulting from free radical attacks on biological structures due to the consequent perturbation of biochemical and physiological functions [8, 39]. Our results revealed that EECM pretreatment significantly protected the liver and kidney from LPO, as evidenced by reduced MDA levels in both liver and kidney tissues. It is plausible that the antioxidants in *C. macroptera* [8], including

Table 3: Semiquantitative scoring of the architectural changes evidenced by histopathological examination of the rats' livers and kidneys.

Scoring parameter	Group						
	1	2	3	4	5	6	7
				Liver			
Degeneration of hepatocytes	—	—	+++	++	++	+	+
Inflammatory cell infiltration	—	—	+++	++	++	+	+
Vascular congestion	—	—	+++	++	+	—	+
Edema	—	—	+++	++	++	+	+
				Kidney			
Tubular necrosis	—	—	+++	++	++	+	+
Vacuolization	—	—	+++	+	++	+	+
Glomerular necrosis	—	—	+++	++	++	+	++

Scoring was performed as follows: none (—), mild (+), moderate (++), and severe (+++).
Group 1 = control; Group 2 = EECM; Group 3 = APAP; Group 4 = T 250; Group 5 = T 500; Group 6 = T 1000; and Group 7 = silymarin.

phenolic acids, flavonoids, and tannins, act synergistically through free radical scavenging, hydrogen donation, singlet oxygen quenching, metal ion chelating, and neutralization of free radical reactions [38, 40] to combat oxidative damage.

The APAP-induced liver and renal damage was consistent with subacute hepatic and tubular necrosis, respectively. Hepatocyte degeneration and necrosis, inflammatory cell infiltration, and vascular congestion with edematous spaces were frequently observed in APAP-intoxicated rat livers. Moreover, epithelial degeneration, necrosis, and localized vacuolization were also found in kidney tissues from rats treated with APAP alone. In the present study, our histopathological findings provided clear evidence of hepatonephrotoxicity following the subacute overdose of APAP. The histopathological changes in the liver and kidney tissues of APAP-treated rats indicated reduced oxygen perfusion that further progressed as a function of the rate of cell death [25]. These findings are in agreement with previous investigations into liver and renal histological alterations following APAP overdose [25, 36]. The hepatorenal protective properties of EECM were further confirmed by the significant improvements in liver and kidney architecture. The best protection was achieved when rats were treated with 1000 mg/kg EECM, while mild or moderate effects were observed in rats treated with 250 or 500 mg/kg EECM, respectively. It is plausible that the protective action against APAP-induced histopathological alterations conferred by phenolics, flavonoids, and other antiradicals/antioxidants [8] may be due to the scavenging of free radicals and inhibition of oxidative damage and the consequent degeneration and necrosis of liver and kidney tissues, which is consistent with our biochemical findings. Further study to elucidate the exact mechanism underlying the hepato- and nephroprotection of *C. macroptera* and to identify the types of antioxidants present in *C. macroptera* is warranted.

5. Conclusion

To the best of our knowledge, our study is the first to report on the hepato- and nephroprotective effects of the *C. macroptera* fruit against acetaminophen-induced oxidative damage in animal model. The protective effects were confirmed at three different doses. Treatment with 1000 mg/kg EECM was the most effective based on the biochemical and histological findings. It is plausible that *C. macroptera* fruit improves the structural integrity of the cell membrane via inhibition of lipid peroxidation while ameliorating the histopathological changes and biochemical perturbations. Therefore, *C. macroptera* is a useful inexpensive food product that can be consumed on a daily basis as a prophylaxis because it confers some protection against toxin-induced hepatotoxicity and nephrotoxicity.

Conflict of Interests

The authors declare that there is no conflict of interests.

Acknowledgments

This research work was supported by the TWAS research Grant no. 14-385 RG/PHA/AS_C, UNESCO FR: 3240283438.

References

[1] E. M. Tanvir, R. Afroz, N. Karim et al., "Antioxidant and antibacterial activities of methanolic extract of BAU kul (*Ziziphus mauritiana*), an improved variety of fruit from Bangladesh," *Journal of Food Biochemistry*, vol. 39, pp. 139–147, 2015.

[2] İ. Gülçin, M. Oktay, Ö. İ. Küfrevioğlu, and A. Aslan, "Determination of antioxidant activity of lichen *Cetraria islandica* (L) Ach," *Journal of Ethnopharmacology*, vol. 79, no. 3, pp. 325–329, 2002.

[3] Y. Liu, E. Heying, and S. A. Tanumihardjo, "History, global distribution, and nutritional importance of citrus fruits," *Comprehensive Reviews in Food Science and Food Safety*, vol. 11, no. 6, pp. 530–545, 2012.

[4] D. L. Dreyer and P. F. Huey, "Coumarins of *Citrus macroptera*," *Phytochemistry*, vol. 12, no. 12, pp. 3011–3013, 1973.

[5] I. A. Abbott, R. R. Leakey, and C. R. Elevitch, *Traditional Trees of Pacific Islands: Their Culture, Environment, and Use*, Permanent Agriculture Resources (PAR), Holualoa, Hawaii, USA, 2006.

[6] T. K. Bose and S. K. Mitra, *Fruits: Tropical and Subtropical*, Naya Prokash, Calcutta, India, 1990.

[7] S. K. Malik and R. Chaudhury, "The cryopreservation of embryonic axes of two wild and endangered *Citrus* species," *Plant Genetic Resources: Characterisation and Utilisation*, vol. 4, no. 3, pp. 204–209, 2006.

[8] N. Uddin, M. R. Hasan, M. M. Hossain et al., "Antioxidant, brine shrimp lethality and antimicrobial activities of methanol and ethyl-acetate extracts of *Citrus macroptera* Montr. fruit using *in vitro* assay models," *British Journal of Pharmaceutical Research*, vol. 4, no. 14, pp. 1725–1738, 2014.

[9] J. K. Grover, S. Yadav, and V. Vats, "Medicinal plants of India with anti-diabetic potential," *Journal of Ethnopharmacology*, vol. 81, no. 1, pp. 81–100, 2002.

[10] M. Rahmatullah, M. A. Khatun, N. Morshed et al., "A randomized survey of medicinal plants used by folk medicinal healers of Sylhet Division, Bangladesh," *Advances in Natural and Applied Sciences*, vol. 4, no. 1, pp. 52–62, 2010.

[11] N. Uddin, M. R. Hasan, M. M. Hossain et al., "In vitro α-amylase inhibitory activity and in vivo hypoglycemic effect of methanol extract of *Citrus macroptera* Montr. fruit," *Asian Pacific Journal of Tropical Biomedicine*, vol. 4, no. 6, pp. 473–479, 2014.

[12] H. Rahman, M. C. Eswaraiah, and A. Dutta, "Neuropharmacological activities of ethanolic extract of *Citrus macroptera* (Varannamensis) fruit peels," *Global Journal of Pharmacology*, vol. 8, no. 4, pp. 609–616, 2014.

[13] S. Paul, M. S. Hossen, E. Tanvir et al., "Antioxidant properties of *Citrus macroptera* fruit and its in vivo effects on the liver, kidney and pancreas in wistar rats," *International Journal of Pharmacology*, vol. 11, no. 8, pp. 899–909, 2015.

[14] M. I. Khalil, E. M. Tanvir, R. Afroz, S. A. Sulaiman, and S. H. Gan, "Cardioprotective effects of tualang honey: amelioration of cholesterol and cardiac enzymes levels," *BioMed Research International*, vol. 2015, Article ID 286051, 8 pages, 2015.

[15] N. Uddin, M. R. Hasan, M. M. Hasan et al., "Assessment of toxic effects of the methanol extract of *Citrus macroptera* Montr. fruit via biochemical and hematological evaluation in female Sprague-Dawley rats," *PLoS ONE*, vol. 9, no. 11, Article ID e111101, 2014.

[16] H. Zimmerman and K. Ishak, "Hepatic injury due to drugs and toxins," in *Pathology of the Liver*, pp. 621–709, Churchill Livingstone, London, UK, 2002.

[17] W. M. Lee, "Drug-induced hepatotoxicity," *The New England Journal of Medicine*, vol. 349, no. 5, pp. 474–485, 2003.

[18] D. Choudhury and Z. Ahmed, "Drug-associated renal dysfunction and injury," *Nature Clinical Practice Nephrology*, vol. 2, no. 2, pp. 80–91, 2006.

[19] D. Gunnell, V. Murray, and K. Hawton, "Use of paracetamol (acetaminophen) for suicide and nonfatal poisoning: worldwide patterns of use and misuse," *Suicide and Life-Threatening Behavior*, vol. 30, no. 4, pp. 313–326, 2000.

[20] J. R. Mitchell, D. J. Jollow, W. Z. Potter, J. R. Gillette, and B. B. Brodie, "Acetaminophen induced hepatic necrosis. IV. Protective role of glutathione," *Journal of Pharmacology and Experimental Therapeutics*, vol. 187, no. 1, pp. 211–217, 1973.

[21] D. Jollow, J. Mitchell, W. Potter, D. Davis, J. Gillette, and B. Brodie, "Acetaminophen-induced hepatic necrosis. II. Role of covalent binding in vivo," *Journal of Pharmacology and Experimental Therapeutics*, vol. 187, no. 1, pp. 195–202, 1973.

[22] W. Z. Potter, S. S. Thorgeirsson, D. J. Jollow, and J. R. Mitchell, "Acetaminophen-induced hepatic necrosis. V. Correlation of hepatic necrosis, covalent binding and glutathione depletion in hamsters," *Pharmacology*, vol. 12, no. 3, pp. 129–143, 1974.

[23] M. Mazer and J. Perrone, "Acetaminophen-induced nephrotoxicity: pathophysiology, clinical manifestations, and management," *Journal of Medical Toxicology*, vol. 4, no. 1, pp. 2–6, 2008.

[24] L. Orlić, I. Mikolasevic, Z. Bagic, S. Racki, D. Stimac, and S. Milic, "Chronic kidney disease and nonalcoholic fatty liver disease—is there a link?" *Gastroenterology Research and Practice*, vol. 2014, Article ID 847539, 6 pages, 2014.

[25] R. Afroz, E. M. Tanvir, M. F. Hossain et al., "Protective effect of Sundarban honey against acetaminophen-induced acute hepatonephrotoxicity in rats," *Evidence-Based Complementary and Alternative Medicine*, vol. 2014, Article ID 143782, 8 pages, 2014.

[26] M. M. Rahman and S. Hossain, "Preventive effect of *Ganoderma lucidum* on paracetamol-induced acute hepatotoxicity in rats," *Journal of Scientific Research*, vol. 5, no. 3, pp. 573–578, 2013.

[27] O. H. Lowry, N. J. Rosebrough, A. L. Farr, and R. J. Randall, "Protein measurement with the Folin phenol reagent," *The Journal of Biological Chemistry*, vol. 193, no. 1, pp. 265–275, 1951.

[28] H. Ohkawa, N. Ohishi, and K. Yagi, "Assay for lipid peroxides in animal tissues by thiobarbituric acid reaction," *Analytical Biochemistry*, vol. 95, no. 2, pp. 351–358, 1979.

[29] S. Shenoy, H. Kumar, N. V. Thashma, K. Prabhu, and P. Pai, "Hepatoprotective activity of *Plectranthus amboinicus* against paracetamol induced hepatotoxicity in rats," *International Journal of Pharmacology and Clinical Sciences*, vol. 2, pp. 32–38, 2012.

[30] S. Manokaran, A. Jaswanth, S. Sengottuvelu et al., "Hepatoprotective activity of *Aerva lanata* Linn. against paracetamol induced hepatotoxicity in rats," *Research Journal of Pharmacy and Technology*, vol. 1, no. 4, pp. 398–400, 2008.

[31] A. Samir, G. Eman, E. Talaat, and Z. Somaia, "Carbamate toxicity and protective effect of vit. A and vit. E on some biochemical aspects of male albino rats," *Egyptian Journal of Hospital Medicine*, vol. 1, pp. 60–77, 2000.

[32] S. Kalender, F. G. Uzun, D. Durak, F. Demir, and Y. Kalender, "Malathion-induced hepatotoxicity in rats: the effects of vitamins C and E," *Food and Chemical Toxicology*, vol. 48, no. 2, pp. 633–638, 2010.

[33] Y. Ruckebush, L. P. Phaneuf, and R. Dunlop, "Lipid metabolism," in *Physiology of Small and Large Animals*, pp. 417–424, B.C. Decker, Philadelphia, Pa, USA, 1988.

[34] J. C. Bartley, "Lipid metabolism and its diseases," in *Clinical Biochemistry of Domestic Animals*, J. J. Kaneko, Ed., pp. 107–135, Academic Press, New York, NY, USA, 4th edition, 1989.

[35] J. G. M. Bessems and N. P. E. Vermeulen, "Paracetamol (acetaminophen)-induced toxicity: molecular and biochemical mechanisms, analogues and protective approaches," *Critical Reviews in Toxicology*, vol. 31, no. 1, pp. 55–138, 2001.

[36] M. Cekmen, Y. O. Ilbey, E. Ozbek, A. Simsek, A. Somay, and C. Ersoz, "Curcumin prevents oxidative renal damage induced by acetaminophen in rats," *Food and Chemical Toxicology*, vol. 47, no. 7, pp. 1480–1484, 2009.

[37] A. R. A. Ali and S. H. Ismail, "The protective effect of honey against amikacin-induced nephrotoxicity in rats," *Iraqi Journal of Pharmaceutical Sciences*, vol. 21, no. 2, pp. 85–93, 2012.

[38] E. M. Tanvir, R. Afroz, M. A. Chowdhury et al., "Honey has a protective effect against chlorpyrifos-induced toxicity on lipid peroxidation, diagnostic markers and hepatic histoarchitecture," *European Journal of Integrative Medicine*, vol. 7, no. 5, pp. 525–533, 2015.

[39] S. J. Stohs and D. Bagchi, "Oxidative mechanisms in the toxicity of metal ions," *Free Radical Biology and Medicine*, vol. 18, no. 2, pp. 321–336, 1995.

[40] K. Robards, P. D. Prenzler, G. Tucker, P. Swatsitang, and W. Glover, "Phenolic compounds and their role in oxidative processes in fruits," *Food Chemistry*, vol. 66, no. 4, pp. 401–436, 1999.

Hindawi Publishing Corporation
Evidence-Based Complementary and Alternative Medicine
Volume 2016, Article ID 8098561, 12 pages
http://dx.doi.org/10.1155/2016/8098561

Research Article

Electroacupuncture Reduces Weight Gain Induced by Rosiglitazone through PPARγ and Leptin Receptor in CNS

Xinyue Jing,[1] Chen Ou,[1] Hui Chen,[1] Tianlin Wang,[1] Bin Xu,[1] Shengfeng Lu,[1] and Bing-Mei Zhu[1,2]

[1] *Key Laboratory of Acupuncture and Medicine Research of Ministry of Education, Nanjing University of Chinese Medicine, Nanjing 210023, China*
[2] *Jiangxi University of Traditional Chinese Medicine, Nanchang 330004, China*

Correspondence should be addressed to Bing-Mei Zhu; zhubm@njutcm.edu.cn

Received 1 November 2015; Accepted 30 December 2015

Academic Editor: Mohamed M. Abdel-Daim

We investigate the effect of electroacupuncture (EA) on protecting the weight gain side effect of rosiglitazone (RSG) in type 2 diabetes mellitus (T2DM) rats and its possible mechanism in central nervous system (CNS). Our study showed that RSG (5 mg/kg) significantly increased the body weight and food intake of the T2DM rats. After six-week treatment with RSG combined with EA, body weight, food intake, and the ratio of IWAT to body weight decreased significantly, whereas the ratio of BAT to body weight increased markedly. HE staining indicated that the T2DM-RSG rats had increased size of adipocytes in their IWAT, but EA treatment reduced the size of adipocytes. EA effectively reduced the lipid contents without affecting the antidiabetic effect of RSG. Furthermore, we noticed that the expression of PPARγ gene in hypothalamus was reduced by EA, while the expressions of leptin receptor and signal transducer and activator of transcription 3 (STAT3) were increased. Our results suggest that EA is an effective approach for inhibiting weight gain in T2DM rats treated by RSG. The possible mechanism might be through increased levels of leptin receptor and STAT3 and decreased PPARγ expression, by which food intake of the rats was reduced and RSG-induced weight gain was inhibited.

1. Introduction

The thiazolidinedione (TZD) class of synthetic peroxisome proliferator-activated receptorγ (PPARγ) agonists is used widely in diabetes to increase insulin sensitivity. Although the underlying mechanisms are complex and incompletely understood, induction of genes involved in glucose and lipid metabolism in macrophages, muscle, and adipose tissue is thought to play roles [1, 2]. However, in addition to enhancing insulin activation, TZDs induce weight gain in humans and rodent models by enhancing adipogenesis and fluid retention and increasing food intake [3, 4]. Weight gain may cause many medical consequences for type 2 diabetic patients, such as overweight or obesity, insulin resistance, and cardiovascular diseases. Few studies have investigated whether TZDs-induced weight gain can be abated, so studies are needed to explore whether the observed TZDs-related weight gain can be prevented by certain interventions.

Acupuncture, as one of the traditional medical approaches, has been used to treat obesity in China for many years. Several clinical trials have been carried out very recently [5–7], and evidences have supported the idea that acupuncture is an effective and safe approach for reducing body weight. Experimental studies are uncovering its mechanisms by which acupuncture could reduce food intake and increase energy consumption [8–10]. A recent study further demonstrated that EA stimulation increased peptide and mRNA levels of α-MSH and its precursors POMC and CART in the arcuate nucleus of hypothalamus (ARH) neurons to inhibit food intake [8]. Cabıoğlu and Ergene reported that EA therapy in obese women reduced serum total cholesterol, triglycerides, and LDL cholesterol

levels [11], suggesting a direct or indirect role of EA in mobilizing energy storage. Based on those studies, questions are raised. Does EA stimulation protect weight gain caused by RSG administration in T2DM rats? What is the possible mechanism in CNS?

The nuclear receptor PPARγ is a ligand-activated transcription factor that promotes adipogenesis and insulin sensitivity [12, 13], and it is expressed in several tissues and cell types including white and brown adipocytes, macrophages, skeletal muscle, liver, pancreatic β-cells [1, 14, 15]. The activation of PPARγ is found to be a key factor of increased body weight when both diabetic mice and patients were treated with TZD [16–20]. In addition to its actions in peripheral tissues, PPARγ plays a role in neuronal systems governing energy balance and insulin sensitivity. PPARγ in hypothalamic neurons is involved in the control of energy balance, glucose metabolism, and autonomic function, suggesting that PPARγ signaling in the CNS may affect energy intake and storage [21–23].

Recent evidence has proven that RSG, a new class of antidiabetic drugs, rather than reducing hyperglycemia and hyperinsulinemia in insulin-resistant states, inhibits leptin expression and its signal transduction in different cells and animal models [24–27]. Leptin, a peptide hormone mainly secreted by adipocytes, is a pleiotropic molecule that regulates food intake, hematopoiesis, inflammation, immunity, cell differentiation, and proliferation [28]. The effect of leptin on food intake is mediated in part via leptin receptors presented in the hypothalamus. Peripherally applied leptin in rodents induces a central signaling pathway that involves activation of signal transducer and activator of transcription 3 (STAT3) [29]. The requirement of this pathway to prevent severe hyperphagia and obesity was recently demonstrated in mice specifically lacking the STAT3-binding site of the leptin receptor [30] and in mice with reduced level of STAT3 protein selectively in the CNS [31]. After binding to the long leptin receptor (OBRb), STAT3 becomes phosphorylated by Janus kinase 2 (JAK2) and acts in the nucleus to regulate transcription [32].

In the present study, we employed T2DM rats as the animal model and treated them with RSG combined with EA on Zusanli (ST36) and Neiting (ST44) acupoints. Our study, for the first time, revealed that EA treatment is effective for inhibiting weight gain in T2DM rats treated with RSG. The possible mechanism might be through increased leptin receptor and STAT3 and decreased PPARγ expressions in CNS, by which food intake of the rats was reduced and so that RSG-induced weight gain was inhibited.

2. Materials and Methods

2.1. Chemicals. STZ was purchased from Sigma Chemical Co. (St. Louis, MO). Rosiglitazone maleate tablets were obtained from Glaxo Smith Kline Pharmaceutical Group (Tianjin, China). The test kits for total cholesterol and triglyceride were purchased from Nanjing Jiancheng Bioengineering Institute (Nanjing, China); iodine [125I] insulin radioimmunoassay kit was purchased from Beijing North Biotechnology Institute (Beijing, China).

2.2. Animals. Male Sprague-Dawley rats, weighted at 100–110 g, were supplied by SLAC Laboratory Animal Company (Shanghai, China). The rats were housed under controlled conditions of temperature (22 ± 2°C) and relative humidity (50 ± 10%) with a 12 h light-dark cycle. They were allowed free access to standard rodent chow. This study was approved by Animal Ethics Committee of Nanjing University of Chinese Medicine (approval number: 16, date of approval: Jan 18, 2007), and all procedures were conducted in accordance with the guidelines of the National Institutes of Health Animal Care and Use Committee.

2.3. Induction of Diabetic Rats. The diabetic rats were induced according to Reed's method with minor modification [33]. Briefly, the rats were fed on high-fat diet (HFD). The HFD consisted of 15% lard, 5% sesame oil, 20% sucrose, 2.5% cholesterol, and 57.5% normal chow. After 4 weeks of dietary manipulation, T2DM rats were administrated with an intraperitoneally injection of STZ (35 mg/kg, dissolved in pH 4.5 citrate buffer). Control rats only received an equivalent volume of citrate buffer. Then experimental rats were continued on their original diets. Fasting blood glucose concentrations, body weight, and food intake were monitored once a week after STZ injection. Biochemical parameters (serum triglyceride, serum total cholesterol, and serum insulin) were measured on day 21 after vehicle or STZ injection. Rats in the T2DM group with nonfasting plasma glucose ≥16.67 mmol/L (300 mg/dL) were chosen as diabetic rats for further study [34].

2.4. Oral Glucose Tolerance Test. On day 22 after STZ or vehicle injection, oral glucose tolerance test (OGTT) was performed. Animals were fasted overnight and then received glucose solution (2 g/kg) orally. Blood samples were collected via the oculi chorioideae vein under light ether anaesthesia at 0 (just before administration), 15, 30, 60, and 120 min after glucose loading. Serum was separated by centrifugation. The concentrations of glucose and insulin in serum were measured using glucometer (Johnson & Johnson Biological Devices Co., Ltd., China) and insulin radioimmunoassay kit (North Institute of Biotech Co., Beijing, China), respectively. Homeostatic model assessment (HOMA) was used to assess the longitudinal changes in insulin resistance (HOMA-IR) [35].

2.5. Grouping of Animals and Parameters of Acupuncture. Normal diet rats were randomly divided into control group (Con) and electroacupuncture group (Con-EA). T2DM rats were randomly divided into T2DM group, T2DM-EA group, T2DM-RSG group, and T2DM-RSG-EA group. All of the rats were fed with normal diet. Rats in the EA group were physically restrained and then electroacupunctured on Zusanli (ST36) and Neiting (ST44), while rats in the control group were restrained in the same way, but without acupuncture. For the rats who received EA treatment, two acupuncture needles (Gauge-28, 0.16 mm) were separately inserted into each acupoint and an electrical current was provided to the needles through an electrical stimulator with parameters of

Table 1: Biochemical parameters in serum of the Con and T2DM rats.

Group	Initial body weight (g)	Final body weight (g)	Serum glucose (mmol/L)	Plasma triglyceride (mmol/L)	Plasma total cholesterol (mmol/L)	Serum insulin (pmol/L)	HOMA-IR
Con	142.33 ± 7.72	363.88 ± 22.95	4.82 ± 0.29	0.49 ± 0.07	1.24 ± 0.20	33.35 ± 3.68	42.02 ± 15.89
T2DM	139.16 ± 7.89	300.91 ± 22.26**	18.97 ± 4.99**	3.48 ± 1.95**	1.96 ± 0.80**	57.00 ± 16.00*	10.42 ± 2.45**

The T2DM rats were fed on high-fat diet for 4 weeks and then were given an intraperitoneally injection of STZ (35 mg/kg). Biochemical parameters (serum triglyceride, serum total cholesterol, and serum insulin) were measured on day 21 after vehicle or STZ injection. Each value is presented as mean ± SD ($n = 6$ in Con group and $n = 26$ in T2DM group). $^{*}p < 0.05$, $^{**}p < 0.01$ versus Con rats using Student's t-test.

2/15 Hz at an intensity level of 1 mA (Han Acuten, WQ1002F, Beijing, China) for 30 minutes, once a day, six days a week. Rats in the RSG group orally received 5 mg/kg of RSG once a day, six days a week. Body weight and food consumption were monitored every week. After 6 weeks of EA or RSG treatment, all the rats were sacrificed with CO_2 and samples were collected.

2.6. qPCR Analysis. Total RNA was isolated using TRIzol® Reagent (Invitrogen, Cat# 15596-026) according to the manufacturer's recommendations. RNA concentrations were quantified and reverse-transcribed using ThermoScript™ RT-PCR System for First-Strand cDNA Synthesis (Invitrogen, Cat# 11146-016). Gene expressions were detected using GoTaq qPCR Master Mix (Promega, Cat# A6001) in Strata gene MX3000P Real-Time PCR system (Genetimes, China). Relative gene expression levels were calculated by ΔΔCt and compared with GAPDH as internal control.

Primers were designed using Primer 5.0 software: PPARγ (NM_001145366; forward: 5′-GTCACACTCTGACAGGAGCC-3′; reverse: 5′-CAC CGCTTCTTTCAAATCTTGT-3′), GAPDH (NM_017008; forward: 5′-AAGGGCTCATGACCACAGTC-3′; reverse: 5′-CAGGGATGATGTTCTGGGCA-3′), OBRb (AF287268; forward: 5′-TCCAGGTGAGGAGCAAGAG-3′; reverse: 5′-TTCAGCGTAGCGGTGATG-3′), and STAT3 (NM_012747; forward: 5′-TATCTTGGCCCTTTGGAATG-3′; reverse: 5′-GTTGTAGGACCATAGGGGTG-3′). Each reaction mixture (25 μL total volume) contained 12.5 μL Maxima SYBR Green Master mix (2X), 0.3 μM of each primer, nuclease-free water, and 20 ng template DNA. Amplification of each gene was performed in duplicate runs and PCR conditions were 95°C for 10 min, followed by 40 cycles of 15 seconds at 95°C, 30 seconds at 60°C, and 30 seconds at 72°C.

2.7. Immunoblotting and Histological Analysis. Proteins were extracted from hypothalamus and the samples in SDS Loading Buffer were heated (100°C, 5 min), subjected to SDS-PAGE, transferred to PVDF or nitrocellulose membranes, and blocked (4°C, overnight) in PBST (PBS with 0.05% Tween 20) containing 5% nonfat dry milk or 5% BSA. Blots were incubated with a primary antibody in blocking buffer (overnight, 4°C) and then with a second antibody (1 : 1000~2000 dilution, 1 hr, RT). Signals were detected using SuperSignal® West Femto Maximum Sensitivity Substrate. Immunodetection of endogenous GAPDH was utilized to indicate that equivalent amounts of protein were present in samples added to the SDS PAGE (wells/lanes·μg/L).

Rabbit anti-GAPDH (Cell Signaling, Cat#2118, 1 : 2000 dilution for Western blot); rabbit anti-PPARγ for Western blot (Cell Signaling, Cat#2443, 1 : 1000 dilution for Western blot); rabbit anti-Stat3 (phospho Y705) for Western blot (Abcam, ab76315, 1 : 1000 dilution for Western blot); and rabbit anti-leptin (Abcam, ab3583, 1 : 1000 dilution for Western blot) were used.

2.7.1. Histological Analysis. Adipose tissue were taken from all the animals and fixed for 24 hours with 10% formaldehyde in phosphate-buffered saline solution. Tissue pieces were washed with tap water, dehydrated in alcohol, and embedded in paraffin. Then, 5 mm sections were placed on glass slides and covered with saline. Hematoxylin-eosin (HE) staining was performed on the slides. HE staining was performed to assess adipocyte size of WAT. The tissue slides were incubated for 5 min in the hematoxylin solution. After water flushing and adding 0.5% ammonium hydroxide for 30 seconds, the tissue slides were put in 0.5% eosin for 2-minute dyeing and measured under microscope (Nikon TE2000, Japan).

2.8. Statistics. Data were presented as means ± standard deviation (SD). Statistics analysis was performed using SPSS 18.0; multiple group comparisons were made by ANOVA, and the comparison between two groups was determined using unpaired 2-tailed Student's t-test. $p < 0.05$ was considered statistically significant.

3. Results

3.1. Establishment of Diabetic Rat Model. Biochemical parameters were measured in serum of the Con and T2DM rats (Table 1). It was found that levels of fasted blood glucose (FBG), triglyceride, and total cholesterol in serum of the T2DM rats were significantly higher than those in the Con rats, accompanied by reduction in body weight. T2DM rats also developed diabetic symptoms such as polyphagia, polyuria, and polydipsia. Higher level of serum insulin and severer HOMA-IR were observed in the T2DM rats. OGTT's result also showed that T2DM rats had significantly higher serum glucose and insulin concentrations induced by glucose loading, resulting in significant increase in AUC values of glucose and insulin (Figure 1). These indexes were similar to pathological state of type 2 diabetes, indicating the DM rats could be considered as type 2 diabetic rats [33, 34].

3.2. Electroacupuncture Treatment Significantly Reduced the Body Weight, Food Intake, and the Ratio of the Weights of WAT

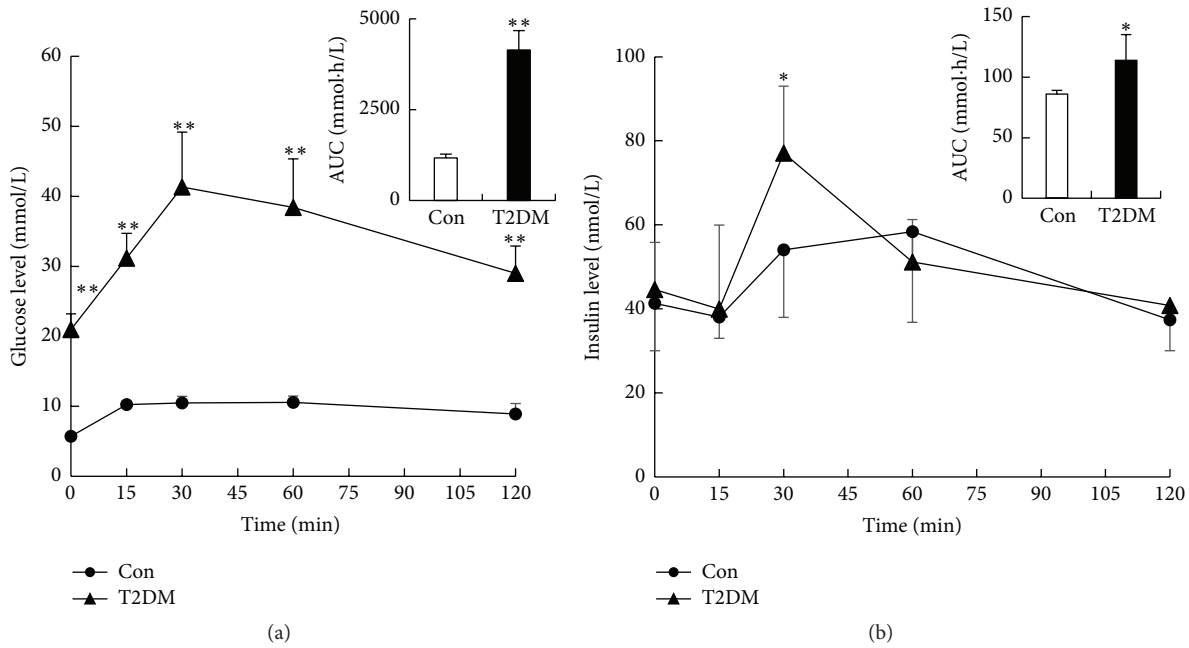

Figure 1: Serum glucose (a) and insulin (b) concentrations in T2DM and Con rats after oral glucose loading. Data were expressed as mean ± SD, $n = 6$ in Con, $n = 26$ in T2DM, and $^{*}p < 0.05$, $^{**}p < 0.01$ versus Con rats.

and BAT to Body Weight. In our study, electroacupuncture on Zusanli (ST36) and Neiting (ST44) markedly reduced body weight and food intake of the T2DM rats treated with RSG compared with the T2DM-RSG rats without acupuncture treatment (Figures 2(c) and 2(d)), whereas electroacupuncture did not significantly change body weight and food intake of Con and T2DM groups which did not receive RSG administration (Figures 2(a) and 2(b)), even after six weeks of intervention. For the first three weeks of treatment, rats in the T2DM-RSG group showed an increased appetite, which, however, had no notable fluctuation in the T2DM-RSG-EA group, suggesting that RSG may enhance appetite but electroacupuncture inhibited it to a certain extent in these rats.

To evaluate the specific effect of EA on adipose tissue, we isolated the inguinal white adipose tissue (IWAT) from the rats in each group and calculated the ratio of IWAT to their individual body weight. We found that, in the T2DM-RSG rats, the ratio was higher than that in the T2DM rats. But after six weeks of treatment with electroacupuncture, the ratios were significantly decreased (Figure 3(a)). We analyzed the sizes of adipocytes by HE staining and observed obviously smaller size of the adipocytes of the IWAT in the T2DM-RSG-EA rats compared with that in the T2DM-RSG rats (Figure 4), suggesting that electroacupuncture might promote lipolysis in obese rats. In addition, after a six-week treatment with electroacupuncture, the ratio of BAT to body weight in rats of the T2DM-RSG-EA group was significantly higher than that in the T2DM-RSG group (Figure 3(b)). Our data suggest that the effectiveness of electroacupuncture on weight gain induced by RSG may be due to the decreased food intake and reduction in the ratio of IWAT to body weight.

3.3. Electroacupuncture Treatment Significantly Improved Metabolism of Cholesterol and Triglyceride in the Obese Rats. We detected serum levels of cholesterol and triglyceride (TG) by using ELISA and found that, compared with the T2DM rats, cholesterol and TG levels were significantly elevated in T2DM-RSG rats after administration of RSG for six weeks; however, six weeks of treatment of RSG plus electroacupuncture completely reversed these levels to the normal levels (Figures 5(a) and 5(b)). FBG levels in the T2DM-RSG-EA rats were significantly decreased compared with the T2DM group (Figure 5(c)). Our data suggested that electroacupuncture effectively reduced the lipid contents in the T2DM rats treated with RSG, without affecting the antidiabetic effect of RSG.

3.4. Electroacupuncture Treatment Changed Ingestion-Related Gene Expression in CNS. We found that the mRNA and protein expression of PPARγ in hypothalamus of the T2DM-RSG rats increased than that in the T2DM rats, but not in the T2DM-RSG-EA group; furthermore, PPARγ was obviously decreased after electroacupuncture treatment compared with the T2DM-RSG rats (Figures 6(a) and 6(b) and Table 2).

To assess leptin responsiveness, we measured the expression of leptin receptor and phosphorylated STAT3, a downstream mediator of intracellular leptin signaling in hypothalamus. Our result shows that the protein expression of leptin receptor increased in the T2DM rats compared with the Con group though its mRNA level did not change and that, after being treated with RSG, the leptin receptor expression was significantly decreased, but EA combined with RSG treatment upregulated it again (Figures 7(a) and 7(b) and Table 2). Unexpectedly, the expression of leptin receptor

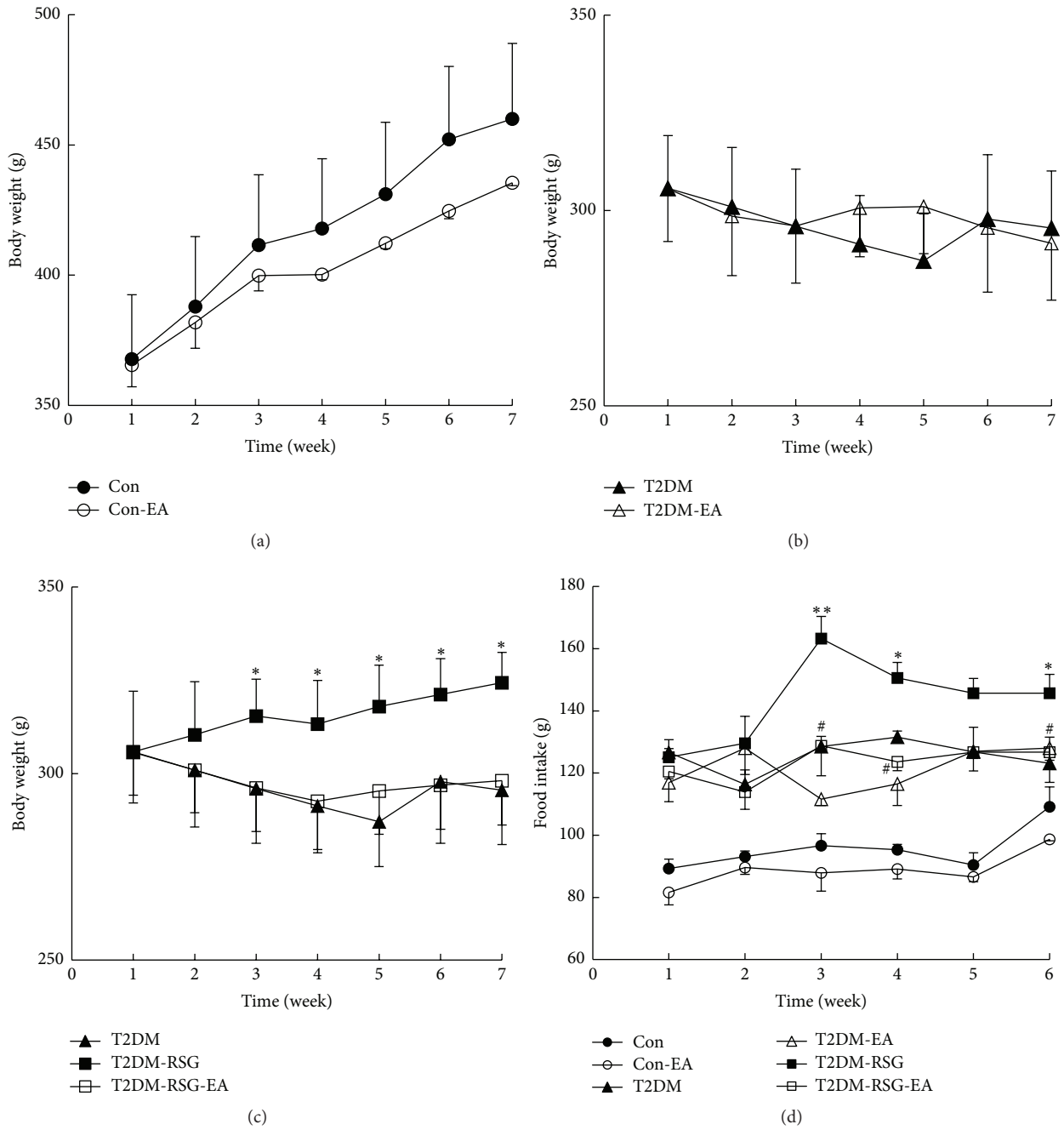

Figure 2: Effects of electroacupuncture and RSG treatment on each group. (a), (b), and (c) Observation of body weight (Con, Con-EA, T2DM, T2DM-EA, T2DM-RSG, and T2DM-RSG-EA groups), $n = 7$ in each group. (d) Measurement of food consumption, $n = 7$ in each group. Data were expressed as mean ± SD, $^{*}p < 0.05$, $^{**}p < 0.01$ versus T2DM rats, and $^{\#}p < 0.05$ versus T2DM-RSG rats.

decreased in hypothalamus in the control group treated with electroacupuncture (Con-EA). We then measured leptin-induced STAT3 phosphorylation in the hypothalamus. As indicated in Figure 7(b), leptin-induced P-STAT3 levels in the hypothalamus of RSG plus EA group were increased significantly compared with the T2DM-RSG rats. These data confirmed that electroacupuncture-inhibited food intake may be attributed to the activation of leptin-STAT3 pathway.

4. Discussion

Weight gain is commonly seen among patients treated with antidiabetic pharmacologic agents [36]. The thiazolidinediones (TZDs), rosiglitazone and pioglitazone, have also been associated with weight gain [37]. The 23-week trials with insulin sensitizing agents have shown consistent and dose-related weight gain ranging from 2.0 to 4.3 kg when used as

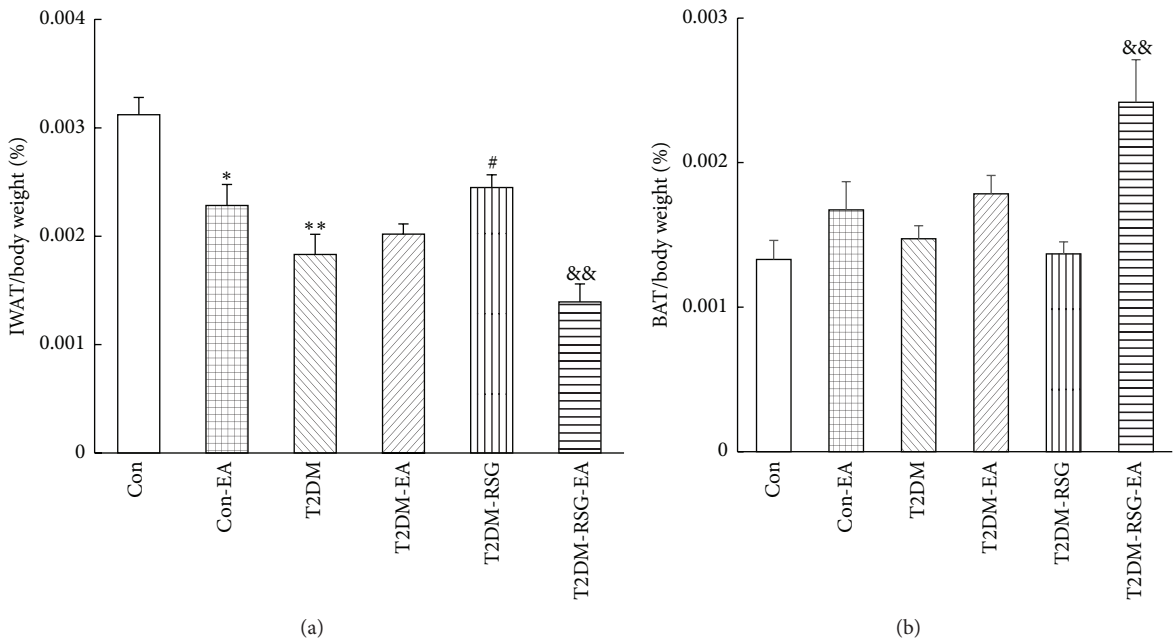

Figure 3: Effects of electroacupuncture and RSG treatment on (a) IWAT/body weight and (b) BAT/body weight. Data were expressed as mean ± SD, $n = 6$, $^{*}p < 0.05$, $^{**}p < 0.01$ versus Con rats, $^{\#}p < 0.05$ versus T2DM rats, and $^{\&\&}p < 0.01$ versus T2DM-RSG rats.

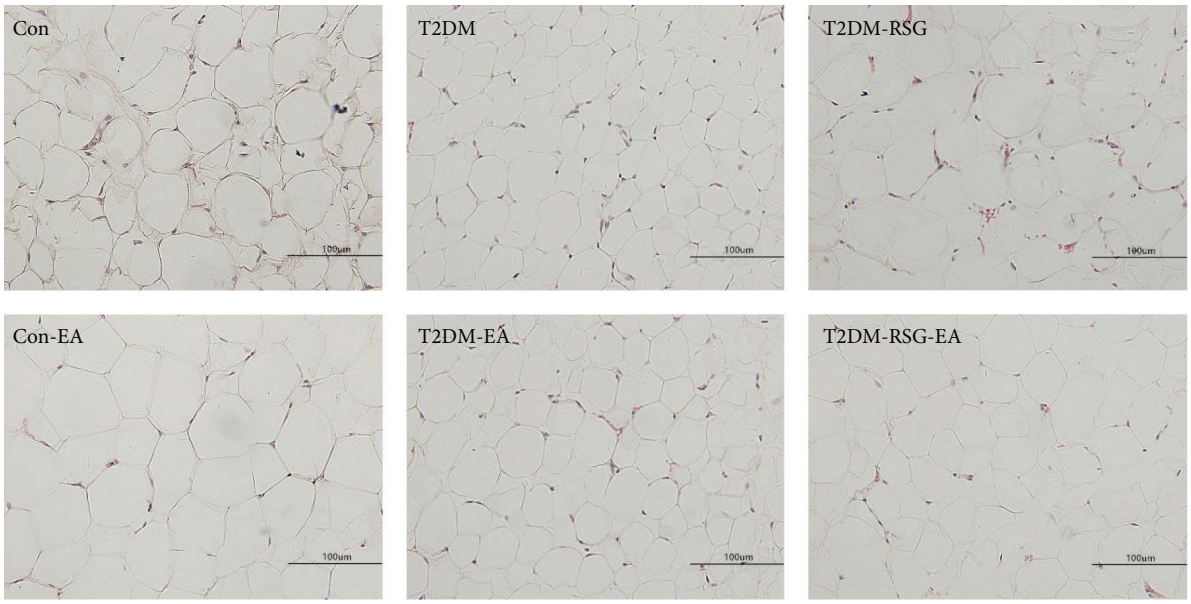

Figure 4: Histologic results of tissues stained with hematoxylin-eosin (HE) staining of each group after six weeks of treatment.

monotherapy [38, 39]. Although conflicting results have been reported, the observed weight gain with TZDs is considered as a result of increased adipose tissue mass and water retention. TZDs are highly potential and selective agonists for PPARγ, which is involved in the regulation of lipid and glucose metabolism [40, 41]. Activation of PPARγ stimulates adipocyte fatty acid uptake, lipogenesis, and differentiation, so that results in weight gain. An adverse consequence of weight gain for patients with type 2 diabetes is overweight or obesity, which is linked to insulin resistance and other medical consequences such as cardiovascular disease. Current conventional therapeutic strategies, including caloric restriction, physical exercise, and drugs, however, can not effectively achieve adequate weight gain. Although exercise can result in short-term weight loss, only 5–10% of subjects can maintain the weight loss for more than a few years

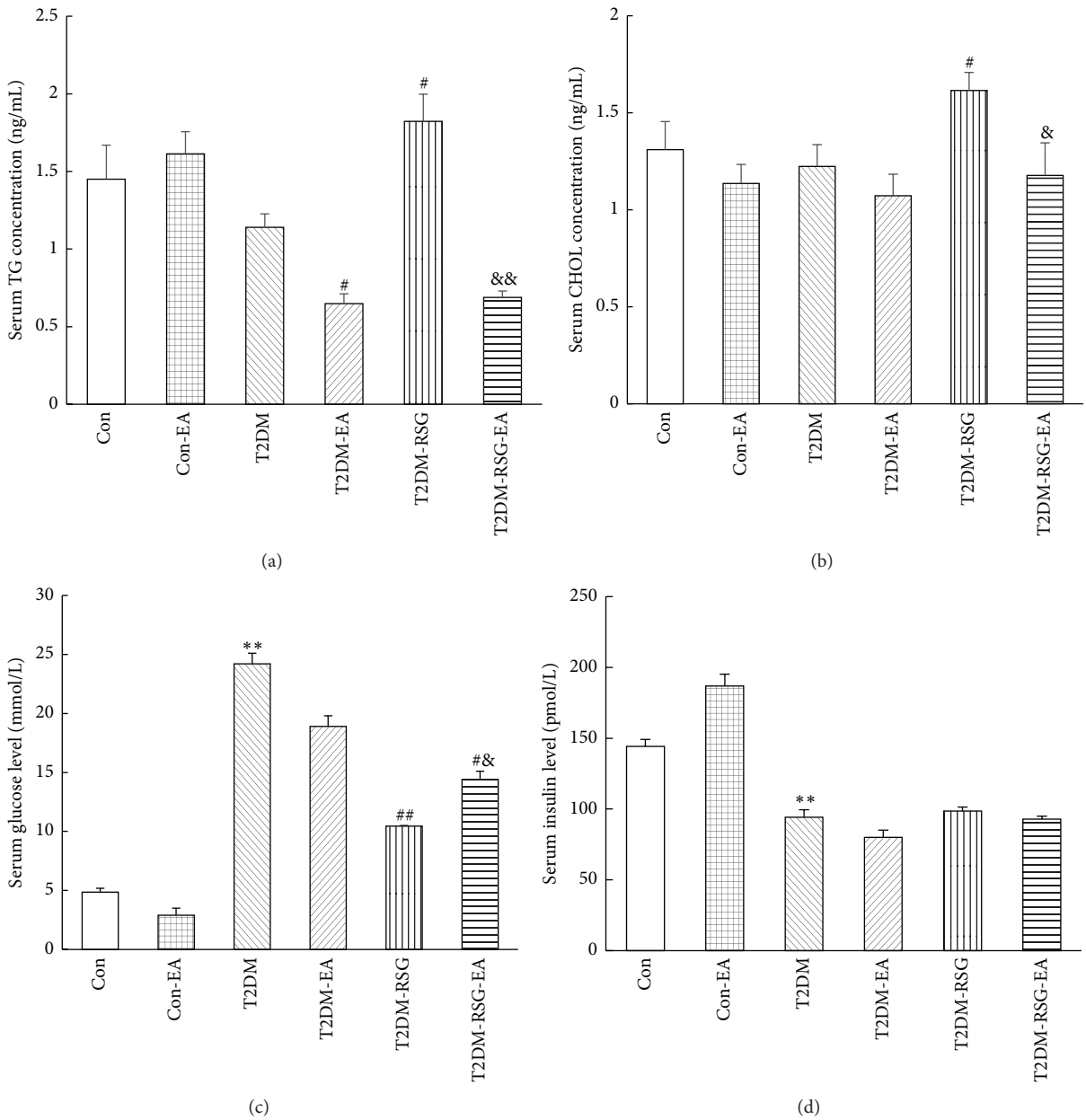

Figure 5: Serum triglyceride (a), total cholesterol (b), glucose (c), and insulin (d) concentrations were measured using a kit, as described in Section 2, respectively. Data were expressed as mean ± SD, $n = 6$, $^{**}p < 0.01$ versus Con rats, $^{\#}p < 0.05$, $^{\#\#}p < 0.01$ versus T2DM rats, and $^{\&}p < 0.05$, $^{\&\&}p < 0.01$ versus T2DM-RSG rats. TG, triglyceride; CHOL, cholesterol.

[42]. Acupuncture has been proved in animal models, such as obese rats, to reduce body weight [8, 9]. In the present study, electroacupuncture on Zusanli (ST36) and Neiting (ST44) markedly reduced body weight in the T2DM-RSG-EA rats and even in the control rats though the effect was mild (Figure 2). The ratio of the weight of IWAT, which is a major tissue for excess energy storage, to the body weight was significantly decreased upon acupuncture applications, suggesting that acupuncture can reduce energy storage to a certain extent. A decreased adipocyte size was observed in the T2DM-RSG-EA group (Figure 4), supporting its effect on inhibiting adipogenesis in the RSG-treated T2DM rats. Studies have shown that decreased appetite is one of the mechanisms by which acupuncture exerted weight loss effect in obese mice [8, 43]. Our present study also confirmed that electroacupuncture decreased food intake to a certain extent in the RSG-treated T2DM rats.

It is well known that weight gain effect of TZDs is a result of activated PPARγ signaling on adipogenesis; however, TZDs also induce hyperphagia in rodent models, which directly linked to the weight gain adverse effect [44–46], suggesting a central site of action. Together with these previous reports, our study suggests that PPARγ signaling in the CNS may influence energy intake and storage. PPARγ is

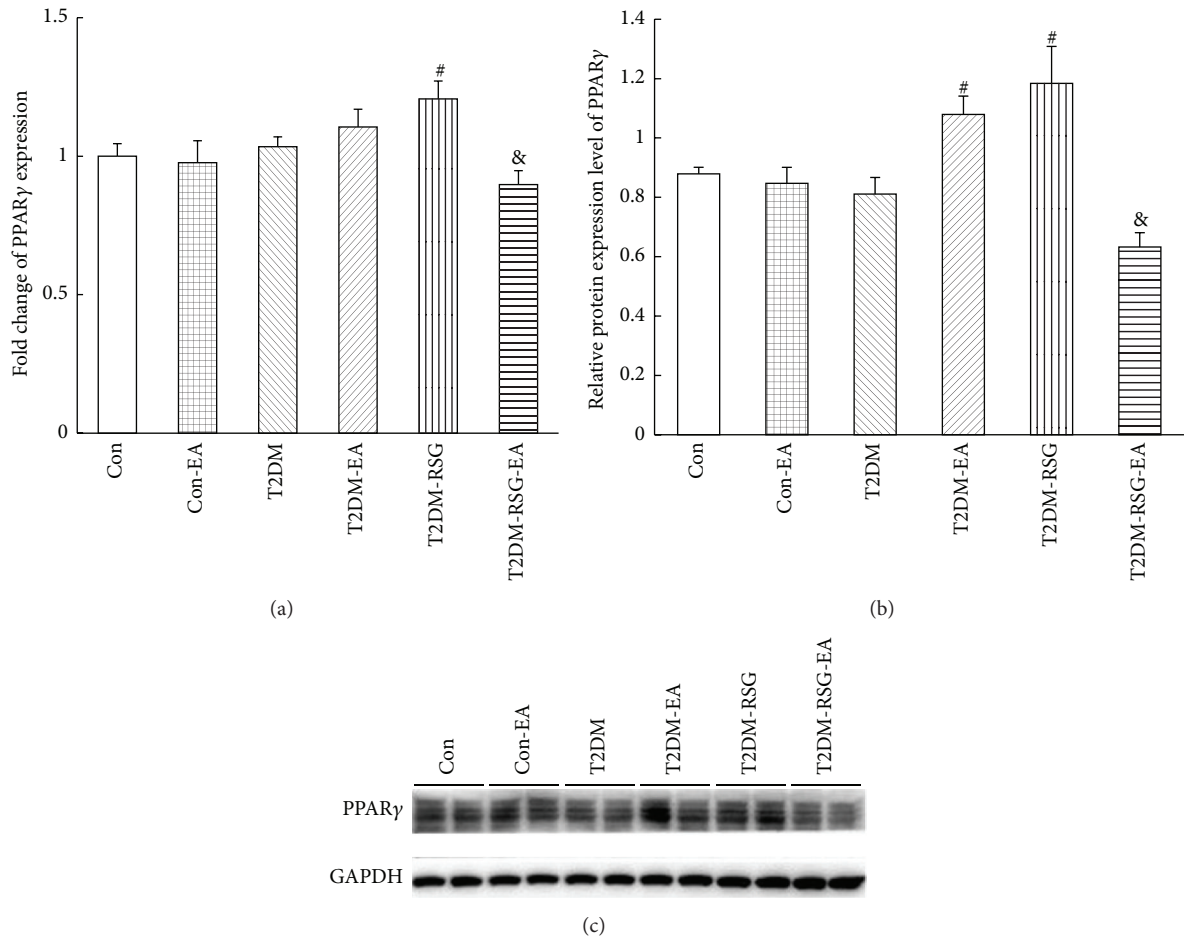

Figure 6: Effects of electroacupuncture and RSG treatment on PPARγ in hypothalamus of each group. (a) mRNA of PPARγ expression was detected by qPCR. Data were expressed as mean ± SD, $n = 6$, $^{\#}p < 0.05$ versus T2DM rats, and $^{\&}p < 0.05$ versus T2DM-RSG rats. (b) Quantitative analysis of PPARγ protein. Data were expressed as mean ± SD, $n = 6$, $^{\#}p < 0.05$ versus T2DM rats, and $^{\&}p < 0.05$ versus T2DM-RSG rats. (c) Western blot result of PPARγ protein in hypothalamus.

Table 2: mRNA fold change of PPARγ, leptin receptor, and STAT3 expression in each group.

Group	PPARγ	Leptin receptor	STAT3
Con	1.00 ± 0.045	1.00 ± 0.303	1.00 ± 0.084
Con-EA	0.98 ± 0.079	1.05 ± 0.104	0.21 ± 0.031*
T2DM	1.03 ± 0.036	1.49 ± 0.176	1.67 ± 0.207*
T2DM-EA	1.11 ± 0.064	1.36 ± 0.088	1.47 ± 0.135
T2DM-RSG	1.21 ± 0.065#	0.97 ± 0.131	0.50 ± 0.073#
T2DM-RSG-EA	0.90 ± 0.050&	1.96 ± 0.258&&	0.61 ± 0.021&

Data were expressed as mean ± SD, $n = 6$, $^{*}p < 0.05$ versus Con rats, $^{\#}p < 0.05$ versus T2DM rats, and $^{\&}p < 0.05$, $^{\&\&}p < 0.05$ versus T2DM-RSG rats using Student's t-test.

expressed in key brain areas, which controls energy homeostasis and glucose metabolism [47], raising the possibility that the CNS might be a previously unrecognized site for TZD action. Lu et al. showed important effects of brain PPARγ on food intake, energy expenditure, and insulin sensitivity [48]. Deletion of brain PPARγ led to both reduced food intake and increased energy expenditure. Our results revealed that RSG treatment increased PPARγ expression in hypothalamus, and electroacupuncture deteriorated the raise of PPARγ in RSG-treated T2DM rats. Our experiment, for the first time, provides the evidence that decreased PPARγ by acupuncture in the CNS can regulate hyperphagia at least partially.

The effect of leptin, a major regulator of body weight and food intake [49], is particularly evident in rodents and humans lacking a functional form of the protein, resulting in severe obesity and greatly increased appetite [50, 51]. Treatment with recombinant leptin reversed the obese phenotype in leptin-deficient humans [52]. The effect of leptin on food intake is mediated in part via leptin receptors present in the hypothalamus. Peripherally applied leptin in rodents induces a central signaling pathway that involves activation of STAT3 [29]. The requirement of this pathway to prevent severe hyperphagia and obesity was recently demonstrated in mice specifically lacking the STAT3-binding site of the leptin receptor [30] and in mice with reduced levels of STAT3 proteins selectively in CNS [31]. After binding to the long leptin receptor, STAT3 becomes phosphorylated by Janus kinase 2

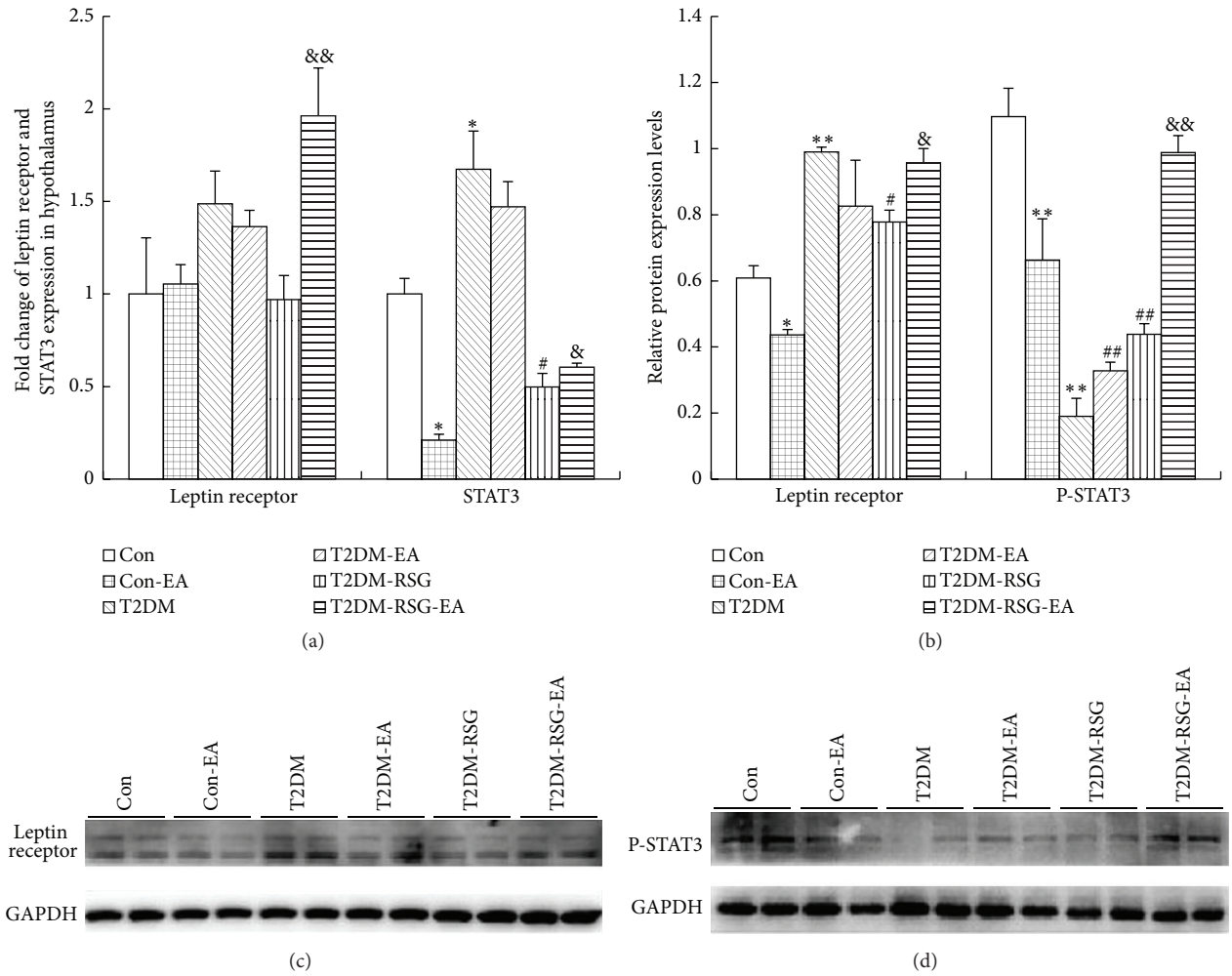

Figure 7: Leptin signaling expressions in hypothalamus of each group. (a) Representative mRNA of leptin signaling expressions was detected by qPCR. Data were expressed as mean ± SD, $n = 6$, $^{*}p < 0.05$ versus Con rats, $^{\#}p < 0.05$ versus T2DM rats, and $^{\&}p < 0.05$, $^{\&\&}p < 0.01$ versus T2DM-RSG rats. (b) Quantitative analysis of leptin signaling proteins. Data were expressed as mean ± SD, $n = 6$, $^{*}p < 0.05$, $^{**}p < 0.01$ versus Con rats, $^{\#}p < 0.05$, $^{\#\#}p < 0.01$ versus T2DM rats, and $^{\&}p < 0.05$, $^{\&\&}p < 0.01$ versus T2DM-RSG rats. (c) and (d) Representative Western blot results of leptin signaling proteins in hypothalamus.

(JAK2) and acts in the nucleus to regulate transcription [32]. El-Haschimi et al. [53] showed that, in diet-induced obesity (DIO) mice, a classical mouse model of leptin resistance and obesity, recombinant leptin completely failed to induce STAT3 activation in hypothalamic extracts, demonstrating severe leptin-resistant signaling in the hypothalamus of DIO mice. This maybe relevant in the pathogenesis of insulin-resistant type 2 diabetes, which is often associated with overweight. In addition, microinjection of leptin into the arcuate nucleus [54], the ventromedial hypothalamus [54, 55], and the nucleus of the solitary tract [56] inhibited food intake. In our study, the protein expression of leptin receptor increased in T2DM rats compared with the control group though its gene level did not change. After treatment with RSG for six weeks, the leptin receptor expression was significantly decreased. After six weeks of treatment with EA on Zusanli (ST36) and Neiting (ST44), the rats with RSG treatment (T2DM-RSG-EA) displayed upregulated leptin receptor expression level. Leptin-induced P-STAT3 level in the hypothalamus of T2DM-RSG-EA group was increased significantly compared with that in the T2DM-RSG rats. These data confirmed that acupuncture may promote reduction of food intake through leptin-STAT3 signaling in the CNS.

Acupuncture is usually used to rectify the imbalance within the body under disease conditions. When the T2DM rats' body weight pathologically reduced, EA may incline to activate the translation of ingestion-related genes such as PPARγ and OBRb to recover the abnormal phenotypes, including the reduced body weight. On the other hand, body weight of the T2DM rats treated with RSG was increased significantly compared with the T2DM group, and then EA may repress the expression of PPARγ and OBRb genes to rectify the imbalance of metabolism, although the mechanisms need to be further studied. As for the unchanged gene expression but elevated protein level of PPARγ and leptin receptor by EA

applied on T2DM rats, some posttranscriptional regulation mechanism might be considered but need to be confirmed by further experimental studies in the future. Recent study reported that leptin signaling contributes to the metabolic features associated with breast cancer malignancy, such as switching the cells' energy balance from mitochondrial β-oxidation to the aerobic glycolytic pathway. Leptin binds to its receptor leading to JAK-mediated tyrosine phosphorylation of the intracellular domain and, through JAK-STAT and MAPK activation, induces phosphorylation and nuclear translocation of glucocorticoid receptor (GR). In the nucleus, GR binds to glucocorticoid-responsive elements in the Leptin gene, resulting in upregulation of leptin expression. Treatment with PPARγ ligands blocks activation of JAK-STAT and MAPK signaling. PPARγ also binds to GR and to glucocorticoid-responsive elements in LEP; formation of a GR-PPARγ complex enables recruitment of nuclear receptor corepressors N-CoR1 and N-CoR2, which inhibit leptin transcription. Moreover, activation of PPARγ also decreases leptin receptor expression and inhibits its transductional pathways [57]. Based on this literature and our present results, we propose that acupuncture may regulate PPARγ expression in hypothalamus and then result in alteration of leptin expression, thus reducing food intake, although more biological experiments are needed to confirm the interaction of PPARγ and leptin pathway in the CNS in the TZDs-treated diabetic models.

5. Conclusion

Taking together, our results, for the first time, provided experimental evidences that EA can inhibit weight gain side effect of RSG through increased level of leptin receptor and STAT3 and decreased PPARγ expressions in CNS, which may contribute to reduced food intake. Further study for determining the interaction of PPARγ and leptin-STAT3 pathway in the CNS of TZDs- treated T2DM rats is of profound significance.

Conflict of Interests

The authors have no relevant affiliations or financial involvement with any organization or entity with a financial interest in or financial conflict with the subject matter or materials discussed in the paper. This includes employment, consultancies, honoraria, stock ownership or options, expert testimony, grants or patents received or pending, or royalties. No writing assistance was utilized in the production of this paper.

Authors' Contribution

Bing-Mei Zhu and Xinyue Jing conceived and designed the experiments. Chen Ou, Xinyue Jing, and Tianlin Wang performed the experiments. Xinyue Jing, Bing-Mei Zhu, Bin Xu, and Shengfeng Lu analyzed the data. Bing-Mei Zhu and Xinyue Jing wrote the paper.

Acknowledgments

This work was supported by National Natural Science Foundation of China (Grants nos. 81303018 and 81273838), the National Natural Science Foundation of Jiangsu Colleges and Universities (Grant no. 11KJB360006), Innovative Entrepreneurial Talent Project in Jiangsu Province (2012), and Jiangxi Provincial "Gan-Po Talents Project 555."

References

[1] A. L. Hevener, J. M. Olefsky, D. Reichart et al., "Macrophage PPARγ is required for normal skeletal muscle and hepatic insulin sensitivity and full antidiabetic effects of thiazolidinediones," *Journal of Clinical Investigation*, vol. 117, no. 6, pp. 1658–1669, 2007.

[2] F. Picard and J. Auwerx, "PPARγ and glucose homeostasis," *Annual Review of Nutrition*, vol. 22, pp. 167–197, 2002.

[3] M. Lehrke and M. A. Lazar, "The many faces of PPARγ," *Cell*, vol. 123, no. 6, pp. 993–999, 2005.

[4] H. Shimizu, T. Tsuchiya, N. Sato, Y. Shimomura, I. Kobayashi, and M. Mori, "Troglitazone reduces plasma leptin concentration but increases hunger in NIDDM patients," *Diabetes Care*, vol. 21, no. 9, pp. 1470–1474, 1998.

[5] S. Darbandi, M. Darbandi, P. Mokarram et al., "Effects of body electroacupuncture on plasma leptin concentrations in obese and overweight people in Iran: a randomized controlled trial," *Alternative Therapies in Health and Medicine*, vol. 19, no. 2, pp. 24–31, 2013.

[6] L. Rerksuppaphol, "Efficacy of auricular acupressure combined with transcutaneous electrical acupoint stimulation for weight reduction in obese women," *Journal of the Medical Association of Thailand*, vol. 95, supplement 12, pp. S32–S39, 2012.

[7] Q. Wang, W.-H. Li, Q.-H. Zhou, X.-D. Tang, X.-X. Zhang, and S. Shu, "Weight reduction effects of acupuncture for obese women with or without perimenopausal syndrome: a pilot observational study," *The American Journal of Chinese Medicine*, vol. 40, no. 6, pp. 1157–1166, 2012.

[8] F. Wang, D. R. Tian, P. Tso, and J. S. Han, "Arcuate nucleus of hypothalamus is involved in mediating the satiety effect of electroacupuncture in obese rats," *Peptides*, vol. 32, no. 12, pp. 2394–2399, 2011.

[9] M. Gong, X. Wang, Z. Mao, Q. Shao, X. Xiang, and B. Xu, "Effect of electroacupuncture on leptin resistance in rats with diet-induced obesity," *The American Journal of Chinese Medicine*, vol. 40, no. 3, pp. 511–520, 2012.

[10] B. Ji, J. Hu, and S. Ma, "Effects of electroacupuncture Zusanli (ST36) on food intake and expression of POMC and TRPV1 through afferents-medulla pathway in obese prone rats," *Peptides*, vol. 40, pp. 188–194, 2013.

[11] M. T. Cabıoğlu and N. Ergene, "Electroacupuncture therapy for weight loss reduces serum total cholesterol, triglycerides, and LDL cholesterol levels in obese women," *The American Journal of Chinese Medicine*, vol. 33, no. 4, pp. 525–533, 2005.

[12] E. D. Rosen, P. Sarraf, A. E. Troy et al., "PPAR gamma is required for the differentiation of adipose tissue in vivo and in vitro," *Molecular Cell*, vol. 4, no. 4, pp. 611–617, 1999.

[13] B. M. Spiegelman, "PPAR-γ: adipogenic regulator and thiazolidinedione receptor," *Diabetes*, vol. 47, no. 4, pp. 507–514, 1998.

[14] P. Escher, O. Braissant, S. Basu-Modak, L. Michalik, W. Wahli, and B. Desvergne, "Rat PPARs: quantitative analysis in adult rat

tissues and regulation in fasting and refeeding," *Endocrinology*, vol. 142, no. 10, pp. 4195–4202, 2001.

[15] E. D. Rosen, R. N. Kulkarni, P. Sarraf et al., "Targeted elimination of peroxisome proliferator-activated receptor γ in β cells leads to abnormalities in islet mass without compromising glucose homeostasis," *Molecular and Cellular Biology*, vol. 23, no. 20, pp. 7222–7229, 2003.

[16] Y. Guan, C. Hao, D. R. Cha et al., "Thiazolidinediones expand body fluid volume through PPARgamma stimulation of ENaC-mediated renal salt absorption," *Nature Medicine*, vol. 11, no. 8, pp. 861–866, 2005.

[17] S. Akazawa, F. Sun, M. Ito, E. Kawasaki, and K. Eguchi, "Efficacy of troglitazone on body fat distribution in type 2 diabetes," *Diabetes Care*, vol. 23, no. 8, pp. 1067–1071, 2000.

[18] Y. Miyazaki, A. Mahankali, M. Matsuda et al., "Effect of pioglitazone on abdominal fat distribution and insulin sensitivity in type 2 diabetic patients," *Journal of Clinical Endocrinology and Metabolism*, vol. 87, no. 6, pp. 2784–2791, 2002.

[19] S. Shadid and M. D. Jensen, "Effects of pioglitazone versus diet and exercise on metabolic health and fat distribution in upper body obesity," *Diabetes Care*, vol. 26, no. 11, pp. 3148–3152, 2003.

[20] S. R. Smith, L. De Jonge, J. Volaufova, Y. Li, H. Xie, and G. A. Bray, "Effect of pioglitazone on body composition and energy expenditure: a randomized controlled trial," *Metabolism: Clinical and Experimental*, vol. 54, no. 1, pp. 24–32, 2005.

[21] S. Moreno, S. Farioli-Vecchioli, and M. P. Cerù, "Immunolocalization of peroxisome proliferator-activated receptors and retinoid X receptors in the adult rat CNS," *Neuroscience*, vol. 123, no. 1, pp. 131–145, 2004.

[22] D. A. Sarruf, F. Yu, H. T. Nguyen et al., "Expression of peroxisome proliferator-activated receptor-γ in key neuronal subsets regulating glucose metabolism and energy homeostasis," *Endocrinology*, vol. 150, no. 2, pp. 707–712, 2009.

[23] A. Mouihate, L. Boissé, and Q. J. Pittman, "A novel antipyretic action of 15-deoxy-Delta12,14-prostaglandin J2 in the rat brain," *Journal of Neuroscience*, vol. 24, no. 6, pp. 1312–1318, 2004.

[24] P. De Vos, A.-M. Lefebvre, S. G. Miller et al., "Thiazolidinediones repress ob gene expression in rodents via activation of peroxisome proliferator-activated receptor gamma," *The Journal of Clinical Investigation*, vol. 98, no. 4, pp. 1004–1009, 1996.

[25] J. Rieusset, J. Auwerx, and H. Vidal, "Regulation of gene expression by activation of the peroxisome proliferator-activated receptor γ with rosiglitazone (BRL 49653) in human adipocytes," *Biochemical and Biophysical Research Communications*, vol. 265, no. 1, pp. 265–271, 1999.

[26] S. Goetze, A. Bungenstock, C. Czupalla et al., "Leptin induces endothelial cell migration through Akt, which is inhibited by PPARγ-ligands," *Hypertension*, vol. 40, no. 5, pp. 748–754, 2002.

[27] J. I. Lee, Y.-H. Paik, K. S. Lee et al., "A peroxisome-proliferator activated receptor-gamma ligand could regulate the expression of leptin receptor on human hepatic stellate cells," *Histochemistry and Cell Biology*, vol. 127, no. 5, pp. 495–502, 2007.

[28] R. S. Ahima and J. S. Flier, "Leptin," *Annual Review of Physiology*, vol. 62, pp. 413–437, 2000.

[29] C. Vaisse, J. L. Halaas, C. M. Horvath, J. E. Dernell Jr., M. Stoffel, and J. M. Friedman, "Leptin activation of Stat3 in the hypothalamus of wild-type and ob/ob mice but not db/db mice," *Nature Genetics*, vol. 14, no. 1, pp. 95–97, 1996.

[30] S. H. Bates, W. H. Stearns, T. A. Dundon et al., "STAT3 signalling is required for leptin regulation of energy balance but not reproduction," *Nature*, vol. 421, no. 6925, pp. 856–859, 2003.

[31] Q. Gao, M. J. Wolfgang, S. Neschen et al., "Disruption of neural signal transducer and activator of transcription 3 causes obesity, diabetes, infertility, and thermal dysregulation," *Proceedings of the National Academy of Sciences of the United States of America*, vol. 101, no. 13, pp. 4661–4666, 2004.

[32] C. Bjørbaek and B. B. Kahn, "Leptin signaling in the central nervous system and the periphery," *Recent Progress in Hormone Research*, vol. 59, pp. 305–331, 2004.

[33] M. J. Reed, K. Meszaros, L. J. Entes et al., "A new rat model of type 2 diabetes: the fat-fed, streptozotocin-treated rat," *Metabolism: Clinical and Experimental*, vol. 49, no. 11, pp. 1390–1394, 2000.

[34] K. Srinivasan, B. Viswanad, L. Asrat, C. L. Kaul, and P. Ramarao, "Combination of high-fat diet-fed and low-dose streptozotocin-treated rat: a model for type 2 diabetes and pharmacological screening," *Pharmacological Research*, vol. 52, no. 4, pp. 313–320, 2005.

[35] E. Bonora, G. Targher, M. Alberiche et al., "Homeostasis model assessment closely mirrors the glucose clamp technique in the assessment of insulin sensitivity: studies in subjects with various degrees of glucose tolerance and insulin sensitivity," *Diabetes Care*, vol. 23, no. 1, pp. 57–63, 2000.

[36] K. Hermansen and L. S. Mortensen, "Bodyweight changes associated with antihyperglycaemic agents in type 2 diabetes mellitus," *Drug Safety*, vol. 30, no. 12, pp. 1127–1142, 2007.

[37] V. Fonseca, "Effect of thiazolidinediones on body weight in patients with diabetes mellitus," *American Journal of Medicine*, vol. 115, supplement 8, pp. 42S–48S, 2003.

[38] A. L. Werner and M. T. Travaglini, "A review of rosiglitazone in type 2 diabetes mellitus," *Pharmacotherapy*, vol. 21, no. 9, pp. 1082–1099, 2001.

[39] J. Chilcott, P. Tappenden, M. L. Jones, and J. P. Wight, "A systematic review of the clinical effectiveness of pioglitazone in the treatment of type 2 diabetes mellitus," *Clinical Therapeutics*, vol. 23, no. 11, pp. 1792–1823, 2001.

[40] J. Vamecq and N. Latruffe, "Medical significance of peroxisome proliferator-activated receptors," *The Lancet*, vol. 354, no. 9173, pp. 141–148, 1999.

[41] S. Kersten, B. Desvergne, and W. Wahli, "Roles of PPARS in health and disease," *Nature*, vol. 405, no. 6785, pp. 421–424, 2000.

[42] A. N. Howard, "The historical development, efficacy and safety of very-low-calorie diets," *International Journal of Obesity*, vol. 5, no. 3, pp. 195–208, 1981.

[43] N. Tian, F. Wang, D.-R. Tian et al., "Electroacupuncture suppresses expression of gastric ghrelin and hypothalamic NPY in chronic food restricted rats," *Peptides*, vol. 27, no. 9, pp. 2313–2320, 2006.

[44] L. C. Pickavance, R. E. Buckingham, and J. P. H. Wilding, "Insulin-sensitizing action of rosiglitazone in enhanced by preventing hyperphagia," *Diabetes, Obesity and Metabolism*, vol. 3, no. 3, pp. 171–180, 2001.

[45] E. Chaput, R. Saladin, M. Silvestre, and A. D. Edgar, "Fenofibrate and rosiglitazone lower serum triglycerides with opposing effects on body weight," *Biochemical and Biophysical Research Communications*, vol. 271, no. 2, pp. 445–450, 2000.

[46] Q. Wang, S. Dryden, H. M. Frankish et al., "Increased feeding in fatty Zucker rats by the thiazolidinedione BRL 49653 (rosiglitazone) and the possible involvement of leptin and hypothalamic neuropeptide Y," *British Journal of Pharmacology*, vol. 122, no. 7, pp. 1405–1410, 1997.

[47] D. A. Sarruf, F. Yu, H. T. Nguyen et al., "Expression of peroxisome proliferator-activated receptor-gamma in key neuronal subsets regulating glucose metabolism and energy homeostasis," *Endocrinology*, vol. 150, no. 2, pp. 707–712, 2009.

[48] M. Lu, D. A. Sarruf, S. Talukdar et al., "Brain PPAR-γ promotes obesity and is required for the insuling-sensitizing effect of thiazolidinediones," *Nature Medicine*, vol. 17, no. 5, pp. 618–622, 2011.

[49] M. W. Schwartz, S. C. Woods, D. Porte Jr., R. J. Seeley, and D. G. Baskin, "Central nervous system control of food intake," *Nature*, vol. 404, no. 6778, pp. 661–671, 2000.

[50] M. A. Pelleymounter, M. J. Cullen, M. B. Baker et al., "Effects of the obese gene product on body weight regulation in ob/ob mice," *Science*, vol. 269, no. 5223, pp. 540–543, 1995.

[51] C. T. Montague, I. S. Farooqi, J. P. Whitehead et al., "Congenital leptin deficiency is associated with severe early-onset obesity in humans," *Nature*, vol. 387, no. 6636, pp. 903–908, 1997.

[52] I. Sadaf Farooqi, G. Matarese, G. M. Lord et al., "Beneficial effects of leptin on obesity, T cell hyporesponsiveness, and neuroendocrine/metabolic dysfunction of human congenital leptin deficiency," *The Journal of Clinical Investigation*, vol. 110, no. 8, pp. 1093–1103, 2002.

[53] K. El-Haschimi, D. D. Pierroz, S. M. Hileman, C. Bjørbæk, and J. S. Flier, "Two defects contribute to hypothalamic leptin resistance in mice with diet-induced obesity," *The Journal of Clinical Investigation*, vol. 105, no. 12, pp. 1827–1832, 2000.

[54] N. Satoh, Y. Ogawa, G. Katsuura et al., "The arcuate nucleus as a primary site of satiety effect of leptin in rats," *Neuroscience Letters*, vol. 224, no. 3, pp. 149–152, 1997.

[55] R. J. Jacob, J. Dziura, M. B. Medwick et al., "The effect of leptin is enhanced by microinjection into the ventromedial hypothalamus," *Diabetes*, vol. 46, no. 1, pp. 150–152, 1997.

[56] H. J. Grill, M. W. Schwartz, J. M. Kaplan, J. S. Foxhall, J. Breininger, and D. G. Baskin, "Evidence that the caudal brainstem is a target for the inhibitory effect of leptin on food intake," *Endocrinology*, vol. 143, no. 1, pp. 239–246, 2002.

[57] S. Andò and S. Catalano, "The multifactorial role of leptin in driving the breast cancer microenvironment," *Nature Reviews Endocrinology*, vol. 8, no. 5, pp. 263–275, 2012.

Hindawi Publishing Corporation
Evidence-Based Complementary and Alternative Medicine
Volume 2016, Article ID 8912184, 8 pages
http://dx.doi.org/10.1155/2016/8912184

Research Article

The Protective Effects of Isoliquiritigenin and Glycyrrhetinic Acid against Triptolide-Induced Oxidative Stress in HepG2 Cells Involve Nrf2 Activation

Ling-Juan Cao,[1,2,3] Huan-De Li,[1,2,3] Miao Yan,[1,2,3] Zhi-Hua Li,[1,2,3] Hui Gong,[1,2,3] Pei Jiang,[1,2,3] Yang Deng,[1,2] Ping-Fei Fang,[1,2,3] and Bi-Kui Zhang[1,2,3]

[1] *Department of Pharmacy, The Second Xiangya Hospital, Central South University, Changsha 410011, China*
[2] *Institute of Clinical Pharmacy, Central South University, Changsha 410011, China*
[3] *School of Pharmaceutical Sciences, Central South University, Changsha 410013, China*

Correspondence should be addressed to Miao Yan; yanmiaocsu@126.com

Received 5 November 2015; Revised 14 December 2015; Accepted 21 December 2015

Academic Editor: Mohamed M. Abdel-Daim

Triptolide (TP), an active ingredient of *Tripterygium wilfordii* Hook f., possesses a wide range of biological activities. Oxidative stress likely plays a role in TP-induced hepatotoxicity. Isoliquiritigenin (ISL) and glycyrrhetinic acid (GA) are potent hepatoprotection agents. The aim of the present study was to investigate whether Nrf2 pathway is associated with the protective effects of ISL and GA against TP-induced oxidative stress or not. HepG2 cells were treated with TP (50 nM) for 24 h after pretreatment with ISL and GA (5, 10, and 20 μM) for 12 h and 24 h, respectively. The results demonstrated that TP treatment significantly increased ROS levels and decreased GSH levels. Both ISL and GA pretreatment decreased ROS and meanwhile enhanced intracellular GSH content. Additionally, TP treatment obviously decreased the protein expression of Nrf2 and its target genes including HO-1 and MRP2 except NQO1. Moreover, both ISL and GA displayed activities as inducers of Nrf2 and increased the expression of HO-1, NQO1, and MRP2. Taken together the current data confirmed that ISL and GA could activate the Nrf2 antioxidant response in HepG2 cells, increasing the expression of its target genes which may be partly associated with their protective effects in TP-induced oxidative stress.

1. Introduction

Triptolide (TP), a major active ingredient extracted from the widely used Chinese herb *Tripterygium wilfordii* Hook f. (TWHF), has been demonstrated to possess various biological activities including anti-inflammation, immune modulation, and antiproliferative activity [1]. However, the clinical application of TP is limited by its narrow therapeutic window and severe toxicities involving hepatotoxicity, nephrotoxicity, and reproductive toxicity [1]. Among these, hepatotoxicity has drawn great attention [2]. A possible mechanism of TP-induced hepatotoxicity was related to oxidative stress damage caused by reactive oxygen species (ROS) [2].

The nuclear factor erythroid 2-related factor 2 (Nrf2) is an emerging regulator of cellular resistance to substances causing oxidative stress [3]. Under physiological condition, Nrf2 is present in the cytoplasm binding to the Kelch-like ECH-associated protein 1 (Keap1). Under stress condition, Nrf2 dissociates from Keap1 and translocates into the nuclear where it binds to antioxidant responsive element (ARE), leading to the expression of its target genes [4]. These include many cytoprotective proteins and drug efflux transporters, such as heme oxygenase 1 (HO-1), NAD (P) H: quinone oxidoreductase (NQO1), glutamate cysteine ligase (GCL), and multidrug resistance-associated protein 2 (MRP2) [5, 6]. Nrf2 pathway is considered as an important endogenous antioxidant signaling pathway and increasing number of studies suggested the potential role of Nrf2 as a therapeutic target to prevent liver injury caused by oxidative stress [7, 8].

Licorice (*Glycyrrhiza uralensis*), a common used Traditional Chinese Medicine (TCM), contains various bioactive compounds including triterpene saponins (mainly

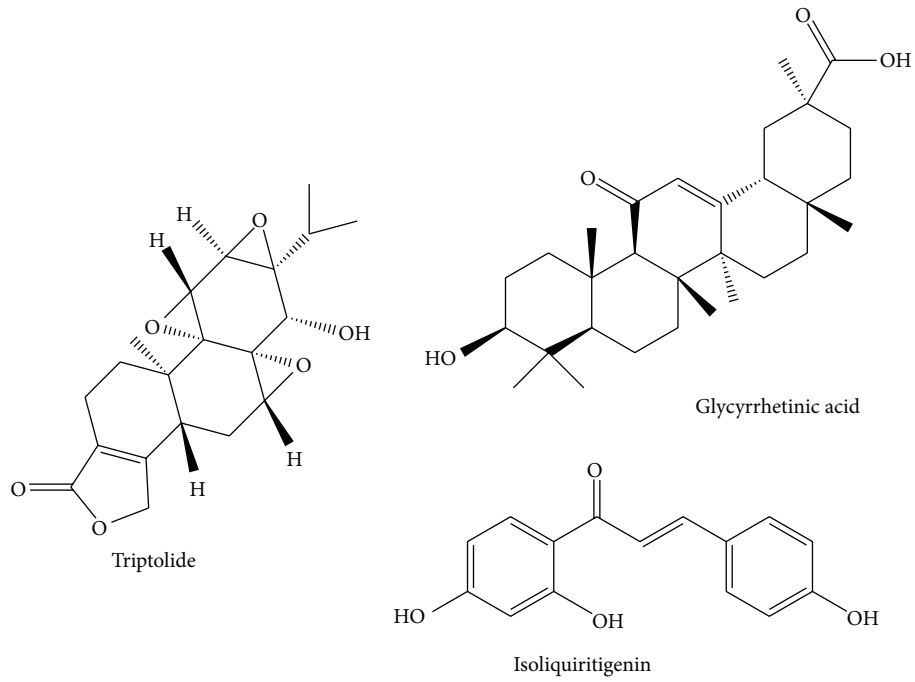

Figure 1: The structures of TP, GA, and ISL.

glycyrrhizin and its bioactive metabolite glycyrrhetinic acid (GA)), flavonoids (such as isoliquiritigenin (ISL)), coumarin, alkaloids, polysaccharides, and amino acids. ISL and GA are two main biologically active components for their useful pharmacological properties such as antioxidation, anti-inflammation, hepatoprotection, and antiviral activity [9]. The structures of ISL and GA are shown in Figure 1.

Licorice is often in combination with TWHF clinically for its toxicity attenuation and efficacy potentiation effect on the treatment of rheumatoid arthritis [1, 10]. Moreover, glycyrrhizin acid has a synergistic effect with TP, thus making TP effective at a lower dosage which may reduce the toxicity of TP since this toxicity is dose-dependent [11]. However, details of the hepatoprotection mechanisms remain to be elucidated. In our previous study, we demonstrated that licorice may intervene in the Nrf2 pathway to induce its target genes, which indicate a novel mechanism for the use of licorice to lower drug toxicity [12]. Based on this observation, our objective was to investigate the regulation effect of ISL and GA on Nrf2 pathway and the protective effects of ISL and GA on TP-induced oxidative stress in human hepatocarcinoma HepG2 cells.

2. Materials and Methods

2.1. Chemicals and Reagents. ISL (purity > 99%), GA (purity > 99%), and TP (purity ≥ 98%) were purchased from On-Road Biotechnology Co., Ltd. (Changsha, China). *tert*-butylhydroquinone (tBHQ), dimethyl sulfoxide (DMSO), and methyl thiazolyl tetrazolium (MTT) were purchased from Sigma-Aldrich (St. Louis, MO, USA). Glutathione (GSH) Detection Kit was purchased from Nanjing Jiancheng Bioengineering Institute (Nanjing, China). Reactive Oxygen Species Assay Kit was purchased from Beyotime Institute of Biotechnology (Shanghai, China). Nrf2 antibody was purchased from Santa Cruz Biotechnology (Santa Cruz, CA, USA). HO-1, NQO1, and MRP2 antibodies were purchased from Abcam Biotechnology Co. (Milton, Cambridge, UK). Other chemicals were of analytical grade from commercial suppliers.

2.2. Cell Culture. Human hepatocarcinoma cell line HepG2 obtained from Xiangya Cell Bank (Changsha, China) was cultured in Dulbecco Modified Eagle's Medium (Hyclone, Logan, USA) supplemented with 10% (v/v) fetal bovine serum (Sijiqing, Hangzhou, China) in a 37°C incubator with 5% CO_2. ISL, GA, tBHQ, and TP were dissolved in DMSO and stock solutions were stored at −20°C. Drugs were freshly diluted to the indicated concentrations with culture medium before use. DMSO concentration in experimental conditions never exceeded 0.1% (v/v).

2.3. MTT Assay. Cell viability was determined by MTT assay. Briefly, cells were counted and plated in a 24-well tissue culture plate and the seeding densities were 2×10^4 cells/well. After 24 h of growth, cells were preincubated with ISL, GA (0, 5, 10, 20, 40, 60, 80, and 100 μM) and TP (0, 10, 20, 40, 50, 60, 80, and 100 nM), respectively, for desired time. Then MTT (5 mg/mL) was added to each well (300 μL) and incubated for 3–5 h, after which the MTT was removed and DMSO (300 μL) was added to each well. After shaking for 10 min, each sample was transferred to a 96-well microtiter plate and the absorbance was recorded at 490 nm.

2.4. Measurement of Intracellular ROS. The fluorescent probe DCFH-DA was used to determine the intracellular

accumulation of ROS. HepG2 cells were seeded in 96-well black plates at a density of 5×10^3 cells/well and then exposed to various concentrations of ISL, GA for 12 h and 24 h, respectively. After that the complete medium was removed and replaced with medium containing TP (50 nM) for 24 h. Then, the cells were washed with serum-free medium and incubated with DCFH-DA (10 μM) for 20 min at 37°C. The fluorescent intensity was measured at an excitation wavelength of 488 nm and emission wavelength of 525 nm.

2.5. GSH Detection. For the measurement of GSH content, HepG2 cells were seeded in 60 cm^2 dishes with 6×10^5 cells/well. Cells were exposed to drugs as described above, after which cells were harvested and lysed by ultrasonication. Following centrifugation at 3500 ×g for 10 min at 4°C, the supernatant was maintained on ice until assayed by GSH detection Kit according to the manufacturer's instructions.

2.6. Preparation of Cell Lysates and Western Blotting. Cells were lysed with RIPA buffer (CW biotech, Beijing, China) and equivalent amounts of protein were separated by 10% SDS-PAGE and transferred to PVDF membranes. After being blocked in 5% nonfat milk in TBST for 1 h at room temperature, the membranes were incubated with the primary antibodies at 4°C overnight. Subsequently, the immunoblots were then incubated with a secondary antibody at room temperature. The membranes were developed using an electrochemiluminescence (ECL) kit (Advansta, USA) according to the manufacturer's protocol.

2.7. Statistics. Results from the experiments were reported as mean ± standard deviation (SD) and conducted with SPSS 19.0. All data were analyzed by one-way ANOVA, followed by Tukey's test. Statistical significance was accepted at a p value less than 0.05.

3. Results

3.1. Cytotoxicity Effects of TP, ISL, and GA. HepG2 cells were treated with tested drugs and cell viability was measured using the MTT assay to evaluate the cytotoxicity effect. As shown in Figures 2(a) and 2(b), ISL decreased the cell viability in dose- and time-dependent manner while GA exhibited no obvious cytotoxicity after 12 h even 24 h of treatment. Based on this observation, the low dose (5, 10, and 20 μM) of ISL and GA treatment for 12 h and 24 h, respectively, was chosen for the following research. After exposure to TP for desired time, the relative cell survival rate decreased dose-dependently (Figure 2(c)). Moreover, the IC_{50} (24 h) was 41.0 nM and a 24 h and the concentration of 50 nM were selected for the following experiment.

3.2. Oxidative Stress. The effects of ISL and GA combining with TP on ROS levels were assessed and tBHQ, a classical activator of Nrf2, was used as positive control. As shown in Figure 3(a), after 50 nM TP treatment for 24 h, the increasing levels of relative ROS were observed, which may lead to increasing probability of cellular damage caused by ROS. However, ISL and GA dose-dependently attenuated TP-induced ROS production compared with TP-treated alone.

3.3. Antioxidant Activity. The intracellular GSH content was detected to confirm the antioxidative activities of ISL and GA. TP significantly decreased intracellular GSH levels after 24 h of treatment as shown in Figure 3(b). Moreover, this decline was attenuated by administration of ISL and GA which both enhanced intracellular GSH content dose-dependently.

3.4. Effects of ISL and GA on the Protein Expression Nrf2 and Its Target Genes. TP pronouncedly suppressed the expression of Nrf2 (Figure 4). In addition, the results indicated that the amount of protein expression of Nrf2 was increased dose-dependently in ISL and GA pretreatment groups compared with TP-treated group. Furthermore, the protein expression of the downstream genes including HO-1, NQO1, and MRP2 was measured (Figures 5 and 6). TP significantly decreased the protein abundance of HO-1 and MRP2 while the expression of NQO1 was significantly increased. Compared with TP-treated group, ISL and GA pretreatment group showed a marked increase in the expression of HO-1, NQO1, and MRP2 in a dose-dependent manner.

4. Discussion

TWHF is a well-known herbal medicine that is widely used to treat various diseases, including rheumatoid arthritis, nephritic syndrome, and lupus [1]. TP is a major active ingredient extracted and isolated from TWHF in 1972, and its pharmacological effects have been extensively investigated. But before this compound can reach its clinical potential, significant challenges remain to overcome, such as severe toxicities involving hepatotoxicity and poor aqueous solubility [13]. To enhance its efficacy and to decrease its toxicity, TWHF is frequently used in combination with other Chinese herbs, such as *Glycyrrhiza uralensis* Fisch. (Licorice) and *Astragalus membranaceus* (Fisch.) Bunge [14]. Licorice has also been a commonly used Traditional Chinese Medicine for many years. ISL and GA, two main active ingredients obtained from licorice, contain a Michael acceptor which is common to many ARE inducers [15]. The α,β-unsaturated carbonyl group has been shown to modify specific cysteine residues of Keap1, which confirm their activation effects on Nrf2 pathway structurally [16]. In addition, our laboratory previously found that ISL (among four compounds derived from licorice) was the most potent Nrf2 pathway inducer in HepG2 [12]. In the present study, we further conveyed that ISL and GA could activate the Nrf2 pathway, increase the protein expression of its target genes, and protect against TP-induced oxidative stress in HepG2 cells.

Activation of Nrf2 pathway plays pivotal role in preventing xenobiotic-related oxidative damage [17]. In current study, the protective role of Nrf2 was found to be attributed partly to its involvement in coordinated induction of phase II enzymes and phase III drug transporters. HO-1 catalyzes the first and rate-limiting step in the catabolism of the prooxidant heme to carbon monoxide, biliverdin, and free iron [18, 19]. It

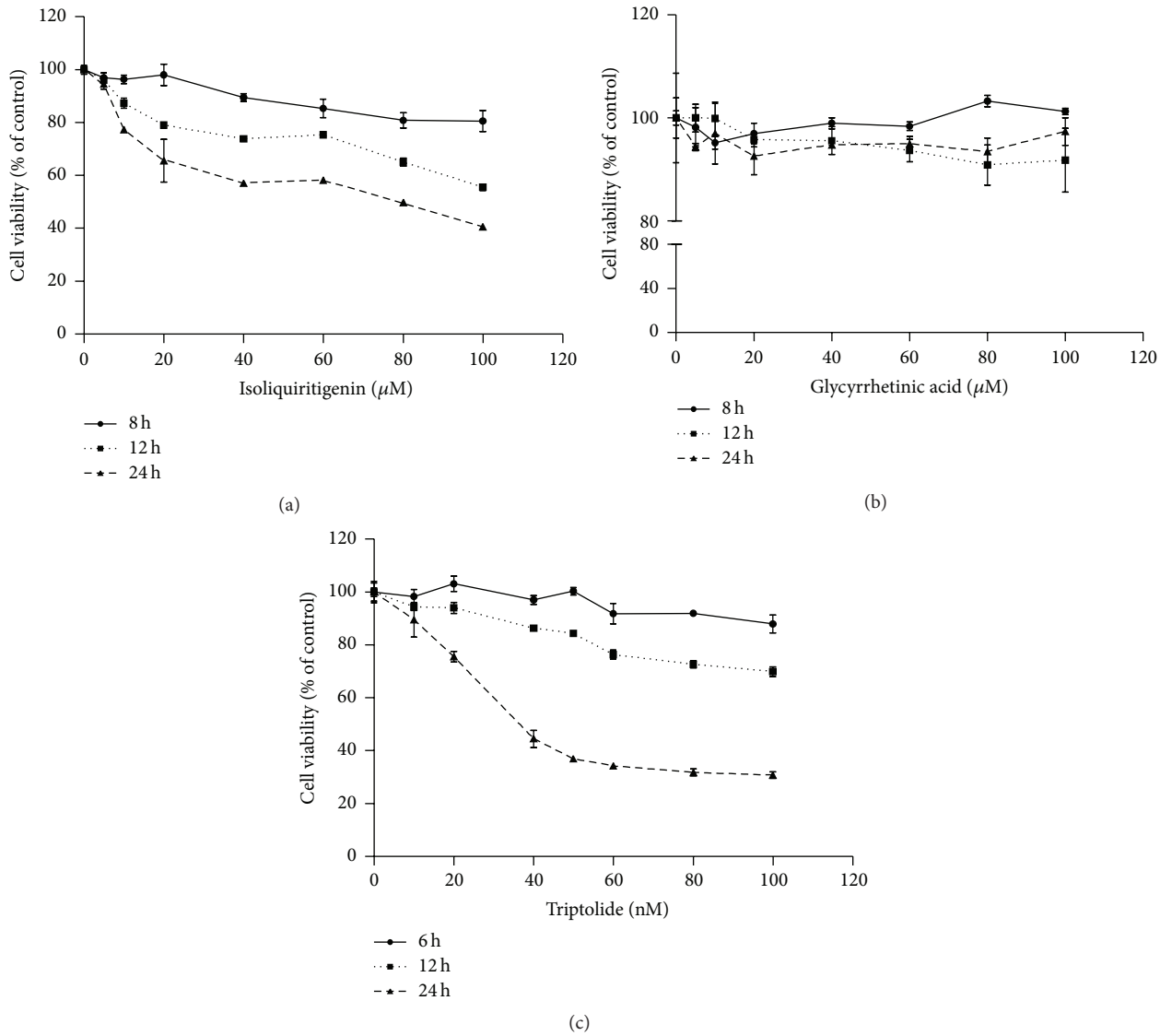

Figure 2: Cytotoxicity of ISL (a), GA (b), and TP (c) in HepG2 cells. Cells were exposed to various concentrations and time of tested drugs before being subjected to the MTT assay ($n = 3$).

has been implicated to play a protective role in antioxidative activity following cellular injury and oxidative stress [20]. NQO1 is a cytosolic flavoprotein catalyzing the electroreductive metabolism and detoxification of endogenous and exogenous chemicals [21]. GCL, consisting of a modulatory (GCLM) and a catalytic (GCLC) subunit, is the rate-limiting enzyme for biosynthesis of GSH [22]. MRP2 participates in excretion of chemicals into bile, especially glutathione-, glucuronide-, and sulfate-conjugated metabolites [23]. All of these are important drug metabolism enzymes and transporters and played vital role in antioxidation and toxicant metabolism and excretion.

A lot of studies including ours had focused on the effect of licorice on Nrf2 pathway [12]. A study found that ISL had suppressive effect on lipopolysaccharide-induced inflammatory responses in murine macrophage which may be associated with inhibiting the Keap1, increasing Nrf2 translocation, and inducing the mRNA expression of UGT1A1, NQO1, and HO-1 [24]. On the other hand, GA delayed the progression of cisplatin-induced renal injury through upregulation of Nrf2 in the BALB/c mice [25]. Moreover, GA protected against CCL_4-induced mice chronic liver fibrosis involving upregulation of Nrf2 [26]. Although numerous studies demonstrated that ISL and GA could activate Nrf2 pathway, the current study is the first to combine ISL and GA with TP to assess their effects on reducing TP-induced hepatotoxicity.

Nrf2 is antioxidant transcription factor leading to protection against oxidative stress by associating with AREs and inducting its target genes described above. The effect of TP to inhibit Nrf2 pathway has been demonstrated in heart tissues and Leydig cells [27, 28]. Consequently, the current study hypothesized that it is also the target of TP in HepG2 cells. It is worthy to notice that the protein expression of Nrf2, HO-1, and MRP2 decreased obviously suggesting that this

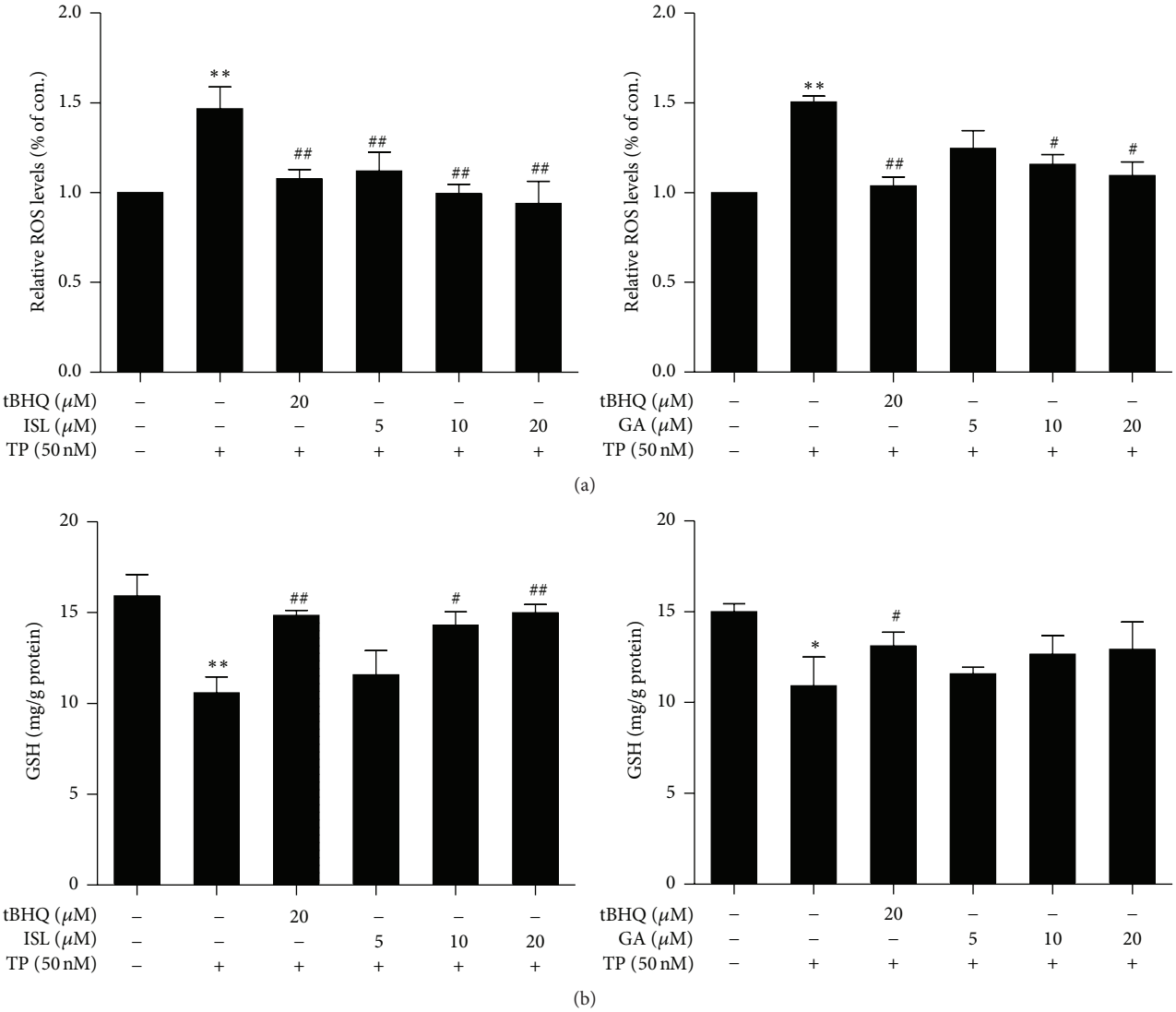

Figure 3: Cells were exposed to 50 nM TP for 24 h after incubation with various concentrations of ISL and GA for 12 h and 24 h, respectively. (a) The content of ROS was measured and normalized to control group. (b) The content of intracellular GSH was measured and normalized to protein content ($n = 3$). $^{*}p < 0.05$ versus control, $^{**}p < 0.01$ versus control; $^{\#}p < 0.05$ versus TP group, $^{\#\#}p < 0.01$ versus TP group. Control (Column 1): 0.1% DMSO.

event may result in lower induction of antioxidant defenses (Figure 5) [29]. In fact, the current results observed a decrease in the GSH content and protein expression of antioxidant enzyme HO-1 in HepG2 cells which is in accordance with a lower Nrf2 activation. However, the results are inconsistent with recent reports in which the expressions of Nrf2 and HO-1 in BALB/C mice were slightly higher than those of control [7]. The difference may be due to different treatment times and experimental subjects. Moreover, increasing protein expression of NQO1 was observed in TP-treated group, indicated that NQO1 may be regulated by other transcription factors. In addition, it is interesting to mention that the protein expressions of HO-1, NQO1, and MRP2 in high dose of ISL-pretreated group were slightly higher compared with tBHQ-treated group. It indicated that the regulation of HO-1, NQO1, and MRP2 expressions by ISL might through independently direct interaction with Nrf2 and other factors such as HIF-1 [30] be involved, but this remains to be elucidated.

There are a few limitations of our study due to the absent of in vivo evaluation since TP-provoked hepatotoxicity is better to be approached in animal model rather than in HepG2 cell model. Moreover, the nuclear accumulation of Nrf2 was not detected to confirm nuclear translocation of Nrf2. Therefore, further studies will be carried out focusing on animals even on Nrf2−/− animals and the nuclear translocation of Nrf2 to further demonstrate the Nrf2 activation mechanisms of ISL and GA.

5. Conclusion

Collectively, the current study demonstrated that ISL and GA effectively attenuated TP-induced oxidative stress and Nrf2 pathway was involved in the protection. To our knowledge,

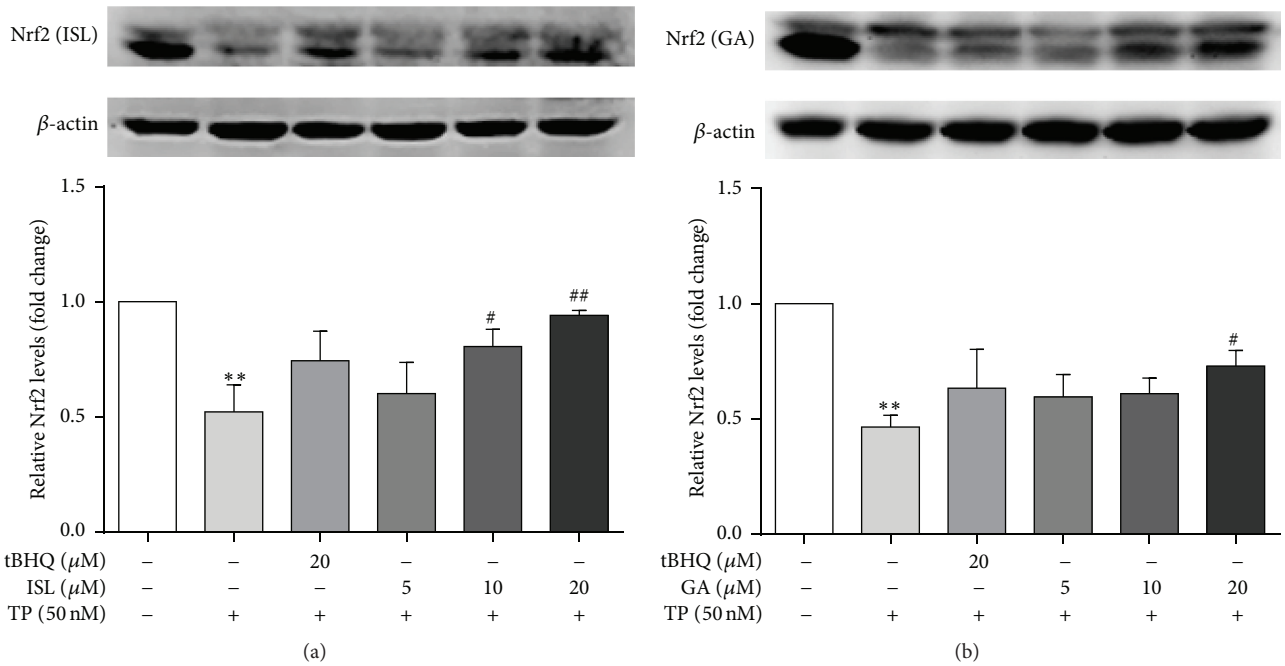

Figure 4: Cells were treated with different concentrations of ISL (a) and GA (b) for 12 h and 24 h, respectively, after which they were exposed to 50 nM TP for 24 h. The protein expression and gray value of Nrf2 was measured ($n = 3$). $^{**}p < 0.01$ versus control; $^{\#}p < 0.05$ versus TP group, $^{\#\#}p < 0.01$ versus TP group. Control (Column 1): 0.1% DMSO.

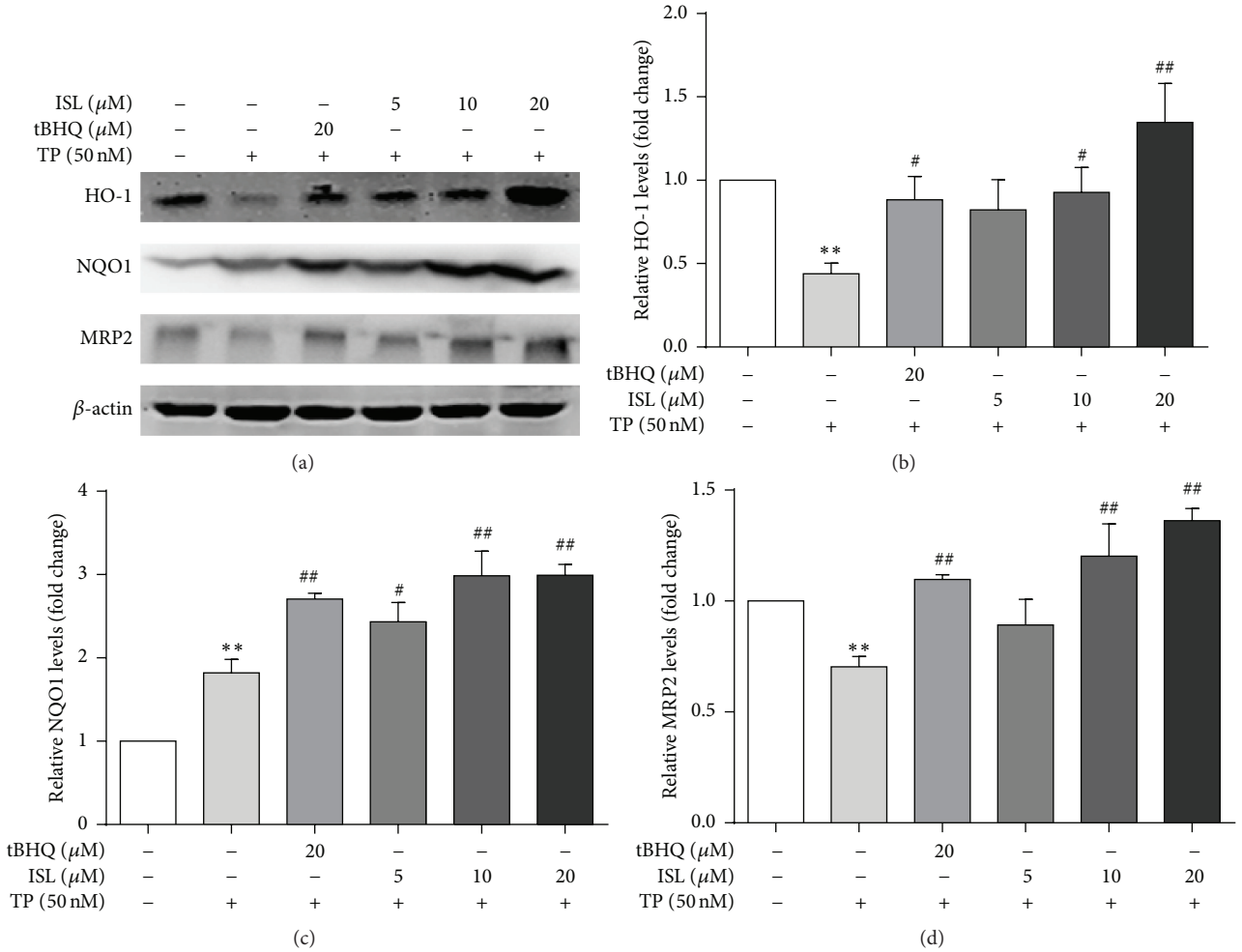

Figure 5: Cells were treated with different concentrations of ISL and tBHQ for 12 h, after which they were exposed to 50 nM TP for 24 h. The protein expressions (a) and gray value of HO-1 (b), NQO1 (c), and MRP2 (d) were measured ($n = 3$). $^{**}p < 0.01$ versus control; $^{\#}p < 0.05$ versus TP group, $^{\#\#}p < 0.01$ versus TP group. Control (Column 1): 0.1% DMSO.

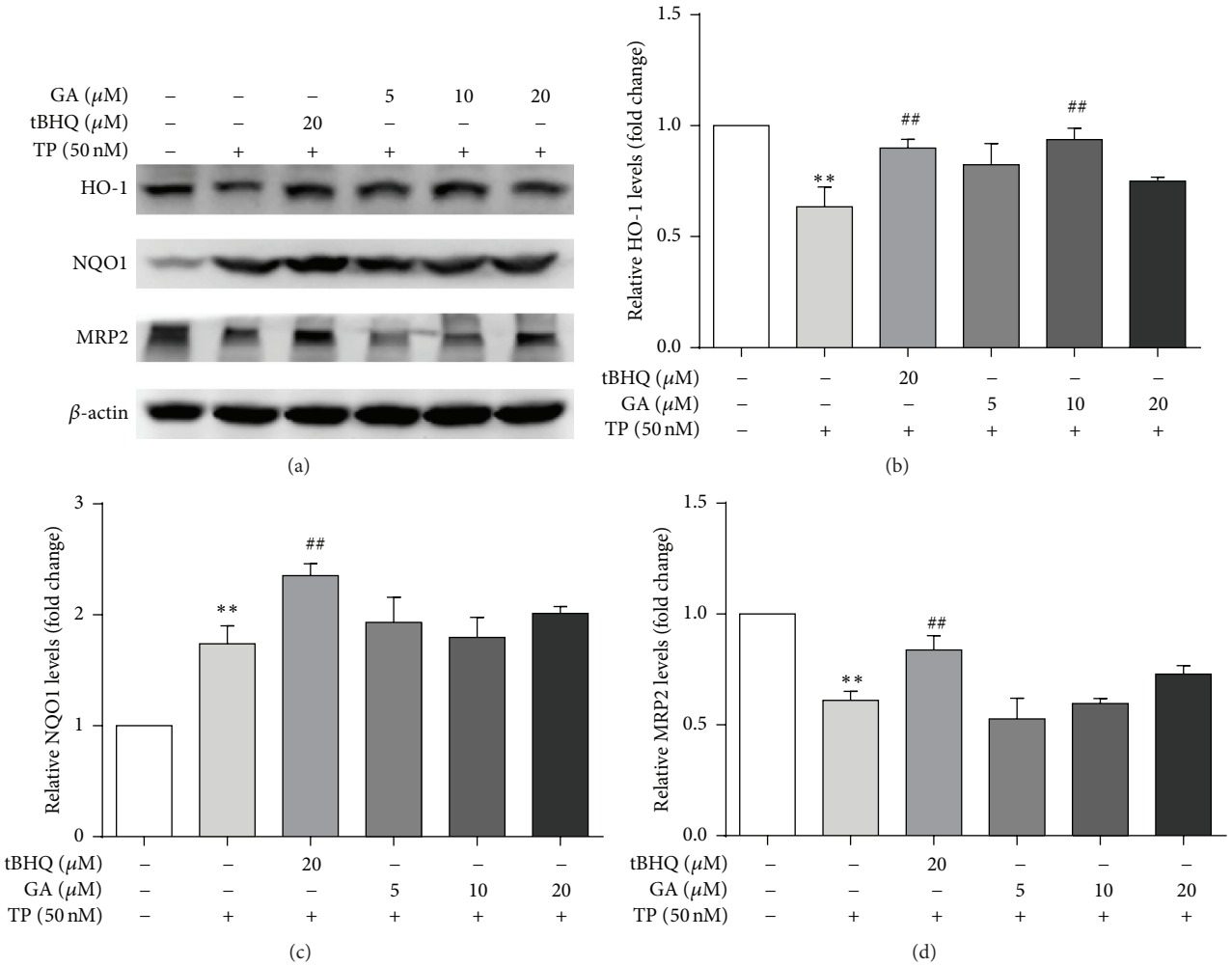

Figure 6: Cells were treated with different concentrations of GA and tBHQ for 24 h, after which they were exposed to 50 nM TP for 24 h. The protein expressions (a) and gray value of HO-1 (b), NQO1 (c), and MRP2 (d) were measured ($n = 3$). $^{**}p < 0.01$ versus control; $^{\#\#}p < 0.01$ versus TP group. Control (Column 1): 0.1% DMSO.

the present study is the first to show that ISL and GA activate Nrf2-associated HO-1, NQO1, and MRP2 in HepG2 cells and exert antioxidative defense against TP-induced hepatotoxicity. Therefore, the results provide new and meaningful insight into protecting against oxidative stress induced by TP. Moreover, this study implies that Nrf2 pathway may present a new biological target and that ISL and GA might be candidates for the prevention of drug-induced hepatotoxicity partly via Nrf2 pathway.

Conflict of Interests

The authors declare that there is no conflict of interests regarding the publication of this paper.

Acknowledgments

This work was supported by the grants of Chinese National Natural Science Foundation (nos. 81202985, 81473411, and 81573686) and the program of China Scholarships Council (no. 201208430206). The authors thank Yanxia Ma for her kind help.

References

[1] X.-J. Li, Z.-Z. Jiang, and L.-Y. Zhang, "Triptolide: progress on research in pharmacodynamics and toxicology," *Journal of Ethnopharmacology*, vol. 155, no. 1, pp. 67–79, 2014.

[2] Z. Mei, X. Li, Q. Wu, S. Hu, and X. Yang, "The research on the anti-inflammatory activity and hepatotoxicity of triptolide-loaded solid lipid nanoparticle," *Pharmacological Research*, vol. 51, no. 4, pp. 345–351, 2005.

[3] Q. Ma, "Role of Nrf2 in oxidative stress and toxicity," *Annual Review of Pharmacology and Toxicology*, vol. 53, pp. 401–426, 2013.

[4] Q. Ma and X. He, "Molecular basis of electrophilic and oxidative defense: promises and perils of Nrf2," *Pharmacological Reviews*, vol. 64, no. 4, pp. 1055–1081, 2012.

[5] G.-W. Hwang, "Role of intracellular defense factors against methylmercury toxicity," *Biological and Pharmaceutical Bulletin*, vol. 35, no. 11, pp. 1881–1884, 2012.

[6] G. Shen and A.-N. Kong, "Nrf2 plays an important role in coordinated regulation of Phase II drug metabolism enzymes and Phase III drug transporters," *Biopharmaceutics and Drug Disposition*, vol. 30, no. 7, pp. 345–355, 2009.

[7] J. Li, F. Shen, C. Guan et al., "Activation of Nrf2 protects against triptolide-induced hepatotoxicity," *PLoS ONE*, vol. 9, no. 7, Article ID e100685, 2014.

[8] Y.-F. Lu, J. Liu, K. C. Wu, Q. Qu, G. Fan, and C. D. Klaassen, "Overexpression of Nrf2 protects against microcystin-induced hepatotoxicity in mice," *PLoS ONE*, vol. 9, no. 3, Article ID e93013, 2014.

[9] T.-C. Kao, C.-H. Wu, and G.-C. Yen, "Bioactivity and potential health benefits of licorice," *Journal of Agricultural and Food Chemistry*, vol. 62, no. 3, pp. 542–553, 2014.

[10] Y. S. Li, P. J. Tong, H. Z. Ma, Q. D. Dai, T. R. Guan, and X. W. Song, "Toxicity attenuation and efficacy potentiation effect of liquorice on treatment of rheumatoid arthritis with *Tripterygium wilfordii*," *Zhongguo Zhong Xi Yi Jie He Za Zhi*, vol. 26, no. 12, pp. 1117–1119, 2006.

[11] M.-X. Liu, J. Dong, Y.-J. Yang, X.-L. Yang, and H.-B. Xu, "Progress in research on triptolide," *Zhongguo Zhong Yao Za Zhi*, vol. 30, no. 3, pp. 170–174, 2005.

[12] H. Gong, B.-K. Zhang, M. Yan et al., "A protective mechanism of licorice (*Glycyrrhiza uralensis*): isoliquiritigenin stimulates detoxification system via Nrf2 activation," *Journal of Ethnopharmacology*, vol. 162, pp. 134–139, 2015.

[13] P. A. Phillips, V. Dudeja, J. A. McCarroll et al., "Triptolide induces pancreatic cancer cell death via inhibition of heat shock protein 70," *Cancer Research*, vol. 67, no. 19, pp. 9407–9416, 2007.

[14] J. Q. Liu, X. J. Ren, J. C. Shu, R. Zhang, and J. X. Pan, "Advances in studies on compatibility of triptolide," *Jiangxi Journal of Traditional Chinese Medicine*, vol. 42, no. 11, pp. 55–57, 2011.

[15] M. Cuendet, C. P. Oteham, R. C. Moon, and J. M. Pezzuto, "Quinone reductase induction as a biomarker for cancer chemoprevention," *Journal of Natural Products*, vol. 69, no. 3, pp. 460–463, 2006.

[16] Y. Luo, A. L. Eggler, D. Liu, G. Liu, A. D. Mesecar, and R. B. van Breemen, "Sites of alkylation of human Keap1 by natural chemoprevention agents," *Journal of the American Society for Mass Spectrometry*, vol. 18, no. 12, pp. 2226–2232, 2007.

[17] M. Lin, X. Zhai, G. Wang et al., "Salvianolic acid B protects against acetaminophen hepatotoxicity by inducing Nrf2 and phase II detoxification gene expression via activation of the PI3K and PKC signaling pathways," *Journal of Pharmacological Sciences*, vol. 127, no. 2, pp. 203–210, 2015.

[18] J. Zhang, X. Cao, S. Ping et al., "Comparisons of ethanol extracts of Chinese propolis (poplar type) and poplar gums based on the antioxidant activities and molecular mechanism," *Evidence-Based Complementary and Alternative Medicine*, vol. 2015, Article ID 307594, 15 pages, 2015.

[19] A. Hervera, S. Leánez, R. Motterlini, and O. Pol, "Treatment with carbon monoxide-releasing molecules and an HO-1 inducer enhances the effects and expression of μ-opioid receptors during neuropathic pain," *Anesthesiology*, vol. 118, no. 5, pp. 1180–1197, 2013.

[20] C.-F. Chang, X.-M. Liu, K. J. Peyton, and W. Durante, "Heme oxygenase-1 counteracts contrast media-induced endothelial cell dysfunction," *Biochemical Pharmacology*, vol. 87, no. 2, pp. 303–311, 2014.

[21] J. H. Lim, K.-M. Kim, S. W. Kim, O. Hwang, and H. J. Choi, "Bromocriptine activates NQO1 via Nrf2-PI3K/Akt signaling: novel cytoprotective mechanism against oxidative damage," *Pharmacological Research*, vol. 57, no. 5, pp. 325–331, 2008.

[22] G. V. Velmurugan, N. R. Sundaresan, M. P. Gupta, and C. White, "Defective Nrf2-dependent redox signalling contributes to microvascular dysfunction in type 2 diabetes," *Cardiovascular Research*, vol. 100, no. 1, pp. 143–150, 2013.

[23] V. Vollrath, A. M. Wielandt, M. Iruretagoyena, and J. Chianale, "Role of Nrf2 in the regulation of the Mrp2 (ABCC2) gene," *Biochemical Journal*, vol. 395, no. 3, pp. 599–609, 2006.

[24] R. Wang, C. Y. Zhang, L. P. Bai et al., "Flavonoids derived from liquorice suppress murine macrophage activation by up-regulating heme oxygenase-1 independent of Nrf2 activation," *International Immunopharmacology*, vol. 28, no. 2, pp. 917–924, 2015.

[25] C.-H. Wu, A.-Z. Chen, and G.-C. Yen, "Protective effects of glycyrrhizic acid and 18β-glycyrrhetinic acid against cisplatin-induced nephrotoxicity in BALB/c mice," *Journal of Agricultural and Food Chemistry*, vol. 63, no. 4, pp. 1200–1209, 2015.

[26] S. Chen, L. Zou, L. Li, and T. Wu, "The protective effect of glycyrrhetinic acid on carbon tetrachloride-induced chronic liver fibrosis in mice via upregulation of Nrf2," *PLoS ONE*, vol. 8, no. 1, Article ID e53662, 2013.

[27] J. Zhou, C. Xi, W. Wang et al., "Triptolide-induced oxidative stress involved with Nrf2 contribute to cardiomyocyte apoptosis through mitochondrial dependent pathways," *Toxicology Letters*, vol. 230, no. 3, pp. 454–466, 2014.

[28] J. Hu, Q. Yu, F. Zhao et al., "Protection of Quercetin against triptolide-induced apoptosis by suppressing oxidative stress in rat leydig cells," *Chemico-Biological Interactions*, vol. 240, pp. 38–46, 2015.

[29] C. Carrasco-Pozo, R. L. Castillo, C. Beltrán, A. Miranda, J. Fuentes, and M. Gotteland, "Molecular mechanisms of gastrointestinal protection by quercetin against indomethacin-induced damage: role of NF-κB and Nrf2," *The Journal of Nutritional Biochemistry*, vol. 27, pp. 289–298, 2016.

[30] M. D. Hjortsø and M. H. Andersen, "The expression, function and targeting of haem oxygenase-1 in cancer," *Current Cancer Drug Targets*, vol. 14, no. 4, pp. 337–347, 2014.